Investigation of the foaming and encapsulation properties of whey proteins

Jenna Lee

Department of Science
School of Science and Computing
South East Technological University

Prepared under the supervision of
Dr. Elaine Duggan

A Dissertation Submitted in Fulfilment of the Requirement for the Degree of Doctor of Philosophy (Ph.D.) by Research

Submitted to South East Technological University, May 2022

Declaration

I hereby certify that this material, which I now submit is entirely my own work and has not been taken from the work of others, save and to the extent that such work has been cited and acknowledged within the text of my own work.

Signed: __Jenna Lee____

ID No.: __20062982___

Date: __30/05/2022____

Acknowledgments

Finally, it comes to the moment as I write the final few lines in my thesis. There was a time in my PhD when I felt as if this moment would never come. Without the contributions of many individuals to whom I am grateful, I would not have made it this far and I would like to express my heartfelt appreciation to everyone who helped me along the way.

I gratefully acknowledge the financial support of the Irish Department of Agriculture, Food and Marine who funded this project as part of the Food Institutional Research Measure (FIRM), project no. 15/F/737.

I would like to thank my supervisor Dr Elaine Duggan, for providing me with the opportunity to pursue this PhD, which has opened up a world of possibilities. Your assistance, support, and guidance has helped me get through the past five years.

I would like to thank the past and present technicians, postgraduate and postdoctoral friends at SETU (formerly known as WIT) who helped along my journey. It has been a roller coaster ride of ups and downs, but I wouldn't have made it through without you all. A big thank you to the crew I had the pleasure of sharing an office with in B18, who were always there for a chat. In particular, I want to thank Stephen and Sean for your time and help with training on instruments and being available to fix anything that broke or decided not to work.

I thank my parents, Liz and Alan for your support and encouragement. Without you, I would not have made it through this journey in one piece. Thank you, Paul, for your patience, compassion, and emotional support, particularly during the last several months, we both made it! Thank you to all my friends for putting up with me, you guys were the welcome distraction I needed. Not forgetting Louie, Teddy, Tilly, and Dora, my four dogs who supplied hairy hugs and instant happiness!

Table of Contents

Page Number

List of Figures

List of Tables

List of Abbreviations

ANS	8-Anilinonaphthalene-1-sulfonic acid
BSA	Bovine serum albumin
DSC	Differential scanning calorimetry
DTNB	5,5-dithiobis (2-nitrobenzoic acid)
EDTA	Ethylenediaminetetraacetic acid
EtOH	Ethanol
G"	Storage modulus
G'	Loss modulus
H_0	Surface hydrophobicity
HTST	High temperature, short time
Hz	Hertz
ICM	Ice cream mixture
kDa	kiloDalton
LMW	Low molecular weight
LTLT	Low temperature, long time
LVR	Linear viscoelastic region
MES	2-Morpholinoethanesulfonic acid
mN/m	MilliNewton meter
mPa	Millipascals
pI	Isoelectric point
RDI	Relative daily intake
RFI	Relative fluorescent intensity
Rpm	Rotations per minute
SDS-PAGE	Sodium dodecyl sulphate polyacrylamide gel electrophoresis
SEM	Scanning electron microscopy
SGF	Simulated gastric fluid

SH	Sulphydryl
SIF	Simulated intestinal fluid
S-S	Disulphide bond
SSF	Simulated salivary fluid
UV-vis	Ultra-violet visible
VD_3	Vitamin D_3
WPI	Whey protein isolate
WPI/VD_3	Whey protein isolate/vitamin D_3
XG	Xanthan gum
α-la	α-lactalbumin
β-lg	β-lactoglobulin
ΔP	Pressure difference
ζ	Zeta potential

Abstract

Foamed foods have been present for years and play an important role in the food we eat, e.g., in bread, carbonated drinks (e.g., beer), ice cream etc. Although aeration offers little nutritional benefit it provides foods with different textures and the air bubbles can help with digestion. However, foams are thermodynamically unstable and must be stabilised for consumer acceptance and product shelf-life.

This work looked at creating stable foams using whey protein isolate (WPI). Whey protein being amphiphilic, can stabilise foamed systems by residing at the air/water interface. Preliminary data found that WPI had good overrun but was unstable and drained within 1–48 h. Due to this instability, WPI microgels were prepared via cold-set gelation and their foamability was assessed, known as Pickering stabilisation. The microgels had lower overrun compared to native WPI, however, stability was much greater than native WPI. The microgels created self-supporting ultra-stable foams, remaining stable for >2 years.

In addition, microgels can also encapsulate compounds. In this work, the microgels encapsulated vitamin D_3 (VD_3), protecting it from stresses found in the food industry such as pasteurisation, UV-light and long-term storage. To the authors knowledge, there has been no published work based on using WPI microgels for encapsulation while also producing stable foams. This project proved that WPI microgels can simultaneously encapsulate VD_3 while also forming an extremely stable foam.

Having established good foaming and encapsulation, the VD_3 loaded WPI microgels (WPI/VD_3) were incorporated into ice cream, whereby the melting rate was significantly reduced. Addition of WPI/VD_3 microgels to ice cream did not negatively affect the ice creams properties and VD_3 content remained stable, indicating the protective effect of WPI microgels from processing and storage conditions.

This demonstrated that WPI microgels could form ultra-stable foams, while acting as a delivery vehicle for VD_3 for food fortification.

Chapter 1
Introduction

The world is experiencing a demographic milestone; the population of people over the age of 60 will reach 1.4 billion by 2030, and is expected to reach 2.1 billion by 2050 (World Health Organization, 2021).

Studies show approximately half of individuals over the age of 65 suffer from dysphagia. Dysphagia is the difficulty or inability to consume regular foods and food products, and this is arguably one of the most common afflictions associated with physiological aging of the human body. The outcomes of dysphagia in the elderly are multifactorial, including abnormal posture, recurrent infections (mostly oropharyngeal yeast), gastroesophageal reflux disease, and frailty (Wimalawansa, 2018). These issues are exasperated further by the considerable quantities of medication in tablet form these individuals are typically required to ingest, which brings with it increased risk of choking and discomfort for the individual generally.

It is not unreasonable to postulate that there is a gap in the field of research and development for products that are designed for consumption by elderly individuals as their capacity to consume regular foods deteriorates with age. Studies all seem to suggest that soft and moist foods are most suitable for the elderly as they are disintegrated and mixed in the mouth with little masticatory forces (Aguilera and Park, 2016). An appropriate example would be foamed food products such as ice cream, mousses, or frozen yoghurt. Foamed foods are growing in popularity amongst the elderly population, primarily due to their suitability and ease of consumption. The incorporated air makes foams soft, easy to chew and digest, which makes them very suitable. However, foamed systems are inherently unstable and are susceptible to collapse.

As people age, their need for vitamin D also increases (World Health Organization, 2002). Vitamin D helps with the absorption of calcium and phosphorus in the body, thereby helping to develop and maintain a healthy skeleton for humans. Having sufficient amounts of vitamin D in the diet can help the elderly maintain bone strength and reduce the number of falls and fractures (Wimalawansa, 2018).

However, vitamin D deficiency is prevalent in Ireland because of Ireland's northerly positioning, resulting in very little UVB light reaching the country. Vitamin D deficiency is defined as the lowest threshold value for plasma 25(OH)D that prevents secondary hyperparathyroidism, increased bone turnover, bone mineral loss or seasonal variations in plasma. It is prevalent amongst elderly people in developed countries who live at higher latitudes, institutionalised elderly, geriatric patients, and patients with hip fractures. It is more difficult for elderly people to obtain exposure to the sun due to changes in their lifestyle such as reduced outdoor activity and wearing more protective

clothing (Mosekilde, 2005). Along with this reduced exposure to sunlight, their ability to make vitamin D is also reduced. With little UVB penetration in conjunction with low dietary intakes, the vitamin D status of Ireland's elderly population is compromised. Due to this, it is necessary for supplementation of vitamin D or consumption of fortified foods (Wimalawansa, 2018).

Food fortification with vitamin D is challenging as it is not soluble in water and is sensitive to environmental stresses such as light, heat, low pH and oxygen which leads to loss of functionality (Ozturk *et al.*, 2015). Vitamin D also has variable oral bioavailability when ingested due to the low pH found in the stomach. Therefore, encapsulation within a carrier is essential for its protection.

This review therefore aims to discuss foam formation and stabilisation using proteins and protein particles. It will also cover the use of protein particles to increase the bioavailability of bioactive compounds.

1.1 Foams

Foams have been present for many years and are used in both traditional and contemporary food products. They are low density, possess large surface area and exhibit both solid and liquid-like behaviour (Hill and Eastoe, 2017). Traditional food products would include those such as bread, whipped cream, meringue, cakes, ice cream etc. However, today there is a growing need for new and improved foods and the inclusion of air can produce foods with unique new textures (Lazidis *et al.*, 2016). The bubbles in foams help the dispersion of flavours and provide body and smoothness while ensuring uniform rheological properties (Kinsella, 1981). Food aeration can also lead to the reduction of density in a product, a change in rheological properties and modification of digestibility, for example protein digestibility was improved in popped cereals (Parker *et al.*, 1999). Aeration in foods also aids the mastication process and enhances flavour delivery to the consumer (Campbell and Mougeot, 1999).

1.1.1 Foam Structure and Formation

Foams consist of two phases; a dispersion of gas in the form of bubbles surrounded by a continuous liquid or solid phase, forming closed cell structures (Hill and Eastoe, 2017). The dynamics of a foam are made up of monolayers of surface active

agents at the air-water interface (molecular), the thin films present between the bubbles known as lamella or films, with a thickness < 1 μm (mesoscopic) and the bubbles and channels present between the bubbles, known as Plateau borders (macroscopic) which are connected to nodes (Fig. 1.1) (Langevin, 2017). The ability of a solution to produce foam is known as foamability (Wang *et al.*, 2016). Foams require energy to be formed, the energy is the product of the surface tension γ and the area created *A*, and is orders of magnitude larger than thermal energies (Rio *et al*., 2014). The interface between the air and water contains an excess of free energy and the interface will try to become as small as possible to reduce this energy (Damodaran *et al*., 2007). The liquid volume fraction of a foam is known as φ and a foam may be distinguished as either a dry foam (<10 % liquid) or a wet foam (>10 % liquid).

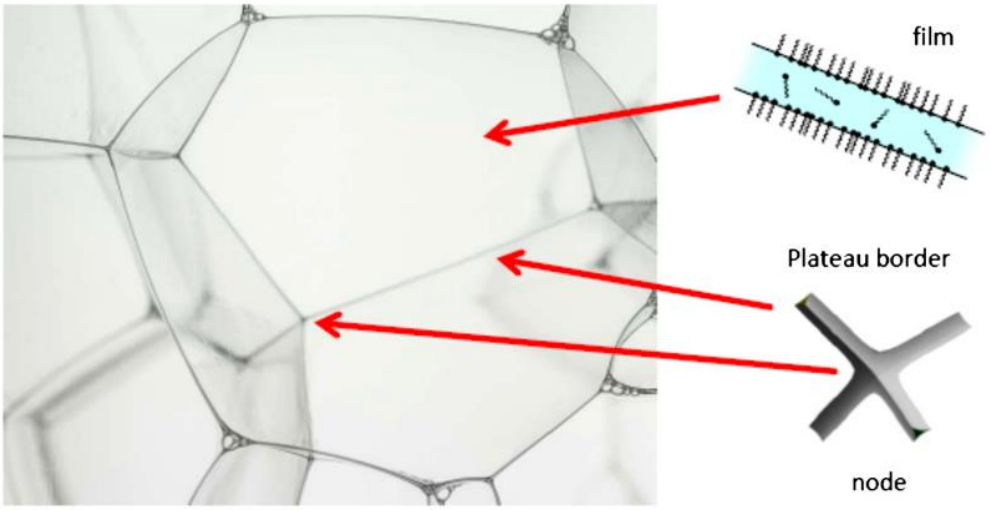

Fig. 1.1 Dry foam. The sides of the bubbles are separated by liquid films, plateau borders and nodes are at the corners. Surfactant molecules are stabilising the liquid films, a polar head facing towards the water and a non-polar tail in contact with air (Langevin, 2017).

When foams are first formed, the low volume fraction of air results in spherical bubbles, however, as the volume fraction of air increases bubbles begin to touch and compress to each other leading to the formation of a polyhedral foam (Langevin, 2017). Foams can be made via sparging, whipping or shaking. Sparging requires the injection of gas into the continuous phase using a single or set of capillaries or a porous plate placed

in the lower part of the foam generator. Due to buoyancy, the bubbles float up from the pores. The gases that are usually used are air, carbon dioxide or nitrogen, however, the use of each affects foam formation and stability. Nitrogen gas has been found to diffuse much slower than carbon dioxide which slows down foam collapse. The slower diffusion of nitrogen is due to the gas being more insoluble in water than carbon dioxide. Air sparging has been used to form foams using the Foamscan apparatus, which controls the gas flow rate (Lech *et al.*, 2016; Marinova *et al*., 2009; Chen *et al*., 2018; Chen *et al*., 2016).

Foams formed by whipping use shear forces to produce foams (Lomolino *et al*., 2015). It is possibly the most common method used for foam formation. Whipping causes shearing of the multiphase liquid creating a new surface. It creates and at the same time disrupts the air/liquid interface (Bos *et al*., 2003). The shaking method involves a vessel that is partially filled with solution and is then shaken and air is incorporated to form bubbles; the pressure difference between the inside of the container and the atmosphere impacts the bubble size (Marinova *et al*., 2009). Disjoining forces between the surfactant films form a thin aqueous film which prevents the bubbles from coming into contact (Kinsella, 1981). The foam is characterised by its overrun, which is the volume of foam formed from the initial liquid (Eq 2.2) or can be defined as the gas holding capacity of the foam.

1.1.2 Foam Instability

The bubbles in foams are naturally unstable and are susceptible to drainage, coalescence or coarsening due to the large density difference between the dispersed phase and the continuous phase, which leads to their collapse and loss of the desired foam structure and texture (Murray and Ettelaie, 2004).

Foams are prone to drainage which causes the flow of water due to gravity through the films of the bubbles (Lazidis *et al.*, 2017). Drainage of foams leads to drier foams due to the liquid fraction being lowered (Fameau and Salonen, 2014). Drainage is dependent on the viscosity of the system; a higher viscosity retards drainage (Kinsella, 1981). With low liquid films, the bubbles are made up of quasi-flat faces at the borders with curved faces at the edges to create polyhedral bubbles (Kinsella, 1981). In polyhedral foams, the lamella is flat while in spherical foams the lamella is rounded. Where three lamellae meet,

a plateau border is formed, a prism-shaped water volume bounded by cylindrical surfaces (Damodaran *et al*., 2007).

Coarsening is caused by the transfer of gas between bubbles induced by capillary pressure differences causing the interfacial films to drain, that causes two or more foam bubbles to join together to form one large bubble (Wang *et al*., 2016). Coalescence occurs when the films between bubbles become thinner and can rupture (Langevin, 2017) (Fig. 1.2). These instability mechanisms are found to be interdependent of each other (Damodaran *et al*., 2007).

Foams have a much shorter lifetime than other colloidal systems such as emulsions and the reason for this is because the interfacial tension at the air/water interface is fivefold larger than that of oil/water. Gas solubility in water is also much higher than that of oil which leads to faster gas transfer from smaller to larger bubbles. Therefore, the kinetics of coarsening in foams are much faster compared to Ostwald ripening in emulsions (Lazidis *et al*., 2017). Ostwald ripening in emulsions (equivalent to coarsening in foams) occurs over a longer time frame of days, weeks or even months compared to foams (Ettelaie and Murray, 2014).

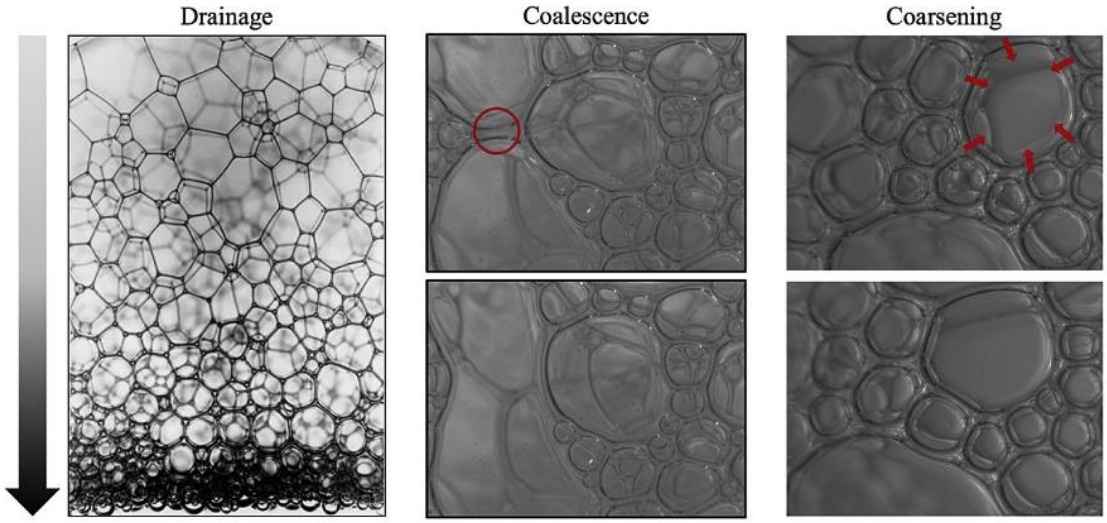

Fig. 1.2 Destabilising mechanisms of foams. The bubbles in drier foams are polyhedral in shape, while wetter foams are spherical. The arrow on the left depicts the gravitational flow of liquid through a foam. Where two bubbles come close and coalesce is indicated by the circle. The gas transfer from smaller to larger bubbles is shown by the arrows (Lazidis *et al*., 2017).

Pure liquid foams do not form stable foams; a stable foam requires a surfactant to form an adsorbed layer of molecules to help prolong their stability (Wierenga and Gruppen, 2010). Surfactants are amphiphilic molecules which means they have a polar (hydrophilic) head and non-polar (hydrophobic) tail. These molecules are adsorbed at the air/water interface alleviating the surface tension (Hunter *et al*., 2008). Surfactants form cohesive deformable films that are capable of resisting excessive localised thinning (Kinsella, 1981). When surfactants reduce the surface tension, less energy is required for the bubbles to survive which in turn increases their life expectancy (Lazidis *et al.*, 2017).

The Marangoni effect is another significant factor which influences drainage. The Marangoni effect relates to the ability of a surfactant to respond to fluctuations in interfacial tension. An interfacial tension gradient is created when liquid drainage occurs in the lamella film. When surfactants adsorb slowly, from low to high interfacial tension, the surface layer moves upward bringing liquid from the lamella with it, leading to reduced drainage. Thinning and breakage of lamella films is more common in foams stabilised by small surfactants compared to proteins (Damodaran, 2005).

There are three classes of surface active agents; low molecular weight (LMW) surfactants (e.g. mono/ diglycerides), amphiphilic polymers (e.g. proteins) and solid particles (e.g. pickering stabilisation) (Wilde, 2000). Low molecular weight surfactants include mono/ diglycerides, phospholipids, polysorbates and the polymeric molecules (high molecular weight surfactants) include whey proteins, caseinates, modified starches and celluloses (Rayner, 2015).

This review will focus on protein stabilised foams. High protein foods are said to be advantageous for growth and maintenance in the body and their ability to control food intake by enhancing satiety (Norton *et al*., 2015). Proteins are widely used as foaming agents in the food industry (ErÇelebi and IbanoĞlu, 2009; Liszka-Skoczylas, Ptaszek and Zmudziński, 2014; Oboroceanu *et al.*, 2014).

1.1.3 Protein Structure

Proteins comprise four levels of structure: primary, secondary, tertiary and quaternary. The primary structure of a protein is the amino acid sequence that is covalently linked through amide bonds known as peptide bonds. The primary structure determines the conformation of the protein; how the protein is folded into its unique three-dimensional structure and ultimately the proteins functional properties (Damodaran *et al*.,

2007). Amino acids are made up of a hydrogen (H), an amine (NH_2), a carboxyl (COOH) and a side (R) group that are covalently linked to a central α-carbon (Ustunol, 2014). Amino acids differ in structure due to their side group, which dictates the physicochemical properties such as net charge, solubility, chemical reactions and hydrogen bonding potential (Damodaran *et al*., 2007). The side groups can be ionic, non-ionic or hydrophobic. All proteins are built by combinations of 20 amino acids, meaning that they can differ with amphiphilic nature and surface activity (Germain and Aguilera, 2014).

The amino acid chain is folded into secondary structural elements known as *α*-helices or *β*-sheets. Most of the *α*-helix structure is amphiphilic in nature, with the polar residues on the outside and the non-polar residues in the interior. In proteins, a sheet like structure is formed when two β-strands of the same molecule interact via hydrogen bonding known as the β-pleated sheet. Two types of β-pleated sheet structures can be formed known as parallel β-sheet and antiparallel β-sheet. β-sheets are more stable than the α-helix structure so therefore proteins with larger segments of β-sheet structures are more likely to have higher denaturation temperatures (Ustunol, 2014; Damodaran *et al*., 2007).

The tertiary structure is the three-dimensional structure of the entire polypeptide. The arrangement of amino acids in the linear polypeptide determines the formation of the tertiary structure of that protein. The protein folding into the tertiary structure defines the shape and size of the protein. The formation of the tertiary structure involves optimisation of various non-covalent interactions between the protein molecules and the solvent to reduce the free energy. Folding of the protein might bring amino acid residues together leading to hydrophobic residues residing in the interior of the molecule, while the hydrophilic residues position themselves at the surface of the molecule. The distribution of the hydrophobic and hydrophilic residues determines if the protein will fold to an elongated, rod-like or globular shape (Ustunol, 2014; Damodaran *et al*., 2007).

The quaternary structure is the three-dimensional arrangement of more than one polypeptide. Quaternary structures are not present in all proteins however, larger proteins are likely to have more than one polypeptide (Ustunol, 2014; Damodaran *et al*., 2007).

The inter- and intra-molecular interactions that occur between protein molecules and the surrounding solvent such as hydrogen bonding, hydrophobic interactions, electrostatic interaction, disulphide bond formation and van der Waals interactions all help to maintain the protein structure. In summary, the formation of protein structures is due to the combination of repulsive and attractive noncovalent interactions and any

covalent disulphide bonds. Changes in the environment such as pH, ionic strength, temperature etc. will cause the protein molecule to adapt its conformation to assume equilibrium. However, denaturation occurs upon drastic environmental changes that alter the secondary, tertiary or quaternary structures causing molecule unfolding or breakage of some interactions (Damodaran *et al*., 2007).

Proteins may be both positively and negatively charged which contribute to electrostatic interactions. At values below pH 10, protonated amino side groups contribute positive charges, whereas at values above pH 2, deprotonated carboxylate side groups contribute negative charge. The isoelectric point is when positive and negative charges are equal giving a zero net charge (Jones and McClements, 2010).

1.1.4 Protein Stabilised Foams

Proteins are of great importance nutritionally and for their functionality in foods. They are the building blocks for synthesis of muscles and tissues in the body while providing structure to the food matrix. Protein stabilised foams are popular in many processes in the food and beverage industry due to their ability to form colloidal structures (Ustunol, 2014).

Proteins' surface activity is influenced by the presence of hydrophobic residues, molecular configuration and the extent and nature of intermolecular bonds (Kinsella, 1981). The large three-dimensional structures of proteins must unfold at interfaces to expose hidden hydrophobic regions. To stabilise a system, the hydrophobic part orientates itself to the air phase (trains) and the hydrophilic parts face towards the aqueous phase (loops), the structure that is formed is often referred to as the loop-train (Wierenga and Gruppen, 2010). When proteins stabilise foams, they create an interfacial layer with viscoelastic properties due to the interactions between the protein molecules at the fluid interfaces (Krägel *et al*., 1999).

Protein foam films are thick and irregular even when only a small amount of protein is used (Rio *et al.*, 2014). The protein molecules must be capable of interacting with neighbouring molecules at the interface to form strong cohesive films (Damodaran *et al*., 2007). At low concentrations, they absorb at the interface with the possibility of more than one layer of protein molecules being adsorbed (Hill and Eastoe, 2017). Random coil proteins such as caseins and globular proteins such as whey protein have different adsorption rates and foaming abilities (Wierenga and Gruppen, 2010). The size of the

native protein molecule is often the same size as the effective thickness of the globular protein monolayer (Dickinson, 1999; Martin *et al.*, 2002; Bos *et al*., 2003).

Foam quality not only measures foam ability and stability but also the rheological properties of foams (Mleko *et al*., 2007). Foams have a multiscale structure and liquid foams display complex mechanical behaviour as they have plastic, elastic and viscous properties (Dollet and Raufaste, 2014). The kinetics of elasticity increase for protein samples in three steps: a rapid increase which indicates adsorption of the proteins at the interface, it then slows down as the molecules unfold and intermolecular interactions develop and then finally a plateau is reached when the proteins are fully adsorbed (Rouimi *et al.,* 2005).

Proteins on their own can create foams with high volume however, they are unstable. Therefore it is essential to expose the protein molecules to different environmental factors to improve its stability such as pH, ionic strength or temperature (Lazidis *et al*., 2017).

1.1.4.1 Whipping time

During foam formation, whipping of liquids causes air to be incorporated in the form of bubbles which rise and disengage from the liquid. The rate of entrainment and disentrainment determines the air content and bubble size (Campbell and Mougeot, 1999). Whipping of protein solutions leads to the unravelling of the protein strands and partial unfolding of the protein tertiary and secondary structure. Kampf *et al.* (2003) found that with continued whipping of an albumin solution, the mean bubble size and their size distribution within the resultant foams decreased as whipping time increased from 1 to 5 min. It has been found that foams with smaller bubbles are more stable than foams with larger bubbles; also when foams have a narrow size distribution the destabilisation mechanisms of coarsening and coalescence are reduced as gas transfer from small to large bubbles is reduced (Yang *et al*., 2009). Whipping time also increased the mechanical strength of the foam formed with increasing whipping time. However, past a certain point, whipping time had no positive effect on the foams and could even lead to partial foam collapse (Kampf *et al*., 2003).

Relatively long whipping times of albumin increased its foaming ability by unravelling of the ovalbumin molecules which formed thicker lamellae that allowed greater intermolecular polymerisation (Lau and Dickinson, 2006). However, prolonged

whipping times caused the albumin to aggregate forming insoluble particles that lost their interfacial activity leading to foam collapse (Lau and Dickinson, 2006). In a study by Vega and Sanghvi (2012), the authors suggested that there is more liquid film thinning, deformation and bubble rupture involved with higher degrees of whipping. Therefore, current research on whipping time of protein foams all seem to indicate that prolonged times negatively affect foaming ability.

1.1.4.2 pH

Protein foam formation is influenced by electrostatic interactions with regards to adsorption and interfacial rheology (Foegeding *et al*., 2006). A protein's hydrophobic exposure and the net charge of the protein affect its adsorption kinetics (Wierenga and Gruppen, 2010). Altering the pH of protein solutions from their native pH can cause them to remain partially unfolded with modified functionalities at extreme pH (pH 1.5, 2.5, 3.5, 10.5, 11.5 or 12.5) followed by partial refolding by readjusting the pH back to the non-denaturing pH range of proteins (pH 4.5, 5.5, 6.5, 7.5 or 8.5) (unfolding/refolding regime) (Liang and Kristinsson, 2006). The modified functionalities due to the unfolding/ refolding regime would include increased surface hydrophobicity which aids in adsorption to the interface and increased flexibility caused by the open configuration due to unfolding, allowing protein molecules to be more surface active, which leads to improved foaming (Liang and Kristinsson, 2006). The authors also found that the unfolding/refolding regime improved the foam texture of the albumin foams, whereby the pH treated foams were noticeable thicker compared to the native protein foams.

Kuropatwa *et al*. (2009) found that whey protein (pI ~ 5) had high overrun and good stability at pH 9 compared to pH 5. The authors proposed that at pH 5 β-lactoglobulin, the main protein found in whey protein forms octamers while at pH 9 it exists in a monomeric form. The octameric structure is believed to hinder the protein unfolding at the air/water interface which is undesirable for foaming. An excess of negative electrostatic charge at pH 9 effected partial unfolding of β-lactoglobulin which increased its flexibility and exposed functional groups, improving the adsorption of whey protein to the air/water interface and thus led to greater foaming properties compared to whey protein at pH 5 (Kuropatwa *et al*., 2009).

Other studies in the literature have found opposite effects of pH on foam ability. At high pH values, proteins carry negative charges and the electrostatic repulsion of

protein molecules may lead to foam destabilisation (Li *et al.*, 2018 & Damodaran *et al*., 2007). Foegeding *et al*. (2006) and Marinova *et al.* (2009) found that at the isoelectric point (pI) of whey protein, electrostatic repulsion is minimal and hydrophobic interactions are favoured. Hydrophobic interactions cause the proteins to come into contact with each other and create stable cohesive foams.

1.1.4.3 Ionic strength

Addition of salt usually leads to an increased amount of adsorbed proteins because electrostatic repulsion between the proteins at the interface are reduced. However, salt's effect on protein foaming depends on the type of salt and the solubility of the protein in that salt solution (Damodaran *et al*., 2007). At low ionic strength, salts can stabilise proteins through electrostatic interactions (salting-in), whereas at high concentrations salts can induce aggregation and sedimentation (salting-out) of proteins depending on the nature and concentration of the salt (Arakawa and Timasheff, 1984).

ErÇelebi and IbanoĞlu (2009) found the addition of low concentrations of NaCl caused the salts to bind to protein-charged groups of whey protein isolate (WPI) and egg white, increasing protein solubility, and led to improved foam stability. However, at higher concentrations the salts decreased protein solubility leading to decreased foam stability. At high ionic strength, solubility decreases as the protein molecules compete with the salt ions to bind with water, thus leading to protein precipitation (ErÇelebi and IbanoĞlu, 2009).

Luck *et al*. (2002) found that the addition of sodium chloride (NaCl) and calcium chloride ($CaCl_2$) increased whey protein foam overrun compared to the control sample without salt. In contrast, Marinova *et al*. (2009) found that the addition of NaCl to whey protein solutions had no substantial effect on the proteins foaming ability. However, the authors did find that NaCl addition improved foaming ability of sodium caseinate. Also, the foams produced by sodium caseinate in the presence of NaCl were more stable than those formed using whey protein (Marinova *et al*., 2009).

Zhu and Damodaran (1994a) assessed the effect of Ca^{2+} and Mg^{2+} on whey protein isolate foaming and found that the stability of Ca^{2+} at any given concentration was higher than that imparted by Mg^{2+}. The authors suggested that this was due to greater binding affinity of Ca^{2+} than Mg^{2+} for the whey proteins leading to the formation of a film with better viscoelastic and mechanical strength properties.

1.1.4.4 Heat treatment

The functional properties of protein can change when exposed to heat treatment (Van der Plancken *et al*., 2007). The thermal denaturation temperature of proteins depends on its unique molecular characteristics as well as solution conditions such as pH and ionic strength (Jones and McClements, 2010). Prior to heat treatment, sulphydryl (SH) groups of proteins are buried in the protein core, deeming them inaccessible (Van Der Plancken *et al*., 2005). Upon heating, the protein unfolds, exposing the SH groups making them available to react with other SH groups to form disulphide bonds (S-S), resulting in the formation of a protein network which can then adsorb at the air/water interface (Van Der Plancken *et al*., 2005; Nicorescu *et al.*, 2011; Jones and McClements, 2010).

Protein aggregates can form a thick rigid interface and increase the interfacial viscoelasticity or remain in the liquid phase where they can become confined, increasing the viscosity leading to the formation of a gel-like network, thus leading to improved foam stability as liquid drainage is decreased (Nicorescu *et al*., 2010; Gharbi and Labbafi, 2019). In contrast, severe heating can cause adverse effects on protein foam ability. It can lead to a reduction in protein solubility, leading to a decrease in the amount of available protein for stabilising the air/water interface because the sulphydryl groups have reacted in the bulk solution.

Grossmann *et al*. (2019) found that with increasing temperature (50 – 80 °C) the aggregate size of the whey proteins increased due to the formation of disulphide bonds. The authors found that on whipping the aggregates, foam overrun and stability improved. During the whipping process shearing forces lead to the creation of new bubbles and also the formation of smaller bubbles due to the breakup of larger bubbles allowing the protein molecules more time to rearrange along the newly created surface. Also, the convection conditions transport the proteins in close proximity to the interface (Grossmann *et al*., 2019). However, even though whipping did improve foaming properties, the authors found that the native protein solutions had better foaming properties, indicating that the aggregates prepared by heating were not able to enhance foaming properties due to their strongly aggregated state and size (Grossmann *et al*., 2019).

Bals and Kulozik (2003a) found that heating of WPI improved the foam overrun however, once the protein was denatured to 50 % the foam overrun was negatively affected due to the viscosity increase. The protein unfolding and the increased interactions between the reactive groups of the protein molecules caused a viscosity increase.

Increasing viscosity hinders the incorporation of air into aqueous systems while improving foam stability (Lau and Dickinson, 2005).

Dry heating of egg albumin was found to produce foams with smaller bubble diameters which aided in an increase in foam overrun and stability (Talansier *et al*., 2009). Van der Plancken *et al*. (2007) also found that the heat-treated egg albumin solutions had a smaller bubble size which resulted in a moist and creamy foam with a low sensitivity to bubble coalescence. In another study, Nicorescu *et al*. (2010) also found that heating whey protein solutions led to a greater number of bubbles with smaller bubble sizes and more uniform size distributions leading to positive changes in foam texture and stability. The results from these studies suggest that temperature is one of several factors to establish optimal foaming properties as excessive heating can have negative effects on foaming.

1.1.4.5 Addition of hydrocolloids

Hydrocolloids are characterised as a diverse group of long-chain polymers that readily disperse in water (Li and Nie, 2016). They can be separated into groups such as tree exudate group, plant group, animal group, natural gums, synthetic gums, non-ionic, anionic etc. (Li and Nie, 2016). Proteins and polysaccharides can link together by covalent bonding to give a specific, strong and permanent 'conjugate'. They can also interact via physical interactions such as non-covalent interactions (electrostatic, hydrophobic, hydrogen bonding etc.). Mixtures of positively charged proteins and negatively charged polysaccharides lead to the formation of strong attractive electrostatic complexes (Rodriguez Patino and Pilosof, 2011).

On mixing of proteins and polysaccharides, one of three outcomes might be observed; complexation, co-solubility or segregation (Fig. 1.3) (Rodriguez Patino and Pilosof, 2011). Complexation involves attractive interactions (ionic, hydrogen bonding or hydrophobic interactions) between the two biopolymers to form soluble or insoluble complexes; co-solubility occurs when the biopolymers form a single homogenous phase and segregation is when the biopolymer compositions separate into two phases; one phase rich in protein and the other rich in polysaccharide.

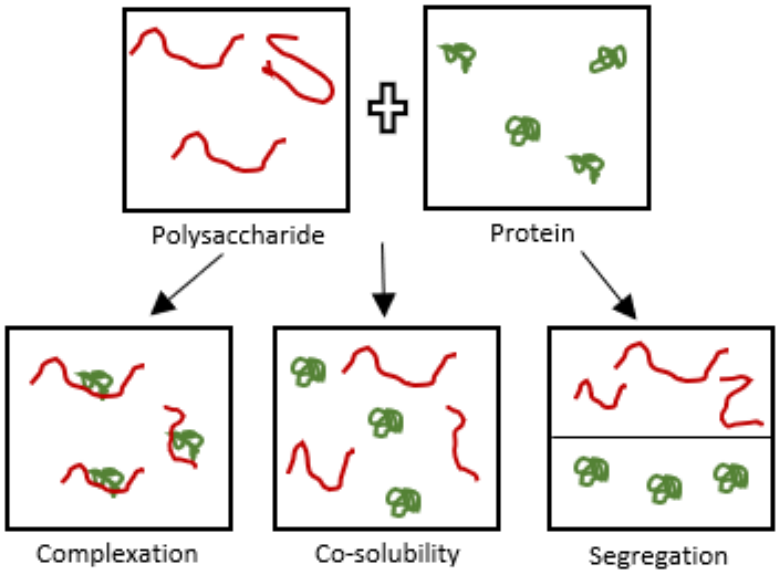

Fig. 1.3 Behaviour of protein-polysaccharide mixtures (Rodriguez Patino and Pilosof, 2011)**.**

Polysaccharides are usually added to food products for their thickening abilities and their ability to modify flow properties and textures of food products (Damodaran *et al*., 2007). Thickening polysaccharides can be used to increase the viscosity of the continuous phase, influence the viscoelastic behaviour and thickness of the adsorbed macromolecular layer while enhancing foam stability (Martínez-Padilla *et al*., 2015). Foam stability is enhanced due to the thinning rate of the bubble lamella being reduced (ErÇelebi and IbanoĞlu, 2009). Polysaccharide addition to foamed systems leads to stronger films as well as improving the water binding capacity of the foam matrix leading to stiffer foams (Kampf *et al*., 2003). Popular gums used in the food industry include sodium alginate, agar, carrageenan, locust bean gum, guar gum among others (Li and Nie, 2016).

For the purpose of this review, xanthan gum (XG) was chosen to be focused on as it is a popular food additive because of its unparalleled rheological properties due to its high molecular weight and anionic nature (Li and Nie, 2016). It is capable of providing long-term stability to colloidal systems due to its weak gel-like properties and its pseudoplastic flow properties (Moschakis *et al*., 2005; Martínez-Padilla *et al*., 2015). Zmudziński *et al*. (2014) describe how xanthan gum can adopt a helical conformation and bind large quantities of water, leading to denser foams. Xanthan gum is soluble in hot and cold water, it is less dependent on temperature and at low concentrations it provides high solution viscosity making the thickening agent unique. In acidic conditions it is soluble and stable and it also works well in the presence of salt (Damodaran *et al*., 2007).

Martínez-Padilla *et al.* (2015) and Liszka-Skoczylas *et al*. (2014) found that in a mixed system of WPI and XG, the average bubble diameter and the drainage rate from the foams decreased leading to increased foam stability. The water binding abilities of gums caused the bubble walls to strengthen giving stiffness to the foams, thus reducing drainage. Zmudziński *et al*. (2014) suggested that when XG and egg albumin were whipped together, the egg albumin unfolded and got stretched and entangled by the network created by XG. More protein molecules became bound which caused the foam to appear denser/ stiffer which also contributed to destabilisation prevention.

The viscosity increase due to XG addition to egg albumin decreased the amount of air incorporation, producing heavier foams (Dabestani and Yeganehzad, 2019). After whipping, the XG molecules were stretched and conformational changes occurred which enhanced the foam elasticity and firmness (Dabestani and Yeganehzad, 2019). Whipping time affects the structure formed by protein/polysaccharide foams. Work by Kampf *et al.* (2003) indicates that XG addition to egg albumin foams required > 3 min to form a strong foam. The network formation does not happen instantaneously and requires both time and energy.

1.1.4.6 Addition of sucrose

Sucrose is a disaccharide, composed of glucose and fructose which occurs naturally in fruits and vegetables. Sucrose is the most commonly understood sugar added to food products. Sucrose is added to food products for its sweetness, colour, flavour formation, alteration of texture, add viscosity, aid fermentation and for preservation (Goldfein and Slavin, 2015).

When proteins are whipped, they adsorb at the newly formed air/water interface, decreasing the surface tension. Addition of sucrose to protein solutions decreases the thermodynamic affinity of proteins for the aqueous environment, limiting protein unfolding, while enhancing protein-protein interactions (Bryant and McClements, 2000; Lau and Dickinson, 2005; Raikos *et al*., 2007; Davis and Foegeding, 2007). However, Rodríguez Niño and Rodríguez Patino (2002) found that the presence of sucrose (0.5 M) increased the diffusion of bovine serum albumin (BSA) toward the interface. The authors found that there were small changes in the structure of BSA, indicating a slight increase in secondary structure and protein-protein interactions in the bulk and at the interface. This may have led to the increased rate of diffusion of BSA for the interface. While,

ovalbumin was found to form hydrogen bonds with sucrose, resulting in reduced hydrophobicity and decreased surface activity, which in turn reduces adsorption at the air/water interface as the protein molecules prefer to remain in the bulk phase (Antipova *et al*., 1999).

Sugars in high concentration are used to form stable confectionery foams (Alavi *et al*., 2020). The addition of sucrose decreased foam overrun, but increased foam stability and this is due to the increased solution viscosity with increasing sucrose concentration (Yang and Foegeding, 2010; Lau and Dickinson, 2005; Ochi *et al*., 2000; Phillips *et al*., 1989). When sucrose is whipped into an egg white protein foam, it dissolves in the protein film present on the air bubbles, increasing viscosity, thus improving stability (Alavi *et al*., 2020). Egg white protein foam stability was improved on addition on sucrose as it lowered the rate of increase in bubble size compared to the control. The presence of smaller bubbles can help to reduce coalescence and coarsening, which in turn improve foam stability (Raikos *et al*.,2007).

1.1.5 Pickering Stabilised Foams

Pickering stabilisation has been found to protect bubbles against coalescence; it involves a monolayer of closely packed solid particles around a bubble interface (Dickinson, 2017). Pickering stabilisation is naturally found in food products such as whipped cream, doughs, batters and ice cream. The presence of fat crystals forms a stable structure by residing in the plane of the bubble surface/droplet interface. The fat crystals can directly crystallise or collect at the oil-water interface reducing coalescence and prolonging product shelf-life (Ghosh and Rousseau, 2011).

Particle stabilised foams have been reported to remain stable for months compared to only hours or days for regular protein stabilised foams (Dhayal *et al.*, 2015; Wang *et al.*, 2017). Pickering stabilisation is not only relevant in foams, but also in emulsions, whereby particles are irreversibly anchored at the oil-water interface (Destribats *et al.*, 2013). In the past, most of the research has focused on using inorganic particles for stabilisation such as silica particles. Silicas were chosen due to their well-defined shape, size variability and their chemical tunability. Inorganic particles have a limited relevance when it comes to an application requiring biocompatibility and biodegradability. They are solid and non-deformable, thus making them unsuitable for food foams (Lam *et al*., 2014).

In recent years there has been increased interest in the use of organic soft particles for foam stability as they are deformable and versatile (Schmitt *et al*., 2014). If the particles used have the correct surface energy or contact angle and have a sufficiently large surface area, the particles are irreversibly adsorbed. This leads to the arrest of disproportionation of bubbles of air in aqueous systems (Murray *et al*., 2011). Examples of particles used for foam stability would include microgels (Li *et al*., 2020a), nanoparticles (Dhayal *et al*., 2015), protein aggregates (Schmitt *et al*., 2007) and fibrils (Peng *et al*., 2017).

Microgel particles are an example of a soft matter that is gaining interest. The manufacture of these particles will be discussed in the next section. Microgel particles are soft porous particles made from polymers such as proteins or polysaccharides. Due to their soft and porous nature, microgels differ considerably from hard particles in interfacial functionality (Dickinson, 2015). They have the ability to hold considerable amounts of solvent within a cross-linked polymer network. Microgel particles can also swell and deswell rapidly in response to changes in environmental conditions such as pH and temperature (Dickinson, 2015).

Studies in recent years have shown that microgels can lead to dispersions being far more stable than those produced by surfactants (Lazidis *et al.*, 2016). Biopolymer-based particles of nanoscale and microscale dimensions have been found to work effectively at stabilising emulsified and aerated systems. The energy of desorption is greater for a particle than for a smaller surfactant and this explains why microgel stabilised dispersions are far more stable than surfactant foams (Cox *et al*., 2009).

There are two main ways, mechanistically speaking, in which microgels function as stabilising agents in emulsions and foams. The particles can create a gel-like network within the spaces amongst the dispersed liquid droplets or gas bubbles when they are present in high concentrations in the bulk continuous phase; thereby increasing the viscosity, leading to reduced drainage (Gharbi and Labbafi, 2019). Alternatively, the particles can generate a particle-loaded surface layer by becoming directly attached to the oil-water or air-water interface, which works to protect the droplets or bubbles (Dickinson, 2017). A combination of these mechanisms can be present in a multi-phase food system as some particles may be dispersed in the bulk phase while others are located within the thin liquid film. This is in comparison to protein stabilised foams where their large three-dimensional structure must unfold at interfaces to expose hidden hydrophobic regions where the hydrophobic part orientates itself to the air phase and the hydrophilic part face towards the aqueous phase.

Murray (2019) suggested that the dangling chains of unfolded protein molecules on the surface of the microgels may allow them to be more surface active than native proteins because they are trapped in a more unfolded state. These microgel particles affect the rheological properties and viscosity of the solution when they form the rigid films (Lazidis *et al*., 2017). The way in which the particles interact with the interface and with each other dictates the way in which they behave within the foam (Fameau and Salonen, 2014).

These particles create a steric barrier consisting of close-packed layers of particles at the gas/liquid interface that works against coalescence which extends the foam's life significantly (Lazidis *et al.*, 2016; Hunter *et al.*, 2008). This mechanism can be seen in Fig. 1.4, whereby protein particles formed a particle loaded layer at the gas/liquid interface of an air bubble. Li *et al*. (2020b) found that egg white protein microgels created a much thicker adsorbed protein layer on air bubbles compared to native egg white protein. Microgel addition to foams improved foam stability compared to egg white only foams, but not necessarily foam overrun. Li *et al*. (2020b) suggested that the lower foam overrun of the microgel stabilised foams could be due to the large and rapid increase in viscosity due to the microgel particles.

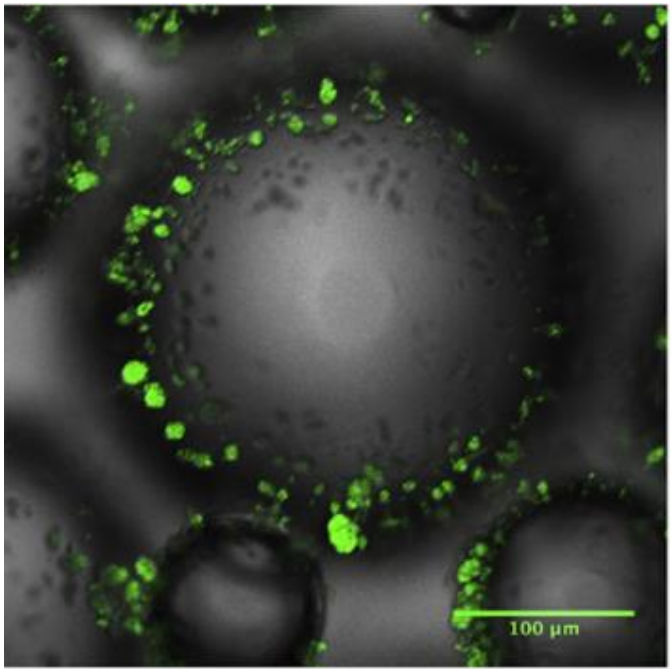

Fig. 1.4 Confocal images of whey protein gels made at pH 5 (stained green) which formed a particle loaded layer around the gas/liquid interface of air bubbles (Lazidis *et al.*, 2016).

A colloidal particle's wettability determines its ability to adhere to the interface, which is defined by the three-phase contact angle, Θ. This contact angle is the angle formed between the tangents of the solid surface and the liquid-gas interface. Particles tend to adsorb on the interface and reduce surface free energy when their contact angle is around 90º (Lazidis *et al.*, 2017; Fameau and Salonen, 2014). The way in which particles behave within a foam depends on how they interact with the interface and with other particles (Fameau and Salonen, 2014). When particles adsorb on the air/water interface they form rigid films that prevent drainage but when there is no adsorption the particles can create a gel-like network when they go through a percolation process, reducing drainage also (Lazidis *et al*., 2017).

Bubbles of different sizes in foams compete for adsorption of nanoparticles (Ettelaie and Murray, 2014). The coverage on the surface of a bubble must reach a critical value of particle adsorption before it is resistant to shrinkage. Smaller bubbles require fewer particles to reach this critical value and thus tend to be stabilised first before larger bubbles (Fig. 1.5) (Ettelaie and Murray, 2014).

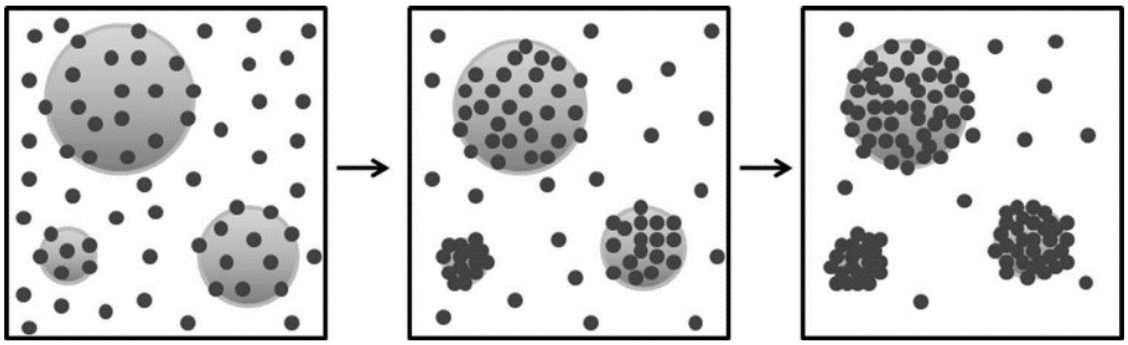

Fig. 1.5 Gas bubbles of different size being stabilised by particles. The smaller gas bubbles are being stabilised first by the particles (Ettelaie and Murray, 2014).

In mixed systems containing LMW surfactants, proteins or particles, competitive adsorption for the air/water interface can occur. LMW surfactants are more effective than proteins in reducing the interfacial tension, however, the foams formed are mostly less stable against coalescence. This is due to the ability of proteins to form a visco-elastic film around air bubbles via non-covalent interactions or via covalent disulphide bonds, while LMW cannot (Bos and Van Vliet, 2001). The displacement of proteins from a solid or liquid interface by LMW surfactants can be described by two mechanisms:

1. Solubilisation: a soluble protein-surfactant complex is formed when the protein is bound by the water-soluble surfactant. The LMW surfactant does not have to adsorb to the interface, but it must interact with the protein
2. Replacement: protein is displaced at the interface when the surfactant adsorbs. In this instance, the LMW surfactant must interact with the interface, but it does not have to interact with the protein.

Rouimi *et al*. (2005) found that competitive adsorption occurred in a mixture containing whey protein and sucrose ester SP 70. The authors found that when the protein and sucrose ester SP 70 were present at the same concentration, the interfacial elasticity nears the value of the film that was only covered by sucrose ester SP 70. This indicated that the LMW surfactant formed a saturated monolayer at the oil-water interface. In a different study, β-lactoglobulin was displaced by the surfactant SDS and Tween 20 (Mackie *et al*., 2000). Once the protein network was broken by surfactant addition, desorption of β-lactoglobulin from the interface took place. Tween 20 completely displaced the protein from the interface at a surface pressure of 30 mN/m, whereas, displacement did not start until 31 mN/m with SDS (Mackie *et al*., 2000).

For mixtures of proteins and protein particles, it is known that the difference in size plays a major role in foaming. Smaller proteins are capable of adsorbing at the air/water interface compared to larger protein particles due to their size and mobility (Li *et al*., 2020b). The smaller protein molecules aid in foam formation, while the larger particles aid in foam stability (Zhu and Damodaran, 1994b; Lazidis *et al*., 2016; Rullier *et al*., 2008).

Protein particles are most readily generated by thermal processing. Globular proteins unfold their polypeptide chain followed by intermolecular association under the influence of hydrophobic and covalent bonding when heated above their denaturation temperature. The microstructure of the microgels formed is dependent on the aqueous solution environment (protein concentration, pH, ionic strength, calcium concentration) and on the processing conditions (temperature, time, and shear-rate) (Oboroceanu *et al*., 2014).

Lazidis *et al.* (2016) found that when whey protein was heat denatured at pH higher or lower than the pI, fibrillar shaped aggregates were formed which appeared to be clear. However, when denaturation occurred close to the pI, the aggregates had a compact spherical shape that appeared opaque. Adjusting the pH of whey protein microgels also influenced the viscosity of a system. Adjustment from pH 5 to pH 8 led to an increase in viscosity which led to improved foam stability. Electrostatic interactions

are therefore important as they influence the structure of these aggregates (Lazidis *et al*., 2016). Murphy *et al*. (2016) found that pH influenced microgel size which in turn influenced their adsorption at the air/water interface. The microgels were found to get smaller with increasing pH from 5.7 to 5.9. Smaller microgels (pH 5.9) diffused and adsorbed at the interface more quickly creating more elastic interfaces than those produced at pH 5.7.

β-Lactoglobulin fibrils formed by heat treatment were found to be sufficient to form and stabilise foams in absence of other foaming agents (Peng *et al*., 2017). The foaming properties of the fibrils were also dependent on pH. Foamability of the fibrils was greater at pH 2 compared to pH 5, whereas foam stability was greater at pH 5 compared to pH 2. At pH 5, which is close to the isoelectric point of β-lactoglobulin, the good stability was due to the lower electrostatic repulsion of the protein molecules which led to increased solution viscosity (Peng *et al*., 2017).

Schmitt *et al*. (2014) also found that whey protein microgels foam ability was dependent on pH (in the range pH 3 – 7). The microgels had the best foaming properties (overrun and stability) at pH 5 compared to the other pH values. The neutral charge of the particles at pH 5 led to bulk self-aggregation that led to reduced drainage.

Dombrowski *et al*. (2016) found that with an increase in β-lactoglobulin aggregate size the foam stability increased. In comparison Rullier *et al*. (2008) found that foam ability and foam stability decreased with an increase in β-lactoglobulin aggregate size, as a longer time was needed for foam formation. It is evident that protein microgels are capable of stabilising foamed systems.

1.2 Protein Microgel Particles

Microgels are a class of deformable soft porous three-dimensional microscopic particles (Shewan and Stokes, 2013; Dickinson, 2017). Protein microgel networks consist of cross-linked protein molecules and their stable structure is due to the presence of covalent bonds and strong noncovalent interactions (Farjami and Madadlou, 2017; Le *et al*., 2017). The microgel structure has been described as ‘smart’ because their cross-linked network allows them to trap solvent within them and they can swell and de-swell reversibly in response to changes in the environmental conditions (e.g. temperature, pH or ionic strength) (Dickinson, 2017). This allows design of engineered particles with controllable and environment-responsive properties.

Most microgels have high water absorption and undergo swelling rather than being dissolved in an aqueous phase, due to the cross-linked nature of their internal structure (Farjami and Madadlou, 2017). The intrinsic characteristics of proteins such as amino acid content, protein concentration, hydrophobicity etc. impact the protein gel functional properties (gel strength, elasticity etc.) (Le *et al*., 2017). The microgel particles can be tuned to alter their composition, dimensions, shape and internal structure (Zhang *et al*., 2015a).

The morphology of the aggregates is affected by the type of protein and the conditions used during fabrication such as concentration, pH and ionic strength (Norton *et al*., 2015). Gels made from globular proteins are categorised as either fine stranded or particulate gels. Fine stranded gels are formed when protein solutions are heated at pH values far from the pI with low ionic strength. Heating globular proteins close to the pI and/or having high ionic strength results in particulate microgels (Le *et al*., 2017; Jones and McClements, 2010).

1.2.1 Fabrication Methods for Protein Microgels

There are several methods to produce microgel particles such as injection, homogenisation, coacervation and atomisation among many more. The following section will discuss some of the available methods.

1.2.1.1 Heat-Set and Cold-Set Gelation

Microgel particles can be made via heat-set or cold-set gelation. Fabrication of microgel particles usually involves unfolding of the native protein structure, which exposes its interactive sites such as thiol groups (Kuhn *et al*., 2010; Ko and Gunasekaran, 2006). The exposure of multiple functional groups could be exploited to create different interactions such as hydrogen bonding, hydrophobic interactions and electrostatic interactions (Chen *et al*., 2006). Protein molecules at high temperatures have a random coil conformation and when cooled below a critical temperature they cross-link with other protein molecules through hydrogen bonding.

For heat-set microgels, proteins are heated above their denaturation temperature under conditions that favour protein-protein interactions causing protein aggregation (Zhang *et al*., 2015a). For cold-set gelation, microgels are fabricated using a two-step

process. First, the proteins are heated under conditions that oppose protein-protein interactions. Secondly, the addition of salt or adjustment of the pH to the pI reduces the electrostatic repulsion between the protein molecules leading to protein aggregation (Bagheri *et al.*, 2014; Beaulieu *et al.*, 2002; Kuhn *et al*., 2010; Alting *et al*., 2000). The formed gels are held together by non-covalent cross-links (hydrophobic, hydrogen bonds) and/ or covalent interactions such as disulphide bonds (Le *et al*., 2017).

Calcium chloride is a popular divalent cation to add due to its ability to act as bridges between the negatively charged carboxylic groups on protein molecules (Kuhn *et al*., 2010). Stronger microgels are formed when they contain high cross-link density (Zhang *et al.*, 2015a). Cross-linking can yield microgels with modulated texture and tuned functional properties such as being indigestible in gastric conditions (Abaee *et al*., 2017).

1.2.1.2 Biopolymer Phase Separation

Electrostatic complexation and thermodynamic incompatibility are examples of biopolymer phase separation methods. To make microgels with electrostatic complexation, a solution using one or two biopolymers can be used (Shewan and Stokes, 2013). Coacervation is the separation of two liquid phases into one concentrated colloid phase, known as the coacervate and another dilute colloid phase (Shewan and Stokes, 2013). Using one biopolymer, simple coacervation occurs and the phase separation occurs due to changes with salt, pH or temperature (Shewan and Stokes, 2013). Complex coacervation involves a solution containing at least two biopolymers with opposite electrical charge (Joye *et al*., 2015). Biopolymers of opposite charge will interact with each other due to electrostatic attraction leading to biopolymer rich particles that are suspended in a biopolymer depleted aqueous phase. Depending on the strength of the attraction and the nature of the polymers, coacervation or precipitation may occur (Fig. 1.6). Cross-linking agents or temperature change can then be used to cause the biopolymers to gel, forming microgel particles (McClements, 2017a). Electrostatic complexation has been used to produce particles using sodium caseinate and sodium alginate (Liu *et al.*, 2018), pectin and β-lactoglobulin (Ron *et al*., 2010) or whey protein isolate with sugar beet pectin (Arroyo-Maya and McClements, 2015).

Thermodynamic incompatibility occurs when repulsive interactions occur between two polymers. The molecular origin is usually steric exclusion (Matalanis *et al*., 2011). The type of behaviour that occurs depends on the biopolymer composition,

biopolymer characteristics and the solution conditions (Matalanis *et al.*, 2010). At low biopolymer concentration, the two biopolymers are mixed and form a one-phase solution but when the biopolymers exceed a certain level, phase separation occurs to form two phases (Fig. 1.6). One phase is rich in one biopolymer and the other phase is rich in the second biopolymer (Matalanis *et al*., 2011).

In a study carried out by Matalanis *et al.* (2010), the authors used segregative and associative phase separation methods to form O/W/W emulsions. Firstly, a segregative phase was produced using sodium caseinate and pectin. This was followed by changing the pH of the system to form droplets through electrostatic attraction.

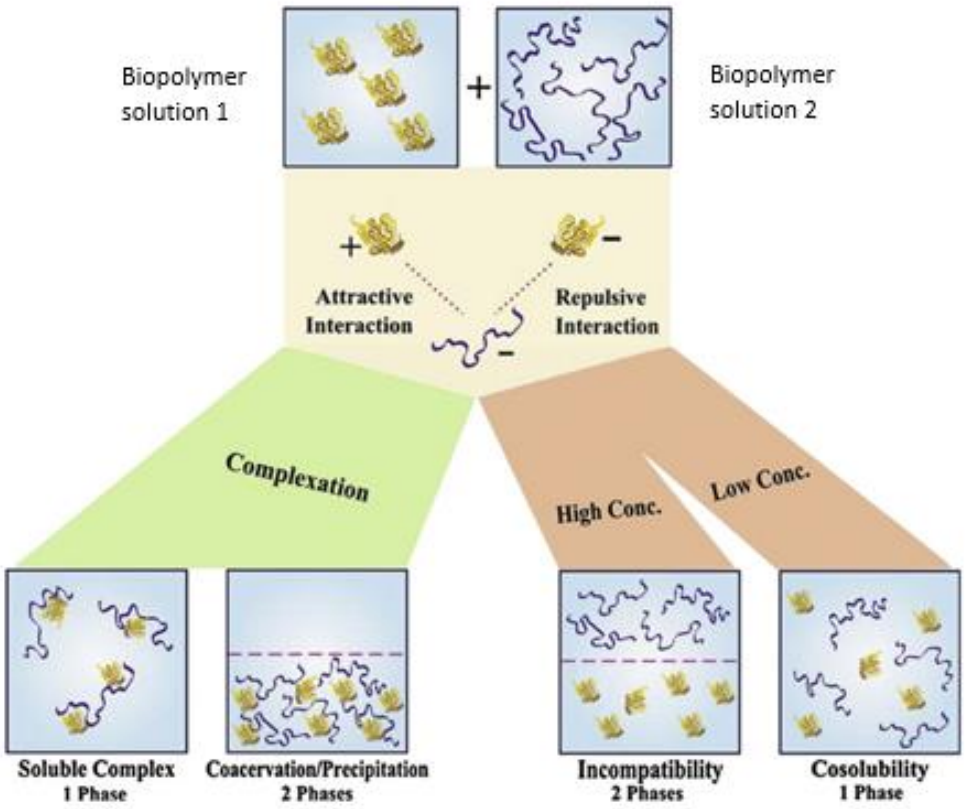

Fig. 1.6 Complexation and thermodynamic incompatibility due to mixing two biopolymers to form particles (Matalanis *et al*., 2011).

1.2.1.3 Antisolvent Precipitation

Anti-solvent precipitation is suitable to produce microgel particles from proteins. It is sometimes known as desolvation, drawing-out precipitation or solvent displacement (Joye and McClements, 2014). The biopolymer solution is known as the good solvent and

this is injected into an anti-solvent (McClements, 2017b). For hydrophobic biopolymers (e.g., zein or gliadin) an organic liquid (such as ethanol or acetone) is usually the solvent with water as the anti-solvent. For hydrophilic biopolymers (e.g. whey protein) the solvent is usually water and the anti-solvent is an organic liquid (McClements, 2017a).

Anti-solvent precipitation works by decreasing the quality of the solvent in which a biopolymer is dissolved. This leads to super saturation which causes solute precipitation (Kakran *et al*., 2012). The main driving force for precipitation is the imbalance of molecular interactions between the solvent and anti-solvent (Joye and McClements, 2014). To produce the particles the solvent and anti-solvent must be miscible over the concentration range at which they will be used (Joye and McClements, 2014). A major advantage of using the anti-solvent method is that it produces relatively small microgels (McClements, 2017a).

This method has been used to fabricate gliadin and zein nanoparticles (Davidov-Pardo *et al*., 2015), zein nanoparticles (Zou *et al*., 2016), protein and grape skin extract particles (Joye *et al*., 2015) and ovalbumin-pectin nanocomplexes (Xiang *et al*., 2020).

1.2.1.4 Injection Methods

A feature that is common amongst this group is that the solution is passed through a narrow orifice to form the particles. The biopolymer mixture is injected or forced through a nozzle into a hardening solution that promotes ion-gelation (Fig. 1.7) (Zhang *et al.*, 2015a). The injection tool can be a pipette, syringe, vibrating nozzle, jet cutter or atomising disk (Nedovic *et al*., 2011). The hardening solutions typically used for their production are glutaraldehyde (chemical), transglutaminase (enzyme), calcium chloride or tripolyphosphate (mineral ions). Alternatively, a change in temperature can also form particles by thermally setting the biopolymers (Farjami and Madadlou, 2017). The microgel particle size depends on the size of the nozzle, the solution viscosity, flow rate and the properties of the gelling environment (Joye and McClements, 2014).

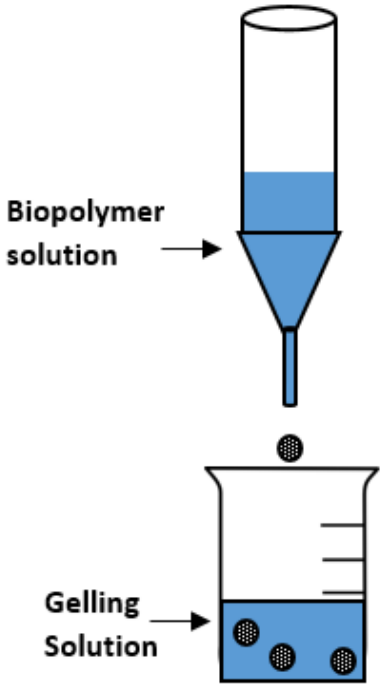

Fig. 1.7 Biopolymer microgels being formed using the injection method. The biopolymer is injected into a gelling solution.

Atomisation methods form large numbers of particles when the biopolymer solution is passed through the nozzle. Spray drying and spray chilling are the most common atomisation methods for producing microgel particles. They are commonly used due to the convenience and shelf-life stability of the dried product (Augustin and Hemar, 2009). For spray drying the biopolymer is dissolved in a suitable solvent that has a low viscosity so that it can be pumped through the nozzle. This solvent is evaporated when heated in the chamber. The biopolymer rich product is then collected from the orifice. The particles are typically of dimensions around 10-100 μm (Zhang *et al.*, 2015a). Operating spray driers are typically heated to temperatures between 150 and 300 °C. This method is often used to dry ingredients that are sensitive to heat, as thermal damage is minimised due to the high surface to volume ratio that allows for rapid drying (Matalanis *et al*., 2011).

Spray cooling involves the same process however instead of heating the chamber, it is cooled. When the biopolymer is passed through the heated nozzle cool air is used to solidify the droplets into microgels (Shewan and Stokes, 2013). These particles can then be collected by centrifugal forces or filtration (Zhang *et al.*, 2015a).

1.2.1.5 Emulsion Based Methods

Emulsion templating begins by homogenising a biopolymer to an oil phase to create a water-in-oil emulsion. Biopolymer rich water droplets are suspended in oil. By varying the homogenisation conditions or the solution composition the size of the water droplets can be controlled (Matalanis *et al*., 2011). When the conditions (pH or temperature) of the system are altered the biopolymer molecules within the water droplet gel (McClements, 2017a). Chemical cross-linking agents can also be added to the system, they diffuse through the oil phase and into the water droplets causing the biopolymers to cross-link. Commonly used gelling agents are calcium, magnesium, barium, copper and zinc ions (Joye and McClements, 2014). The microgel beads can then be removed from the oil phase once they are formed via centrifugation, filtering or solvent extraction (McClements, 2017a; Matalanis *et al*., 2011). WPI microcapsules were formed using this process (Sağlam *et al.*, 2014; Betz *et al.*, 2012) and an oil-in-water-in-oil whey protein emulsion was prepared (Sung *et al*., 2015).

1.2.2 Microgel Characteristics

The functional properties of microgels within food structures depends on the particles structure, electrical charge and physicochemical properties.

1.2.2.1 Microgel Structure

Microgel composition can be controlled by the appropriate selection of ingredients and processing technique (McClements and Xiao, 2012). Particle size is an important characteristic of biopolymer-based delivery systems (Joye and McClements, 2014). The particles can range in size from a few hundred nanometers to a few millimetres due to different starting materials and fabrication methods. Their dimensions influence the mouthfeel of a food product; if they are > 50 μm they can be perceived as separate particles by the human mouth as it will present a grainy rather than smooth texture. Microgel shape also affects the mouthfeel of a product (McClements, 2017b). Particles below 100 μm appear homogenous to the human eye, however, particles above 100 μm appear as discrete particles (McClements, 2017a). Particles can be formed with different sizes and morphologies depending on the pH, ionic strength and type of salt and protein concentration (Kharlamova *et al*., 2018). A gel's appearance is a good indicator of the

network formed by the protein molecules. Translucent gels are formed by an ordered structure while opaque gels are formed due to larger and random aggregated particles (Kuhn *et al*., 2010; Hongsprabhas and Barbut, 1997).

Cross-linking has been found to influence particle size. Cross-linking whey protein with transglutaminase almost halved the size of the particles from 155 to 81 nm, while cross-linking with citric acid only reduced the particle size from 155 to 143 nm (Bagheri *et al*., 2014). Abaee *et al*. (2017) found that cross-linking whey protein cold-set hydrogels with citric acid at various pH values influenced particle size. The particle size at pH 9 was larger than the particles formed at pH 7 (297 vs. 127 nm). The authors suggested that at pH 9, the protein structure is more unfolded than at pH 7, resulting in more reactive sites accessible for cross-linking with citric acid.

The diameter of whey protein particles was found to be dependent on pH. Arroyo-Maya and McClements (2015) found that at pH 4 the smallest particles were formed (< 200 nm) and the particle size increased to 250 – 260 nm above this pH value (Schmitt *et al*., 2014). However, when the pH was adjusted to 4 – 5.5, larger particles were formed with a diameter of 5.5 µm. The authors suggest that the larger particle size at this pH range was likely to correspond to the aggregation at this pH as it is in close proximity to the isoelectric point of whey protein (Schmitt *et al*., 2014).

For an emulsification/cold-set gelation process of whey protein beads, $CaCl_2$ concentration had an effect on both size and particle appearance (Beaulieu *et al*., 2002). An emulsion was firstly prepared followed by gelation using $CaCl_2$. With an increase in concentration from 10 to 20 % $CaCl_2$, the particle size decreased from 2.1 to 1.8 mm. At lower salt concentrations Hongsprabhas and Barbut (1997) found that increasing $CaCl_2$ concentration from 10 mM to 120 mM increased the size of whey protein particles.

Microgel shape can vary between spherical, ellipsoidal or fibrous and this has an impact on its functional attributes (McClements, 2017a). WPI particles made via emulsion templating at different pH values created differently shaped particles with different pore sizes (Fig. 1.8) (Sağlam *et al*., 2014). At pH 5.5, the particles made were irregularly shaped with an uneven distribution of large pores; whereas at pH 6.8 the particles were spherical, smoother and had more evenly distributed smaller pores (Sağlam *et al*., 2014). The authors suggested that at pH 5.5 the irregular shapes were caused by a heating step which caused the particles to shrink.

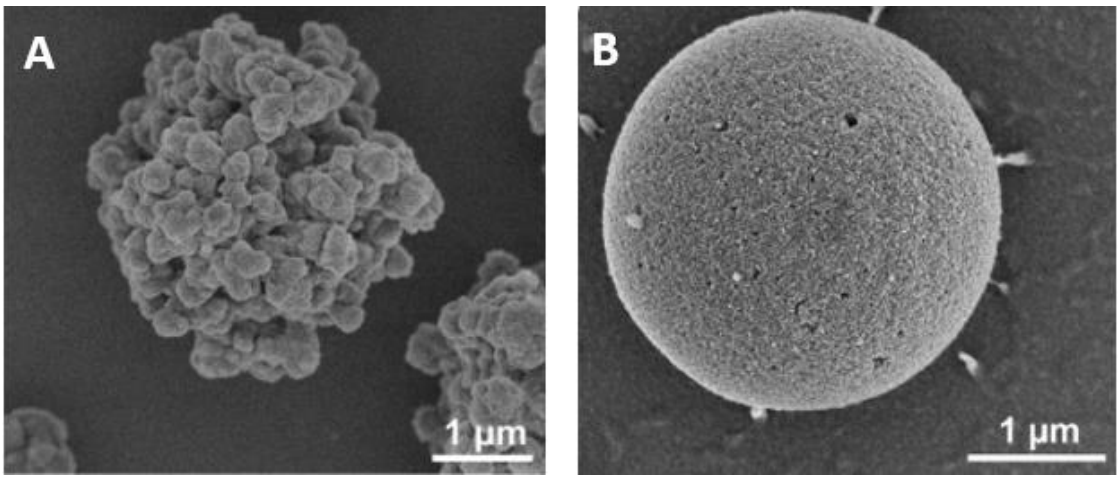

Fig. 1.8 Effect of pH on the microstructure of whey protein particles observed by SEM. 25 % whey protein solution prepared at pH 5.5 (A) and pH 6.8 (B) (Sağlam *et al*., 2014).

At pH 7.2 using a double emulsion technique, Je Lee and Rosenberg (2000) produced microcapsules from whey protein isolate and anhydrous milk fat, finding that the particles varied in size (10-100 µm) with a smooth dent-free outer surface. These particles also contained some spherical surface pores (0.2 – 0.4 µm). In contrast, at pH 4.5 or 5.5, the particles were extremely porous, wrinkled and presented many irregularities indicating aggregation of protein matrices instead of the formation of a continuous film. The internal structure of the particles at pH 7.2 was not connected through channels or pores to the outer surface while the particles produced at the lower pH (4.5 or 5.5) contained large aggregated proteins separated by voids of various sizes (Je Lee and Rosenberg, 2000).

Increasing the calcium chloride concentration when preparing microgels using the cold-set gelation method was found to form more regular shaped particles. Beaulieu *et al*. (2002) suggested that the increase in sphericity of the particles was due to the increased kinetic mechanism of gelation with increased calcium chloride concentration. Over a period of 3.5 h using a concentration of 10 mM $CaCl_2$, whey protein particles with evenly dispersed small pores were formed, however, after 6.5 h the particle size and pore size increased (Hongsprabhas and Barbut, 1997). This indicated that over time, $CaCl_2$ was changing the microstructure of the gels.

The morphology of protein particles was found to change with the addition of copolymers. Davidov-Pardo *et al*. (2015) formed biopolymer particles using zein and gliadin in the absence or presence of copolymers of pectin or sodium caseinate. Tightly

packed spherical particles were formed from zein (Fig. 1.9), and when coated with sodium caseinate they remained spherical however, the sodium caseinate was in excess which resulted in a clumpy surface (Davidov-Pardo *et al*., 2015). Bare gliadin particles produced clusters which were joined together but still distinguishable. When coated with pectin, the clusters formed into single particles that were spherical in shape but of varying sizes. The particles were held together by a net-like structure (Davidov-Pardo *et al*., 2015). Pectin addition to gliadin also affected the particle structure. This indicates that copolymer addition affects microgel morphology.

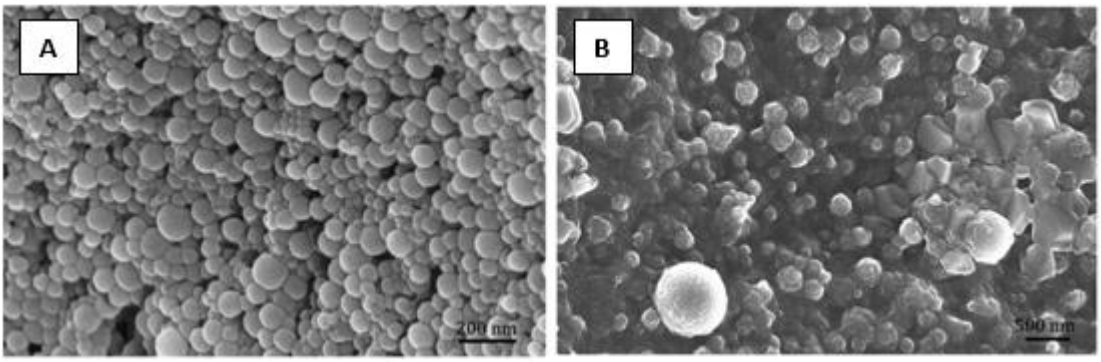

Fig. 1.9 SEM images of bare zein (A) and sodium caseinate coated zein (B) (Davidov-Pardo *et al*., 2015).

1.2.2.2 Electrical Characteristics

The electrical properties of microgels have an important job in determining physicochemical properties, stability, and functional performance. Microgels are exposed to different pH conditions when present in foods as well as inside the human gut when ingested. Therefore, it is useful to establish the impact of pH on microgel properties (Su *et al*., 2019).

The electrical characteristics include the ionisable groups on the biopolymer molecules as well as any associated ionic species (e.g. mineral ions) (McClements, 2017a). The surface potential of the microgel particles determines its overall electrical properties which depends on the nature of the charged molecules at their surfaces. Particles can be highly positive or negative depending on their composition. The electrical charge on the particles influences whether the particles will aggregate or remain separated. Interactions with other ingredients in food products are also influenced by

particle charge, as an electrostatic complex may form if another ionic ingredient is present (Matalanis *et al*., 2011).

By measuring the change in ζ-potential with pH the surface potential can be characterised. It is important to ensure that the ζ-potential of the microgels exceeds a value (± 30 mV) to ensure that the electrostatic repulsion is stronger than any attractive interactions such as van der Waals, electrostatic, hydrophobic or depletion to prevent aggregation between microgel particles. Therefore when two compounds are mixed together to form particles or complexes, the opposite surface charge of two compounds is important (Yangchao Luo *et al*., 2011).

The ζ-potential of native WPI, WPI aggregates and WPI microgels were analysed by Yang *et al.* (2019). The authors found that the ζ-potential of the samples increased with a change in protein form from the native to the aggregated state followed by the microgel state. The loss of positively charged groups of the aggregates' and microgels' surface was due to the positive charged groups being buried within the hydrophobic regions upon aggregation, and thus increased negative charge (Yang *et al*., 2019)

Colloidal stability of whey protein microgels was explained due to the ζ -potential values of ± 20 mV at pH far from the protein pI, whereas when the pH was close to the pI, the ζ -potential dropped. At this point, colloidal stability was lost and aggregation of the microgels occurred (Schmitt *et al*., 2014).

The overall electrical charge of microgels might be different from the biopolymers used to fabricate them. Also, by coating particles with a layer of charged biopolymers, their functional attributes can be changed. Davidov-Pardo *et al*. (2015) coated zein and gliadin particles with sodium caseinate and pectin at different pH due to the different charge and stability characteristics of the hydrophilic copolymers. With increasing pectin and zein concentration, the ζ -potential of the particles went from positive to increasingly negative.

Deshmukh *et al.* (2015) suggested that microgels do not need to carry much electrical charge to be stable, as they can deform in the bulk or at the interface. The particles can stretch out when the surface coverage is low, whereas when the microgels are in high concentration, they come in contact with each other and less stretching occurs, however the interface is still covered (Deshmukh *et al*., 2015).

1.2.2.3 Rheological Properties

Microgels possess the rheological properties of both polymer solutions and solid-sphere suspensions (Shewan and Stokes, 2013). The amount and strength of cross-links between biopolymer molecules affects the rheological properties of microgels (McClements, 2017a). Like any colloid, the rheology and viscosity is controlled by the interactions between particles and the resulting network (Shewan and Stokes, 2013). The viscosity of the biopolymer suspension increases with increasing biopolymer concentration. When biopolymer particles entrap more solvent within their network they increase the viscosity of the system (Jones and McClements, 2010). Rheological measurements of protein gels are classified by small or large strain measurements. Small strain techniques non-destructively measure rheological properties, while large strain techniques tend to destroy or fracture the sample (Li *et al*., 1999).

The rheological properties of protein gels are influenced by the network structure and interactions within the structure (Li *et al*., 1999). The functional attributes of microgels are influenced by their rheological properties. Incorporating microgels into food products would require the final product to have the desired textural and flow properties (McClements, 2017a). It is desirable for some foods to have low viscosity e.g. beverages while other foods require high viscosity such as dressings or dips (Jones and McClements, 2010). It is beneficial to understand the rheological properties of microgels because it helps to determine their stability during storage and transportation and finally their tendency to breakdown when exposed to mechanical forces (McClements, 2017a).

Microgel suspensions are attractive in the food industry as their rheology can be controlled by varying composition, the cross-link density, particle size, shape and surface properties to meet the requirements for applications (Stokes, 2011). By altering the environmental conditions such as pH, temperature or ions, it can cause the microgels to swell or deswell which allows a higher phase volume to be obtained compared to hard spheres of equal size (Stokes, 2011; Shewan and Stokes, 2013).

1.2.3 Encapsulation

Microgels are known for their capability to stabilise foamed systems, however, microgels are also popular for their ability to entrap and protect substances within their cross-linked network. Encapsulation is a process that entraps one substance (active agent) within another substance (wall material). The substance being encapsulated is also known

as the core, active, bioactive, or internal. The substance that encapsulates is sometimes called the wall material, coating, shell, capsule, external phase or matrix (Nedovic *et al*., 2011). The wall material should not react with the core and be capable of retaining the core within the particle, protect the core from environmental conditions, be edible, non-toxic, economically available and also be capable of promoting bioactive bioavailability by releasing bioactive components upon digestion (Dhakal and He, 2020)

Encapsulation has been used to entrap, protect, and deliver sensitive components while improving the sensory properties of foods. Substances are encapsulated because they are susceptible to environmental, processing or gastrointestinal conditions (Nedovic *et al*., 2011). Encapsulation of compounds is also needed to mask unpleasant tastes, convert a liquid to a solid or powder, improve the effectiveness of the compound, broaden the application range, ensure the optimal dosage, control of the release properties, improve the heat stability, protect unstable and volatile compounds, or to prolong shelf life (Gouin, 2004; Zagury *et al*., 2021; Zhang *et al*., 2015b; Torres *et al*., 2016; Diarrassouba *et al*., 2015; Luo *et al*., 2012 & Teng *et al*., 2013). A range of substances can be used to encapsulate compounds and to be good carriers they must be of food-grade, be biodegradable and capable of forming a barrier between the internal phase and the surrounding conditions. Examples include starches, plant exudates, proteins and lipids (Nedovic *et al*., 2011; Abbasi *et al*., 2014; Luo *et al*., 2012; Zhang *et al*., 2020; Ozturk *et al*., 2015; Mitbumrung *et al*., 2019)

For this review, protein particle systems will be focused on. Milk proteins are the most common proteins used as encapsulating materials i.e., casein, whey protein, β-lactoglobulin, lactoferrin etc., and vegetable proteins such as soy, zein and gliadin. Protein-based particle systems can encapsulate both hydrophilic and hydrophobic substances (Dima *et al*., 2020). Proteins' functional properties, such as solubility, gel formation, emulsification, or digestibility, are related to their structure. This makes it easy to modify proteins functional properties either chemically or physically (Sobhaninia *et al*., 2018). Whey proteins are suitable for encapsulating heat-sensitive nutraceuticals due to their ability to form cold-set hydrogels and they are also completely biodegradable (Abaee *et al*., 2017; Gunasekaran *et al*., 2007; O'Neill *et al*., 2015). Whey proteins have surface-active properties, antioxidant properties, high tensile and low oxygen permeability and wide availability making them suitable for encapsulating compounds (Khan *et al*., 2020). Proteins are also useful as they are easily digested within the gastrointestinal tract of humans for the release of bioactive compounds (Joye and McClements, 2014).

1.2.3.1 Retention and release properties

There are two main mechanisms in the retention of bioactive agents within microgels; pore size and specific interactions (Zhang *et al.*, 2015a). The presence of pores within microgels is of importance as they will impact the retention, protection, and release of bioactives from the particle (Fig. 1.10). Pore sizes in microgels are typically between 5 – 500 nm depending on the degree of cross-linking, pH, or temperature. If the molecule being encapsulated is larger than the pore size then it will be retained within the particle, however, if it is smaller, the molecule can be easily released (Zhang *et al.*, 2015a). If this occurs the bioactive is susceptible to chemical degradation as chemicals can diffuse into the microgels (McClements, 2017b). Retention of the bioactive therefore depends on the conditions used to fabricate the microgels.

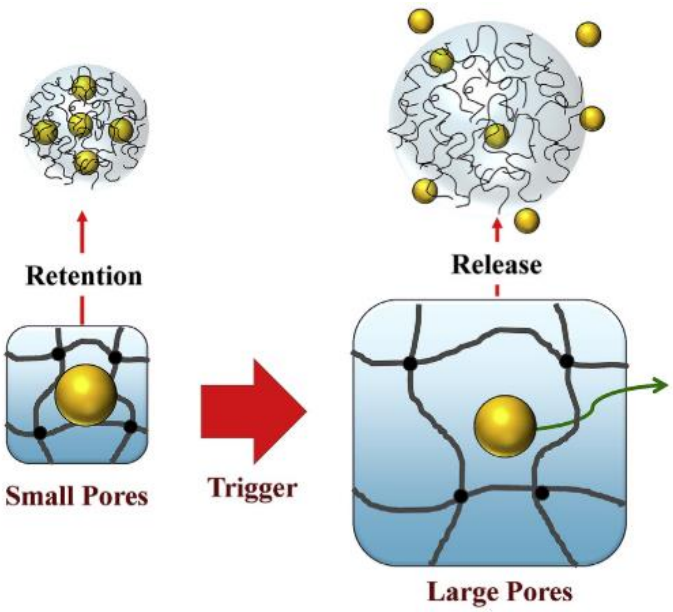

Fig. 1.10 Bioactive agent will be retained within the microgel particle if their dimensions are larger than the pores, whereas they will be released if they are smaller than the pores (McClements, 2017b)**.**

It is popular to engineer the particles to retain bioactives due to attractive and repulsive interactions. The molecule being encapsulated will be retained well if there is a strong attraction between the molecule and wall material (McClements, 2017b). Therefore, particles with large pores can still retain bioactives within their structure if

there is an attractive interaction. The presence of covalent and non-covalent interactions (e.g., van der Waals, hydrogen bonding, hydrophobic interactions) can help to retain bioactives within their core.

The main purpose of encapsulation is to protect bioactive agents from harmful environmental conditions, however, this is meaningless if the bioactive cannot be released from the particle at the desired site or time (Dhakal and He, 2020). The release of a bioactive compound from a microgel is determined by the bioactive location and its interaction with the microgel network (Zhang *et al.*, 2015a). The concentration of the encapsulated compound and the transport rate also affect release (Matalanis *et al*., 2011). The bioactive can also be released by increasing the ionic strength which weakens the attractive electrostatic interactions through screening effects (McClements, 2017a). The active substance can be released from the microgel by simple diffusion through the pores.

It can occur that the active substance is evenly distributed throughout the particles and is not strongly attracted or repelled by the biopolymer network (McClements, 2017a). In this circumstance, the main factors which influence the rate of release are the dimensions of the active substance, the pore size of the microgel, its shape and structure and the viscosity of the solvent. The extent to which the bioactive is released increases when the dimensions of the bioactive itself are decreased and the pore size of the microgel is increased. The bioactive may interact strongly with the biopolymer network through electrostatic, hydrophobic or hydrogen bonding (McClements, 2017a). However, once the conditions are altered (pH, ionic strength) and the charges on the molecules become similar, the bioactive can be released (Matalanis *et al*., 2011).

When particles absorb solvent they swell increasing the pore size of the biopolymer network which could release the encapsulated compound (Matalanis *et al*., 2011). The small pore sizes can also swell due to environmental changes such as pH or ionic strength (McClements, 2017a). Therefore, creating pH- or ionic- induced triggered release of bioactive substances can be used to control the swelling of the microgel. For example, the particles can be fabricated so that they release the compounds at the desired site e.g. small intestine for uptake into the body (Ray *et al.*, 2016; Winuprasith *et al.*, 2018; O'Neill *et al.*, 2015).

Release from particles can also occur due to degradation of the biopolymer network which may occur due to surface or bulk erosion, fragmentation, weakening of cross-links or chemical breakdown of the biopolymers (Zhang *et al.*, 2015a). When the microgel encounters specific environmental conditions, it can lead to the release of the bioactive agent. It occurs usually due to physical (e.g. high temperature), chemical (e.g.

acids or bases) or enzymatic (e.g. lipases etc.) mechanisms (McClements, 2017a; Zhang *et al*., 2015a). For microgels intended for human consumption, breakdown usually happens due to exposure to compounds present in the stomach and small intestine such as proteases or saliva. These mechanisms will be discussed in more detail in section 1.2.3.2.

1.2.3.2 Gastrointestinal fate of bioactive loaded protein microgels

It is necessary to consider the complex physiology of the human gastrointestinal tract (GIT) when designing delivery systems for bioactive agents (Cook *et al*., 2012). Most proteins are easily digested within the human GIT which is essential for the eventual release of the bioactives after ingestion (Joye and McClements, 2014). The bioactive agent should be retained within the microgel for one set of environmental conditions but released from the particles under a different set of environmental conditions. Alterations in pH, ionic strength or temperature trigger changes in the surface charge and hydrophobicity of protein particles, deeming them sensitive delivery systems (Joye and McClements, 2014).

In the oral stage, the particles after ingestion are exposed to several changes. They are mixed with saliva, exposed to pH change, ionic conditions, change in temperature, digestive enzymes and interact with surfaces in the mouth (McClements and Xiao, 2012). In the stomach the food bolus containing the microgel particles is exposed to acidic conditions and is mixed with enzymes, surface active substances and experiences a flow/force profile (McClements & Xiao, 2012). Food is physically digested into a thick semifluid mass known as chyme which is then transferred to the duodenum (Bao *et al*., 2019). In some cases it is desirable to retain and protect bioactives within the stomach phase, however, in other cases it is desirable to release bioactives in the stomach (Zhang *et al*., 2015a).

Bioactive compounds are usually absorbed in the small intestine where they cross the epithelial cell layer (Bao *et al*., 2019). After entering the small intestine, particles are mixed with alkaline digestive juices which contain bile salts, phospholipids, pancreatic lipase, colipase and bicarbonate that brings the pH to almost neutral (McClements and Xiao, 2012). The combined effect of proteases (trypsin, chymotrypsin and elastase) present in pancreatin catalyse the hydrolysis of peptide bonds leading to protein degradation (Beaulieu *et al*., 2002). The various proteases work differently to degrade protein. Trypsin works on the peptide links that involve the carboxylic groups of lysine

and arginine, hydrophobic residues preceding the scissile peptide bond are attacked by chymotrypsin and elastase is specific to small neutral residues (Beaulieu *et al*., 2002).

Several studies have used particle systems to protect bioactive compounds under gastric conditions while allowing release under intestinal conditions, for example whey protein microgels containing retinol (Beaulieu *et al*., 2002), β-lactoglobulin nanoparticles containing riboflavin (Madalena *et al.*, 2016), carboxymethyl chitosan-soy protein nanoparticles containing vitamin D (Teng *et al*., 2013; Khan *et al*., 2020 and Zhang *et al.*, 2020), ovalbumin-pectin containing vitamin D (Xiang *et al*., 2020), β-lactoglobulin-lysozyme complexes protecting vitamin D (Diarrassouba *et al*., 2015), β-lactoglobulin micro- and nanospheres containing riboflavin and quercetin (Simoes *et al*., 2020).

1.2.3.3 Applications

Today, foods are not just needed for human life, but they have become crucial to prevent and treat chronic illnesses. Designing foods is a complex process which involves the consumer, doctors, technologists, biologists, economists and sociologists (Dima *et al*., 2020). Below is a list of examples of bioactive substances which have been encapsulated using particles due to their sensitivity to environmental conditions.

1.2.3.3.1 Vitamins

Vitamins play a vital role in human life, they regulate metabolic and cellular functions, promote health, reproduction and growth while also preventing illness. Vitamins are sensitive molecules and are susceptible to chemical and physical factors and should therefore be preserved from harmful agents like heat, light, pH and oxygen to prevent nutrient losses (Katouzian and Jafari, 2016; Dhakal and He, 2020).

Riboflavin, also known as vitamin B_2, is known for its antioxidant, anti-aging, anti-inflammatory and anti-cancer properties. Riboflavin is highly photosensitive and has low solubility in water (Djoullah and Saurel, 2021). Riboflavin was successfully encapsulated and protected within whey protein microgels via hydrophobic interaction (O'Neill *et al*., 2014; Egan *et al.*, 2014)

Vitamin C has a wide range of pharmacological properties such as anti-aging, anti-oxidation and anti-cancer. However, its stability is low and most of its functionality is lost during food processing or storage due to exposure to envionmental conditions such

as pH, light, heat and oxygen (Peng *et al*., 2016). A novel vitamin C loaded nano hydrogel was fabricated by self-assembly which consisted of citrus peel pectin and bovine serum albumin to overcome the instability of vitamin C and the authors suggested that the ordered three-dimensional and porous network of the structures were responsible for vitamin C encapsulation (Peng *et al*., 2016).

Vitamin D, a fat-soluble vitamin, plays an important role in the human body as it helps with the absorption of calcium and phosphorous, thereby helping to develop and maintain a healthy skeleton for humans (Mitbumrung *et al*., 2019; Wimalawansa, 2018). Fortifying foods with vitamin D is challenging due to the fat-soluble nature of vitamin D as it has low water solubility and it is sensitive to oxidation and UV light (Kiani *et al*., 2017). Several studies have successfully encapsulated vitamin D_3 using whey protein (Liu *et al.*, 2020a), β-lactoglobulin (Ron *et al*., 2010;Diarrassouba *et al*., 2015), soy protein (Khan *et al*., 2020), zein (Yangchao Luo *et al.*, 2011), ovalbumin (Xiang *et al*., 2020), potato protein (David and Livney, 2016) among more.

Vitamin E is the main fat-soluble dietary antioxidant and comprises a family of tocopherols and tocotrienols (Damodaran *et al*., 2007). Vitamin E has poor solubility in water and is unstable when exposed to environmental factors such as light, heat and oxygen (Luo *et al.*, 2011). Tocopherols are the main compounds having vitamin E activity in food and α-tocopherol has the highest biological activity (Damodaran *et al.*, 2007). α-Tocopherol has been encapsulated using zein/chitosan based nanoparticles; electrostatic interactions, hydrogen bonds and hydrophobic interactions were responsible for the complex formation between α-tocopherol, zein and chitosan (Luo *et al*., 2011). Yin *et al*. (2020) encapsulated α-tocopherol within whey protein particles and found that the percentage of α-tocopherol encapsulated increased with increasing protein concentration. The authors suggested that α-tocopherol got bound to the internal cavity and surface hydrophobic pocket of β-lactoglobulin.

Carotenoids contribute significant vitamin A activity to foods of animal and plant origin (Damodaran *et al.*, 2007). β-Carotene is a member of the carotenoid family with strong antioxident capacity and high provitamin A activity (Liu *et al.*, 2018). β-Carotene is highly susceptible to chemical degradation when exposed to light, heat or oxygen due to the large number of conjugated double bonds found in its structure. Caseinate- alginate microparticles were used to encapsulate and improve the stability and bioaccessibility of β-carotene (Liu *et al.*, 2018).

1.2.3.3.2 Phenolic compounds

Resveratrol is a polyphenol extracted from grape skins, it has poor water solubility, poor UV stability and low oral bioavailability. For this reason, Davidov-Pardo *et al*. (2015) analysed the encapsulation ability of zein or gliadin particles uncoated or coated with pectin or sodium caseinate. Coating with copolymers increased the encapsulation efficiency of both particles.

Curcumin has extremely low water solubility, about 11 ng/ml which makes it difficult to incorporate into food (Alavi et al., 2018a). Curcumin has been encapsulated within whey protein aggregates mixed with k-carrageenan (Alavi et al., 2018a), zein-carrageenan nanoparticles (Chen *et al*., 2020) and lysozyme-carrageenan nanoparticles (Huang *et al*., 2020). Curcumin was found to bind to the hydrophobic regions of the protein complexes which protected the chemically reactive groups of the phenol from environmental conditions such as light and heat.

Epigallocatechin gallate (EGCG) is a polyphenol found in tea that has strong medicinal and therapeutic values (Liang *et al*., 2017). However, EGCG is oxidised easily by high temperatures, oxygen and pH and therefore needs protection against degradation. Liang *et al*. (2017) used zein-chitosan nanoparticles to analyse their ability to enhance EGCG stability. Electrostatic interactions and hydrogen bonds were responsible for the interaction between EGCG with zein-chitosan complexes.

Anthocyanins are found in fruits and vegetables which has been linked to the prevention of heart disease, cancer and inflammation (Arroyo-Maya and McClements, 2015). Arroyo-Maya and McClements (2015) encapsulated anthocyanin within whey protein/ beet pectin nanoparticles due to their poor chemical structure causing stability issues. Nascimento *et al.* (2020) assessed the capability of casein hydrogels for the encapsulation and release of jaboticaba extract. Jaboticaba is a fruit high in polyphenols with elevated levels of anthocyanin. The authors found that hydrogels cross-linked with transglutaminase formed a denser more compact protein structure, protecting jaboticaba (Nascimento *et al*., 2020).

Quercetin a natural flavonoid has been found to be beneficial for human health including anti-oxidation, anti-inflammatory, anti-cancer, anti-diabetic, and anti-atherosclerosis properties (Liu *et al.*, 2020b). However, due to its low solubility in water it is necessary to develop a delivery system to improve its solubility. Liu *et al.* (2020b) encapsulated quercetin in whey protein coated by lotus root amylopectin hydrogels and found that the hydrogels could protect the active groups on the C ring of encapsulated quercetin (Liu *et al*., 2020b).

1.3 Scope of thesis

Many foam products suffer from destabilisation mechanisms such as drainage, coalescence, and coarsening. Studies have indicated that proteins are capable of forming and stabilising foams which can be manipulated by altering the environmental conditions such as protein concentration, whipping time, pH, ionic strength, heat, addition of sucrose or a polysaccharide such as xanthan gum. However, protein microgels have also been reported to have a positive impact on foaming which can lead to foams remaining stable for months compared to several hours or days for native protein foams. The microgels are capable of residing at the air/water interface or remaining in the bulk continuous phase improving foam stability. It has been reported that the stabilising capability of microgels is in some way dependent on particle size, electrical characteristics, and rheological properties.

Another functionality of microgels is their ability to entrap and protect sensitive compounds within their cross-linked biopolymer network and act as oral delivery systems. The development of edible delivery systems is important to improve the stability of active materials during storage and enhance bioavailability. Cold-set gelation is a suitable method for heat labile compounds as it comprises the active material being added to the cooled solution of pre- heat-denatured proteins. Previous studies have indicated that microgel structures can vary in size and morphology depending on the type of salt, ionic strength, pH or protein concentration used.

The aim of this project is to obtain an understanding of the conditions necessary to form and stabilise protein foams and more specifically whey protein foams and to use this understanding to better control foaming behaviour based on foam overrun and stability. The WPI microgels will be formed using cold-set gelation and their properties will be characterised to determine the ability of the microgels to form and stabilise foams for prolonged periods. The use of whey protein microgels is also used to encapsulate and protect vitamin D_3, as vitamin D is sensitive to food processing conditions such as light, heat, oxygen and low pH. The release of vitamin D_3 from the microgels is monitored using a standardised *in vitro* digestion model to establish if the microgels can protect and release vitamin D_3 at the correct site of action. The vitamin D_3 loaded microgels are analysed for their ability to form and stabilise foams when exposed to several environmental conditions commonly used in the food industry. The microgels capacity to protect vitamin D_3 from environmental conditions followed by mechanical whipping is also investigated. The vitamin D_3 loaded microgels will be incorporated into a model food

system, in this case ice cream, to act as a delivery vehicle for vitamin D_3. Evaluation will be carried out on the effect of microgels on ice cream properties, vitamin D_3 stability within the food product followed by monitoring VD_3 release using a standardised *in vitro* digestion model.

Chapter 2
Materials and Methods

2.1 Materials

Whey protein isolate (WPI) (BiPRO 97.8% w/w total protein) was purchased from Agropur Inc. (Le Sueur, MN, USA). Sodium chloride (NaCl), calcium chloride ($CaCl_2$), sodium azide, cholecalciferol, sodium cacodylate and glutaraldehyde were purchased from Lennox (Dublin, Ireland). Xanthan gum (XG) from *Xanthomonas campestris*, 8-anilinonaphthalene-1-sulfonic acid (ANS), 5,5-dithiobis (2-nitrobenzoic acid) (DTNB, Ellman's Reagent), absolute ethanol (EtOH), hydrochloric acid (HCl), sodium hydroxide (NaOH), α-amylase, porcine pepsin, porcine pancreatin and bovine bile were purchased from Sigma-Aldrich (Wicklow, Ireland). SeeBlue Plus2 pre-stained protein standard and MES SDS running buffer, InstantBlue Coomassie Stain, dialysis tubing (10 kDa molecular cut off) and dialysis clips purchased from ThermoFisher Scientific (Dublin, Ireland). Ice cream ingredients: milk, cream, eggs, sugar, vanilla extract were purchased from a local supermarket (Tesco, Ireland).

2.2 Methods

2.2.1 Whey protein

2.2.1.1 Whey protein isolate solution preparation

Whey protein isolate was prepared by dissolving the powder in deionised water at room temperature using a magnetic stirrer to make a 10 % w/w protein solution at pH 6.8, unless stated otherwise. Sodium azide was added (0.02 %) to prevent microbial growth. The rehydrated samples were kept in the refrigerator overnight at 4 ºC to fully hydrate.

2.2.1.2 Surface Tension

The surface tension of the WPI solutions was measured using a drop shape analysis method (Drop Shape Analysis, KRÜSS G10 system, Hamburg, Germany). Using a syringe (1.8 mm diameter), 1 mL of each sample was collected and used for analysis. The syringe was placed in the syringe holder. Each drop was left to equilibrate for 3 min before the reading was taken. The surface tension was calculated using the Young-Laplace equation using the DSA version 1.65.0.7 software (KRÜSS G10 system).

Laplace Equation $\Delta P = \frac{2\gamma}{r}$ Eq 2.1

Where:

ΔP = pressure difference

γ = surface tension

r = radius of the air bubbles

2.2.1.3 ζ-potential

The ζ-potential of WPI solutions was determined between pH 3 and 7 at 25 °C by dynamic light scattering (Nanotrac Wave II, Microtrac, Germany). Samples were diluted to a concentration of approximately 0.1 % (w/w) to avoid multiple scattering effects.

2.2.1.4 Particle size

The hydrodynamic diameter of whey protein aggregates formed after being subjected to heat treatment were measured by dynamic light scattering (Nanotrac Wave II, Microtrac, Germany). The solutions were diluted (1:20) to prevent multiple scattering effects. Equilibrium time before measurement start was set to 1 min.

2.2.2 Microgels

2.2.2.1 Preparation of whey protein isolate microgels

Whey protein isolate solutions were prepared according to section 2.2.1.1. Cold-set gelation was used to create the microgels. The protein solution was pre-heated in a water bath at 80 ℃ for 30 min followed by cooling on ice to room temperature. Calcium chloride was used to cross-link the denatured protein samples to form microgels. To establish the optimum method of manufacture, a number of procedures were trialled:

A. 20 – 100 µL of denatured whey protein isolate was pipetted into 0.1 M $CaCl_2$ solution.
B. Denatured WPI was submerged in 0.1 M $CaCl_2$ solution.
C. Denatured WPI was dispensed through a 100 µL pipette tip using a peristaltic pump (MasterFlex, Console Drive, Cole-Parmer, UK) into 0.1 M $CaCl_2$ solution.

D. $CaCl_2$ at concentrations of 0.02, 0.05 and 0.1 M was added to the denatured WPI solution. The solution was thoroughly mixed using a pin stirrer.

All samples when placed in $CaCl_2$ were left to cross-link at 4 ℃ for 24 h. After 24 h the gels from methods A – C were washed three times with deionised water to remove excess $CaCl_2$. Once the optimum fabrication method was chosen on the basis of optimum foam overrun and stability, the effect of cross-linking time was analysed at 0 or 24 h.

2.2.2.2 Preparation of vitamin D_3 loaded microgels

Whey protein isolate solution was prepared as per section 2.2.1.1. Vitamin D_3 stock (2 mg/ mL) was prepared in absolute ethanol.

To form the vitamin D_3 loaded WPI (WPI/VD_3) microgels, vitamin D_3 was added to the denatured WPI solutions (pH 3 – 8) to make a final concentration of 20 µg VD_3 followed by addition of 0.1 M calcium chloride and the samples were vortexed. The samples were left under gentle shaking (100 rpm) to cross-link at room temperature for 24 h unless stated otherwise before analysis was carried out. All tubes were flushed with nitrogen and covered with aluminium foil to be protected from light.

2.2.2.3 Determination of encapsulation efficiency of WPI microgels

The encapsulation efficiency (EE) of the microgels (pH 6.8) was determined according to the method of Luo *et al*. (2012) with minor modifications. To test the effect of pH on encapsulation efficiency, WPI was altered from native pH (6.8) to pH 3, 4.5, 4.8, 5.5, 7.5 and 8. These pH values were chosen to determine if the electrical charge of WPI influenced encapsulation efficiency. Vitamin D_3 loaded microgels were centrifuged at 4,000 rpm for 40 min at room temperature. The supernatant was collected, filtered, and analysed by UV-vis spectrophotometer (Jenway 6305 Spectrophotometer, Stone, UK) at 265 nm as unencapsulated vitamin D_3. A sample containing WPI microgels without VD_3 was used as a blank.

The encapsulated vitamin D_3 in the microgels was also extracted from the pellet. Five mL of ethanol was added and vigorously shaken on a vortex mixer for 30 s, then 5 mL of hexane was added and shaken for another 30 s. Five mL of pure water was then added to the above mixture and the tube was sealed tightly and shaken on a multipurpose rocker for 30 min. After the mixture had been centrifuged at 4,000 rpm for 10 min at 4

°C to separate the hexane phase and the water/ethanol phase, the vitamin D_3 in the hexane layer was measured as described in the previous paragraph. A standard curve was prepared (0.1 – 20 µg/ mL) of vitamin D_3 in absolute ethanol.

2.2.2.4 Particle size

Particle size distributions of the microgels were determined using static light scattering. Malvern Mastersizer Hydro 2000S (Malvern Instruments, UK) was used to obtain the surface weighted mean ($d_{3,2}$). Samples were diluted in distilled water to avoid multiple scattering. A refractive index of 1.33 and 1.456 was used for water and whey protein, respectively. All size measurements were carried out in three replicates.

2.2.2.5 Differential scanning calorimetry (DSC)

Differential scanning calorimetry analysis of WPI powder, VD_3 powder and the WPI and WPI/VD_3 microgel solutions were performed using a DSC Q 2000 (TA instruments, New Castle, DE, USA). Samples (5 mg) were added to an aluminium pan and hermetically sealed. Samples were heated from room temperature to 200 °C with a constant heating rate of 10 °C/ min under continuous purging with nitrogen. A sealed empty aluminium pan was used as a reference.

2.2.2.6 Stability of VD_3 to environmental stresses

The influence of environmental stresses such as long-term storage at 20, 4 and – 20 °C, UV-light (254 nm), dairy pasteurisation temperature (72 °C for 15 s or 63 °C for 30 min) or foaming on the stability of VD_3 were determined. A control sample of unencapsulated VD_3 in ethanol was exposed to the same conditions as reference for (i – iii). All samples were analysed as per section 2.2.2.3.

i. Long-term storage: The WPI/VD_3 microgel solutions were stored at fridge (4 °C), freezer (- 20 °C) or room temperature (20 °C), and a sample was taken each week for 4 weeks.
ii. UV- light: The WPI/VD_3 microgel solutions were exposed to UV light (254 nm) in a UV light box. Samples were taken every hour for 5 hours.

iii. Temperature: The WPI/VD_3 microgel solutions were submerged in a water bath at 72 °C for 15 s or 63 °C for 30 min.

iv. Foaming: After exposure to the various conditions (pH, ionic strength, heat, sucrose and XG) followed by mechanical whipping, the microgel foams were stored in closed tubes covered with aluminium foil and stored at 4 °C for 4 weeks. Vitamin D_3 stability was measured at the end of the fourth week.

2.2.3 Analysis of rheological properties

Viscosity and rheological measurements were performed on a shear stress controlled rotational rheometer (AR-G2 rheometer, TA instruments, New Castle, DE). A parallel plate geometry with a diameter of 40 mm with a gap of 500 μm was used. Viscosity values were measured at a shear rate of 100 s^{-1} at 20 °C.

The linear viscoelastic region (LVR) was determined by an amplitude sweep (0.02 – 100 % strain). A strain-controlled frequency sweep (0.01 – 10 Hz) at a strain (0.2 %) within the LVR was applied. Time sweeps (120 min) were also carried out at 0.2 % strain and 1 Hz. The storage (G') and loss modulus (G'') were recorded. All measurements were carried out in triplicate.

The same methods were followed for the ice cream samples, however they were carried out at 4 °C.

2.2.4 Sodium dodecyl sulphate polyacrylamide gel electrophoresis

The protein fractions were characterised by sodium dodecyl sulphate polyacrylamide gel electrophoresis (SDS-PAGE). The protein solutions were diluted to a final protein concentration of ~0.2 %. Samples were prepared with an SDS-PAGE buffer under reducing conditions (0.125 M Tris-HCl pH 6.8, 4% SDS, 20% glycerol, bromophenol, 10% β-mercaptoethanol) or non-reducing conditions (without β-mercaptoethanol). A mixture of sample and sample buffer (1:1 v/v) was heated to 100 °C for 5 min and cooled on ice. The microgel samples were centrifuged at 10,000 rpm for 10 min. Five μL of each sample were loaded into Bolt Bis-Tris gel (ThermoFisher Scientific, Dublin, Ireland) consisting of a 4 – 12 % gradient capable of separating proteins up to 260 kDa. Molecular weights of the protein bands were estimated by means of the protein marker (SeeBlue Plus2 Pre-stained protein standard). The running buffer, MES SDS

(20X) was diluted to 1X and the migration was performed at a constant voltage of 200V for 22 min. Gels were stained with InstantBlue Coomassie Stain. Images of the gels were captured using the iBright FL1000 Imaging system (ThermoFisher Scientific, Dublin, Ireland).

2.2.5 Determination of accessible sulphydryl content

The concentration of free sulphydryl groups were measured according to the Ellman's Reagent protocol (ThermoScientific, 2020) using Ellman's reagent. The amount of free sulphydryl groups (SH) were analysed. Protein solutions were diluted (1:5) with distilled water and 500 µL of the protein sample was mixed with 5 mL reaction buffer (0.1 M sodium phosphate, 1 mM EDTA, pH 8.0) and 100 µL Ellman's reagent. Samples were left to incubate for 15 min at room temperature. Samples were then centrifuged at 4,000 rpm for 15 min and their absorbance was measured using a UV-vis spectrophotometer at 412 nm (Jenway 6305 Spectrophotometer, Stone, UK). The concentration of accessible SH was determined using a standard curve (0.25 – 1.5 mM cysteine).

2.2.6 Surface hydrophobicity

The surface hydrophobicity of samples was determined using the fluorescence probe, 8-anilinonaphthalene-1-sulfonic acid (ANS) (8 mM in 0.01 M phosphate buffer, pH 8.0) according to the method of Alavi *et al.* (2018b) with slight modification. A series of protein solutions with concentration from 0.0025 – 0.02 % was prepared by diluting native, heat denatured and WPI microgel solutions with 0.01 M phosphate buffer, pH 8. Forty µL of ANS solution was added to 4 mL of each protein solution and the fluorescence intensity was recorded by a spectrophotometer (Cary Eclipse fluorescent spectrophotometer, Agilent, Middelburg, The Netherlands) at the excitation and emission wavelengths of 365 and 484 nm respectively. A control sample containing phosphate buffer without WPI was mixed with ANS; the fluorescent intensity of the control was used to estimate the relative fluorescent intensity (RFI). The RFI was calculated for each sample by dividing the fluorescent intensity of the sample by the fluorescent intensity of the control. RFI was plotted against the protein concentrations and the slope (H_0) of the line for each sample was the surface hydrophobicity.

2.2.7 Foaming

2.2.7.1 Effect of environmental factors on foaming

Several conditions were investigated to assess their effect on the foaming ability of native WPI and microgels. The effect of protein concentration, ionic strength, pH, whipping time, sucrose concentration and heat were studied. Sample conditions were altered prior to mechanical whipping. Refer to section 2.2.7.2 for the whipping method and instrument.

2.2.7.1.1 Whey protein solutions

i. Native protein concentration was altered to 2.5, 5, 7 and 10 %.

ii. The whipping times used were 2.5, 5, 7, 10, 15 and 20 min.

iii. The pH of the samples was adjusted from their native pH (6.8) to pH 3, 4, 4.5, 5, 8 or 9 using 1 M NaOH or 1M HCl.

iv. Sodium chloride was added at concentrations of 0.05, 0.1, 0.2 and 0.4 M.

v. Sucrose was added at 12, 15 or 20 %.

vi. For heat treatment, WPI samples in covered beakers were submerged in a water bath at 70 – 80 ℃ for 30 min, followed by cooling on ice to reach room temperature.

vii. WPI solutions were supplemented with 0.1, 0.2 and 0.3 % xanthan gum and stirred to make uniform dispersions using a stirrer bar. The rehydrated samples were kept in the refrigerator at 4 °C overnight to fully hydrate. The whey protein isolate/xanthan gum (WPI/XG) solutions were subjected to several treatments to determine the effect of foaming.

- The whipping time was analysed at 3, 5, 7 and 10 min.
- The pH of the solutions was adjusted to pH 3, 4, 5, 6, 8, 9 using 1 M NaOH or 1 M HCl.
- To test the effect of ionic strength, concentrations of 0.05, 0.1, 0.2 and 0.4 M sodium chloride were added to the solutions before foaming.

2.2.7.1.2 Microgel sols

i. The whipping times used were 5 and 10 min.

ii. The pH of the samples was adjusted from their native pH (6.8) to pH 3, 4, 4.5, 5, 8 or 9 using 1 M NaOH or 1 M HCl.
iii. Sucrose was added at 12, 15 or 20 %.
iv. For heat treatment the microgels were exposed to dairy pasteurisation temperatures of 72 ℃ for 15 s and 63 ℃ for 30 min in a water bath followed by cooling on ice.
v. Sodium chloride was added at concentrations of 0.05, 0.1, 0.2 and 0.4 M.
vi. The microgels were supplemented with 0.3 % XG (chosen as the optimum concentration for foaming in chapter 4) and stirred to make uniform dispersions.

2.2.7.2 Preparation of foams

Foams were prepared using a standard kitchen hand blender (Kenwood), at speed 3 for 5 min for native WPI solutions and 10 min for WPI microgels, unless stated otherwise. Samples were whipped in modified 100 mL disposable cups (Sarstedt, Wexford) which were pre-drilled with a 0.5 cm hole at the centre of the bottom of the cup. This hole was covered with duct tape for the whipping duration. After completion of whipping, the beaters were carefully removed from the foam to prevent foam damage.

2.2.7.3 Foam characterisation

Immediately after whipping, the foam volume was read from the graduated scale on the container. After that, the duct tape was removed from the container and the container was placed over a beaker. The stability of the foam was measured by collecting the drained liquid in the beaker after 60 min. The drained liquid was collected via pipette for measurement. The following equations were used to measure foam overrun and stability respectively. Maximum foam stability is 100%.

$$\text{Foam overrun (\%)} = \frac{V1}{V2} \times 100 \qquad \text{Eq. 2.2}$$

$$\text{Foam stability (\%)} = \frac{V2-V3}{V2} \times 100 \qquad \text{Eq. 2.3}$$

Where:

V1 = Foam volume at 0 min (mL)

V2 = Volume of the initial liquid phase (mL)

V3 = Volume of liquid drainage after 60 min (mL)

2.2.7.4 Analysis of foam structure

Foam bubble size was assessed using a light microscope equipped with a CCD camera (Olympus BX51 Microscope, Mason Technology, Dublin, Ireland). A drop of water was placed on a glass slide and a small amount of foam was transferred to this water droplet using a spatula. Singular bubbles that were not overlapping were analysed within 10 min after foaming. ImageJ software was used to determine bubble area (mm^2) and bubble wall thickness (mm) from at least 130 bubbles per sample.

2.2.7.5 Foam textural properties

Texture parameters of the samples were obtained using a texture analyser (TA.XT.plus, Texture Analyser, Stable Microsystems, Godalming, UK). The method was followed as per Dabestani & Yeganehzad (2019) with slight modification. To prevent any edge effect, the foamed samples in 120 mm diameter containers were penetrated with an aluminium cylinder (36 x 36 mm) at a constant velocity of 1 mm s^{-1} for a distance of 10 mm. The force at target and the positive area of the curve were used as firmness and consistency, respectively. Foam texture was assessed immediately after foaming and after 6 months storage.

2.2.8 Scanning electron microscopy (SEM)

The morphology of the WPI microgels and WPI/VD_3 microgels were studied by SEM according to the method by Egan *et al*. (2013) with minor modifications. Microgels were fixed over night at 4 °C in 2.5 % glutaraldehyde. The microgels were then rinsed three times (15 min each) with 0.1 M sodium cacodylate followed by dehydration in an ethanol series of 30, 50, 70, 80, 90, 100 % (v/v) for 10 min each. Samples were then left to dry in a vacuum oven (Memmert V0500 Vacuum drying oven, Germany) at 25 °C. Following this, the dried microgels were mounted onto SEM specimen stubs and were sputter coated using an Emitech K550 gold sputter coater. SEM studies were carried out using a TM4000 SEM-EDX system (Hitachi Technologies) at 15 kV.

The WPI microgel foam and WPI/VD_3 microgel ice cream microstructure was evaluated by scanning electron microscopy using a method by Nooshkam *et al*. (2022) and Yu *et al*. (2021). Samples were frozen in liquid nitrogen and then freeze dried. The samples were mounted onto SEM specimen stubs and were sputter coated using an

Emitech K550 gold sputter coater. SEM studies were carried out using a TM4000 SEM-EDX system (Hitachi Technologies) at 10 kV.

2.2.9 Ice cream

2.2.9.1 Ice cream manufacture and incorporation of microgels

To make the cream mixture, 250 mL full fat cream, 300 mL milk, 57.5 g sugar and 5 mL vanilla extract were heated over a low heat until it almost boiled. At this point the sample was taken off the heat and set aside for 30 min to cool. In a separate bowl, 3 large egg yolks and 57.5 g sugar were beaten using a standard kitchen blender (Kenwood) at speed 3 until the mixture thickened. One hundred mL of the cooled cream mixture was added to the egg mixture and beaten. The cream mixture was reheated just to the boil and taken off the heat. The egg mixture was added and stirred. The saucepan was returned to a low heat to allow it to cook, under constant stirring until the mixture coated the back of the spoon. The ice cream mixture was transferred to a bowl over ice water to cool. The mixture was covered and kept at 4 °C for 24 h.

WPI microgels at different concentrations (3, 7, 10, 13 and 17 %) were incorporated into the ice cream to determine the effect of microgel concentration. The ice cream mixture (ICM) and WPI/VD_3 loaded ice cream mixture (WPI/VD_3 ICM) are the names given for the samples. The RDI of vitamin D for older adults over the age of 70 is 20 µg (Food Safety Authority of Ireland, 2020). This study aimed to incorporate 6 µg VD_3 (30 % RDI) into ice cream, which was kept constant across the varying microgel concentrations. Samples were mixed using a stirrer bar for 10 min followed by homogenization using a laboratory homogeniser standard unit (Staufen, Germany) at 8,000 rpm for 1 min. The ice cream mixture was poured into the ice cream maker (Cuisinart 2L Ice cream maker, Ireland) and churned for 30 min. The soft ice cream was transferred to plastic containers and stored at -20 °C to harden until analysis.

2.2.9.2 Vitamin D_3 extraction from ice cream

The ice cream was stored at -20 °C and a sample was taken each week for 4 weeks to analyse vitamin D_3 stability. Ice cream with WPI microgels without vitamin D_3 was used as a control. For VD_3 extraction a method described by Kazmi *et al.* (2007) was

followed with minor modification. The ice cream was thawed and diluted with deionised water (1:3). Diluted samples (1g) were weighed into 10 ml centrifuge tubes containing 0.5 ml of potassium hydroxide (60 % w/v). Samples were nitrogen flushed, capped, shaken, and transferred to a water bath at 70 °C for 30 min. The centrifuge tubes were shaken once after 5 min. After 30 min, the samples were cooled in ice water for 10 min.

A mixture containing 3.75 ml of methanol:chloroform (2:1) was added and each tube was vortexed. A further 1.25 ml of chloroform was added and vortexed. Samples were centrifuged at 4 °C for 10 min at 1500 x g. The top layer was removed, and the clear bottom layer was kept and analysed via UV-vis spectroscopy at 254 nm for vitamin D_3 content. A blank consisting of ice cream with WPI microgels was used.

2.2.9.3 Ice cream hardness and melting rate

After fabrication the ice cream was stored at -20 °C and a sample was taken each week for 4 weeks to analyse hardness and ice cream melting rate. Hardness (N) of ice cream samples was determined using a texture analyser (TA.XT.plus, Stable Microsystems, Godalming, UK). The ice cream samples were penetrated with a P/30C perspex cone probe. The peak positive force was recorded as the probe penetrated the ice cream to a depth of 20 mm at a speed of 2 mm^{-1} (Chansathirapanich *et al*., 2016).

To study the melting behaviour of the ice cream, samples were taken after 24 h and at the end of the fourth week. Ice cream samples (50 g) were removed from containers and placed on a wire mesh grid over a beaker at room temperature (20 °C). The weight of the drip was recorded at 10 min intervals until the ice cream completely melted. The melting rate of the ice cream was determined as the slope as a function of time over the dripped portion (Soukoulis *et al.*, 2008).

2.2.10 *In vitro* digestion model

The release profile of vitamin D_3 from WPI microgels and from ice cream was evaluated under simulated *in vitro* gastrointestinal conditions using dialysis tubing. The INFOGEST international consensus model was used (Minekus *et al.*, 2014). Two mL of sample was filled into a dialysis bag (10 kDa molecular cut off) and sealed with dialysis clips.

Simulated saliva fluid (SSF), gastric fluid (SGF) and intestinal fluid (SIF) electrolyte stock solutions were prepared as described below. Dialysis bags were placed in the simulated fluids made up to 100 mL with 0.01 M phosphate buffer at pH 7.0. At predetermined time points, 1 mL of sample was withdrawn and equal volume of fresh medium was simultaneously replaced. Samples were analysed for vitamin D_3 release as per section 2.2.2.3

i. *Oral phase:* 1.6 mL of SSF electrolyte stock followed by the addition of 10 µL of 0.3 $CaCl_2$, 0.19 mL of water and 0.2 mL of α-amylase solution. The mixtures were incubated at 37 °C for 2 min under agitation in a shaking incubator at 120 rpm.
ii. *Gastric phase:* To simulate the gastric phase, 3.2 mL SGF electrolyte stock, 0.5 ml of pepsin solution and 2 µL of 0.3 M $CaCl_2$, 0.191 mL of 1 M HCl to reach pH 3 and 0.107 mL of water were added. The samples were incubated at 37 °C for 2 h under agitation in a shaking incubator at 120 rpm.
iii. *Intestinal phase:* To simulate the intestinal phase, 3.4 mL of SIF electrolyte stock, 2 mL of pancreatin solution, 1 mL of bile solution, 16 µL of 0.3 M $CaCl_2$, 0.14 mL of 1 M NaOH to reach pH 7 and 1.44 mL of water were added. The samples were incubated at 37 °C for 2 h under agitation in a shaking incubator at 120 rpm.

The KinetDS software for dissolution test data analysis was used to analyse kinetic VD_3 release (Mendyk *et al*., 2012). In this study five kinetic models were used to investigate the mechanism of VD_3 release: zero order, first order, Korsmeyer-Peppas, Hixson-Crowell and Higuchi model.

2.2.11 Statistical analysis

All experiments were carried out in triplicate and data (n=3) were reported as mean ± standard deviation. Differences between means were evaluated by ANOVA using the Tukey posthoc test using Minitab statistical software version 18 (Minitab Inc., Pennsylvania, USA). Differences were considered significant if $P < 0.05$.

Chapter 3
Foaming properties of whey protein isolate

3.1 Introduction

Whey is a co-product of the cheese making process which was once seen as waste. However, today, it has become a valuable material in the agri-food, biotechnology and medical markets due to it being an excellent source of proteins and peptides, lipids, minerals, vitamins and lactose (Smithers, 2008). Depending on the end use of the product, whey can go through various processes to form powders that are enriched with protein for specialised formulations. Examples include chromographic, electro-dialysis and membrane techniques (microfiltration, ultra-filtration) for demineralisation and purification of whey to form high protein and low-fat functional whey ingredients such as whey protein concentrate (WPC) and whey protein isolates (WPI) (Smithers, 2008). In this study, whey protein isolate was used, meaning that the whey has gone through ion exchange and cold-filtered processing techniques, removing almost all the fat, lactose and other impurities to produce an ultra-purified protein powder (Smithers, 2008).

The aims of this study were to investigate the effect of several environmental factors on the foaming behaviour of WPI. The factors that were investigated were protein concentration, whipping time, pH, ionic strength, heat treatment and addition of sucrose. The WPI foams were characterised based on their overrun and stability.

3.2 Results and discussion

3.2.1 Effect of WPI concentration and whipping time on foaming properties

The foaming properties of WPI were assessed to find the optimum protein concentration for foam overrun and stability by testing four different concentrations: 2.5, 5, 7 and 10 %. The overrun was found to increase up to 5 % WPI, after this concentration the overrun decreased that led to a small but significant difference (Table 3.1). The possible reason as to why this decrease occurred may be due to the rise in solution viscosity with increasing protein concentration (Table 3.1). The viscosity increased from 2.07 ± 0.12 to 3.42 ± 0.10 mPa as concentration increased from 2.5 to 10 % WPI. Increased viscosity minimises the incorporation of air into the solution, thus reducing foam formation. Marinova *et al.* (2009) and Britten and Lavoie (1992) found similar results, where the foam overrun increased with increasing concentration and then plateaued or decreased past a certain point. Britten and Lavoie (1992) suggested that at

high protein concentrations, the solubility of proteins decrease, thus leading to a decrease in foam overrun.

In contrast, an increase in protein concentration increased the foam stability. Stability values increased from 72 to 93 % as the protein concentration increased from 2.5 to 10 %. Increasing viscosity and a reduction in the surface tension of the continuous phase with increasing protein concentration may have helped to reduce liquid drainage therefore preventing foam destabilisation (Table 3.1). Initially the surface tension was 50.16 ± 0.69 mN/m, however when the protein concentration was increased to 10 % to surface tension decreased to 46.84 ± 0.31 mN/m. With increasing viscosity, the formation of a protein multilayer at the interface is facilitated and the reduced surface tension helps to alleviate the pressure differences at the air/water interface (Vega and Sanghvi, 2012). A greater concentration of protein in foams form thicker and more rigid interfacial films that help reduce drainage within the lamella present in foams (Britten and Lavoie, 1992).

10 % WPI was chosen for the remainder of experiments as at this concentration a relatively good foam overrun (650 %) can be obtained with good stability (93 %).

Table 3.1 The effect of protein concentration on whey protein solution viscosity, surface tension, foam overrun and stability. Data (n=3) are presented as the mean ± SD. Data with different superscript letters within a column indicate significant differences.

Whey protein (%)	Viscosity (mPa)	Surface tension (mN/m)	Overrun (%)	Stability (%)
2.5	2.07 ± 0.12^{c}	50.16 ± 0.69^{a}	$689 \pm 19.25^{a,b}$	72 ± 7.18^{c}
5	3.10 ± 0.10^{b}	$48.89 \pm 0.95^{a,b}$	700 ± 0.00^{a}	$81 \pm 6.39^{b,c}$
7	3.14 ± 0.28^{b}	$47.13 \pm 0.25^{b,c}$	678 ± 28.87^{b}	$86 \pm 5.77^{a,b}$
10	3.42 ± 0.10^{a}	46.84 ± 0.31^{c}	650 ± 0.00^{c}	93 ± 3.85^{a}

Whipping time is one of the factors that effects foam formation. Whipping of protein solutions leads to the unravelling of the protein strands and partial unfolding of the protein tertiary and secondary structure. Whey protein solutions were whipped for 2.5 - 20 min to establish optimum whipping time for good foaming properties. The optimum overrun (761 %) was reached when the samples were whipped for 5 min (Fig. 3.1).

Increasing whipping time above 5 min led to decreased overrun. At 5 min, the improved functionality might be due to an appropriate amount of mechanical energy, allowing sufficient protein to adsorb and aggregate on the interfacial lamellae leading to improved foaming ability. At shorter whipping times the reduced overrun may have occurred due to under-beating, resulting in fewer air bubbles being incorporated into the protein solution. At longer whipping times > 5 min, excessive over-beating of WPI could have occurred, leading to protein denaturation or aggregation, limiting the proteins function of adsorbing to the air/water interface (Dabestani and Yeganehzad, 2019). If aggregation of the protein molecules did occur, the size of aggregated proteins can reduce their ability to diffuse to the interface, leading to lower foam overrun (Rullier *et al*., 2008).

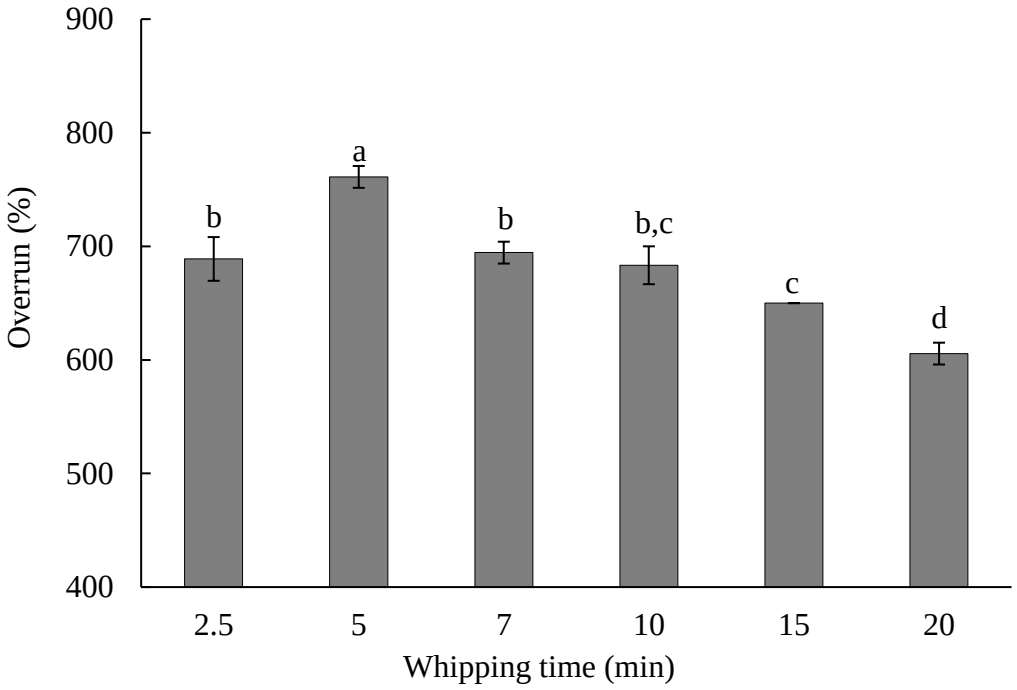

Fig. 3.1 Effect of whipping time on 10 % WPI (pH 6.8) foam overrun. Data (n=3) are presented as the mean ± SD. Data with different letters indicate significant differences.

The most unstable protein foams were produced after 2.5 min whipping (82%). As the whipping time increased for longer than 2.5 min the stability of the foam increased. There was no significant effect on foam stability between 5 – 20 min whipping, with foam stability values ranging between 94 – 98 %. These results may indicate that even though foam overrun was hindered by possible protein aggregation, foam stability was not. In

fact, it has been found that protein aggregates help to improve foam stability (Davis and Foegeding, 2007; Gharbi and Labbafi, 2019; Moro *et al*., 2011). The aggregates can adsorb at the interface, increase the viscoelasticity of the interface or the aggregates can remain in the aqueous phase forming a gel-like network (Rullier *et al*., 2008).

From these results, 5 min whipping time was chosen for the rest of the study unless stated otherwise, as at this time, foam with good overrun and stability was produced.

3.2.2 The effect of pH, ionic strength, heat treatment and sucrose concentration on WPI foaming ability

3.2.2.1 Effect of pH

The pH of a solution has a major influence on the protein solubility, which is of primary importance as this influences other functional properties required by proteins such as good emulsion, gelation, foam and whipping properties (Pelegrine and Gasparetto, 2005).

The pH values used in this study were pH 3 – 9, ranging from below and above WPI isoelectric point (pI). Fig. 3.2 (inset) shows the ζ-potential of WPI solutions effected by pH. The isoelectric point of WPI was found to be in the range $4.5 < pH < 5$ where the ζ-potential was zero. This zero net charge promotes protein-protein interactions, causing aggregation between the protein molecules. Below the pI, WPI was positively charged, above they were negatively charged indicating electrostatic repulsion between the molecules. Understanding the net charge of the protein molecules is important to understand the electrostatic interactions that are occurring, which has a big influence on WPI foaming.

Results showed that WPI foamed best close to the isoelectric point, where foam overrun reached 906 and 928 % for pH 4.5 and 5 respectively (Fig. 3.2). When the pH was altered above or below this, the overrun decreased. The same outcome occurred for foam stability, with high stability close to the pI and increased drainage occurring at pH values further from the pI. Phillips *et al.* (1990) also found that at pH 5, the most stable WPI foams were formed. Protein-protein interactions at the pI can lead to the formation of aggregates, which when whipped take time to diffuse at the air/water interface which could explain why the foams were more stable than at other pH values. The increased surface activity and the reduction in electrostatic interactions of proteins close to the pI might have aided at increasing the foaming ability of whey protein (Zhang *et al*., 2004).

At pH < 5 α-lactalbumin, one of the proteins present in WPI, loses bound calcium ions and takes on a molten globular state, causing it to be more surface-active as protein-protein interactions are increased which results in the formation of a viscoelastic film (Zhang *et al*., 2004; Lajnaf *et al*., 2018). Also, protein adsorption of β–lactoglobulin is increased at the isoelectric point due to the lack of net charge which leads to weaker repulsive interactions between the protein molecules, thus increasing protein hydrophobicity (Engelhardt *et al*., 2013). Also, Engelhardt *et al*. (2013) suggested that at the pI, due to the increased protein-protein interactions, a dense multilayer of β–lactoglobulin can form. The combined effect of increased surface activity of the two proteins found in whey protein (β–lactoglobulin and α-lactalbumin) at pH close to the pI could explain the high overrun and stability values at this point.

The reduction in overrun of WPI at higher pH values may be explained by the high level of solubility resulting from high electrostatic repulsion between the protein molecules, leading to fewer proteins being adsorbed at the interface. Solubilisation is promoted by electrostatic repulsion and hydration of the charged residues on the proteins surface (Damodaran *et al*., 2007). Protein-water interactions are favoured over protein-protein interactions which causes increased charge repulsion between the protein molecules, decreasing the amount of protein aggregates capable of stabilising foams (Rodriguez Patino *et al*., 1995).

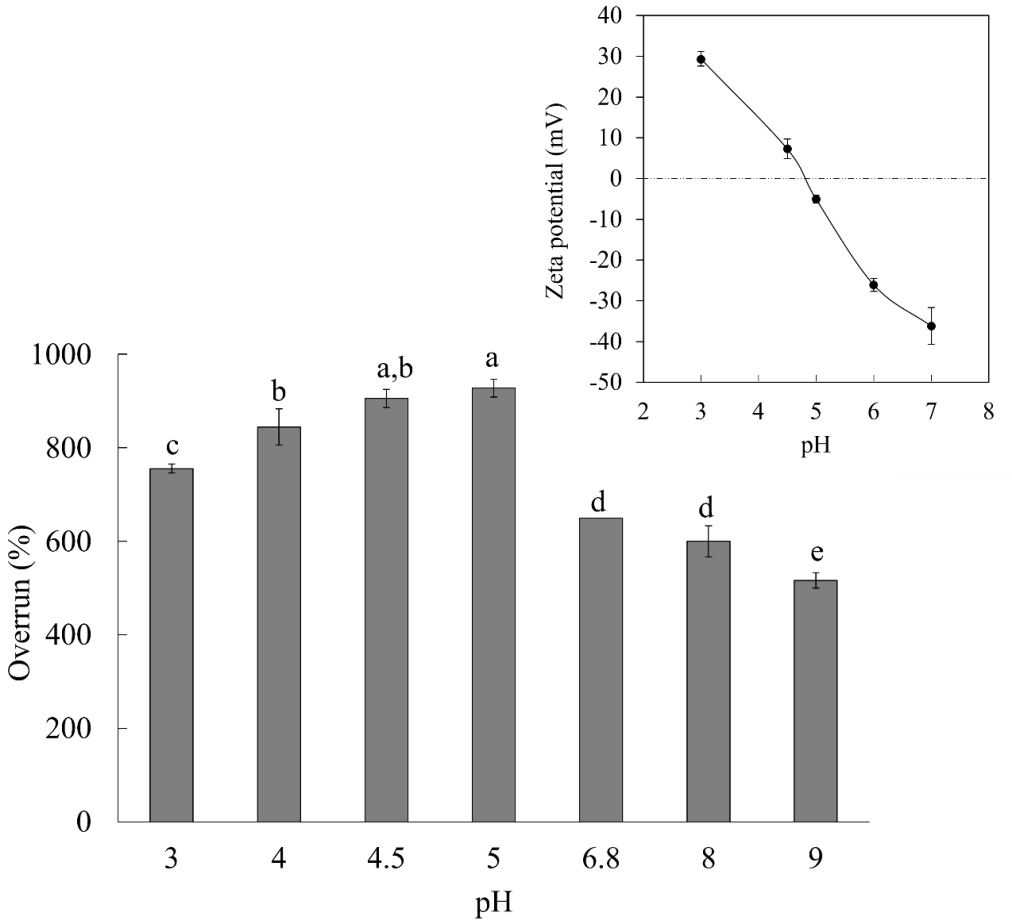

Fig. 3.2 Influence of pH on 10 % WPI electrical charge (ζ) (inset) and on 10 % WPI foam overrun. Data (n=3) are presented as the mean ± SD. Data with different letters indicate significant differences.

3.2.2.2 Effect of heat

Often, denaturation of molecules can be destructive because of the loss of some properties. However, in the case of food proteins it is usually desirable (Damodaran *et al*., 2007). In this study, a combined effect of heat treatment (70 – 80 °C) at various pH values (pH 3 – 9) were compared against their corresponding non-heated samples to see the effect of heat on foaming properties (Table 3.2). At pH 6.8 - 9, heat treatment increased foam overrun compared to the non-heated samples. For non-heated proteins increased solubility at higher pH usually leads to lower overrun values. However, the improvement in overrun of these samples after heating could be due to the protein molecules unfolding, exposing the inner hydrophobic region which then interacts with other protein molecules forming protein aggregates (Pelegrine and Gasparetto, 2005).

Table 3.2 Effect of pH and temperature on 10 % WPI foam overrun (%). Data (n=3) are presented as the mean ± SD. Data with different superscript letters within a column indicate significant differences.

Temperature (°C)	**Overrun (%) at different pH values**					
pH	**3**	**4**	**5**	**6.8**	**8**	**9**
No heat	756 ± 10^{a}	844 ± 29^{a}	928 ± 19^{a}	650 ± 0^{c}	600 ± 36^{b}	517 ± 19^{c}
70 °C	644 ± 19^{b}	739 ± 19^{b}	711 ± 26^{b}	694 ± 48^{c}	750 ± 10^{a}	872 ± 38^{a}
75 °C	756 ± 19^{a}	244 ± 19^{c}	217 ± 26^{c}	850 ± 48^{a}	839 ± 10^{a}	922 ± 38^{a}
80 °C	750 ± 48^{a}	128 ± 36^{d}	178 ± 53^{c}	789 ± 45^{b}	772 ± 10^{a}	783 ± 0^{b}

Close to the protein isoelectric point, foam overrun was negatively affected. This decrease in overrun was more pronounced at 80 °C and 75 °C for pH 4 and 5 respectively. The viscosity of the unheated WPI solution at native pH (6.8) was 3.42 mPa, which increased more than five-fold to 19.97 mPa at 80 °C (Table 3.3). After exposure to 80 °C, at pH 4 and 5 the viscosity of the solution increased substantially from ~ 4 to 7780 and 9091.54 mPa respectively. This increased viscosity impeded air incorporation into the continuous phase of the system which has also been found by Dabestani and Yeganehzad (2019).

Also, at pH close to the pI after heat exposure, solubility is decreased due to the increase in hydrophobicity of the protein surface as a consequence of unfolding and this could also contribute to decreased overrun (Damodaran *et al*., 2007).

Heating improved foam stability at pH 3, 6.8, 8 and 9. At pH 3 with no heat treatment, stability had a value of 68 % which increased to 83 % at 70 ºC and then further increased to 100 % stability at 75 – 80 ºC. Close to the isoelectric point with or without heat, foam stability did not change and remained at 100 %. At pH 6.8, 8 and 9 stabilities improved reaching 100 %, regardless of the temperature (70 – 80 ºC).

Table 3.3 Viscosity values (mPa) of 10 % whey protein isolate exposed to heat treatment and a control sample that was unheated. Data (n=3) are presented as the mean ± SD. Data with different superscript letters within a column indicate significant differences.

Temperature (℃)	**Viscosity (mPa) at different pH**		
	4	**5**	**6.8**
No heat	4.34 ± 0.43^{b}	4.21 ± 0.92^{d}	3.42 ± 0.10^{c}
70 ℃	7.01 ± 0.40^{b}	35.18 ± 2.74^{c}	6.44 ± 0.40^{c}
75 ℃	45.65 ± 4.18^{b}	728.16 ± 38.98^{b}	13.81 ± 1.63^{b}
80 ℃	7780.22 ± 1224.9^{a}	9091.54 ± 1197.24^{a}	19.97 ± 5.05^{a}

Heating of the protein solutions above their denaturation temperature led to aggregation of the protein molecules. Heating of the protein samples formed particles with a diameter of 18 - 19 nm across the three temperatures at native pH (6.8). The particle size at pH 4 -5 increased with increasing temperature with larger particles formed at pH 5 (Table 3.4).

Aggregates can interact with several bubble interfaces, forming a matrix where they are interlinked forming a cohesive network (Nicorescu *et al*., 2009). These particles can form a thick rigid interface or remain in the continuous phase where viscosity is increased leading to stability increase (Gharbi and Labbafi, 2019). A study by Rullier *et al*. (2008) found that the foaming ability of β-lactoglobulin aggregates made from heat treatment was influenced by aggregate size as this affects adsorption rate. The authors found that the larger the particles, the lower the overrun. However, the presence of aggregates of any size resulted in more stable foams compared to the non-aggregated protein foams. In this study the large particles found at pH 4 – 5 after heat treatment might explain the low overrun but high stability of the foams. The increased viscosity of these samples as a result of the large particle size could also contribute to form stable foams as it minimises gas diffusion between the bubbles.

Table 3.4 Particle size of WPI at pH 4, 5 and 6.8 after heat treatment at 70 – 80 °C. Data (n=3) are presented as the mean ± SD. Data with different superscript letters within a column indicate significant differences.

pH	Particle size	Temperature °C		
		70	**75**	**80**
4	**µm**	43.85 ± 4.13^{b}	83.70 ± 19.6^{b}	405.20 ± 41.6^{a}
5	**µm**	174.20 ± 36.7^{a}	1052.70 ± 102^{a}	N/A
6.8	**nm**	19.71 ± 0.52^{c}	18.44 ± 0.04^{c}	18.57 ± 0.79^{b}

Note: N/A indicates that the sample formed into a monolith gel and could not be measured by the Mastersizer.

3.2.2.3 Effect of ionic strength

On addition of 0.05 – 0.2 M sodium chloride to whey protein solutions, the foam overrun significantly increased (Fig. 3.3). However, at 0.4 M NaCl, the overrun reduced such that it did not significantly differ from the control sample (0 M). Foam stability was unaffected by ionic strength as the samples did not differ from the control sample, reaching stability values between 93 – 95 %. Electrostatic repulsion between proteins at the interface is reduced with salt addition, leading to an increase in protein adsorption (Nicorescu *et al.*, 2008). Addition of salt affects the solubility of protein; low concentrations enhance the solubility whereas higher concentrations decrease it. The increased solubility at low ionic strength is caused by the decrease in the ionic activity of the protein macroion (Damodaran *et al*., 2007). Salt ions bind to the protein charged groups at low ionic strength and reduce the electrostatic repulsions between proteins (Zhang *et al*., 2004).

With excess salt addition, the solubility decreases due to the protein molecules competing with the salt molecules to bind with water leading to protein precipitation (ErÇelebi and IbanoĞlu, 2009). This may suggest why the overrun improved with 0.2 M but decreased at 0.4 M NaCl. At low ionic strength protein solubility is increased improving foaming but at higher ionic strength protein solubility is decreased which decreases overrun. This result is in agreement with Zhang *et al*. (2004) who found that whipping ability of WPI increased with 0.1 M NaCl addition, but decreased with further salt addition. Marinova *et al*. (2009) found that NaCl addition to whey protein concentrate had little effect on foaming, however when NaCl was added to sodium caseinate at 0.15 M foaming was improved compared to the solutions without salt.

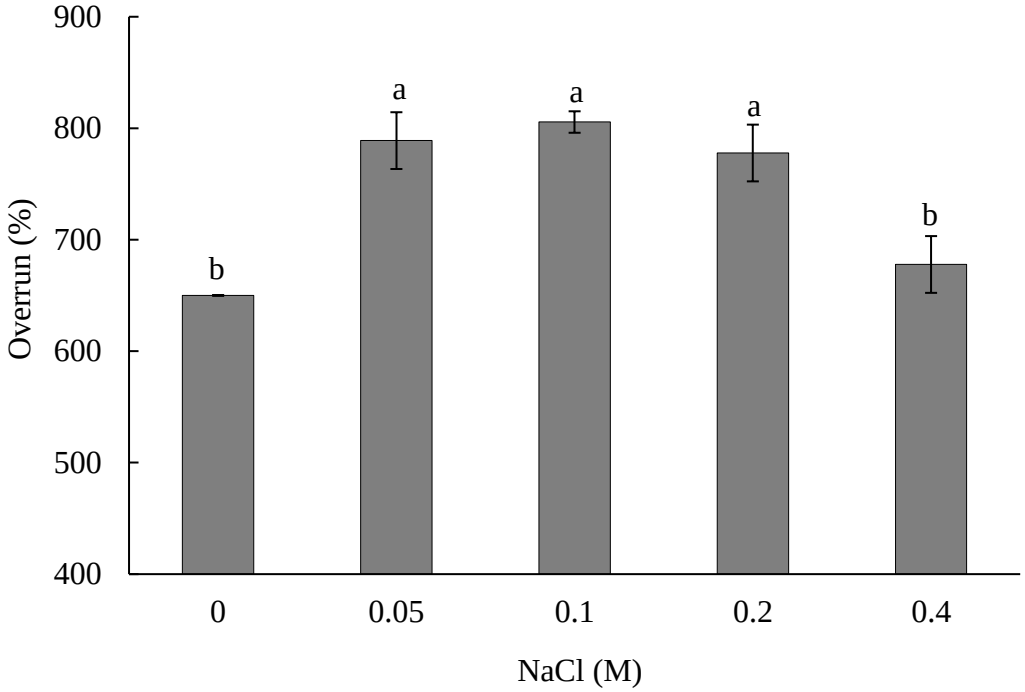

Fig. 3.3 Foam overrun of 10 % WPI (pH 6.8) with varying concentrations of NaCl. Data (n=3) are presented as the mean ± SD. Data with different letters indicate significant differences.

3.2.2.4 Effect of sucrose

In chapter 8 of this thesis, ice cream was chosen as the real food system and sucrose is one of the main ingredients in ice cream products, which is typically added at 9 - 12 % (Goff, 1997). Therefore, a range of sucrose concentrations were tested to determine the effect on WPI foaming.

The addition of sucrose significantly altered the foaming properties of WPI depending on sucrose concentration. Increasing the concentration of sucrose from 12 to 20 % led to increased solution viscosity from 7.03 to 8.74 mPa respectively (Table 3.5). Yang and Foegeding (2010) and Nastaj (2021) also found that the viscosity of their protein solutions increased with increasing sucrose concentration. Subsequently, WPI foam overrun decreased with increasing sucrose concentration, while stability increased (Table 3.5). The interactions between protein molecules can be negatively affected as sucrose can impede protein unfolding limiting protein-protein interactions (Nastaj, 2021). Sucrose is known to improve stability of systems by increasing the viscosity of lamellar water which retards drainage (Kinsella, 1981).

Table 3.5 Effect of sucrose concentration on 10 % WPI (pH 6.8) foam overrun and stability. Data (n=3) are presented as the mean ± SD. Data with different superscript letters within a column indicate significant differences.

Sucrose (%)	Viscosity (mPa)	Overrun (%)	Stability (%)
0	3.42 ± 0.10^{c}	650 ± 0.00^{a}	93.33 ± 3.85^{b}
12	7.03 ± 0.71^{b}	458 ± 8.33^{b}	$97.50 \pm 0.83^{a,b}$
15	7.66 ± 0.19^{b}	411 ± 9.62^{c}	$96.39 \pm 1.92^{a,b}$
20	8.74 ± 0.34^{a}	376 ± 8.39^{d}	98.89 ± 0.48^{a}

3.3 Conclusion

Many factors affected the functional properties of whey proteins such as concentration, pH, temperature, sucrose concentration and ionic strength. Protein concentration was initially tested as it is vital to establish the optimum concentration to produce foam with good foaming ability. Lower concentrations were found to produce the best overrun while higher concentrations produced foam with better stability. Whipping time was also essential to foam formation as a substantial amount of time was required for the protein to unfold and adsorb at the interface, while overbeating caused negative effects leading to foam collapse.

Altering the pH of WPI to its isoelectric point led to the formation of foams with good overrun and stability due to the protein-protein interactions. At other pH values, overrun and stability were decreased. When these samples were heated overrun was found to decrease at the pI and increase at the other pH values which could be due to increased viscosity or larger aggregate size at the pI. Heat treatment at all pH values led to increased foam stability.

Sodium chloride addition was found to increase foaming ability at 0.05 - 0.2M while further addition led to negative effects, due to solubility issues. Heat treatment of WPI caused the proteins to unfold and interact with each other and form small aggregates at the nanometre scale which helped to increase the overrun and stability of the system. Increasing the concentration of sucrose led to reduced overrun but increased stability due to the rise in solution viscosity or the ability of sucrose to impede protein unfolding. Results from this research showed that exposing WPI to a range of treatments can aid at forming foams with suitable foam volume and stability that can be considered for the production of foodstuffs.

Chapter 4

The effect of xanthan gum on whey protein foams

4.1 Introduction

Foams are considered metastable systems and are thermodynamically unstable leaving them to be susceptible to coarsening, coalescence and drainage due to the influence of van der Waals forces and gravity. Foam stability is an important factor as it affects the shelf life and product appearance of foods for consumer consumption (ErÇelebi and IbanoĞlu, 2009). In chapter 3, WPI foaming properties varied depending on the environmental factor. However, in all cases, the WPI foams collapsed in ≤ 60 min.

Polysaccharides are usually added to food products for their thickening abilities and their ability to modify flow properties and textures of food products. Therefore, in this study, the addition of a polysaccharide, xanthan gum, was investigated for its ability to improve the foam stability of WPI. Xanthan gum (XG) is a microbial anionic hetero-polysaccharide (Damodaran *et al*., 2007). Lateral charged chains composed of three saccharides as well as acetyl and pyruvate groups are attached to xanthan gum's cellulose backbone (Bertrand and Turgeon, 2007). Xanthan gum is soluble in hot and cold water and at low concentrations it provides high solution viscosity, which is not affected by temperature, making the thickening agent unique. In acidic conditions, it is soluble and stable and it also works well in the presence of salt (Damodaran *et al*., 2007). The purpose of this study was to analyse the effect of xanthan gum on the foaming properties of whey protein solutions.

4.2 Results and discussion

4.2.1 Effect of XG concentration on whey protein foam overrun and stability

Whey protein (10 % v/v) was chosen as at this concentration good foaming properties were found in chapter 3. A range of xanthan gum concentrations (0.1 – 0.3 %) were used to determine the effect on WPI foaming. The viscosity of 10 % whey protein solution increased and the surface tension decreased with xanthan gum addition (Table 4.1). With increasing xanthan gum concentration, there was a progressive increase in the solution viscosity which increased ten-fold on addition of 0.3 % XG.

Table 4.1 Viscosity and surface tension of whey protein/xanthan gum solutions and of the bubble area and bubble wall thickness of whey protein/ xanthan gum foams. Data (n=3) are presented as the mean ± SD. Data with different superscript letters within a column indicate significant differences.

10 % WPI	Viscosity (mPa)	Surface tension (mN/m)	Bubble area (mm^2)	Bubble wall thickness (mm)
0 % XG	3.42 ± 0.10^{d}	46.84 ± 0.31^{a}	0.028 ± 0.02^{a}	0.060 ± 0.02^{c}
0.1 % XG	15.01 ± 0.16^{c}	46.88 ± 0.38^{a}	0.018 ± 0.01^{b}	$0.063 \pm 0.01^{b,c}$
0.2 % XG	28.51 ± 0.23^{b}	46.37 ± 0.51^{a}	$0.014 \pm 0.01^{b,c}$	$0.076 \pm 0.01^{a,b}$
0.3 % XG	36.32 ± 0.54^{a}	44.49 ± 0.47^{b}	0.013 ± 0.01^{c}	$0.079 \pm 0.02^{a,b}$

Addition of xanthan gum (0.1 – 0.3 %) to whey protein solutions led to a decrease in foam overrun which was more pronounced at higher gum concentrations i.e. 0.3 % (Table 4.2). Xanthan gums linear structure gives it the capability to increase the bulk viscosity of solutions even at low concentrations (Dabestani and Yeganehzad, 2019). A decrease in overrun can be a consequence of increased viscosity and fluid resistance against air incorporation (Dabestani and Yeganehzad, 2019; Liszka-Skoczylas *et al*., 2014; Zmudziński *et al*., 2014). This leads to a limited number of protein molecules unfolding and diffusing at the interface, thus a lower overrun in the resultant foam (Lau & Dickinson, 2004).

Whipping time affected the foam overrun of these samples. The protein only sample had an optimum overrun after 5 min whipping; increasing whipping time decreased foam overrun. When XG (0.1 – 0.3 %) was introduced, increasing the whipping time from 3 to 10 min led to increases in the foam overrun (Table 4.2).

Table 4.2 Effect of xanthan gum concentration and whipping time on 10 % whey protein foam overrun. Data (n=3) are presented as the mean ± SD. Data with different lowercase superscript letters within a column and uppercase superscript letters within a row indicate significant differences.

Whipping time	**Foam overrun (%)**			
Min	**0 % XG**	**0.1 % XG**	**0.2 % XG**	**0.3 % XG**
3	689 ± 9.62^{bA}	489 ± 19.25^{cB}	378 ± 38.49^{dC}	122 ± 26.29^{dD}
5	761 ± 19.25^{aA}	522 ± 28.87^{cBC}	539 ± 45.53^{cB}	511 ± 19.25^{cC}
7	694 ± 9.62^{bA}	650 ± 28.87^{bB}	633 ± 28.87^{bBC}	606 ± 9.62^{bC}
10	683 ± 19.25^{bB}	706 ± 9.62^{aA}	706 ± 9.62^{aA}	650 ± 19.25^{aC}

Foam stability was greatly improved with XG incorporation. For the protein only sample extending whipping for longer than 2.5 min improved foam stability. At 2.5 min the foams had a stability of 82 %, which increased to 98 % for 5 – 20 min whipping. However, the foam drained within the duration of the assay. With xanthan gum addition foam stability increased to 100 % regardless of whipping time. At 0.1 and 0.2 % XG the foams remained stable for 24 h but drained thereafter. With 0.3 % XG addition, the foam remained stable for considerably longer (approx. 48 h.) before any drainage occurred. Both increased viscosity and decreased surface tension can help retard drainage and impede gas diffusion. Xanthan gum's weak gel-like properties and pseudo-plastic flow properties enable it to provide colloidal systems with long-term stability (Moschakis *et al*., 2005).

Foams containing XG appeared denser and creamier compared to the protein only samples. This observation can be supported by results from Zmudziński *et al*. (2014) who describes how xanthan gum can adopt a helical conformation and bind large quantities of water, therefore making a foam more dense. This increase in foam density has been reported by previous studies (Liszka-Skoczylas *et al*., 2014; Zmudziński *et al*., 2014).

Image analysis showed that whey protein only foams appeared polydisperse whereas WPI/XG foams appeared more monodisperse (Fig. 4.1). With xanthan gum addition the bubble area decreased with increasing XG concentration from 0.1 – 0.3 % (Table 4.1). The bubble walls were also found to gradually thicken with XG addition (Table 4.1). Studies have found that in foams smaller bubbles typically burst at the expense of larger bubbles (coarsening) or the smaller bubbles join to form larger bubbles (coalescence) (Lau and Dickinson, 2005; Lomolino *et al*., 2015; Pithia and Edwards,

1994; Yang *et al*., 2009). These destabilisation mechanisms lead to unstable foams and eventually foam collapse. With the incorporation of xanthan gum, it showed that the bubbles were both smaller and appeared more monodisperse. This may suggest that the destabilisation mechanisms are reduced or prevented as the bubbles are of more uniform size. Kampf *et al*. (2003) found that xanthan gum addition strengthened the bubble films of the foams, by providing an additional polymeric network and increasing wall stiffness. This strengthening mechanism explained by Kampf *et al*. (2003) may explain the increased foam stability.

Even though the addition of xanthan gum resulted in reduced overrun compared to the protein only samples, it was found that with increased whipping time the overrun was improved. Whey protein required 5 min whipping to produce the highest overrun whereas when XG (0.1 – 0.3 %) was added, the solution required 10 min whipping. Since 0.3 % XG produced foams with good overrun and stability, this concentration was chosen for the remainder of experiments.

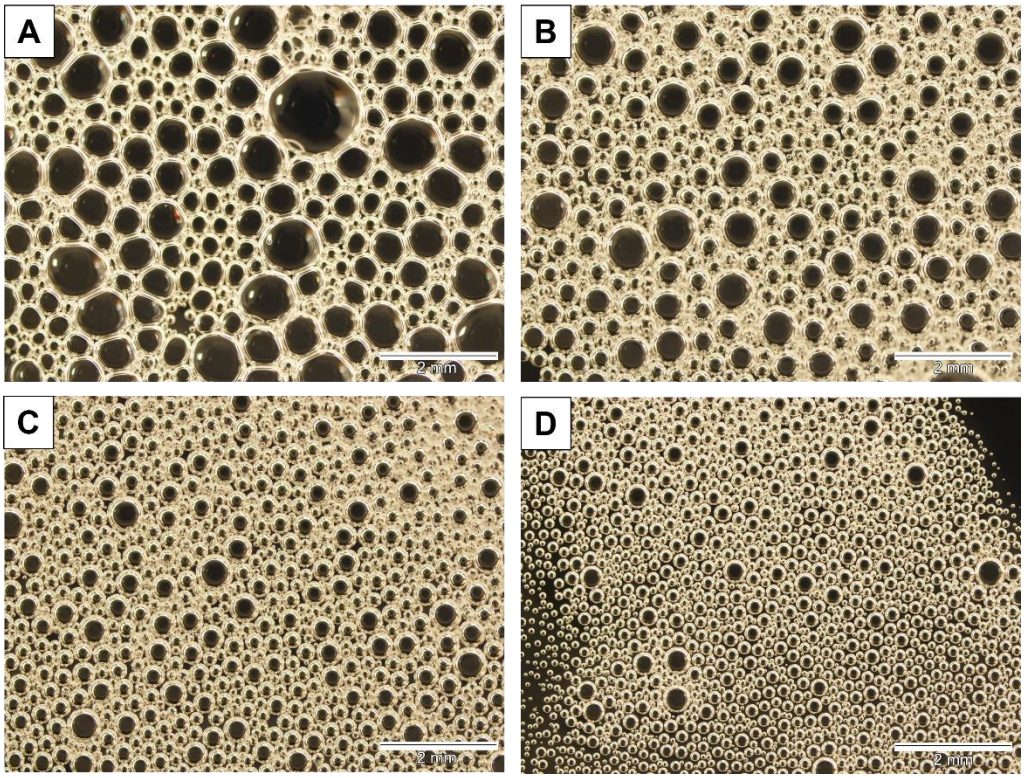

Fig. 4.1 Light microscope images of 10 % whey protein foams prepared using whey protein only (A), with 0.1 % XG (B), with 0.2 % XG (C) and with 0.3 % XG (D), within 10 min of foaming. Scale bar for each concentration represents 2 mm.

4.2.2 Effect of pH on WPI/XG foams

Protein/polysaccharide coacervation is dependent on the electrical charges on the biopolymers which dictates if segregative or associative phase separation will occur (Souza and Garcia-Rojas, 2017). Proteins have a positive net charge at pH below their pI and carry a negative net charge above the pI. Xanthan gum is a highly charged anionic polysaccharide. Complete compatibility can occur when protein and XG exist in solution with opposite charges forming strong electrostatic complexes (Rodriguez Patino and Pilosof, 2011; Laneuville *et al*., 2000). However, repulsive interactions between proteins and polysaccharides occurs when they are present with the same charge which can lead to mutual exclusion. However, at high polymeric concentration with the same surface charge, thermodynamic incompatibility occurs, which is the main cause of synergistic effects (Rodriguez Patino and Pilosof, 2011; Doublier *et al*., 2000).

Adjusting the pH (pH 3 – 8) of whey protein only foams was found to significantly affect foam overrun (Fig. 4.2). Whey protein foam overrun increased gradually when the pH was adjusted from pH 3 up to pH 5, where the highest overrun occurred. As found in chapter 3, the isoelectric point of WPI was in close proximity to these pH values (4 – 5). At the isoelectric point of a protein, foaming properties are optimal due to electrostatic repulsion being minimised and hydrophobic interactions being favoured (Foegeding *et al*., 2006). In chapter 3, when the pH was altered above pH 5, the overrun decreased. At higher pH, the reduction in foam overrun may be due to increased protein solubility as a result of the high electrostatic repulsion between the protein molecules, leading to fewer proteins being adsorbed at the air/water interface (Kuropatwa *et al.*, 2009). With the addition of xanthan gum, the overrun was highest at pH 3 and 4 and decreased thereafter with increasing pH (Fig. 4.2). At these pH values, the complexes of WPI and XG are neutral (zero-net charge) and thus leads to increased foam overrun.

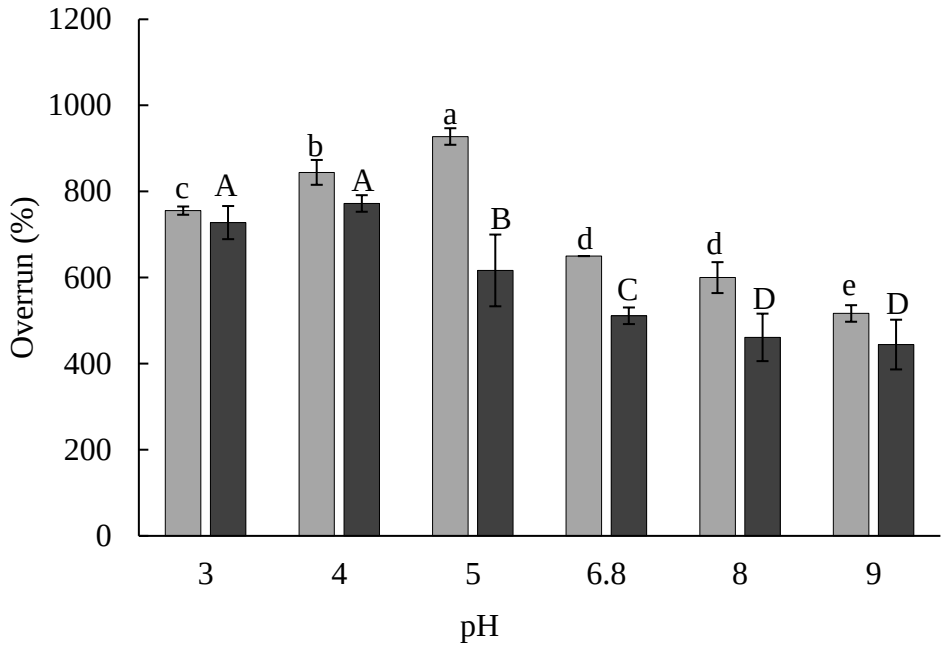

Fig. 4.2 Effect of pH on foam overrun of 10% WPI (grey) and 10 % WPI with 0.3% XG (black). Data (n=3) are presented as the mean ± SD. Data with different letters indicate significant differences. Small letters indicate significant differences between WPI only foams, capital letters indicate significant differences between WPI/XG foams.

Whey protein foams were most stable close to the isoelectric point, however, with 0.3 % XG addition, the least stable foams were produced at this pH. With added xanthan gum the most stable foams was found at pH above the protein isoelectric point. Above this pH, proteins carry a net negative charge. It is possible therefore that thermodynamic incompatibility occurred due to the presence of the same charge on each biopolymer. According to Rodriguez Patino and Pilosof (2011), the unfavourable repulsive interactions between the proteins and xanthan gum may have led to the separation of the biopolymers into two distinct phases. This commonly occurs with semi-dilute or concentrated mixed solutions of protein and polysaccharides and is the main cause of synergistic effects (Rodriguez Patino and Pilosof, 2011). Perez *et al.* (2010) found that at neutral pH, the adsorption of β-lactoglobulin in the presence of xanthan gum could have been positively influenced by thermodynamic incompatibility that resulted in better surface-active and viscoelastic properties of the adsorbed film as protein-protein interactions were favoured.

It is likely that several different interactions can occur between proteins and polysaccharides. As previously described by Zmudziński *et al.* (2014), protein molecules

can get entangled and inter-linked with xanthan gum molecules when the solutions are whipped which is followed by the formation of structures that can increase the viscosity of the continuous phase, improving stability. On the other hand, thermodynamic incompatibility can occur depending on the electrical charge of the solution, leading to synergistic effects. Indeed, it is possible that either of the mentioned interactions could occur.

4.2.3 Effect of NaCl on WPI/XG foams

Addition of NaCl (0.05 – 0.2 M) to the protein only sample increased the foam overrun (chapter 3). With further addition to 0.4 M, foam overrun decreased. As found by Nicorescu *et al*. (2008), electrostatic repulsion between the proteins at the interface are reduced with salt addition, leading to an increase in protein adsorption (Nicorescu *et al*., 2008). The addition of low concentrations of salt to protein solutions increases the protein solubility, whereas high ionic strength decreases the solubility (Damodaran *et al*., 2007).

In contrast, the addition of NaCl to WPI/XG foams decreased the foam overrun which became more pronounced with increasing ionic strength (Fig. 4.3). These results indicate that WPI/XG foams were affected by NaCl addition. The addition of salt to protein/polysaccharide complexes has been found to have a dissociating effect on the complexes (De Kruif *et al*., 2004). Souza and Garcia-Rojas (2017) found that complex formation of egg albumin and xanthan gum was inhibited with the addition of NaCl as the ions screened the reactive sites at the biopolymer's surface. The results from these studies could explain why overrun values decreased with XG addition in the presence of sodium chloride.

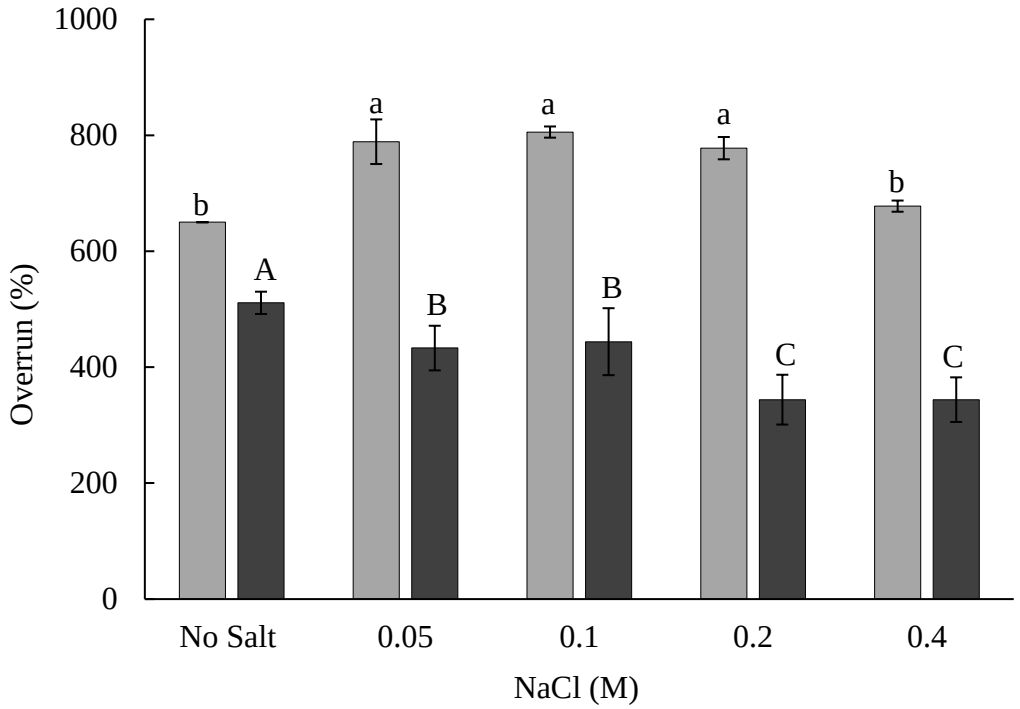

Fig. 4.3 Effect of NaCl concentration on 10% WPI (grey) and 10 % WPI with 0.3% XG (black) foam overrun. Data (n=3) are presented as the mean ± SD. Data with different lowercase and uppercase letters indicate significant differences for WPI only foams and WPI/XG foams respectively.

Foam stability for the control whey protein solution was unaffected by salt addition, with stability ranging 93 – 96 % irrespective of NaCl concentration. Similarly, NaCl did not have an effect on the foam stability of WPI/XG solutions, remaining at 100 % stability. The overrun and stability of whey protein was affected differently by xanthan gum and ionic strength. The rationale as to why foam overrun decreased cannot be used to describe what occurred for foam stability. The inhibition of complex formation between the proteins and xanthan gum due to NaCl as suggested by Souza and Garcia-Rojas (2017) did not affect the foam stability. Stability could have remained unaffected due to the high viscosity, low surface tension or smaller bubble area of the protein/polysaccharide solutions.

4.3 Conclusion

The present study clearly indicates that xanthan gum addition to whey protein leads to both positive and negative effects on the foam properties. Its addition reduced

the foam overrun regardless of concentration used (0.1 – 0.3 %) while it enhanced foam stability extending it for a period of days rather than hours. The increased viscosity with increasing xanthan gum concentration prevented incorporation of sufficient amounts of air into the solutions, thus lowering foam overrun. However, this increased viscosity along with smaller bubbles areas, thicker bubble walls and lower surface tension values positively improved foam stability.

Both pH and ionic strength were found to influence foam formation. The optimum foam overrun for the WPI protein only solutions occurred at pH 5. With xanthan gum addition the highest overrun occurred at pH 3 and 4, due to the neutral charge of the complex. The WPI protein only solutions were also found to be most stable at the pI. However, with xanthan gum addition stability was lowest at this pH, which could be due to thermodynamic incompatibility because of electrostatic repulsion between the molecules. Salt addition impaired the WPI/XG foams overrun, however, it did not affect foam stability.

From a food product perspective, these environmental conditions can be considered as they influence the protein/ polysaccharide foams differently. If a voluminous food is required, the use of less XG could be pursued but if a product with low volume, high stability is required, larger amounts of XG can be used.

Chapter 5
Whey protein microgels for stabilisation of foams

Data in this chapter has been published in *International Dairy Journal* (Lee, J., Duggan, E. 2022 Whey protein microgels for stabilisation of foams). https://doi.org/10.1016/j.idairyj.2022.105399

*Additional fabrication methods have been included in this chapter

5.1 Introduction

Foams consist of air bubbles distributed throughout a continuous aqueous phase separated by films called lamellae. The surface tension between the air/water interface is five times larger than that between water and oil (Lazidis *et al*., 2016). According to Hill & Eastoe (2017) the surface tension phenomenon is due to the imbalance of attractive intermolecular interactions at the surface of the liquid. Additional energy is required to create the interface between air and water which is attributed to the surface tension. Therefore, foams require amphiphilic entities to adsorb at the surface to reduce the tension.

Pickering stabilisation has been found to protect bubbles against coalescence, whereby closely packed solid particles adsorb at the interface forming a monolayer around a bubble. When two bubbles come in to close proximity, the particle layer prevents coalescence, thus stabilising the bubble (Dickinson, 2017). In the past, most of the research has focused on using inorganic particles for stabilisation, such as silica particles (Lam *et al*., 2014). However, inorganic particles have limited relevance when it comes to an application requiring biocompatibility and biodegradability, thus making them unsuitable for food foams (Lam *et al*., 2014).

In recent years there has been increased interest in the use of microgels for foam stability as they are deformable and versatile (Schmitt *et al.*, 2014). These microgel particles are soft porous particles made from polymers such as proteins or polysaccharides. Studies in recent years have shown that microgels can lead to dispersions being far more stable than those produced by surfactants (Lazidis *et al*., 2016; Li *et al*. (2020b) ; Asghari *et al*., 2016; Ellis *et al*., 2019). The reason for this is because the energy of desorption is greater for a particle than for a smaller surfactant (Cox *et al*., 2009).

Food proteins are defined as those that are non-toxic, easily digestible, available in abundance, nutritionally adequate and sustainable agriculturally (Damodaran *et al*., 2007). Whey proteins are known for their high nutritional value and functional properties and are widely used in the food industry for nutritional purposes such as prevention of cancers (Gill and Cross, 2000), antioxidant activity (Bayram *et al*., 2008) and use for weight management due to the satiety effect of whey proteins (Weigle *et al*., 2005). Many proteins are insoluble at their isoelectric point (pI), making it difficult to use them in solution around this pH. However, whey proteins are soluble at their pI and can be utilised, making them applicable for addition into acidic beverages such as fruit juices or

soft drinks (Ustunol, 2014 & Ron *et al.*, 2010). Whey proteins are also utilised as functional ingredients in foods due to their ability to form gels and emulsions and can act as delivery vehicles for bioactive compounds (Lee & Duggan, 2022; Bryant & McClements, 2000; Lazidis *et al*., 2016; Li *et al.*, 2022; Abbasi *et al.*, 2014; Madadlou *et al*., 2020; Tan *et al*., 2019).

In this study, cold-set gelation was used to make microgel particles. This involves heating a solution of native protein while controlling pH and protein concentration; this causes partial protein unfolding which exposes thiol groups (Kuhn *et al*., 2010). Reducing the electrostatic repulsion between the protein aggregates will initiate cold-set gelation. This is done by increasing the mineral content or adjusting the pH of the solution (Bryant and McClements, 2000).

There are two main ways, mechanistically speaking, for microgel particles to function as stabilising agents and foams. The particles can create a gel-like network within the spaces amongst the gas bubbles when they are present at high concentrations in the bulk continuous phase. On the other hand, the particles can generate a particle-loaded surface layer by becoming directly attached to the air-water interface, which works to protect the bubbles (Dickinson, 2017). A combination of these mechanisms can be present in a multi-phase food system as some particles may be dispersed in the bulk phase while others are located within the thin liquid film.

The objective of this study was to investigate the potential of whey protein microgel particles to produce and stabilise foamed systems for prolonged periods. The particle stabilised foams were compared with foams produced with native whey protein.

5.2 Results and discussion

5.2.1 Effect of manufacturing method on WPI gel formation

Several methods were trialled to ascertain the optimal method for microgel formation. The methods which consisted of (A) pipetting denatured WPI into 0.1 M $CaCl_2$, (B) submerging denatured WPI in 0.1 M $CaCl_2$, (C) dispensing denatured WPI through a pipette tip using a peristaltic pump into 0.1 M $CaCl_2$ or (D) adding $CaCl_2$ (0.02 – 0.1 M) to denatured WPI under stirring, formed different microgels. The various fabrication methods (A - D) were found to have a significant effect on the WPI gel appearance. The particles formed from methods A and B were too large and unable to be

measured using the Mastersizer, instead, they were measured using a ruler. For method A, the particles varied in size depending on the quantity of protein solution pipetted into the gelling solution ($CaCl_2$). When an aliquot of 20 µL of WPI was used smaller particles were formed (1 – 1.5 cm), whereas when a larger volume of 100 µL was used the particles were larger (1.5 – 2 cm) (Fig. 5.1A). When the WPI was first pipetted into the $CaCl_2$ solution the particles appeared almost transparent, however, over time they became opaque. Method B led to the formation of a monolith gel which was formed directly on submerging the denatured WPI in the calcium chloride solution. This monolith had a diameter of about 6 cm (Fig. 5.1B).

The smaller particles produced from method C and D could be measured using the Mastersizer. For method C, a peristaltic pump was used to continuously inject denatured WPI into 0.1 M $CaCl_2$ solution, forming particles dispersed in a calcium chloride solution (Fig. 5.1C). Method D formed opaque sols after the addition of 0.02 - 0.1 M $CaCl_2$ to denatured WPI, as varying $CaCl_2$ concentration has been found to have different effects on whey protein aggregation and particle size (Beaulieu *et al*., 2002; Zhu & Damodaran, 1994a). The use of 0.02 M $CaCl_2$ formed a macro gel block rather than discrete particles, therefore particle size could not be measured. The macro gel appearance was similar to Fig. 5.1B.

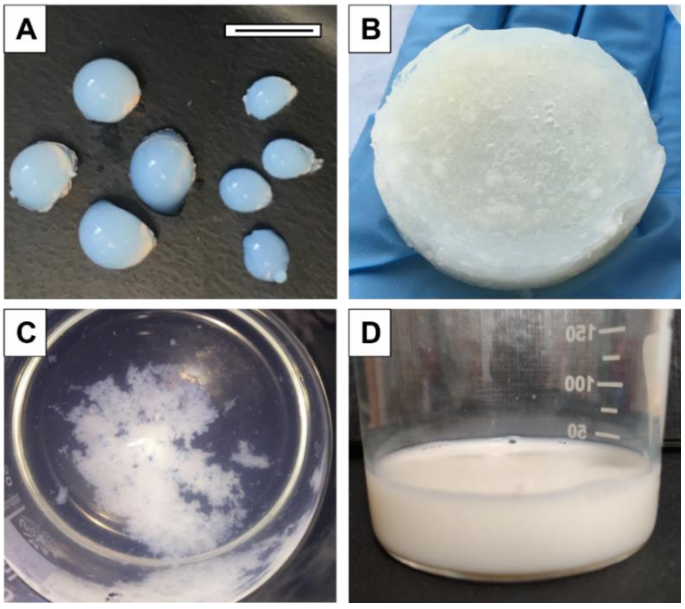

Fig. 5.1 Digital images of microgels fabricated using method A - D. (A) Method A - microgels made with 100 µl $CaCl_2$ (left) and 20 µl $CaCl_2$ (right), scale bar represents 2 cm, (B) Method B - monolith microgel, (C) Method C - peristaltic pump and (D) Method D - microgels formed by 0.1 M $CaCl_2$.

Table 5.1 Particle size of whey protein microgel particles fabricated from method C and D. Data (n=3) are presented as the mean ± SD. Data with different superscript letters indicate significant differences.

	Method ($CaCl_2$)			
	C	**D (0.02 M)**	**D (0.05 M)**	**D (0.1 M)**
D (3,2) (µm)	26.37 ± 0.44^{c}	N/D	97.30 ± 0.13^{a}	43.88 ± 2.46^{b}

*Addition of 0.02 M $CaCl_2$ formed a macro-gel and could not be measured by the Mastersizer.

For particles formed by addition of $CaCl_2$ to denatured WPI, the particle size was dependent on calcium concentration; as the calcium chloride concentration increased the particle size decreased. More available $CaCl_2$ could have led to higher aggregation activity of the unfolded interactive sites of whey protein leading to smaller more tightly packed microgel particles. With less $CaCl_2$ present, it could be possible that the unfolded loose strands of whey protein were not fully aggregated due to insufficient $CaCl_2$ to screen electrostatic repulsion, leading to larger particles. It is also possible that more available calcium ions led to more protein aggregation sites which would in turn lead to more numerous but smaller aggregates, whereas lower concentrations of calcium could have led to the formation of fewer but larger protein aggregates which further led to the formation of a protein macro-gel at 0.02 M $CaCl_2$. Other studies have also found that the aggregation of WPI increased progressively with increased concentration of $CaCl_2$ and also the size of the particles decreased with increased calcium (Beaulieu *et al*., 2002; Zhu and Damodaran, 1994a).

5.2.2 Establishing the optimum microgel fabrication method for foaming

In this study, the foaming properties of the microgels were tested 24 h after $CaCl_2$ addition. Samples were whipped for 5 or 10 min to establish if whipping time affected the overall foaming ability of the microgels. The particles made by pipetting denatured WPI into excess $CaCl_2$ were too large and solid to be whipped alone, therefore they were directly incorporated into a whey protein solution to analyse their foaming ability. However, when whipped they were too large and did not become integrated within the foam matrix and precipitated instantly from the foam. Therefore, this method for microgel

formation was not pursued, due to the incapability of the particles to be incorporated into protein solutions for foam formation.

It was thereafter decided to whip the microgels directly rather than trying to incorporate them to another protein solution. In doing this, several options were explored, described as methods B – D. It was found that whipping for 10 min led to slightly better foam overrun values compared to 5 min whipping regardless of $CaCl_2$ concentration or microgel preparation method (Table 5.2).

There was little foam production from method B (monolith gel) as there were only small amounts of air incorporated into the gel. The foam overrun only increased by 6 and 39 % when whipped for 5 and 10 min respectively. It appeared that whipping of the monolith led to the break-up of the gel into smaller pieces. For method C, air incorporation was also very low (Table 5.2). Image analysis of these samples showed the presence of pieces of gel with very few bubbles (image not shown). As air incorporation into the samples was very low and there was mostly only gel pieces present, these were not true foams but rather whipped gels. The stability of the whipped gels from method B – C were good (87 – 93 %), which did not differ with whipping time. These methods were not pursued for further analysis due to their inability to form foam sufficiently.

Table 5.2 Foam overrun (%) at 5 or 10 min whipping of microgel particles fabricated by methods B - D. Data (n=3) are presented as the mean ± SD. Data with different lower case superscript letters within a column and data with different upper case superscript letters between rows indicate significant differences.

	Overrun (%)	
Method	**Whipping time**	
	5 min	**10 min**
Native WPI	761 ± 9.62^{aA}	683 ± 16.67^{aB}
B	106 ± 9.62^{dB}	133 ± 28.87^{dA}
C	106 ± 9.62^{dB}	133 ± 28.87^{dA}
D (0.02 M)	189 ± 19.25^{cB}	289 ± 19.25^{cA}
D (0.05 M)	283 ± 28.87^{bA}	317 ± 28.87^{cA}
D (0.1 M)	306 ± 9.62^{bB}	378 ± 19.25^{bA}

The addition of calcium solutions to denatured WPI (method D) to form microgels led to better foam formation. With increasing calcium concentration and increased

whipping time from 5 to 10 min, the foam overrun increased. This could be due to the smaller particle size at higher ionic concentrations. The smaller particles could be more capable of adsorbing at the air/water interface than the larger microgels. Other studies have also found that the foamability of β-lactoglobulin (β-lg) microgels or whey protein fluid gels depended on particle size (Rullier *et al*. 2008; Murphy *et al*. 2016; Lazidis *et al*., 2016). The authors found that smaller protein particles could adsorb more quickly at the interface than larger particles facilitating foam formation. In addition, the microgels formed at lower ionic strength had higher viscosity values, which could have contributed to lower foam overrun. On addition of 0.02 M $CaCl_2$ the microgel sol viscosity was 7576 mPa which decreased to 1659 mPa when 0.1 M $CaCl_2$ was added (Table 5.3). Increased viscosity minimises the incorporation of air into the system which leads to reduced foam overrun (Rodriguez Patino *et al*., 1995). Tomczyńska-Mleko (2013) used a similar method to form aerated gels, however, differences occurred as the authors formed a semisolid continuous gel with air bubbles present within the continuous gel. In this study, microgel solutions were formed whereby when whipped, the microgels resided in the continuous phase stabilising the air bubbles. Additionally, the concentrations used by Tomczyńska-Mleko (2013) are similar to the low concentration of 0.02 M used in this study which in both cases led to the formation of a continuous gel.

Table 5.3 Viscosity values of native WPI and microgels left to cross-link with $CaCl_2$ after 0 and 24 h. Data (n=3) are presented as the mean ± SD. Data with different superscript letters within a column indicate significant differences.

	Viscosity (mPa)	
$CaCl_2$ (M)	**0 h**	**24 h**
Native WPI	3.42 ± 0.10^{c}	N/D
0.02	181.42 ± 10.56^{a}	7576.32 ± 171.74^{a}
0.05	114.43 ± 3.35^{b}	3095.10 ± 253.80^{b}
0.1	108.83 ± 2.63^{b}	1659.26 ± 649.33^{b}

Regardless of the concentration of $CaCl_2$ added, small amounts of liquid drainage did occur with stability values ranging 88 – 93 %. After the 60-min test period the liquid drainage from these foams stopped.

The foams produced from the microgels fabricated from methods that involved the addition of denatured WPI to an excess of $CaCl_2$ (Methods A – C) were not true foams as the overrun values were so low that there was little air incorporated to be lost; thus, were not pursued further. However, the microgels produced by the addition of 0.02 - 0.1 M $CaCl_2$ to denatured WPI (method D) did produce true foams as the overrun values were substantially higher while also having excellent stability. Therefore, the remainder of the study focussed on the microgel foams formed from method D.

5.2.3 Native whey protein vs. whey protein microgel foaming

Having established the optimum microgel fabrication method for foaming, the foaming properties of microgels (cross-linked for 24 h) were compared with native WPI foams. Foaming of native whey protein solutions were found to be significantly affected by whipping time. The highest overrun occurred with 5 min whipping (761 %), but it decreased in volume when whipping was carried out for 10 min (683 %) (Table 5.2). The foam overrun of native WPI was significantly higher than the microgel foams regardless of whipping time (Table 5.2). Stability of the WPI foams was not significantly different between the two whipping times (94 – 98 %), however, these foams slowly drained after the 60-min test time and foams typically collapsed within 2 h.

For the microgels, small amounts of liquid drainage did occur with stability values ranging 88 – 93 % regardless of the concentration of $CaCl_2$ added. Stability of foams formed from 0.02 M $CaCl_2$ microgels were significantly lower than WPI foam stability. However, after the 60-min test period no further liquid drained from these foams. The remaining foam remained stable without further drainage for an extended period of > 2 years. This was measured periodically over 2 years by monitoring drainage from the covered foams stored at 4 °C, and in that time period no drainage occurred, and the foams remained visually intact. Another study formed aerated gels, however, they were not as stable as air only remained within the gels for 41 days compared to 2 years in this study (Tomczyńska-Mleko, 2013).

The microgel foams were found to have lower overrun but better foam stability compared to foams produced using native whey protein. The difference in overrun could have occurred because of the ability of the native whey protein to adsorb at the air/water interface at a faster rate than microgels due to the smaller size and mobility of native proteins (Li *et al.*, 2020b). Microgels at interfaces may take longer to adopt a favourable adsorption orientation compared to native WPI (Li *et al*., 2020b). Li *et al*. (2020b) found

that egg white protein foams had higher overrun than those formed using egg white protein microgels due to the size differences between protein molecules and microgels. Zhu & Damodaran (1994b) also found that smaller monomeric whey proteins were more capable of producing foam with higher overrun, but the larger polymeric protein molecules contributed to foam stability. The monomeric species were capable of rapidly migrating, adsorbing, and unfolding at the air/water interface contributing to foam formation while the aggregated proteins increased the viscoelastic properties of the films leading to more stable foams (Rullier *et al.*, 2008; Rullier *et al.*, 2010). Similarly Lazidis *et al.* (2016) found that their smaller protein particles could diffuse faster to the interface. The authors also found that their whey protein fluid gels could create the same amount of foam as native whey protein but with improved stability. The foam overrun of their native whey protein and whey protein fluid gels ranged from 197 – 240 % (Lazidis *et al.*, 2016). In this study, the WPI microgels foaming properties were greater as the microgel foams had significantly greater overrun (378 %), while also providing excellent stability.

Viscosity is another factor which influences the whipping ability of the samples. As shown in Table 5.3, native WPI had a much lower viscosity compared to the microgels. The viscosity of the microgels was greater due to their aggregated cross-linked structure. The large disparity between the viscosity values correlates with the overrun results as more viscous systems minimise the incorporation of air into the solution leading to lower overrun values.

The storage and loss moduli of the microgels were greater than those of native WPI (Fig. 5.2). The protein solutions without $CaCl_2$ remained in their native state where the protein molecules were flexible and free to move around displaying an entangled solution. However, with calcium addition to heat denatured WPI, much larger aggregates were present due to cross-linking of the protein molecules, and this contributed to a more interconnected elastic structure.

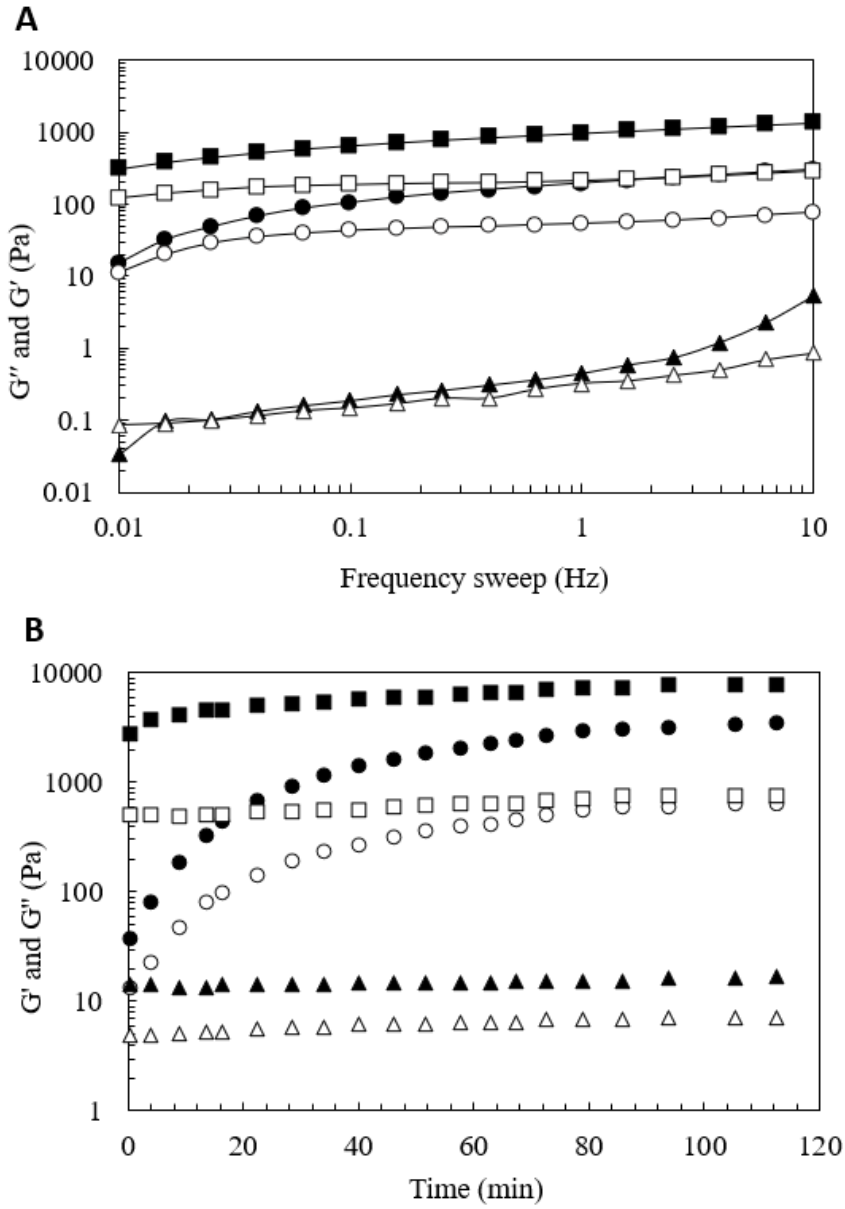

Fig. 5.2 Rheological properties for microgels formed using 0.1 M $CaCl_2$ (0 h vs. 24 h) and native WPI. (A) Frequency sweep. (B) Time sweep. ● 0 h G', ○ 0 h G", ■ 24 h G', □ 24 h G", ▲ Native WPI G' and △ G". Data (n=3).

The higher G' values of the microgels indicated that heat denaturation followed by $CaCl_2$ addition induced gel formation of the protein solutions (Nicorescu *et al.*, 2008). Whey protein microgels are not a build-up of simple polymer chains, but they possess a complex hierarchical structure that consists of clusters of aggregated denatured proteins (Schmitt *et al.*, 2010). The stronger microgel sols could have resulted in more stable foams as increased elasticity has been found to aid with foam solidity and thus foam stability (Nicorescu *et al.*, 2008; Rouimi *et al.*, 2005).

The addition of $CaCl_2$ to heat denatured WPI improved the foam textural properties as both foam firmness and consistency increased (Table 5.4). The addition of $CaCl_2$ strengthened the protein bonds to form cross-linked gelled networks which when whipped led to the formation of stronger foams.

Table 5.4 Texture parameters of native WPI, microgel foams calcium-cross-linked for 0 and 24 h and microgel foams stored for 6 months. Data (n=3) are presented as the mean ± SD. Data with different superscript letters within a column indicate significant differences.

Sample	Firmness ($N\ s^{-1}$)	Consistency ($N\ s^{-1}$)
Native WPI	0.58 ± 0.05^{d}	7.12 ± 0.31^{d}
0h cross-linked microgel foam	2.51 ± 0.20^{c}	22.60 ± 2.31^{c}
24h cross-linked microgel foam	0.75 ± 0.06^{d}	9.10 ± 0.75^{d}
0h cross-linked microgel foam stored for 6 months	6.58 ± 0.37^{a}	46.10 ± 1.67^{a}
24h cross-linked microgel foam stored for 6 months	3.89 ± 0.33^{b}	40.27 ± 0.82^{b}

Image analysis of these foams indicated that the microstructure of the native whey protein and the microgel foams differed (Fig. 5.3). On a macroscopic level both foams appear similar, however, the bubbles were visibly larger in the native WPI foam (Fig. 5.3A and 5.3C). On a microscopic level, the native protein foam appeared as just bubbles surrounded by their liquid wall (Fig. 5.3B) while the microgel foams showed bubbles surrounded by cloudy gel-like white regions (Fig. 5.3D). The native protein foams had an average bubble area of $0.03 \pm 0.02\ mm^2$ and a bubble wall thickness of 0.06 ± 0.02 mm. The bubble area or wall thickness could not be measured for the microgel stabilised foams as the presence of gel-like white regions hindered the ability of the software to accurately measure these values as the white regions obstructed the bubbles. However, visually, it is evident that the bubbles in the microgel foams were smaller than those in the native whey protein foams. This difference in microstructure could potentially contribute to the extreme stabilising ability of microgels to form ultra-stable foams.

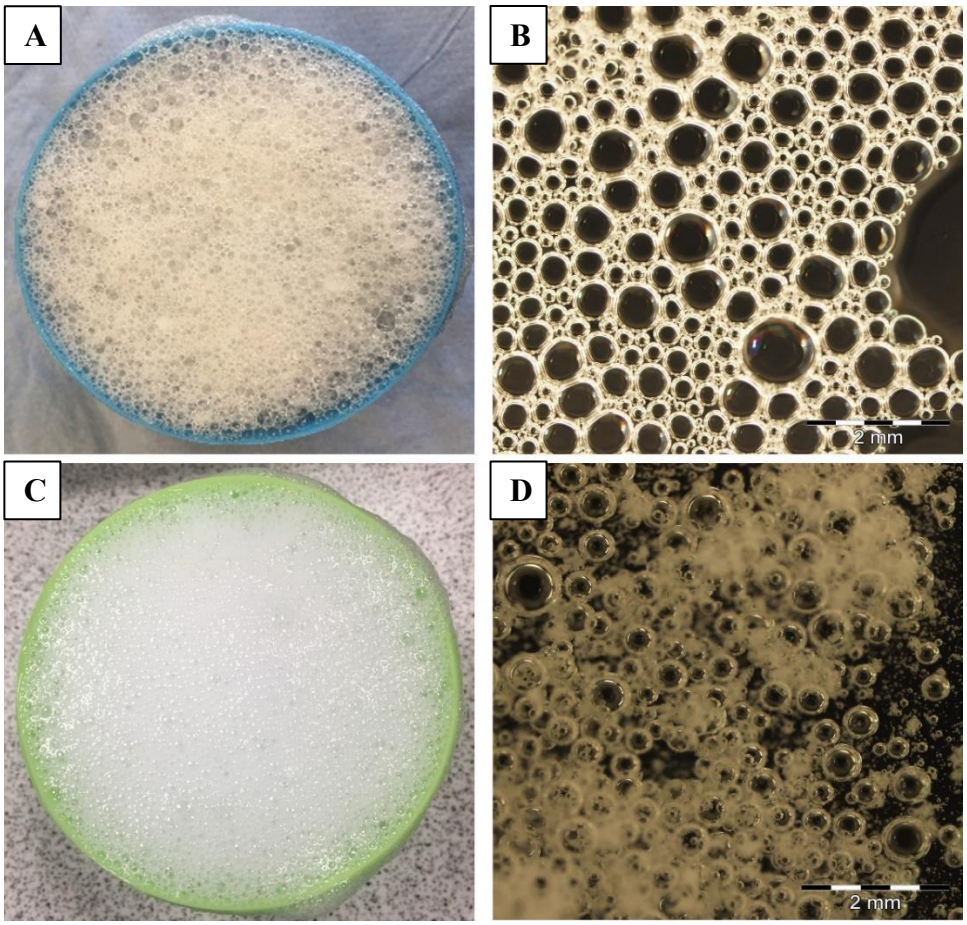

Fig. 5.3 Images of 10 % WPI foam; macroscopic foam (A) and a microscopic foam (B). Microgel foam formed from 0.1 M $CaCl_2$ and whipped; macroscopic (C) and microscopic (D). Scale bar represents 2 mm.

The presence of a gelled network amongst the bubbles could have reduced foam destabilisation by preventing/ reducing bubble coalescence. The scanning electron microscopy image in Fig. 5.4 showed microstructures of a porous interconnected structure suggesting that the air bubbles were trapped and stabilised amongst a cohesive network formed by the microgels. Other studies have found that particles can remain in the liquid phase where they could act as corks and increase the viscosity thus, slowing down or eliminating drainage (Gharbi and Labbafi, 2019; Rullier *et al*., 2008).

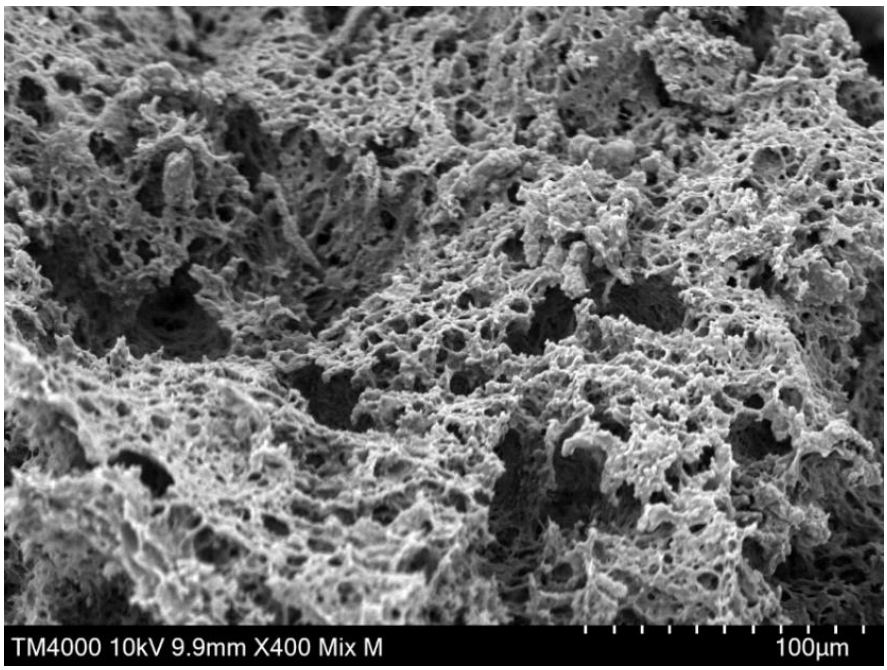

Fig. 5.4 Scanning electron microscopy image of WPI microgel foams.

5.2.4 Effect of cross-linking time on microgels

The effect of crosslinking time of the microgels rheological, textural, and foaming properties was investigated. As shown in Table 5.2, native WPI produced foams with high overrun but low stability, while the opposite occurred for the WPI microgels. Therefore, it was decided to examine foaming microgels immediately on $CaCl_2$ addition (0.1 M) without any crosslinking time (0 h cross-linking) to see whether the foams could benefit from being unfolded while also forming cross-links upon $CaCl_2$ addition to produce foams with a combined functionality with greater overrun and stability.

Frequency and time sweep of the microgels that were left to cross link for 0 and 24 h were compared (Fig. 5.2). Frequency sweeps are carried out to characterise biopolymer systems where entangled solutions, weak gels and strong gels can be identified (Garrec and Norton, 2012). The microgels were found to be marginally dependent on frequency, G' and G" increased slightly as the frequency increased from 0.01 – 10 Hz and they were found to be more elastic than viscous (Fig. 5.2A). The storage and loss moduli of the microgels that were cross-linked for 24 h were considerably greater than those cross-linked for 0 h. This suggests that longer cross-linking allowed proteins more time to aggregate and become internally covalently cross-linked, leading to the formation of stronger microgels.

After $CaCl_2$ addition (0 h), G' and G" increased markedly until approx. 40 min, thereafter G' and G" plateaued (Fig. 5.2B). In comparison, the microgels cross-linked for 24 h showed slight increase in G' and G" before reaching a plateau. This suggested that on addition of $CaCl_2$ the denatured WPI formed microgels with increased structuring within the sample, whereas after 24 h there was little structuring occurring as the microgels were mostly formed. For both samples (0 h vs. 24 h) the storage modulus was greater than the loss modulus which signifies typical features of an interconnected structure (Moakes *et al*., 2015).

Foam overrun values were considerably higher for foams cross-linked at 0 h compared to those cross-linked for 24 h regardless of $CaCl_2$ concentration (Table 5.5). The stability of the 0 h cross-linked microgel foams was also greater (100%) as there was no drainage, whereas the microgels that were left to cross-link for 24 h had ~ 10% loss as liquid drained from the foams. The microgel foams remained stable for > 2 years forming ultra-stable foams.

Table 5.5 Overrun values of microgels that were left to cross-link with $CaCl_2$ for 0 h and 24 h. Data (n=3) are presented as the mean ± SD. Data with different superscript letters within a column indicate significant differences.

	Overrun (%)	
$CaCl_2$ (M)	**0 h**	**24 h**
0.02	683 ± 48.11^{b}	289 ± 19.25^{b}
0.05	717 ± 15.91^{b}	317 ± 28.87^{b}
0.1	756 ± 9.62^{a}	378 ± 19.25^{a}

The viscosity of the microgel sol measured directly after calcium addition was lower compared to that cross-linked for 24 h (Table 5.3). This lower viscosity coupled with weaker storage and loss moduli might have allowed more air to be incorporated into the system leading to greater foam formation while also allowing the microgels to adsorb at the air/water interface at a faster rate than the 24 h cross-linked microgels. Also, because the microgels cross-linked for 0 h were forming over time they could have been continually strengthening the foam leading to a more stable structure.

The textural parameters in Table 5.4 indicated that the 0 h cross-linked microgel foams were firmer and more consistent than foams formed from 24 h cross-linked

microgels. Similar results were found by Nooshkam *et al*. (2022), whereby foams with the greatest overrun had greater texture parameters. However, the authors suggested that the air bubbles within the continuous phase acted as active filler particles, enhancing the strength of the foam as a consequence of their close packing and connection.

The texture of the microgel foams were also measured 6 months after formation. Foam firmness and consistency significantly increased regardless of cross-linking time, however, foams formed from 0 h cross-linked microgels had higher firmness and consistency after 6 months. Fig. 5.5 shows an image of foams made from 0 h and 24 h cross-linked microgels. The picture of the foams was taken 6 months after they were made. The 0 h cross-linked microgel foam held its shape better than the 24 h cross-linked microgel foam. The cross-linking was not saturated in the 0 h sample, and post foaming, it continued to cross-link, forming stronger interparticle cross-linking around the air bubbles. On the other hand, cross-linking was saturated in the 24 h sample, which led to much less interparticle cross-linking post foaming. However, both foams were very stable, displaying self-supporting structures. Foams stabilised by WPI microgels clearly show stability well in excess of food surfactants in aerated systems.

Texture analysis of the foams supports the stability results of the microgels cross-linked for 0 or 24 h. The foams formed from WPI whipped directly after $CaCl_2$ addition (0 h) had zero drainage and were found to be firmer and more consistent compared to the 24 h cross-linked microgel foams. The improved texture of the foams could have aided to prevent liquid drainage.

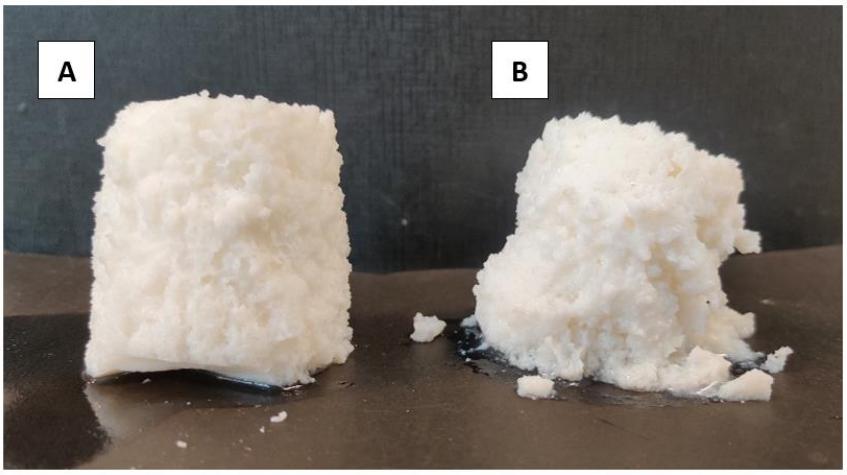

Fig. 5.5 Foams formed from microgels cross-linked for (A) 0h and (B) 24h. Image taken 6 months after foams production.

5.2.5 SDS-Page, free sulphydryl content and surface hydrophobicity

SDS-PAGE images of the samples are represented in Fig. 5.6. Whey protein heated to 80 °C was analysed to show the effect of heat on protein structural changes. Upon heating WPI to 80 °C and cross-linking for 0 and 24 h, the electrophoretic patterns under non-reducing conditions showed polymeric bands at the top of the gel which were unable to enter indicating that the molecular weight of the sample was >260 kDa. Monomeric bands corresponding to α-lactalbumin (α-la) (~14 kDa), β-lg (~18 kDa) and bovine serum albumin (BSA) (~66 kDa) were evidently less visible than those found in native WPI, indicating that the monomeric proteins were polymerised into aggregates. Similar results have been found by Zhu & Damodaran (1994b) & Hongsprabhas and Barbut (1997) whereby heated whey protein molecules aggregated and could not enter the gel. There are differences between the 0 and 24 h cross-linked microgel bands, the monomeric bands of α-la and β-lg are less visible for the 24 h cross-linked gels indicating that more of the monomeric proteins were polymerised into microgels. It can also be seen that the 24 h cross-linked microgels could barely enter the gel indicating their larger size due to the longer cross-linking time for polymer network formation. Under reducing conditions in all lanes, the bands corresponding to the protein aggregates that were unable to enter the gel disappeared and instead there were strong distinct bands corresponding to α-la, β-lg and BSA. The electrophoretic patterns of the heated WPI and the microgels were indistinguishable from native WPI, indicating that the protein aggregates and microgels were formed via disulphide-sulphydryl interchange reactions (Davis and Foegeding, 2004).

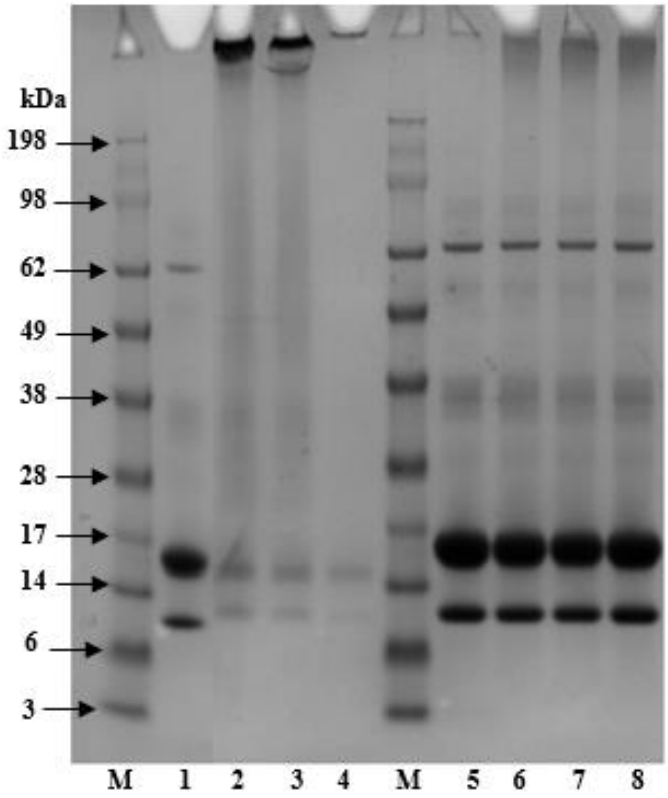

Fig. 5.6 SDS-polyacrylamide gel electrophoresis of WPI dispersions at 0.2 %. Lanes M represent the standard marker. Lane 1 – 4 nonreduced and lane 5 – 8 reduced. Nonheated native WPI (lane 1), WPI heated to 80 °C (lane 2), 0 h cross-linked microgel (lane 3), 24 h cross-linked microgel (lane 4), nonheated native WPI (lane 5), WPI heated to 80 °C (lane 6), 0 h cross-linked microgel (lane 7), 24 h cross-linked microgel (lane 8).

The content of accessible sulphydryl groups increased when WPI was heated to 80 °C as a result of WPI unfolding and exposing buried sulphydryl groups (Table 5.6). The microgels cross-linked for 0 h had the highest free sulphydryl content (2.12 mM), which decreased to 1.11 mM when cross-linking time increased to 24 h indicating the formation of disulphide bonds. The SDS-PAGE data supports the free SH results in that the microgels were formed by disulphide bonds and that the disulphide bond content was greater for the 24 h cross-linked microgels.

Table 5.6 Protein hydrophobicity (H_0) and free sulphydryl (SH) content. Data (n=3) are presented as the mean ± SD. Data with different superscript letters within a column indicate significant differences.

Sample	H_0	Free SH (mM)
Native WPI	365.56 ± 17.97^{b}	0.14 ± 0.06^{d}
WPI at 80 °C	545.25 ± 12.86^{a}	1.45 ± 0.25^{b}
0 h cross-linked microgels	375.75 ± 4.14^{b}	2.12 ± 0.12^{a}
24 h cross-linked microgels	35.83 ± 2.03^{c}	1.11 ± 0.00^{c}

The surface hydrophobicity of native WPI, heat denatured WPI, 0 h and 24 h cross-linked microgels are also shown in Table 5.6. Heat treatment of WPI to 80 °C for 30 min, exposed the hydrophobic regions of WPI. This was expected as heat treatment unfolds protein structures promoting hydrophobic interactions (Jia *et al*., 2015). On addition of $CaCl_2$ to heat denatured WPI, the surface hydrophobicity decreased. The addition of $CaCl_2$ screened the protein surface charges leading to protein aggregation and thus gel network formation which reduced the number of available binding sites for ANS (Liu *et al.*, 2020a; Schmitt *et al.*, 2007). The microgels cross-linked for 24 h had significantly lower amount of exposed hydrophobic regions compared to the microgels cross-linked for 0 h. This suggests that the microgels were not fully formed on immediate addition of $CaCl_2$ indicating that the protein solution was not fully aggregated, whereas the microgels crosslinked for 24 h, had more time to allow the protein molecules to crosslink forming more disulphide bonds, thus reducing surface hydrophobicity. The SDS-page also showed that crosslinking for 24 h led to larger protein aggregates, indicating that the microgels are made up of protein-protein hydrophobic interactions and covalent disulphide bonds.

5.3 Conclusion

Whey protein microgels produced via cold-set gelation showed foaming properties which were dependent on particle size, calcium concentration, cross-linking time, rheological properties, free sulphydryl and free surface hydrophobicity content. The microgels could form stable foams and image analysis indicated the ability of microgels to alter the microstructure of the bubbles in foams by creating an interconnected protein

network stabilising the air bubbles. The strength of the microgels could be manipulated by altering the cross-linking time which in turn affected the foaming and textural properties. This can be used to create softer or more firm foams depending on the needs of the end product.

Foam overrun for microgel foams was lower than that of native protein foams, however, stability was greatly improved. The differing foaming abilities of native WPI and WPI microgels was due to differences in their rheological properties which can be tailored by altering the $CaCl_2$ concentration or cross-linking time. Microgels can also alter the textural properties of foams, as both foam firmness and consistency were improved. This can be of use to the end user to tailor foods for specific needs such as low-calorie or high density foods.

This study demonstrated that the microgels had exceptional stabilisation ability, significantly beyond that of previously published work in the literature on microgel stabilised systems. The microgels decreased and even prevented liquid drainage which led to the formation of ultra-stable foams remaining stable for > 2 years. The microgel properties can be manipulated by controlling particle size, $CaCl_2$ concentration, rheological and textural properties. The unique properties of microgel stabilised foams have much to offer in developing the science of food structuring and formulating novel and versatile structures to be used in the food industry. The WPI microgels can be used to prolong the lifetime of normally unstable foamed food products.

Chapter 6
Improved stability of vitamin D_3 encapsulated in whey protein isolate microgels

Data in this chapter have been published in *International Dairy Journal* (Lee, J., Duggan, E. 2022 Improved stability of vitamin D3 encapsulated in whey protein isolate microgels). https://doi.org/10.1016/j.idairyj.2022.105351

6.1 Introduction

Vitamin D is a fat-soluble vitamin that plays an important role in the human body as it helps with the absorption of calcium and phosphorous, thereby helping to develop and maintain a healthy skeleton for humans (Mitbumrung *et al*., 2019; Wimalawansa, 2018). Vitamin D_3 is synthesized in our skin when exposed to sunlight (Walia *et al*., 2017). However, vitamin D deficiency is common among populations worldwide (Diarrassouba *et al*., 2015). Reduced exposure to sunlight, the angle of the sun reaching the earth, cloud cover/ pollution, skin type, use of sun cream, wearing protective clothing and reduced dietary intake are among the causes of vitamin D deficiency (Mitbumrung *et al*., 2019; Tan & McClements, 2021). Due to this, it is necessary for supplementation of vitamin D or consumption of fortified foods (Wimalawansa, 2018). However, fortifying foods with vitamin D is challenging due to the fat-soluble nature of the vitamin, as it has low water solubility and it is sensitive to oxidation and UV light (Kiani *et al*., 2017).

Several studies have investigated vitamin D stability in food products after thermal heating and storage conditions and in all instances there were vitamin D losses (Zareie *et al.*, 2019; Ložnjak and Jakobsen, 2018; Jakobsen and Knuthsen, 2014; Tabibian *et al*., 2017; Bajaj and Singhal, 2021). Encapsulation is therefore an ideal solution for this problem as it can protect the vitamin from harmful processing conditions. The main reason for protecting bioactive agents is to increase their stability and bioavailability after consumption (Pinheiro *et al*., 2017).

To overcome vitamin D instability, encapsulation has mostly been done by delivery systems such as nanoemulsions (Winuprasith *et al*., 2018; Ozturk *et al*., 2015; Guttoff *et al*., 2015), nanoparticles (Abbasi *et al*., 2014; Levinson *et al.*, 2014; Lin *et al*., 2016; Berino *et al*., 2019), complex coacervate particles (Teng *et al*., 2013; Ron *et al*., 2010; Luo *et al*., 2012; Xiang *et al*., 2020), casein micelles (Semo *et al*., 2007; Cohen *et al*., 2017; Haham *et al*., 2012; Loewen *et al*., 2018) and lipid nanocapsules (Kiani *et al*., 2017; Park *et al*., 2017). However, to date few studies have used whey protein microgels for encapsulation of vitamin D without the use of adding or coating with a second protein or polysaccharide to improve encapsulation properties.

Microgels are unique systems which differ from other colloidal systems such as those aforementioned. Microgels are deformable soft porous three-dimensional microscopic particles and their stable structure of cross-linked biopolymer molecules is due to the presence of covalent bonds and strong noncovalent interactions (Farjami and Madadlou, 2017). The disulphide bonds, thiol groups, the degree of unfolding,

electrostatic repulsion among proteins, pH and ionic strength determine the size and surface properties of the particle (Zhang *et al.*, 2015a). They can retain bioactive compounds due to physical entrapment inside the pores, attractive physical interactions or covalent bonding (McClements, 2017a). Additionally, microgels are known to have excellent interfacial properties, stabilising foams and emulsions for prolonged periods. Microgels exhibit combined properties of different classes of materials (e.g. rigid particles, flexible macromolecules and micellar aggregates), uniting the best of the colloidal, polymer and surfactant world, thus making them advantageous over other particle systems (Plamper and Richtering, 2017).

In this study, cold-set gelation was used to fabricate the WPI microgels. Cold-set gelation is a popular method for encapsulation of heat labile compounds. To fabricate protein microgels, the protein must undergo conformational changes i.e. unfolding of the molecule by heat treatment under conditions that oppose protein-protein interactions, exposing interactive sites such as thiol groups and disulphide bonds (Ko and Gunasekaran, 2006). This is followed by the addition of salt that screens the electrostatic repulsion between protein molecules causing protein aggregation (Bagheri *et al.*, 2014; Beaulieu *et al.*, 2002).

Therefore, this study determines if WPI microgels can successfully encapsulate and protect vitamin D_3 following exposure to environmental stresses routinely encountered in the food industry. The WPI microgels will also be passed through an *in vitro* digestion model to determine if the microgels can protect vitamin D_3 from degradation during gastric transit, but release at the correct site of action, in the small intestine. It is an important step to evaluate the capability of WPI microgels to encapsulate and protect vitamin D as the results will provide useful information for the use of WPI/VD_3 microgels in food applications.

6.2 Results and discussion

6.2.1 Encapsulation efficiency of whey protein microgels

The particle size of the WPI and WPI/VD_3 microgels fabricated at the various pH values were measured and results can be found in Table 6.1. Visually, both microgel solutions were opaque in appearance at all pH values, indicating the formation of large complexes (Zhang *et al.*, 2016). The incorporation of VD_3 within WPI microgels did not

significantly change the particle size at any pH (Table 6.1). For both microgel solutions, the microgels formed at pH 4.5 and 4.8 were significantly larger (>150 μm) than microgels formed at the other pH values (< 56 μm). As found in chapter 3 and shown again in Fig. 6.1, the isoelectric point (pI) of whey protein isolate was in the range 4.5 < pH < 5 as the ζ-potential was zero leading to protein-protein interactions. This caused the protein molecules to aggregate prior to $CaCl_2$ addition, leading to the formation of larger particles. Additionally, the reduction in ζ-potential to ~ ± 6 mV, resulted in a drop below the critical stability value of ± 20 mV. Schmitt *et al.* (2014) further indicated that at pH 4.5 and 4.8 aggregation of the microgels into larger colloidal particles occurred due to their instability. In comparison, at the other pH values, the electrostatic repulsive forces could have prevented aggregation of the protein molecules prior to $CaCl_2$ addition.

Table 6.1 The effect of pH on microgel particle size. Particle size displayed as surface weighted mean d(3,2). Data (n=3) are presented as the mean ± SD. Data with different lowercase superscript letters within a column and different uppercase superscript letters within a row indicate significant differences.

	Particle size	
pH	**WPI**	**WPI/VD_3**
3	28.72 ± 2.85^{cA}	26.20 ± 1.88^{bA}
4.5	162.34 ± 15.85^{aA}	186.65 ± 25.99^{aA}
4.8	178.88 ± 20.52^{aA}	182.68 ± 18.65^{aA}
5.5	$50.85 \pm 5.66^{b,cA}$	45.98 ± 7.95^{bA}
6.8	$43.88 \pm 2.46^{b,cA}$	30.11 ± 5.24^{bA}
7.5	$40.21 \pm 6.19^{b,cA}$	29.74 ± 6.21^{bA}
8	55.30 ± 14.92^{bA}	37.45 ± 4.56^{bA}

β-Lactoglobulin, the main protein in whey protein is a member of the lipocalin protein family and it is known for its ability to bind to hydrophobic bioactive compounds (Ha *et al.,* 2019). The encapsulation efficiency of WPI was found to be dependent on pH. At whey protein's native pH 6.8, the highest encapsulation efficiency occurred with > 98 % VD_3. As shown in Fig. 6.1, when the pH was altered to the other pH values less than

50 % of vitamin D_3 was encapsulated. At approx. pH 4.5 - 5 where it is close to zero net charge (Fig. 6.1), protein-protein interactions occurred to form aggregates, which could have reduced the interactive sites available for binding with VD_3. At pH values further from the pI, protein molecules are more charged (Totosaus *et al*., 2002). Therefore, it is hypothesised that the low encapsulation efficiency at pH 3, 7.5 or 8 is due to the greater net charge on the protein molecules. The greater the net charge the greater the electrostatic repulsion, preventing the interactions required to form a protein network suitable to protect VD_3 (Totosaus *et al*., 2002).

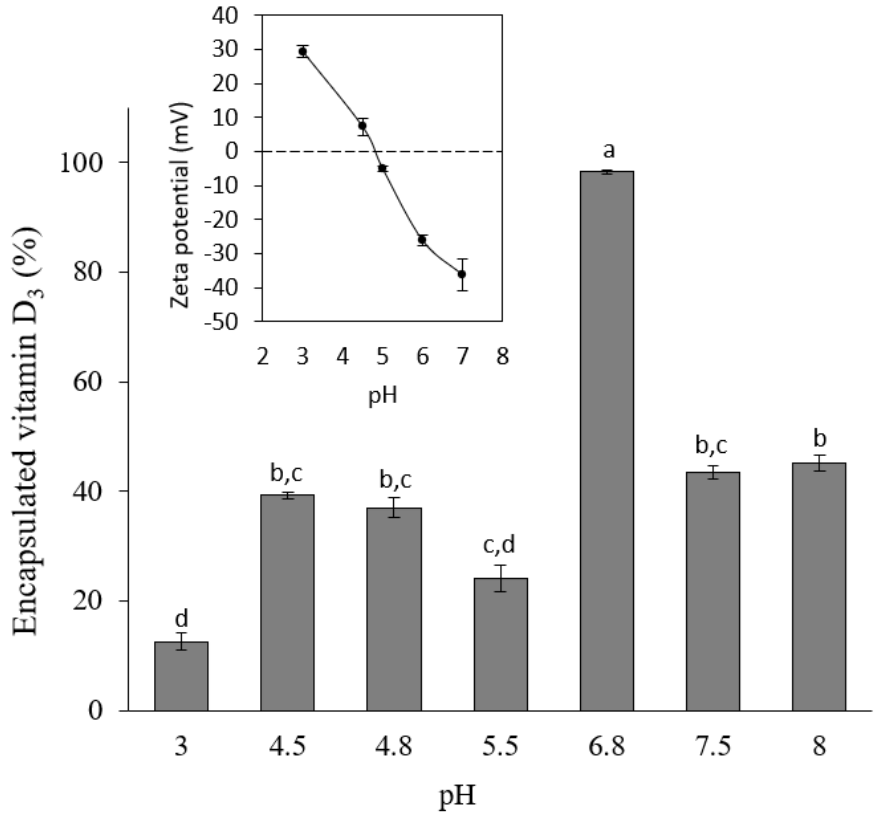

Fig. 6.1 Influence of pH on WPI electrical charge (ζ) (inset) and encapsulation efficiency (%) of microgels. Data (n=3) are presented as the mean ± SD. Data with different letters indicate significant differences.

The microgels at pH 6.8 were chosen as the optimum fabrication pH as the highest amount of VD_3 was encapsulated. Cold-set gelation is a suitable method for encapsulation of heat sensitive bioactive compounds, as the bioactive is added to the cooled, denatured WPI solution, creating a bioactive loaded solution. During the heating step for particle

formation, WPI was denatured, exposing hydrophobic regions for potential interaction with VD_3. The addition of $CaCl_2$ shields electrostatic repulsion between the protein molecules resulting in intermolecular aggregation and thus formation of microgels (O'Neill *et al*., 2014; Giroux *et al*., 2010). Addition of $CaCl_2$ increases the polarity of the aqueous phase, which could possibly lead to an additional driving force for hydrophobic interaction between WPI and VD_3 (O'Neill *et al*., 2014).

The morphology of the microgels at pH 6.8 was analysed using scanning electron microscopy to distinguish if VD_3 incorporation altered the WPI microgel structure (Fig. 6.2). The microgels appeared as particulate structures with an uneven coarse surface. There was a mix of both small and large aggregates with smaller aggregated particles attached to the surface of larger aggregates. This indicates that network formation occurred as smaller particles aggregated to form larger particles. The morphology of the WPI and WPI/VD_3 microgels in the SEM images were not noticeably different from one another, indicating that VD_3 incorporation did not alter the microgel morphology.

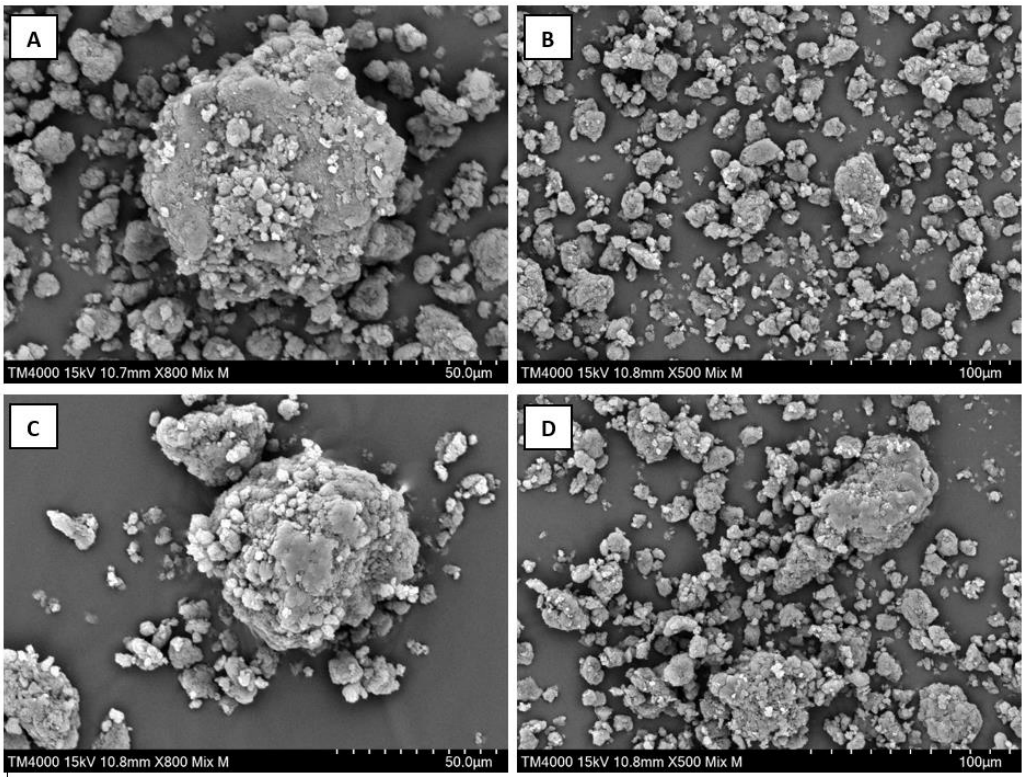

Fig. 6.2 Scanning electron microscopy micrographs of (A, B) WPI microgels and (C, D) WPI/VD_3 microgels at pH 6.8.

6.2.2 Thermal stability

The DSC thermograms corresponding to WPI and VD_3 powder and WPI and WPI/VD_3 microgel solutions are shown in Fig. 6.3. Whey protein and vitamin D_3 exhibited endothermic peaks at 88.44 and 83.93 °C respectively. The DSC curve of WPI powder exhibited a broad endothermic peak which can be associated with evaporation of bound water. In Fig. 6.3 the WPI powder endotherm is highlighted, as the endothermic peak reduced in size due to the lower heat flow required to evaporate the free bound water. When the WPI formed microgels, the endothermic peak shifted to a higher temperature (103. 57 °C); this was probably due to the aggregated, cross-linked nature of the microgels which in turn improved the microgel stability. The denaturation temperature of a sample rises as the number of crosslinks within the molecule increases (Liu *et al.*, 2020). Both microgel systems, WPI and WPI/VD_3 displayed almost the same endothermic peak at ~103.57 °C, this single peak demonstrates the successful incorporation of VD_3. The vitamin D_3 peak shifted from 83.93 °C to an endothermic peak identical to the WPI microgel (103.57 °C). This resulted in the WPI and WPI/VD_3 microgels having the same endothermic peak (103.57 °C), which indicated that vitamin D_3 was encapsulated and protected by the WPI microgel. Similar results have been found by Luo *et al*. (2012) & Park *et al*. (2017) whereby the authors successfully encapsulated vitamin D_3 within zein and lipid nanoparticles respectively.

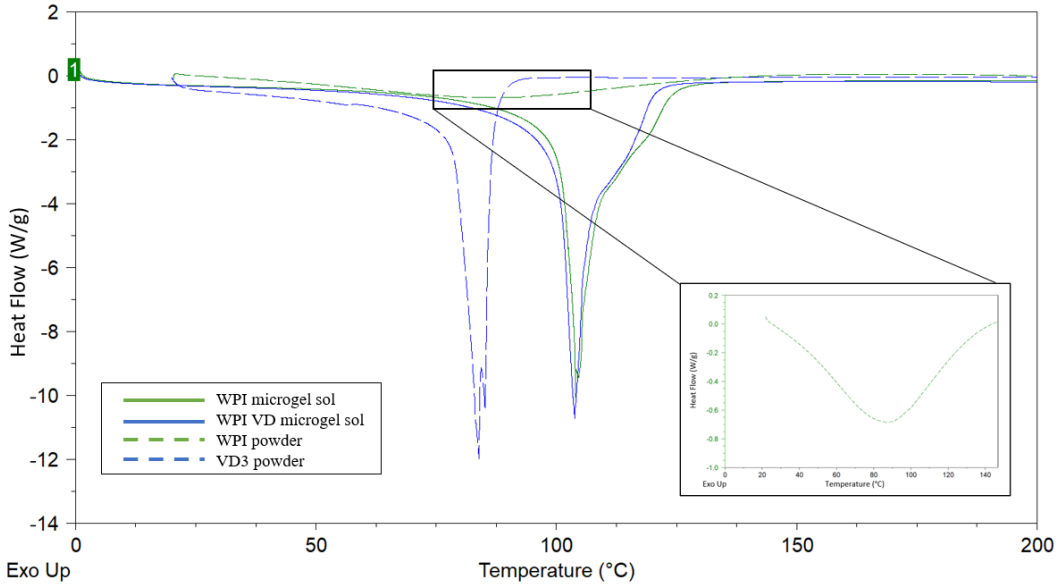

Fig. 6.3 Differential scanning calorimetry (DSC) thermograms of WPI microgel (green continuous line), WPI/VD_3 microgel (blue continuous line), WPI powder (green dashed line) (inset) and VD_3 powder (blue dashed line).

6.2.3 Stability of vitamin D to environmental stresses

The protective effect of WPI microgels on VD_3 encapsulated within them was compared with a control sample containing unencapsulated VD_3. Vitamin D_3 is susceptible to degradation upon exposure to light, heat and oxygen, which are commonly experienced during food production and storage (Kiani *et al*., 2017). It is therefore essential to analyse the protective effect of WPI microgels before proposing the microgels as a functional food ingredient.

Pasteurisation is a common processing treatment in the food industry, but the process can be partially destructive to sensitive compounds such as vitamin D_3 (David and Livney, 2016). To determine whether the WPI microgels could protect VD_3 from degradation during pasteurisation, a thermal experiment was carried out. The WPI/VD_3 microgels and unencapsulated VD_3 were exposed to heat treatment at 72 °C for 15 s (high temperature short time) or 63 °C for 30 min (low temperature long time). Regardless of temperature, the WPI microgels protected VD_3 from degradation compared to unencapsulated VD_3. Upon exposure to 72 °C for 15 s or 63 °C for 30 min, unencapsulated VD_3 degraded by 25 %, whereas 97 % of the encapsulated VD_3 remained intact within the microgels. The antioxidant activity of the free thiol groups of β-lactoglobulin in whey protein can provide a protective barrier for vitamin D_3 (Diarrassouba *et al*., 2015).

Storage temperature is an important factor to preserve the quality of food products, therefore a range of routinely used storage temperatures were analysed. The WPI microgels were stored for 4 weeks at 20, 4 and -20 °C and their ability to protect vitamin D_3 was investigated (Fig. 6.4). Temperature is an important factor to preserve the quality of food products. The WPI microgels were found to significantly protect VD_3 compared to unencapsulated VD_3 at all storage temperatures over the four-week period. For unencapsulated VD at 20, 4 and -20 °C there was a loss of 28, 28 and 8 % respectively after the first week followed by a total loss of 35, 33 and 24 % respectively at the end of the fourth week. In comparison, when VD_3 was encapsulated within the microgels, there was a < 1 % VD_3 loss at the end of the first week regardless of storage temperature followed by a total loss of 8, 8 and 5 % at 20, 4 and - 20 °C, respectively at the end of the fourth week. After four weeks the microgels retained > 93 % VD_3 whereas ~ 69 % of unencapsulated VD_3 remained, demonstrating the ability of the microgels to protect and maintain the activity of vitamin D_3 during long term storage.

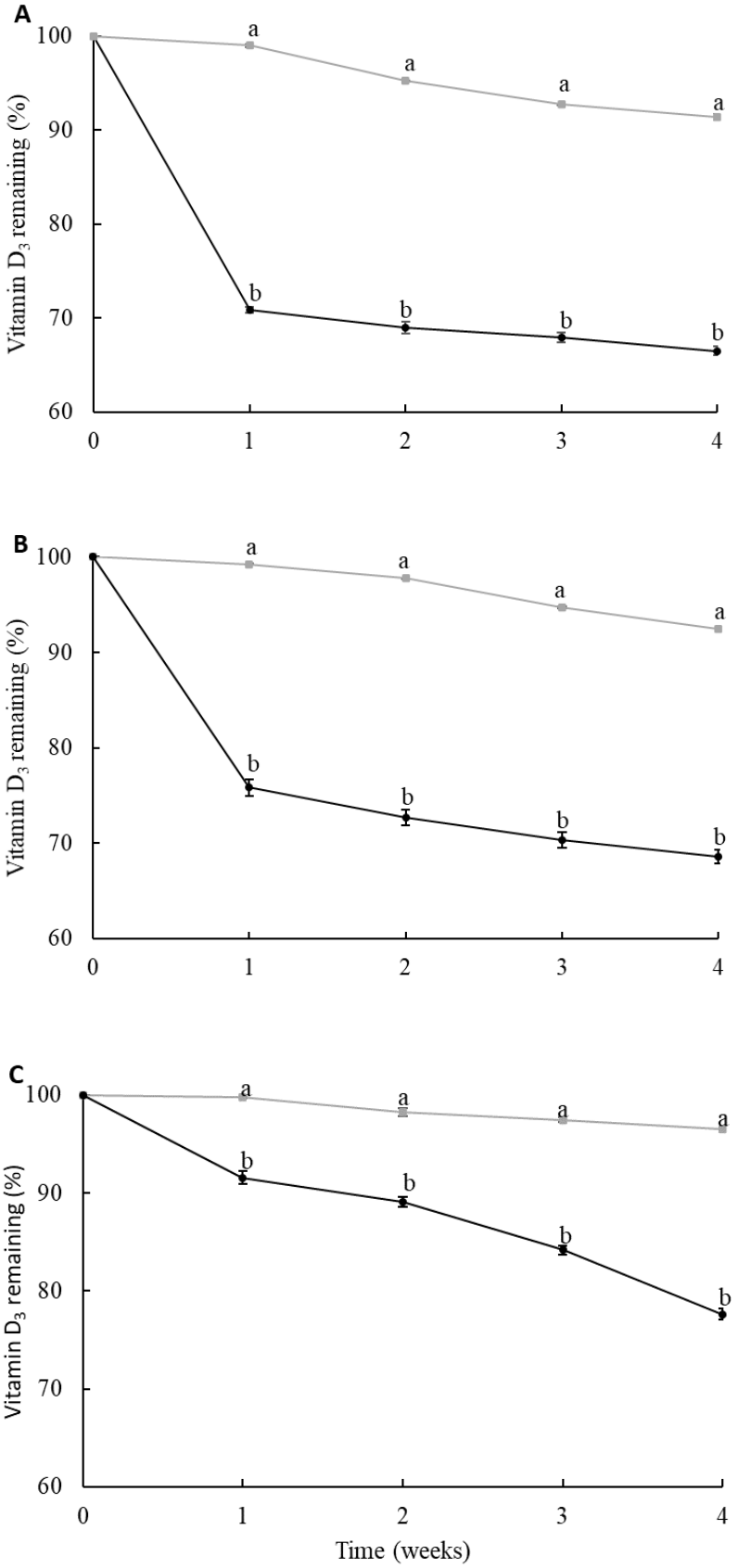

Fig. 6.4 Effect of 4 week storage at (A) 20 °C, (B) 4 °C and (C) – 20 °C, on WPI/VD_3 microgels (■) and unencapsulated VD_3 (●). Data (n=3) are presented as the mean ± SD. Data with different letters indicate significant differences.

Khan *et al*. (2020) also found that whey protein/soy protein microcapsules protected vitamin D_3 for four weeks at 4 °C. More than 94 % of free vitamin D_3 was degraded, while > 93 % VD_3 remained intact within the microcapsules. The authors suggested that the mobility of vitamin D_3 was reduced within the protein matrix, decreasing the vitamins reactivity, hindering contact with oxidising agents. Liu *et al*. (2020a) found that whey protein isolate-lotus root amylopectin (WPI-LRA) composite gels provided a protective barrier for vitamin D_3, as 61 % remained intact after 30 day storage at room temperature. The hydrophobic interaction between vitamin D_3 and the whey protein isolate-lotus root amylopectin composite gels protected vitamin D_3 from oxidative degradation.

UV-light is commonly used in the food industry to reduce the microbial load in food products; therefore, it is of interest to determine whether the WPI microgels can protect VD_3 when exposed to UV-light. Upon UV-light exposure, the unencapsulated VD_3 experienced rapid degradation with a loss of 71 % after 1 hour followed by complete degradation after 4 hour exposure (Fig. 6.5). In contrast, the microgels displayed protective effects for vitamin D_3 against UV-light, with 97 % still remaining intact after 5 hour exposure, indicating that the WPI microgels can protect VD_3 from UV-light. Photochemical stability of vitamin D_3 is one of the major hurdles for fortified food products. Other studies have utilised different protective structures to protect vitamin D_3 from UV-light, such as β-lactoglobulin-lysozyme complexes (Diarrassouba *et al*., 2015), whey protein isolate nanoparticles (Abbasi *et al*., 2014) and whey protein isolate/lotus root amylopectin composite gels (Liu *et al.*, 2020a). The authors suggest that the dense protein matrix composed of amino acids with aromatic side groups and double bonds can protect vitamin D_3 by absorbing UV-light thereby reducing the absorption of UV-light by vitamin D_3.

Overall, it is evident that WPI microgels provided significant protection to VD_3 against degradation when exposed to environmental conditions commonly found in food production compared to the unencapsulated VD_3 dispersion. Subsequently, the microgels had higher concentrations of VD_3 compared to unencapsulated VD_3.

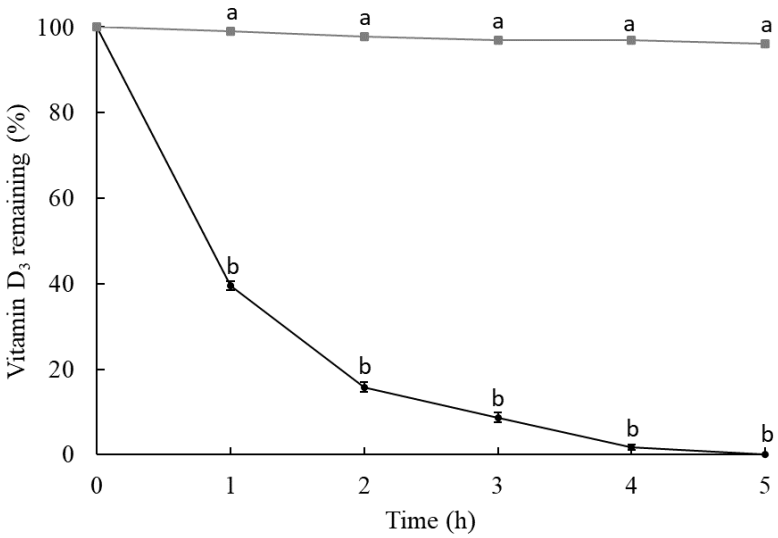

Fig. 6.5 Effect of UV-light on WPI/VD_3 microgels (■) and unencapsulated VD_3 (●). Data (n=3) are presented as the mean ± SD. Data with different letters indicate significant differences.

6.2.4 *In vitro* digestion

The physiological environment of the human gastrointestinal tract is complicated because of the differences in pH, salt ions and presence of several digestive enzymes, thus foods are easily digested making it difficult to obtain targeted release. In this study, the digestive behaviour of WPI/VD_3 microgels in SGF and SIF were analysed to achieve VD_3 release in SIF to improve the stability and bioavailability of vitamin D_3.

The WPI/VD_3 microgels and unencapsulated VD_3 in dialysis bags were passed through a static *in vitro* digestion model and 1 mL samples were taken at specific time points and analysed. The *in vitro* digestion model consists of two min in the oral stage, two hours in the gastric and two hours in the intestinal stage, mimicking human digestion.

The cumulative release rate of VD_3 from WPI/VD_3 microgels is shown in Fig. 6.6. It can be seen that during the first 120 min, representing the oral and gastric phase, 99 % of unencapsulated VD_3 was detected, however, when encapsulated, release from the WPI microgels was low, with 12 % VD_3 released. This indicates the protective effect of the WPI microgels during gastric transit. Pepsin found in the stomach cleaves peptide bonds of hydrophobic amino acids in proteins destroying the protein structure. However, this destruction is reduced when proteins form complexes due to cold-set gelation as the hydrophobic amino acids get protected within the protein network leading to the

formation of a protective outer layer, preventing degradation by pepsin (Xiang *et al*., 2020; O'Neill *et al*., 2015 ; Ha *et al*., 2019; Beaulieu *et al*., 2002).

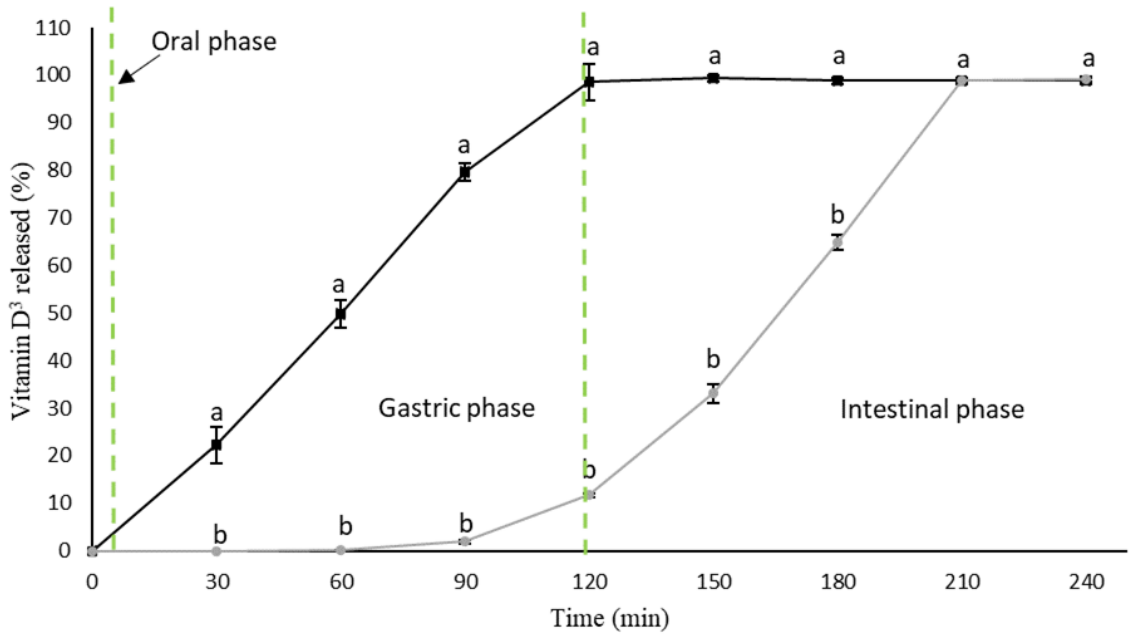

Fig. 6.6 Vitamin D_3 release (%) from microgels after exposure to *in vitro* digestion. WPI/VD_3 microgels (●) and unencapsulated VD_3 (■). Data (n=3) are presented as the mean ± SD. Data with different letters indicate significant differences.

On exposure to SIF, the WPI microgels offered little protection to VD_3. After the first 30 min in the intestinal phase 33 % of VD_3 was released, while after one hour this had increased to 64 %. At 210 min of *in vitro* digestion, the release of VD_3 from the microgels was not statistically different from that of unencapsulated VD_3, reaching full release. β-lactoglobulin, the main protein in whey protein is susceptible to pancreatic proteases, destroying the protein structure resulting in the release of VD_3 (Xiang *et al*., 2020; Ozel *et al*., 2020; Chavoshpour-Natanzi and Sahihi, 2019). These results showed that the use of WPI microgels decreased VD_3 release in SGF and promoted VD_3 release in SIF, improving VD_3 bioavailability. The intestinal absorption of vitamin D_3 depends on its solubilisation in the aqueous intestinal environment. Hydrophobic compounds can get trapped in the bile salts and get carried through the intestinal cell barriers into the blood circulation (Lin *et al*., 2016).

The protein hydrolysis of the WPI/VD_3 microgels was investigated using SDS-PAGE to understand the release of vitamin D_3 (Fig. 6.7A). The simulated digestive fluids of the oral, gastric, and intestinal stages are shown in Fig. 5.7B. To form microgels, the monomeric proteins of α-lactalbumin (α-la) (~14 kDa), β-lg (~18 kDa) and bovine serum albumin (BSA) (~66 kDa) polymerise into aggregates. In Fig. 6.7A in lane 1, the electrophoretic pattern showed a polymeric band at the top of the gel as the undigested WPI/VD_3 microgels were unable to enter indicating that the molecular weight of the sample was > 260 kDa. It is possible that not all the monomeric proteins polymerised into aggregates as a faint band is present at ~ 14 kDa, representing α-la. For the oral and gastric phase in lane 2 and 3 respectively, most of the WPI/VD_3 microgels remained intact as there are bands present at the top of the gel where they were too large to enter the gel and the presence of a continuous smear of high molecular weight proteins indicating the presence of aggregates. Similar results have been found by Li *et al*. (2022). However, there are visible bands at ≤ 14 kDa, indicating the presence of α-la and smaller polypeptide chains, which is possibly due to minor proteolysis of the microgels. There are also distinct bands at 38 and 49 kDa which matches the bands found in the oral (lane 1) and gastric (lane 2) simulated digestion fluids in Fig. 6.7B. Lanes 4 - 7 of Fig. 6.7A shows protein bands of samples taken at 30 min intervals during the intestinal phase digestion. The bands present correspond with those found in the SIF (lane 3 Fig. 6.7B), however there is no evidence of large aggregates still present nor a band corresponding to α-la (~14 kDa) or β-lg (~18 kDa). This verified the hydrolysis of protein in the microgels in the intestinal phase as there was no protein bands present leaving just the pancreatic proteases present on the gel, similar to the results found by Sousa *et al*. (2020); Alavi *et al*. (2018) and Xiang *et al*. (2020).

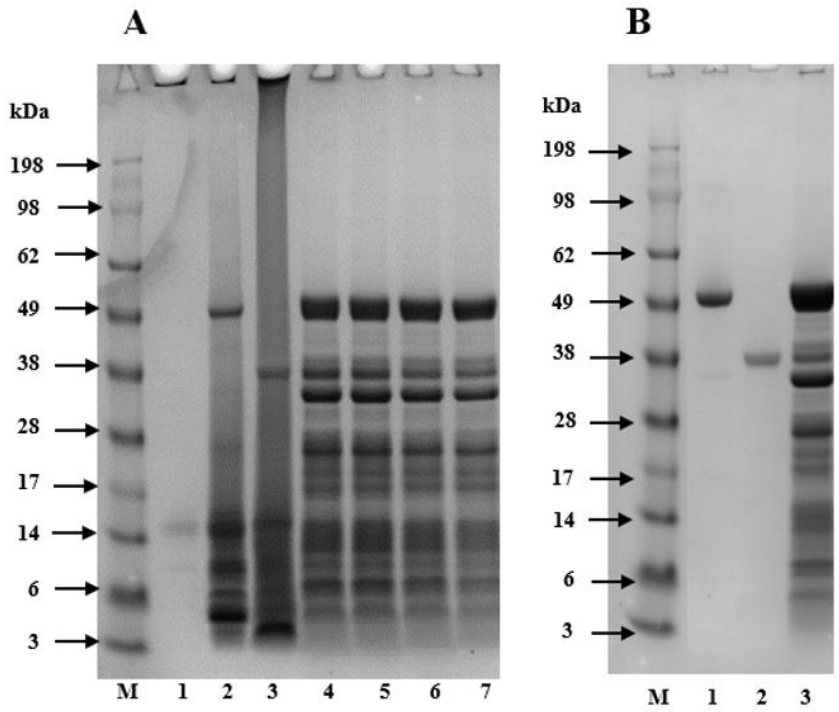

Fig. 6.7 SDS-polyacrylamide gel electrophoresis patterns of (A) undigested/digested WPI/VD_3 microgels and (B) simulated digestion fluids without WPI/VD_3 microgels. Lanes M represent the standard marker. In A, undigested WPI/VD_3 microgel (lane 1), digested WPI/VD_3 passed through oral, gastric and 30, 60, 90, 120 min intestinal (lane 2 – 7 respectively). In B, simulated oral fluids (lane 1), simulated gastric fluids (lane 2) and simulated intestinal fluids (lane 3).

To further investigate the release mechanism of vitamin D_3 from the WPI microgels in a simulated *in vitro* digestion model, the cumulative release rate from WPI microgels was assessed by five kinetic models; zero order, first order, Korsmeyer-Peppas, Hixson Crowell and Higuchi and the R^2 values are shown in Table 6.2.

For zero-order kinetics the release of an active agent as a function of time takes place at a constant rate independent of the active agent concentration. In comparison, first-order kinetics measures the change in concentration over time which is dependent on the active agents concentration (Bruschi, 2015). The Higuchi model is based on Fickian diffusion and it explains the release of an active agent from a solid matrix, with a linear relationship between the cumulative release and the square root of time (Chavoshpour-Natanzi and Sahihi, 2019). The Korsmeyer-Peppas model is used for systems whereby more than one type of phenomenon of active agent release is involved; diffusion or erosion (Panizzon *et al.*, 2014). The Hixson-Crowell model describes release from systems that depend on the change in surface area and diameter with time i.e., systems that have dissolved or eroded (Panizzon *et al*., 2014).

Table 6.2 Kinetic model fitting results of WPI/VD_3 microgels.

Model	R^2
Zero order	0.844
First order	0.693
Korsmeyer-Peppas	0.484
Hixson-Crowell	0.965
Higuchi	-0.730

It is indicated by Brodkorb *et al*. (2019) that the INFOGEST method is unsuitable for detailed kinetic analysis, however there are several authors who have applied kinetic release models to similar *in vitro* digestion methods (Chavoshpour-Natanzi and Sahihi 2019; Remondetto *et al*. 2004; Xiang *et al*. 2020; O'Neill *et al*. 2015 & Chen and Subirade, 2006).

The release of VD_3 from the microgels was not linear and the values from the regression coefficient (R^2) have shown best fit to Hixson-Crowell release model. This suggests that the release was controlled mainly by disintegration of the microgels, it applies to particles that dissolve or erode. The release of VD_3 from the microgels depends on the change in surface area and diameter of the microgels over time (Panizzon *et al*., 2014).

The particle size data corroborates the kinetic model results in that the particles decreased in size in the small intestinal phase, where 85 % VD_3 was released. The initial particle size prior to *in vitro* digestion was 30.11 ± 5.24 µm, which decreased to 0.93 ± 0.02 µm at the end of digestion (Table 6.3). Pancreatic proteases are known to destroy β-lg structure, therefore it can be hypothesised that the WPI microgel structure broke down resulting in VD_3 release.

Table 6.3 The effect of gastrointestinal juices on microgel particle size. Particle size displayed as surface weighted mean d (3,2). Data (n=3) are presented as the mean ± SD. Data with different superscript letters indicate significant differences.

Gastrointestinal phase	Particle size (μm) D (3,2)
Initial	30.11 ± 5.24^{a}
Oral	36.84 ± 3.4^{a}
Gastric	40.37 ± 3.14^{a}
30 min intestinal	38.20 ± 1.00^{a}
60 min intestinal	28.69 ± 7.20^{a}
90 min intestinal	0.77 ± 1.95^{b}
120 min intestinal	0.93 ± 0.02^{b}

6.3 Conclusion

In this work, WPI microgels were successfully developed using cold-set gelation and were further used as a delivery system for vitamin D_3. Incorporation of VD_3 did not significantly alter the particle size and the microgels displayed high encapsulation efficiency (> 98 %) which was pH dependent. Results showed that the microgels effectively protected VD_3 against degradation from UV-light, dairy pasteurisation temperature and long-term storage. The *in vitro* digestion data indicated that the WPI microgels could provide a protective barrier for VD_3 in the gastric phase, while allowing release in the small intestine. These findings clearly show that WPI microgels may be used as viable delivery systems for VD_3 which have good potential in the food industry.

Chapter 7
Foamability of vitamin D_3 loaded microgels

7.1 Introduction

As found in the previous chapters, microgels can form ultra-stable foams and they can also encapsulate vitamin D_3. This chapter, therefore, looks at combining both processes to form VD_3 loaded WPI microgel stabilised foams. This is believed to be the first time microgels have been combined in the same process to stabilise a foamed system while encapsulating and delivering vitamin D_3.

The WPI and WPI/VD_3 microgels were subjected to alterations in pH, ionic strength, heat treatment, sucrose concentration and XG addition. The effect of the various environmental factors on the rheological, foaming and textural properties of the microgels were analysed and compared.

7.2 Results and discussion

Results of the encapsulation efficiency of WPI can be found in chapter 6. The WPI microgels (pH 6.8) successfully incorporated VD_3 within its cross-linked polymeric matrix, showing good encapsulation efficiency of > 98 %. The encapsulation efficiency was also confirmed using dynamic scanning calorimetry as the WPI and WPI/VD_3 microgels displayed the same endothermic peak at 103.57 °C, demonstrating successful incorporation. The encapsulation of VD_3 within the WPI microgels did not significantly change the particle size of the microgels, with sizes of 43.88 ± 2.46 and 30.11 ± 5.24 µm for WPI and WPI/VD_3 microgels respectively. The morphology of the WPI microgels did not change upon incorporation of VD_3, as observed by SEM. The results indicate that encapsulation of vitamin D_3 did not negatively affect the morphology or particle size of the microgels. Having established good encapsulation efficiency, the foaming ability of the WPI/VD_3 microgels were analysed upon exposure to several environmental factors.

7.2.1 Effect of pH on WPI and WPI/VD_3 microgels

The effect of pH (3, 4, 4.5, 5, 6.8, 8, 9) on the WPI and WPI/VD_3 microgel rheological, foaming and foam textural properties were assessed. The viscosity of both microgel systems (WPI and WPI/VD_3) were significantly greater at pH values close to the pI of WPI (Table 7.1). As shown in previous chapters, the viscosity of the continuous

phase influences the rate of foam drainage. In chapter 3 of this thesis, the ζ-potential data indicated that the pI of WPI was between pH 4 and 5 as the value was zero. At the pI of whey protein, protein-protein interactions occur due to the zero net charge leading to protein aggregation (Zhang *et al*., 2004). As the microgels are made up of aggregated, cross-linked protein molecules, this zero net charge may have led to further aggregation leading to increased viscosity. The results in Table 7.1 show that at some of the pH values, the addition of VD_3 reduced the solution viscosity.

Table 7.1 Viscosity values of WPI and WPI/VD_3 microgels. Data (n=3) are presented as the mean ± SD. Data with different lowercase superscript letters within a column and uppercase superscript letters within a row indicate significant differences.

pH	**Viscosity (mPa)**	
	WPI	**WPI/VD_3**
3	501 ± 109.55^{cA}	172 ± 16.57^{dB}
4	1503 ± 157.05^{bA}	854 ± 23.57^{cB}
4.5	2720 ± 456.63^{aA}	1177 ± 3.19^{bB}
5	2667 ± 335.40^{aA}	2124 ± 22.83^{aA}
6.8	206 ± 43.93^{cA}	105 ± 5.74^{dA}
8	224 ± 80.20^{cA}	110 ± 21.02^{dA}
9	386 ± 24.64^{cA}	104 ± 60.89^{dB}

Dynamic strain sweeps indicated that the linear viscoelastic region was up to 0.2 % strain for both microgel systems at all pH values and the storage modulus, G', dominated over the loss modulus, G". Fig. 7.1 A displays G' and G" of both microgel systems at pH 6.8, which shows that the storage and loss moduli decreased at approx. 2 – 3 % strain. This also occurred for both microgel samples at pH 3 – 5. At pH 9 for both microgel systems, G' also started to decrease at approx. 2 - 3 % strain. However, G" increased at approx. 14 % strain, followed by a decrease when the strain increased further (Fig. 7.1 B). Both microgel systems at pH 8 behaved in a similar way. A peak in G" suggests that there is an associated network between molecules in a sample (TAInstruments, 2020). In associated networks, the deformed molecules pull each other in the same direction due to their attraction, however, eventually this interaction between the molecules is overcome. The new freedom of molecules means that they are free to

move about and dissipate energy leading to an increase in G". However, once deformation is too high, the structure breaks down and thus G" decreases (TAInstruments, 2020).

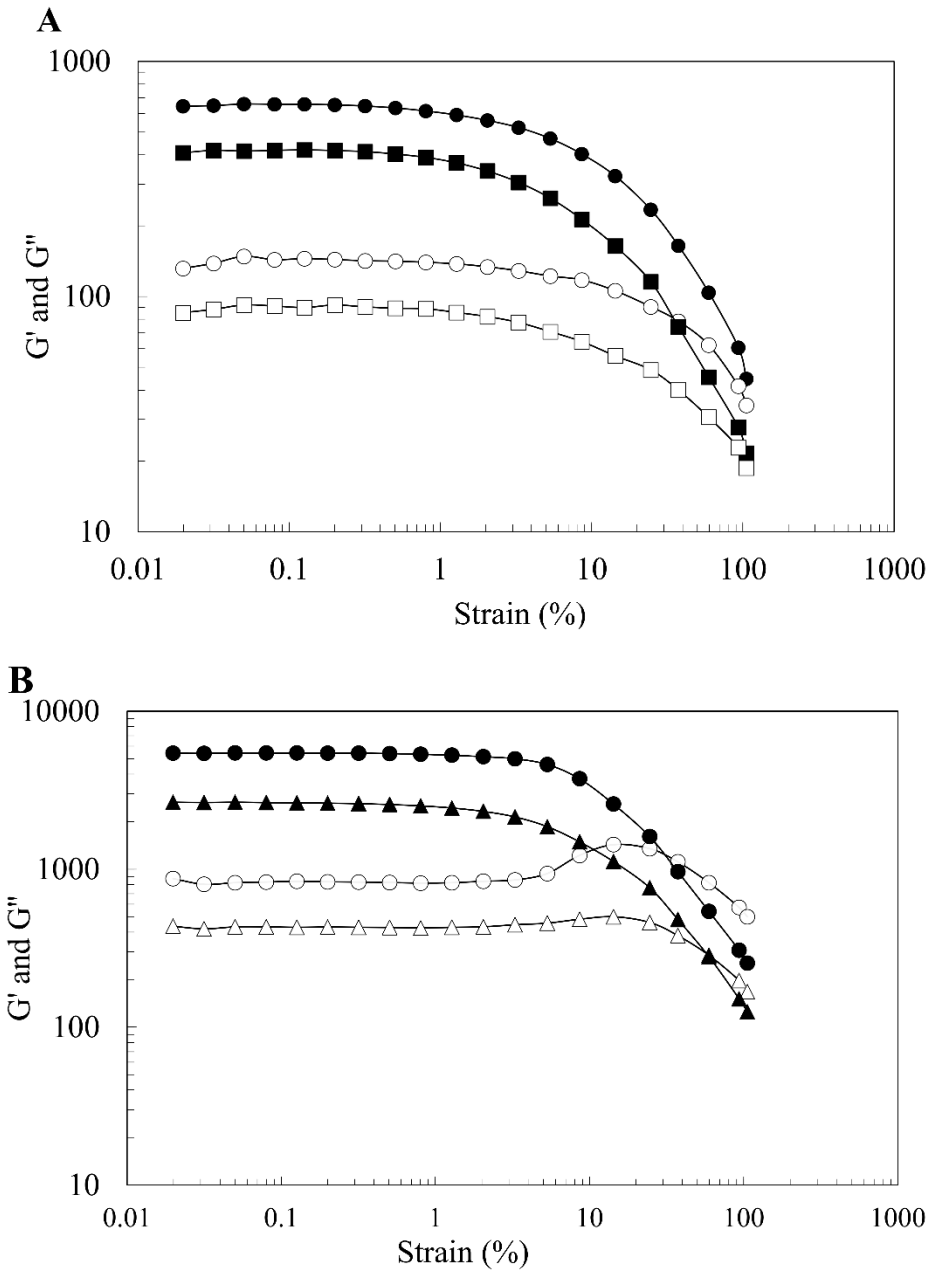

Fig. 7.1 Strain sweep of (A) WPI microgels G' (●) and G" (○) and WPI/VD_3 microgels G' (■) and G" (□) at pH 6.8. (B) WPI microgels G' (●) and G" (○) and WPI/VD_3 microgels G' (▲) and G" (△) at pH 9. Data (n=3).

The microgels were subjected to frequency and time sweeps to determine their internal structure and stability of the microgels during storage after pH alteration. G' values are only shown for clarity (Fig. 7.2). The rheological data for the WPI and WPI/VD_3 microgels revealed that the storage modulus (G') was greater than the loss modulus (G") regardless of pH, indicating that the microgels behaved like an elastic material (Liu *et al*., 2019; Mleko *et al*., 2007). A gel behaves principally as an elastic material due to the presence of a continuous network (Khan *et al*., 1997).

The encapsulation of vitamin D_3 within the WPI microgels resulted in a slight decrease in G' and G", however, the gels were still classified as structured materials. Both microgel systems, regardless of pH, displayed a slight frequency dependence as G' and G" marginally increased from 0.1 to 10 Hz (Fig. 7.2 A, B). Due to the slight frequency dependence, the gels can be classified as strong gels (Chen and Dickinson, 1998), signifying that the microgel systems are gelled, three-dimensional network systems. A greater loss modulus and increased frequency dependence would indicate that the systems consisted of isolated particles that did not form a network (Khan *et al*., 1997). For the WPI microgels, when the pH was altered to above its native pH (6.8) to pH 8 and 9, G' and G" increased significantly, increasing the network structure, whereas when altered below pH 6.8, G' and G" decreased (Fig. 7.2A). Alteration of the WPI/VD_3 microgels from their native pH (6.8) to the other pH values caused G' and G" to increase, with a substantial increase at pH 8 and 9 (Fig. 7.2B). At all pH values, for both microgel systems, the slopes of G' and G" did not markedly change with frequency, indicating that there was no change in the microgel network.

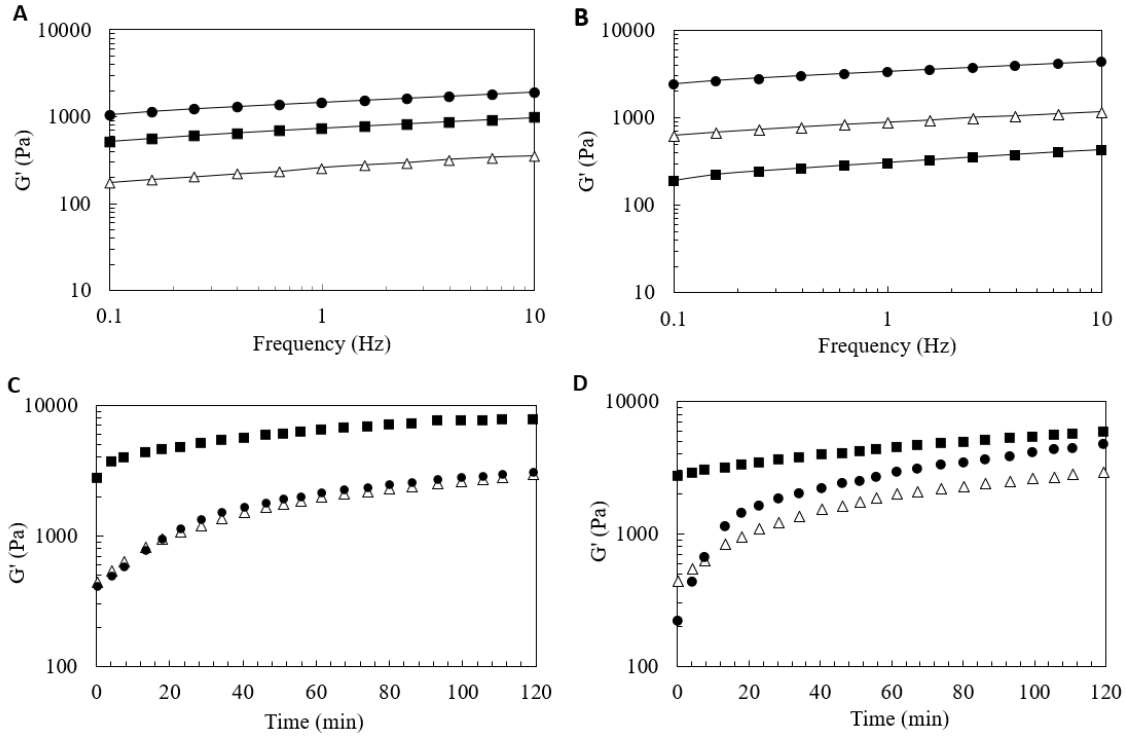

Fig. 7.2 Frequency sweeps of (A) WPI and (B) WPI/VD_3 microgels. Time sweeps of (C) WPI and (D) WPI/VD_3 microgels at pH (△) 4, (■) 6.8 and (●) 8. Data (n=3).

The storage and loss modulus of the WPI and WPI/VD_3 microgels were monitored over a period of 120 min (Fig. 7.2 C and D). Time sweeps provide information about how a material might change after it has been loaded. For both microgel systems, G' and G" remained stable over the 120-min period with an exception at pH 4 and 8 where G' and G" initially increased at a fast rate until this increase slowed at approx. 20 min.

Foaming of WPI microgels was assessed and compared with the foaming properties of WPI/VD_3 microgels. The encapsulation of vitamin D_3 did not lead to any significant changes in the foaming properties of the WPI microgels. For both microgel systems the lowest overrun was around pH 4 – 5 and the highest overrun occurred at pH 6.8 – 9 (Table 7.2). The overrun values correlate with the viscosity values, as the highest viscosity occurred at pH 4 – 5. More viscous systems minimise the amount of air that can be incorporated which consequently leads to lower overrun values.

Table 7.2 Foam overrun and stability of WPI and WPI/VD_3 microgels at various pH values. Data (n=3) are presented as the mean ± SD. Within each parameter, data with different uppercase superscript letters within a row and data with different lowercase superscript letters within a column indicate significant differences.

pH	Overrun (%)		Stability (%)	
	WPI	**WPI/VD_3**	**WPI**	**WPI/VD_3**
3	$317 \pm 16.50^{a,b,cA}$	$278 \pm 69.34^{a,b,cA}$	96 ± 1.53^{aA}	93 ± 2.55^{aA}
4	$261 \pm 9.81^{b,cA}$	$256 \pm 53.58^{b,cA}$	95 ± 2.00^{aA}	93 ± 0.96^{aA}
4.5	239 ± 25.53^{cA}	$239 \pm 34.69^{b,cA}$	95 ± 2.89^{aA}	92 ± 1.67^{aA}
5	256 ± 41.79^{cA}	228 ± 9.62^{cA}	96 ± 1.15^{aA}	93 ± 1.67^{aA}
6.8	361 ± 41.79^{aA}	$344 \pm 41.94^{a,bA}$	97 ± 1.53^{aA}	95 ± 1.67^{aA}
8	$356 \pm 19.63^{a,bA}$	$322 \pm 25.46^{a,b,cA}$	98 ± 0.58^{aA}	93 ± 0.00^{aA}
9	$333 \pm 57.74^{a,b,cA}$	378 ± 19.25^{aA}	98 ± 0.00^{aA}	94 ± 2.55^{aA}

Interactions in the bulk solution are influenced by the net charge of proteins, that consequently influence their foaming properties (Kuropatwa *et al.*, 2009). The foam overrun values of the microgels differ from the overrun values that were previously found for native WPI in chapter 3. Native WPI foamed best at pH close to the pI at pH 4.5 – 5, whereas for the microgel systems, foams with the lowest overrun were formed at this pH. At pH near the pI there is zero net charge which leads to the minimisation of electrostatic repulsion, thereby promoting protein-protein interactions, increasing protein adsorption (Engelhardt *et al*., 2013). Due to the reduction in net charge at the pI, protein molecules aggregate, however, as the microgels are already in an aggregated state it is hypothesised that altering the pH close to the pI might have resulted in extensive aggregation, negatively affecting foaming.

Grossmann *et al*. (2019) proposed that at the air/water interface of foamed systems monomeric proteins act as anchors for aggregated proteins. In chapter 5, electrophoretic patterns indicated that the microgels were made up of aggregates and some monomeric proteins. Consequently, it is possible that at the pI, the monomeric proteins decreased due to protein aggregation, reducing the number of monomeric proteins available to act as anchors for the microgels, resulting in poor foaming properties.

At pH 9, protein solubility is high due to the high electrostatic repulsion between protein molecules leading to reduced foam overrun, however, this did not occur for either of the microgel systems. As microgels are already aggregated cross-linked structures, it

is proposed that the alteration of pH did not cause any changes and consequently did not negatively affect foaming.

The foam stability of the WPI and WPI/VD_3 microgels was not significantly affected by pH change, ranging from 92 to 98 % (Table 7.2). In chapter 5, the protein microgels when whipped were found to be capable of surrounding the bubbles as cloudy gel-like regions preventing gas diffusion between the bubbles. Consequently, changing the environmental pH had no negative effects on the microgels stabilising capabilities.

Stable foams can be characterised by greater textural properties such as high firmness or consistency (Bals and Kulozik, 2003b). In this study, all foams remained stable, but the foam textural parameters decreased as the pH decreased from pH 9 to pH 3 (Fig. 7.3), suggesting that in this case the stabilising ability of the microgels is not correlated to foam textural properties.

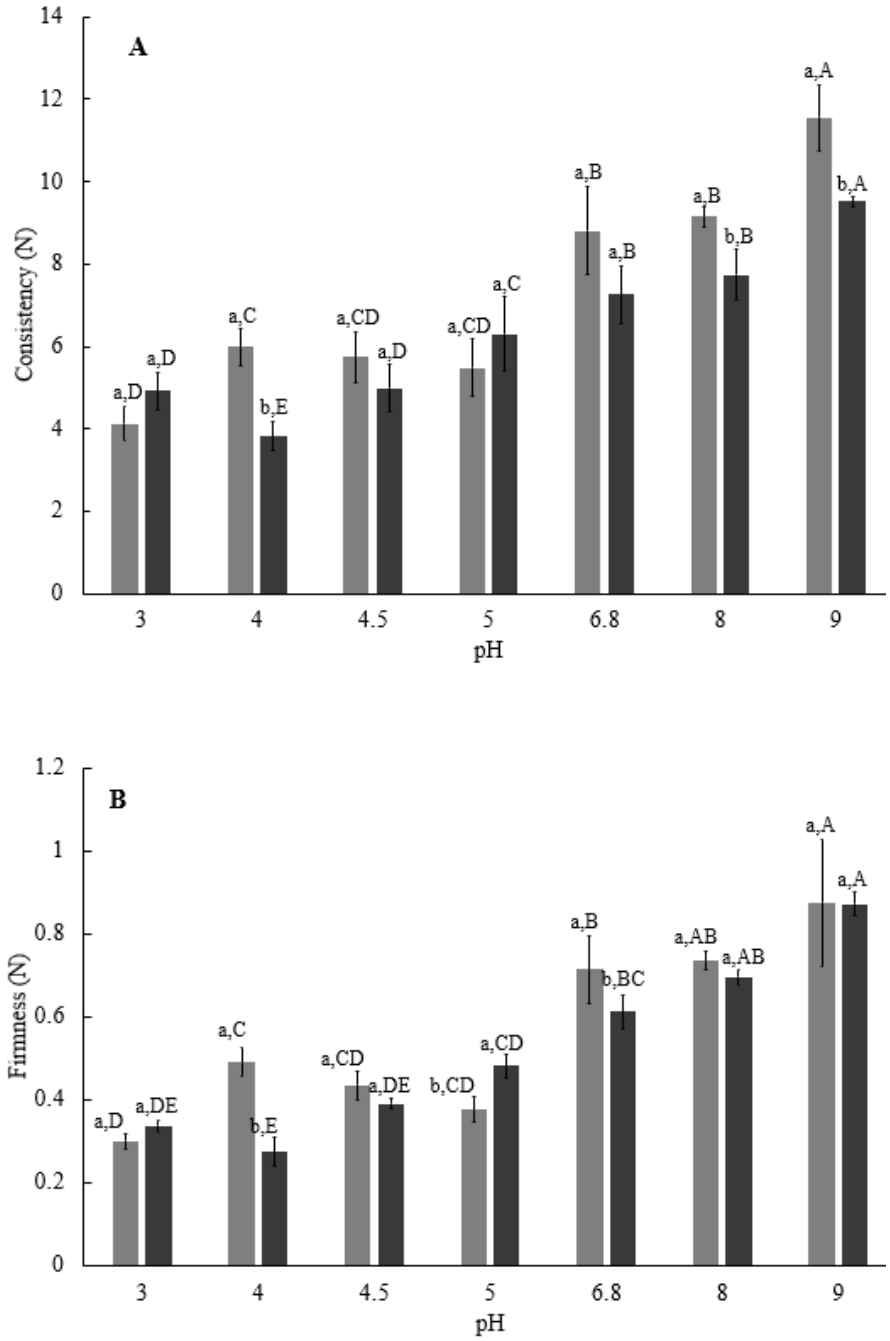

Fig. 7.3 Foam consistency (A) and foam firmness (B) of WPI (grey) and WPI/VD_3 (black) microgel foams. Data (n=3) are presented as the mean ± SD. Data with different lowercase letters indicate significant differences between pH values; different uppercase letters indicate significant differences between each microgel system.

7.2.2 Effect of NaCl on WPI and WPI/VD_3 microgels

In this section, the effect of NaCl concentration (0.05, 0.1, 0.2 and 0.4 M) on WPI and WPI/VD_3 microgel rheological, foaming and foam textural properties was investigated. The viscosity of both microgel systems increased with increasing NaCl

concentration (Table 7.3). In chapter 5, electrophoretic patterns of microgels indicated that some monomeric proteins were present that did not polymerise into aggregates. Consequently, it is hypothesised that addition of NaCl promoted aggregation between the free monomeric proteins present among the microgels, thus increasing viscosity. Equally, the excess salt from NaCl addition could have caused the proteins to precipitate, increasing viscosity.

Table 7.3 Viscosity of microgels with NaCl. Data (n=3) are presented as the mean ± SD. Data with different uppercase superscript letters within a row and data with different lowercase superscript letters within a column indicate significant differences.

NaCl (M)	**Viscosity (mPa)**	
	WPI	WPI/VD_3
0	206 ± 43.93^{bA}	104 ± 5.74^{bA}
0.05	488 ± 53.20^{aB}	654 ± 46.89^{aA}
0.1	456 ± 55.97^{aB}	627 ± 45.04^{aA}
0.2	437 ± 13.03^{aA}	623 ± 49.11^{aA}
0.4	564 ± 38.96^{aA}	734 ± 65.48^{aA}

Similar to the results in the previous section, the incorporation of vitamin D_3 led to slight changes in the storage and loss moduli however, its addition was not detrimental to the strength of the WPI microgels upon addition of NaCl and all samples were found to be more elastic than viscous. Strain sweeps revealed that at all NaCl concentrations for both microgel systems, their structures began to breakdown at approx. 0.8 – 1 % strain. For both microgel systems at all concentrations the storage and loss moduli values became equal at 100 % strain, indicating full structure breakdown.

The G' and G" for all samples displayed a weak frequency dependence which indicated that the rheological response of the microgels were not markedly affected by the applied deformation (Fig. 7.4 A and B). Over the frequency range (0.1 – 10 Hz), the addition of NaCl decreased the storage and loss modulus of the WPI microgels. However, as the concentration of NaCl increased, G' and G" increased, so that 0.4 M was similar to the control sample. For the WPI/VD_3 microgels, 0.05 M NaCl decreased G' and G" while the microgel strength increased at the other NaCl concentrations.

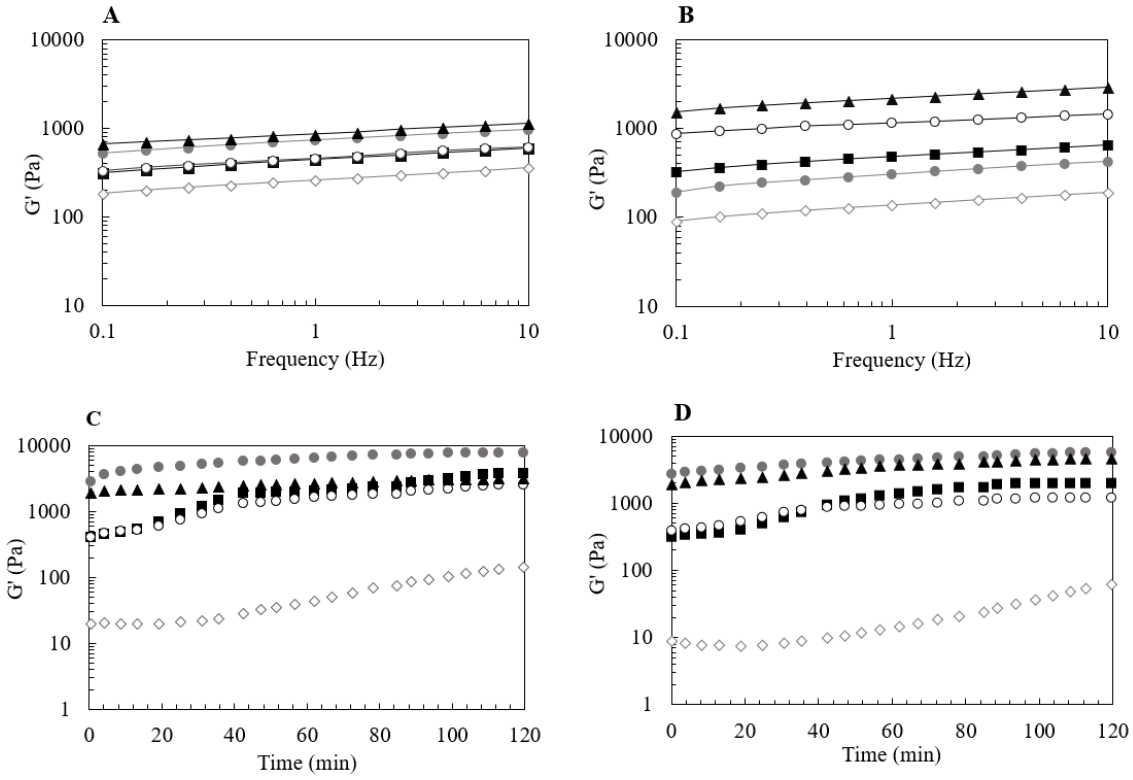

Fig. 7.4 Frequency sweeps of (A) WPI and (B) WPI/VD_3 microgels. Time sweeps of (C) WPI and (D) WPI/VD_3 microgels at (●) 0 M, (◊) 0.05 M, (■) 0.1 M, (○) 0.2 M and (▲) 0.4 M NaCl. Data (n=3).

Analysing G' and G" over a duration of 120 min revealed that the WPI and WPI/VD_3 microgels did not remain stable, as G' and G" increased initially followed by a plateau (Fig. 7.4 C and D). As discussed in chapter 5, G' and G" of the microgels increased on addition of $CaCl_2$, due to the salt screening the electrostatic repulsion between the protein molecules leading to the formation of a protein network. Also, present are some monomeric proteins amongst the microgels, therefore, it is suggested that NaCl interacted with the remaining free monomeric proteins causing G' and G" to increase initially as the strength of the microgel structure was increasing while interactions occurred between the salt and protein molecules. This increase eventually plateaued.

However, the incorporation of NaCl decreased the microgel strength compared to the control regardless of concentration. As the microgels are made up of $CaCl_2$ induced cross-links, the addition of more salt could have led to a higher aggregation rate of the available monomeric protein molecules creating large aggregates forming a structure with decreased G'. Similar results were found by Wang *et al*. (2018), whereby on increasing

the ionic concentration, extremely large aggregates were formed leading to an inhomogeneous structure resulting in a coarser gel with decreased storage modulus.

On foaming the WPI and WPI/VD_3 microgels, there was no significant difference between the foaming properties of both systems in the presence of NaCl (Table 7.4). The addition of NaCl to both microgel systems had no significant effect on foam overrun when compared to the control, except when 0.2 M NaCl was added, which improved foam overrun. Stability of the microgel foams was unaffected by NaCl addition, as stability remained at 89 – 98 %. The viscosity of both microgel systems increased on addition of NaCl, regardless of concentration, however, this viscosity increase did not affect foaming. For native WPI (chapter 3), foam stability was also unaffected by NaCl addition.

Table 7.4 Foam overrun and stability of microgels with NaCl. Data (n=3) are presented as the mean ± SD. Within each parameter, data with different uppercase superscript letters within a row and data with different lowercase superscript letters within a column indicate significant differences.

NaCl (M)	Overrun (%)		Stability (%)	
	WPI	**WPI/VD_3**	**WPI**	**WPI/VD_3**
0	361 ± 41.79^{bA}	344 ± 41.94^{bA}	$97 \pm 1.53^{a,bA}$	$95 \pm 1.67^{a,bA}$
0.05	383 ± 0.00^{bA}	367 ± 16.67^{bA}	$98 \pm 0.33^{a,bA}$	$97 \pm 0.96^{a,bA}$
0.1	394 ± 9.62^{bA}	389 ± 9.62^{bA}	98 ± 0.58^{aA}	$94 \pm 2.55^{a,bA}$
0.2	472 ± 25.46^{aA}	450 ± 16.67^{aA}	$96 \pm 0.96^{a,bA}$	97 ± 1.67^{aA}
0.4	356 ± 38.49^{bA}	344 ± 34.69^{bA}	94 ± 1.92^{bA}	89 ± 5.09^{bA}

The addition of salt affects the stability, solubility, and biological activity of proteins. At low concentrations the addition of salt can stabilise proteins through electrostatic interactions as the protein solubility is enhanced (i.e. salting in) while at high concentrations solubility is reduced as protein and salt molecules compete to bind with water leading to precipitation and low foaming properties (i.e. salting out) (Arakawa and Timasheff, 1984). Zayas (2001) states that salting out with neutral salts occurred above 1.0 M, however, other studies have found that salting-out of whey protein isolate with Ca^{2+} or Mg^{2+} occurred at a lower concentration of 0.04 M or 0.1 M $CaCl_2$ for silver carp myosin (Zhu and Damodaran, 1994; Jia *et al.*, 2015). In this study, the mechanism of

salting-out did not seem to occur as the foaming properties of WPI and WPI/VD_3 microgels were not affected by the higher ionic concentration of 0.4 M NaCl, remaining similar to the control.

As previously mentioned, stable foams can result in greater textural properties, however, the foam firmness and consistency of WPI and WPI/VD_3 microgels slightly decreased in the presence of NaCl but did not have a detrimental effect on foaming properties (Fig. 7.5).

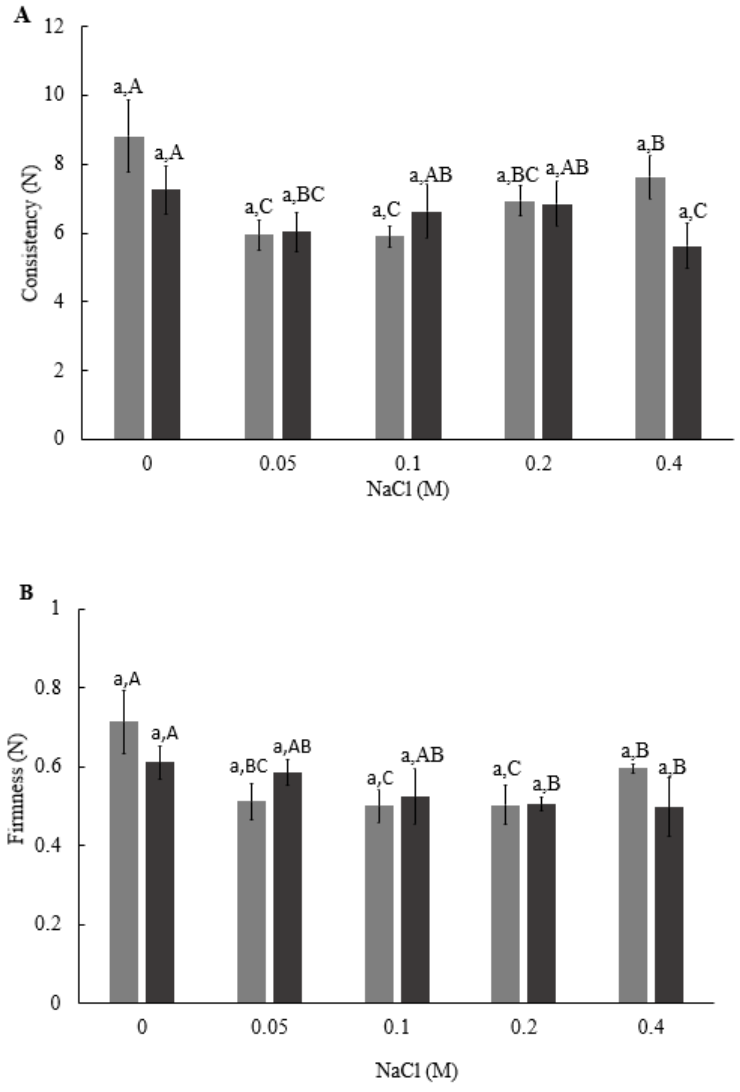

Fig. 7.5 Foam consistency (A) and foam firmness (B) of WPI (grey) and WPI/VD_3 (black) microgel foams. Data (n=3) are presented as the mean ± SD. Data with different lowercase letters indicate significant differences between NaCl concentration; different uppercase letters indicate significant differences between each microgel system.

7.2.3 Effect of sucrose on WPI and WPI/VD_3 microgels

Sucrose is a common ingredient used in the manufacture of food products and therefore, its effect on WPI and WPI/VD_3 microgel rheological, foaming and foam textural properties was studied. At approx. 1 % strain, the storage and loss moduli of both microgel systems at all sucrose concentrations began to decrease and a viscoelastic behaviour was observed with G' being greater than G". The results demonstrate that at all sucrose concentrations, G' and G" of both microgel systems were slightly frequency dependent as G' and G" increased from 0.1 to 10 Hz (Fig. 7.6 A and B), however, there was no change in the microgel network as the slope of G' and G" did not change. However, the addition of sucrose decreased the microgel strength compared to the control, decreasing the storage and loss moduli.

Time sweeps revealed that as the sucrose concentration increased from 12 to 20 %, G' and G" increased, but they were still less than the control (0 % sucrose) (Fig. 7.6 C and D). High sucrose concentrations increase the viscosity, which leads to a reduction in the mobility in the environment, resulting in a drop in gel strength (Khemakhem *et al.*, 2019).

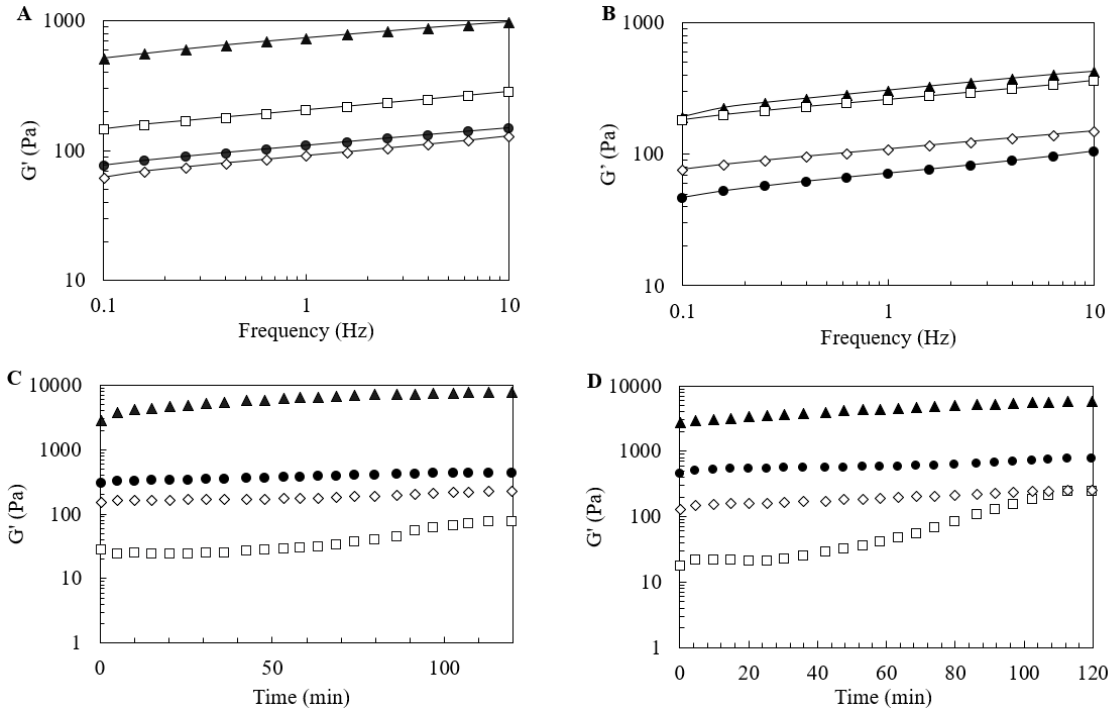

Fig. 7.6 Frequency sweeps of G' of (A) WPI and (B) WPI/VD_3 microgels. Time sweeps of (C) WPI and (D) WPI/VD_3 microgels at (▲) 0 %, (□) 12 %, (◊) 15 % and (•) 20 % sucrose. Data (n=3).

Addition of sucrose significantly increased the WPI and WPI/VD_3 microgel viscosity, however, the foam overrun and stability were not affected by the addition of sucrose (Table 7.5). The foam overrun remained at 322 – 378 % while stability remained at 93 – 99 %. Sucrose decreases the thermodynamic affinity of proteins for the aqueous environment while enhancing protein-protein interactions (Bryant and McClements, 2000). Therefore, the protein molecules do not adsorb at the air-water interface as they prefer to stay in the continuous phase, affecting foamability (Nastaj, 2021). Sucrose is known to increase the viscosity of systems which in turn leads to reduced foam overrun and increased stability (Yang and Foegeding, 2010). This mechanism occurred for native WPI in chapter 3, whereby sucrose addition decreased foam overrun but increased foam stability. However, the addition of sucrose did not affect WPI or WPI/VD_3 microgel foaming properties as foam overrun or stability did not significantly differ from the control foam samples. Other studies have also found that sucrose addition increased foam stability (Davis and Foegeding, 2007; Raikos *et al*., 2007).

Table 7.5 Viscosity, foam overrun and stability of WPI and WPI/VD_3 microgels on addition of sucrose. Data (n=3) are presented as the mean ± SD. Within each parameter, data with different uppercase superscript letters within a column and data with different lowercase superscript letters within a row indicate significant differences.

		Sucrose (%)			
		0	**12**	**15**	**20**
Viscosity (mPa)	WPI	206 ± 43.93^{cA}	385 ± 30.84^{bB}	364 ± 17.02^{bB}	563.26 ± 33.97^{aA}
	WPI/VD_3	104 ± 5.74^{cA}	508 ± 0.44^{bA}	510 ± 0.57^{bA}	616 ± 151.78^{aA}
Overrun (%)	WPI	361 ± 41.79^{bA}	372 ± 9.62^{aA}	356 ± 9.62^{aA}	333 ± 16.67^{aA}
	WPI/VD_3	344 ± 41.94^{aA}	378 ± 9.62^{aA}	372 ± 9.62^{aA}	322 ± 63.10^{aA}
Stability (%)	WPI	97 ± 1.53^{aA}	99 ± 0.96^{aA}	96 ± 1.92^{aA}	97 ± 2.55^{aA}
	WPI/VD_3	95 ± 1.67^{aA}	97 ± 3.35^{aA}	93 ± 1.27^{aA}	95 ± 3.37^{aA}

Foam textural properties showed that foam firmness and consistency did not significantly differ between the WPI and WPI/VD_3 microgels (Fig. 7.7). Even though the addition of sucrose did not significantly affect the foaming properties of either microgel system, sucrose addition (regardless of concentration) decreased the foam firmness and

consistency of both microgel systems. The storage and loss moduli of WPI and WPI/VD_3 microgels also decreased on addition of sucrose, indicating weakening the microgel structure. It is possible that the weakened gel structure when whipped also formed a weak foam structure that could not withstand the penetration test resulting in reduced textural properties.

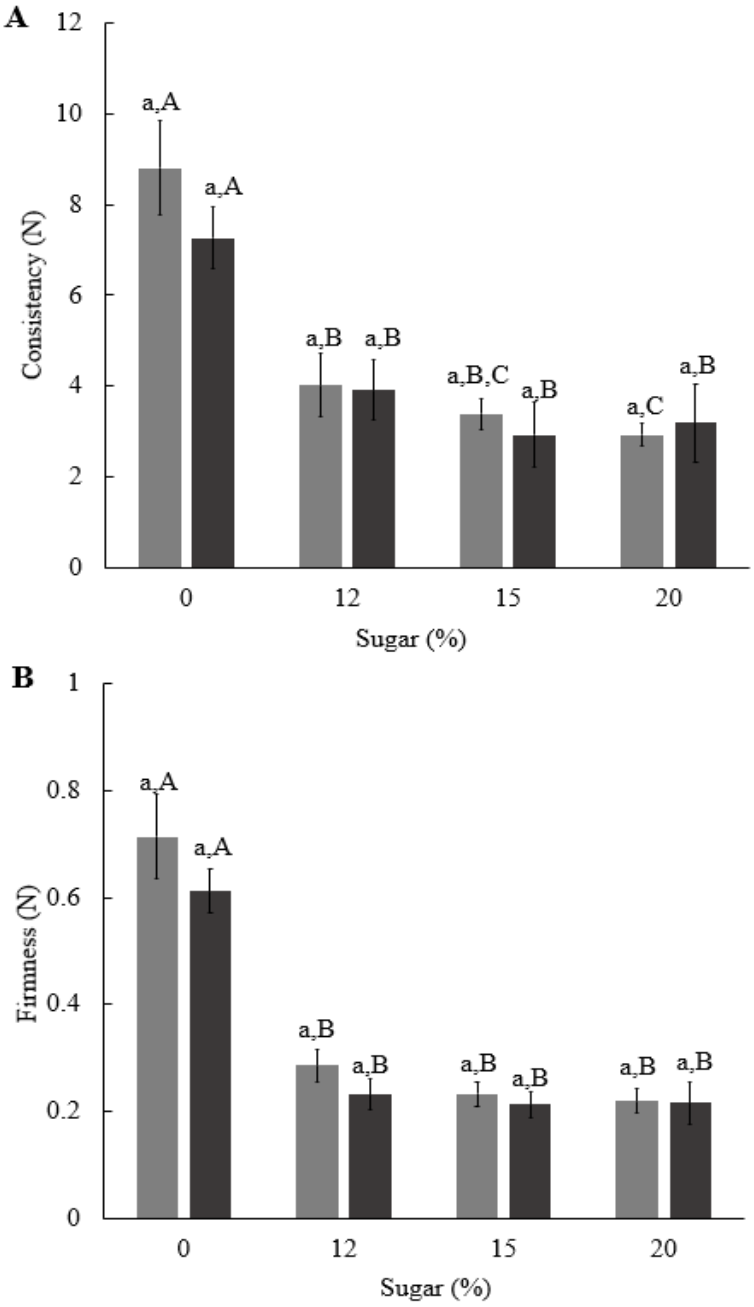

Fig. 7.7 Foam consistency (A) and foam firmness (B) of WPI (grey) and WPI/VD_3 (black) microgel foams. Data (n=3) are presented as the mean ± SD. Data with different lowercase letters indicate significant differences between sucrose concentrations; different uppercase letters indicate significant differences between each microgel system.

7.2.4 Effect of xanthan gum on WPI and WPI/VD_3 microgels

Xanthan gum (XG) is commonly used in the food industry for its stabilising properties, it increases the solution viscosity which enhances foam stability by retarding drainage (Martínez-Padilla *et al*., 2015). In chapter 4, it was found that 0.3 % xanthan gum produced foams with the best overrun and stability, therefore, this concentration was used in this study. Xanthan gum's effect on WPI and WPI/VD_3 microgel rheological, foaming and foam textural properties was therefore examined.

Similar to the previous sections, all microgel systems showed that G' dominated over G", indicating that the microgels were more viscoelastic. Strain sweeps showed that the WPI and WPI/VD_3 microgels began to breakdown at approx. 2 - 3 % strain as G' and G" started to decrease. The systems had an extremely low dependency on frequency, and the addition of 0.3 % XG presented marginally higher values of G' and G" in comparison to the control microgels, indicating that the presence of XG strengthened the gel system. A study by Zmudziński *et al.* (2014) also found that the addition of XG to egg white protein foams increased G' and G".

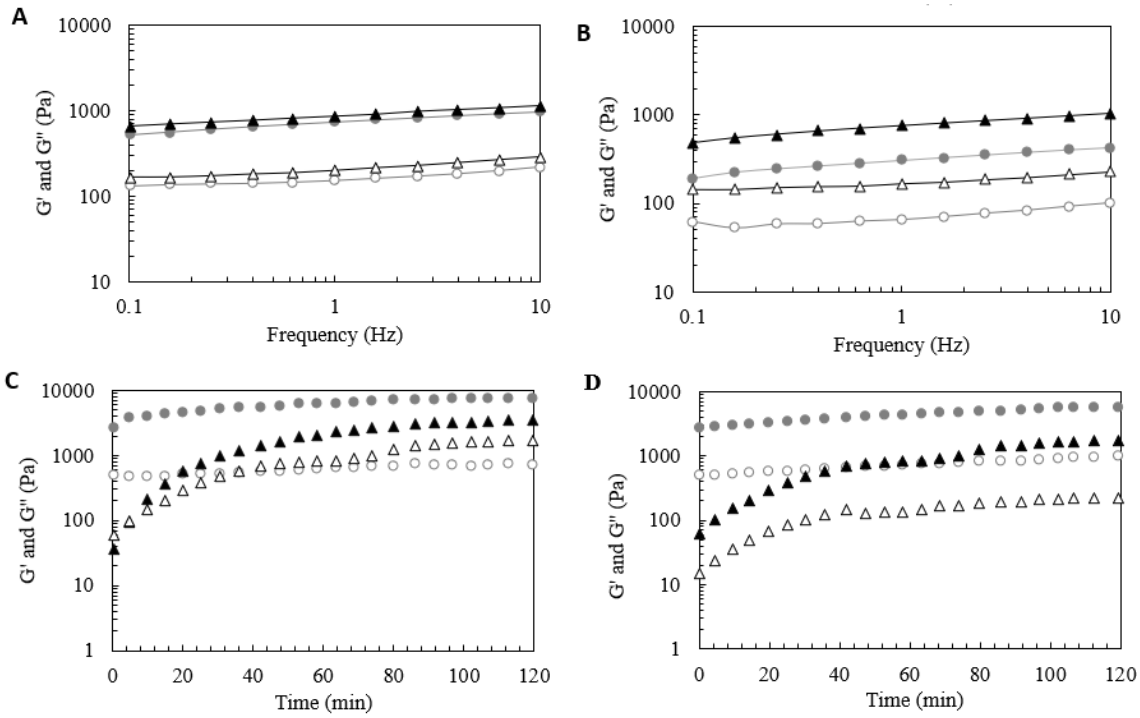

Fig. 7.8 Frequency sweeps of (A) WPI and (B) WPI/VD_3 microgels. Time sweeps of (C) WPI and (D) WPI/VD_3 microgels at (•) 0 %, (▲) 0.3 % xanthan gum. Closed symbols represent G' and open symbols represent G". Data (n=3).

Time sweeps indicated that the addition of XG to both microgel systems formed unstable structures as G' and G" increased initially until about 50 min and thereafter plateaued (Fig. 7.8 C and D) which was also seen with pH. Several interactions can occur between proteins and polysaccharides such as complexation, co-solubility or segregation, which likely caused G' and G" to increase as XG strengthened the microgel structure before reaching equilibrium (Rodriguez Patino and Pilosof, 2011). Bryant and McClements (2000) found that thermodynamic incompatibility occurred between 8.5 % whey protein and at comparable XG concentration (0.05 – 0.2 %) at pH 7, where both molecules are negatively charged, leading to electrostatic repulsion between the molecules. The authors state that thermodynamic incompatibility is more pronounced in an aggregated solution than one containing individual proteins (Bryant and McClements, 2000). However, Benichou *et al*. (2007) found that in a mixture containing 4 – 10 % WPI and 0.5 – 2 % XG, molecular interactions occurred without phase separation. The authors suggested that there is a metastable zone between coacervation and a solution-like phase where the molecules do not precipitate but are in a supersaturated state with one another.

In this study, the microgels were negatively charged as they were at pH 6.8. It is possible that there are several positively charged sites on the microgels which strongly interacted with XG. The initial increase in G' and G" on addition of XG could be due to new interactions taking place between the microgels and XG forming new structured entities. Xanthan gum imposes its elasticity and may have adsorbed on the protein surface, which led to strengthening of the microgels which when fully adsorbed, equilibrated. Similar results were documented by Benichou *et al*. (2007). Visually no separation occurred in the mixture.

Addition of 0.3 % xanthan gum increased the viscosity of both microgel systems and subsequently decreased foam overrun, while foam stability was unaffected (Table 7.6). For native WPI in chapter 4, the addition of XG increased solution viscosity which also decreased foam overrun, however, XG improved native WPI foam stability. Upon foaming, the mechanical forces propel the re-orientation of XG molecules, which increases the viscosity (Zmudziński *et al*., 2014). Xanthan gum's weak gel-like properties and pseudo-plastic flow properties enable it to provide colloidal systems with long-term stability (Moschakis *et al*., 2005). In chapter 5, the WPI microgels displayed extreme stabilising abilities, forming foams that remained stable for > 2 years and the addition of XG in this study did not alter this ability as the foam stability did not change.

Table 7.6 Viscosity, foam overrun and stability of WPI and WPI/VD_3 microgels. Data (n=3) are presented as the mean ± SD. Within each parameter, data with different uppercase superscript letters within a column and data with different lowercase superscript letters within a row indicate significant differences.

		Xanthan gum (%)	
		0%	**0.30%**
Viscosity (mPa)	**WPI**	206 ± 43.93^{bA}	1338 ± 511.31^{aA}
	WPI/VD_3	104 ± 5.74^{bA}	1436 ± 54.23^{aA}
Overrun (%)	**WPI**	361 ± 41.79^{aA}	217 ± 16.67^{bA}
	WPI/VD_3	344 ± 41.94^{aA}	194 ± 34.70^{bA}
Stability (%)	**WPI**	97 ± 1.52^{aA}	100 ± 0.00^{aA}
	WPI/VD_3	95 ± 1.67^{aA}	100 ± 0.00^{aA}

Textural results of the WPI and WPI/VD_3 microgel foams showed that foam consistency and foam firmness did not change on addition of XG, as they did not significantly differ from the control (Fig. 7.9). The foam textural results correlate with foam stability as there was no significant change on addition of XG. In chapter 4, the addition of XG was found to increase the textural properties of native WPI foams. Zmudziński *et al*. (2014) states that during the whipping process, the XG molecules undergoes conformation changes and stretches which can interpenetrate with the unfolded protein molecules. This increase did not occur for the microgels as they are already in an aggregated state, capable of retaining their structure, and so XG might not have been able to interpenetrate to the same extent.

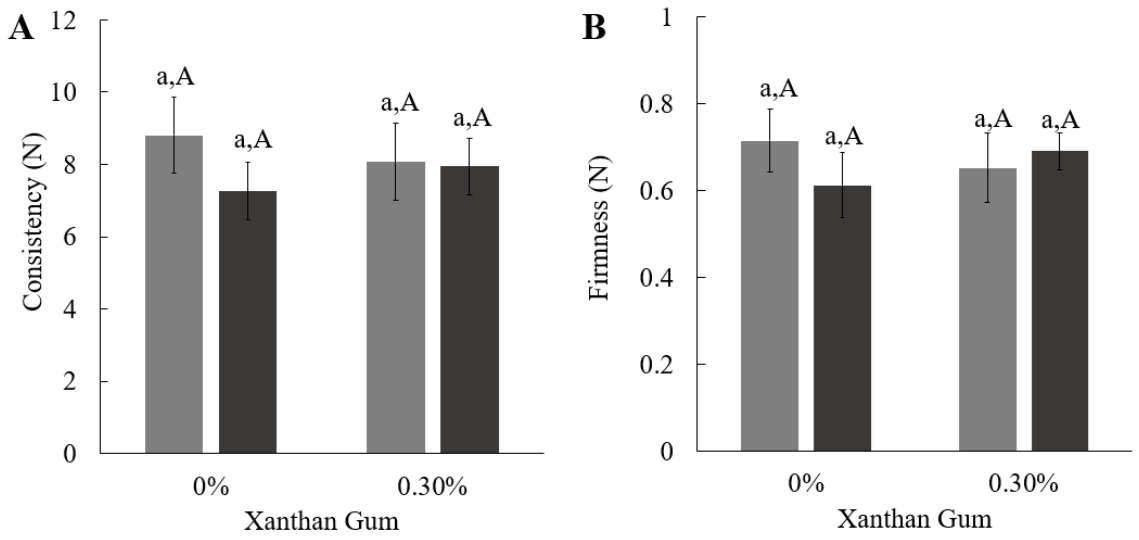

Fig. 7.9 Foam (A) consistency and (B) foam firmness of WPI (grey) and WPI/VD_3 (black) microgel foams. Data (n=3) are presented as the mean ± SD. Data with different letters at each XG concentration indicate significant differences.

7.2.5 Effect of heat treatment on WPI and WPI/VD_3 microgels

The WPI and WPI/VD_3 microgels were exposed to dairy pasteurisation temperatures of 72 °C for 15 s or 63 °C for 30 min and the effect on rheological, foaming and foam textural properties were assessed. Heating to 72 °C for 15 s is known as the continuous method and is referred to as high temperature, short time (HTST) heating. Heating at 63 °C for 30 min is considered a batch method or low temperature long time (LTLT) heating (Meunier-Goddik and Sandra, 2002).

Fig. 7.10 shows G' as a function of frequency for both microgel systems when subjected to heat treatment. The slope of G' for each heat treatment was similar for both systems with very little change which indicates that the gel structure was not altered. Heating at either temperature increased the strength of the microgels, increasing the G' and G" compared to the unheated microgels. The increase in G' and G" was substantially greater when the microgels were heated at 72 °C for 15 s. Time sweeps indicated that the storage and loss moduli of both microgel systems were not stable and significantly increased over the duration of 120 min. As previously discussed, the microgels are made up of monomeric and polymeric protein molecules. It is possible that heating caused the monomeric proteins to aggregate further causing the protein network in the microgels to strengthen leading to increased storage and loss moduli.

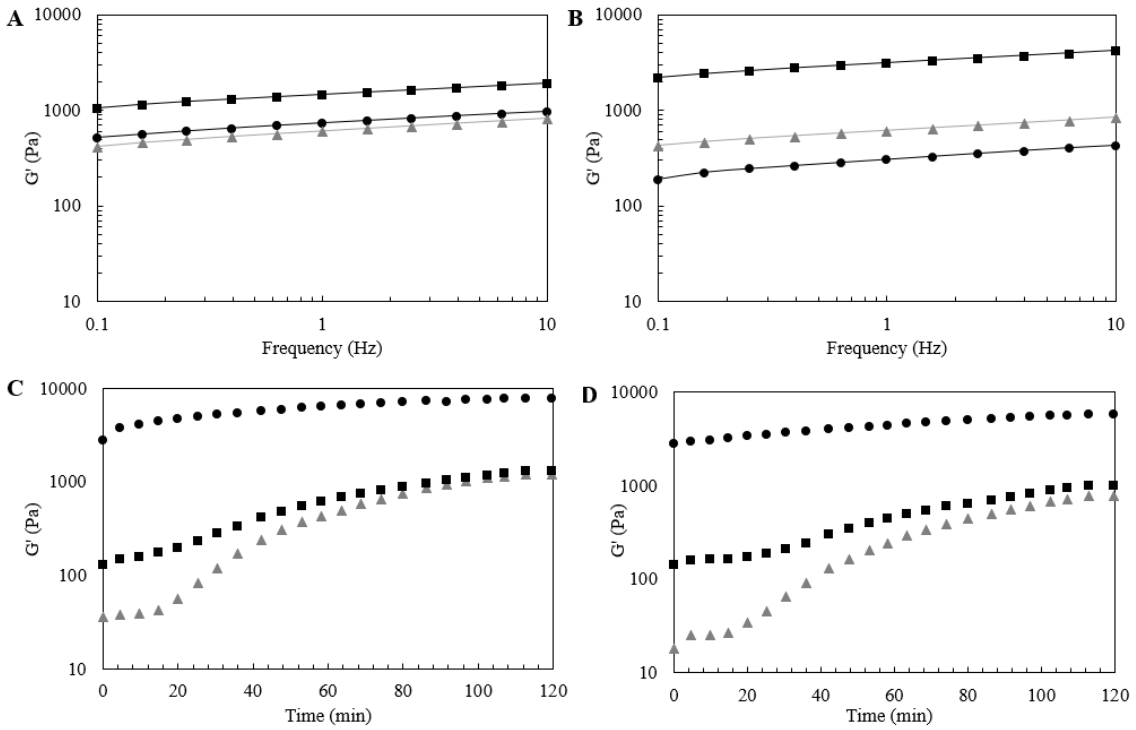

Fig. 7.10 Frequency sweeps (G') of (A) WPI and (B) WPI/VD_3 microgels. Time sweeps (G') of (C) WPI and (D) WPI/VD_3 microgels at (•) no heat, (▲) 72 °C 15 s and (■) 63 °C 30 min. Data (n=3).

The effect of heat treatment on the WPI and WPI/VD_3 microgel foaming properties is shown in Table 7.6, with heat treatment resulting in reduced overrun at both temperatures. As discussed above for the rheological data, it is possible that heating caused the monomeric proteins to aggregate. In chapter 3, native WPI was altered to pH close to the pI, where protein-protein interactions are favoured which was further aggravated by heat treatment, leading to reduced foam overrun. Therefore, in this chapter, the increased aggregation due to heat treatment increased the microgel sol viscosity leading to reduced overrun (Table 7.7).

Table 7.7 Viscosity, foam overrun and stability of WPI and WPI/VD_3 microgels. Data (n=3) are presented as the mean ± SD. Within each parameter, data with different uppercase superscript letters within a row and data with different lowercase superscript letters within a column indicate significant differences.

		Temperature (°C)		
		No heat	**72°C 15 s**	**63°C 30 min**
Overrun (%)	**WPI**	361 ± 41.79^{aA}	283 ± 0.00^{bA}	267 ± 16.67^{bA}
	WPI/VD_3	344 ± 41.94^{aA}	275 ± 22.06^{bA}	261 ± 4.81^{bA}
Stability (%)	**WPI**	97 ± 1.52^{aA}	93 ± 1.67^{aA}	82 ± 4.41^{bA}
	WPI/VD_3	95 ± 1.67^{aA}	92 ± 1.67^{aA}	84 ± 1.92^{bA}
Viscosity (mPa)	**WPI**	206 ± 43.93^{bA}	221 ± 9.20^{aA}	216 ± 1.45^{aA}
	WPI/VD_3	104 ± 5.74^{bA}	187 ± 27.15^{aA}	137 ± 23.06^{aA}

Foam stability was not affected by heating at 72 °C for 15 s, whereas heating at 63 °C for 30 min decreased the foam stability. Although heating at LTLT slightly reduced the foam overrun, good foaming properties were still achieved, however, heating at HTST was less detrimental to the microgels foaming properties. The use of HTST is more common in the food industry as it is more energy efficient and cost effective.

Heating significantly decreased the foam textural properties of both microgel systems as the foam firmness and consistency reduced by more than half upon heat exposure (Fig. 7.11). This could be linked to the foam overrun values, as they were also negatively affected by heat treatment.

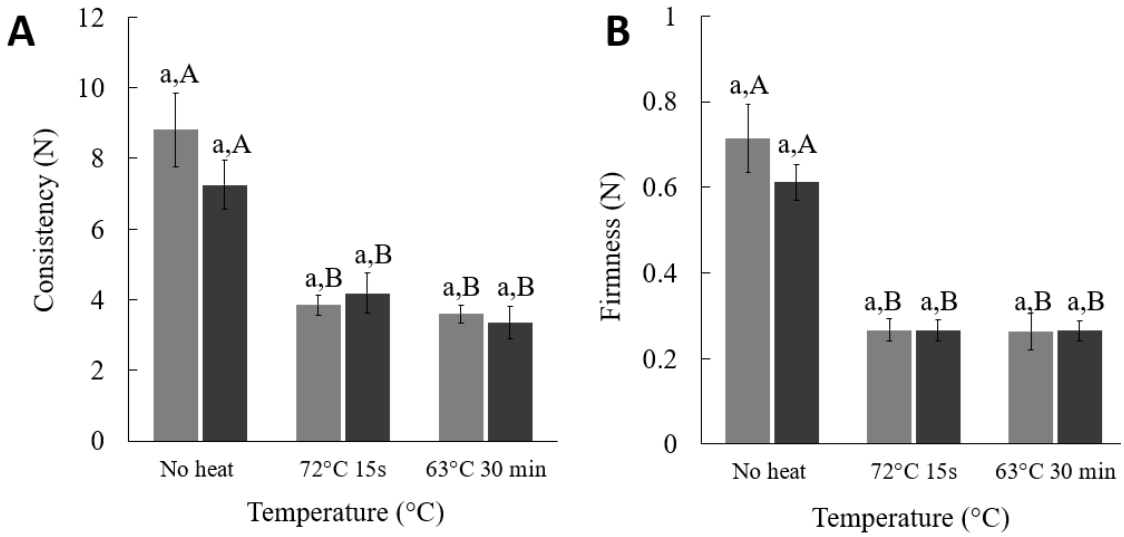

Fig. 7.11 Foam consistency (A) and foam firmness (B) of WPI (grey) and WPI/VD_3 (black) microgel foams. Data (n=3) are presented as the mean ± SD. Data with different lowercase letters indicate significant differences between heat treatments; different uppercase letters indicate significant differences between each microgel system.

The WPI and WPI/VD_3 microgels regardless of environmental condition displayed similar behaviours in G' and G", demonstrating how vitamin D_3 addition did not negatively affect the WPI microgel rheological properties. Results showed that in most cases the foaming ability of both microgel systems were not significantly different from each other, indicating that vitamin D_3 can be added to WPI microgels without causing any negative effects. Results indicated that the WPI and WPI/VD_3 microgel foaming properties can be tailored by altering pH, ionic strength, sucrose content, heat treatment or xanthan gum addition. The WPI and WPI/VD_3 microgels across the various conditions displayed good foaming properties, indicating that their incorporation into a complex food formulation is possible.

7.2.6 Vitamin D stability after foaming

Previously, in chapter 6 the ability of WPI microgels to protect VD_3 from various environmental conditions was established. It was proposed that the antioxidant activity of the free thiol groups of β-lactoglobulin in whey protein provided a protective barrier for vitamin D_3, as the mobility of VD_3 was reduced within the protein matrix composed of amino acids with aromatic side groups and double bonds (Khan *et al.*, 2020;

Diarrassouba *et al*., 2015; Liu *et al*., 2020a). However, it is essential to assess the protective effect of WPI microgels after exposure to various conditions followed by mechanical whipping before proposing the microgels as a functional food ingredient.

Upon exposure to the various environmental conditions and subsequently foamed, the WPI/VD_3 microgel samples were stored at 4 °C for 4 weeks. Vitamin D_3 stability was analysed at the end of the fourth week to determine if the microgels could protect VD_3 after being mechanically whipped. In Fig. 7.12, the total amount of VD_3 released (%) for each condition at the end of the four weeks is presented. The WPI microgels whipped at pH 3 – 9 led to small amounts of VD_3 being released with the maximum amount released at pH 4 with a loss of 2.85 %.

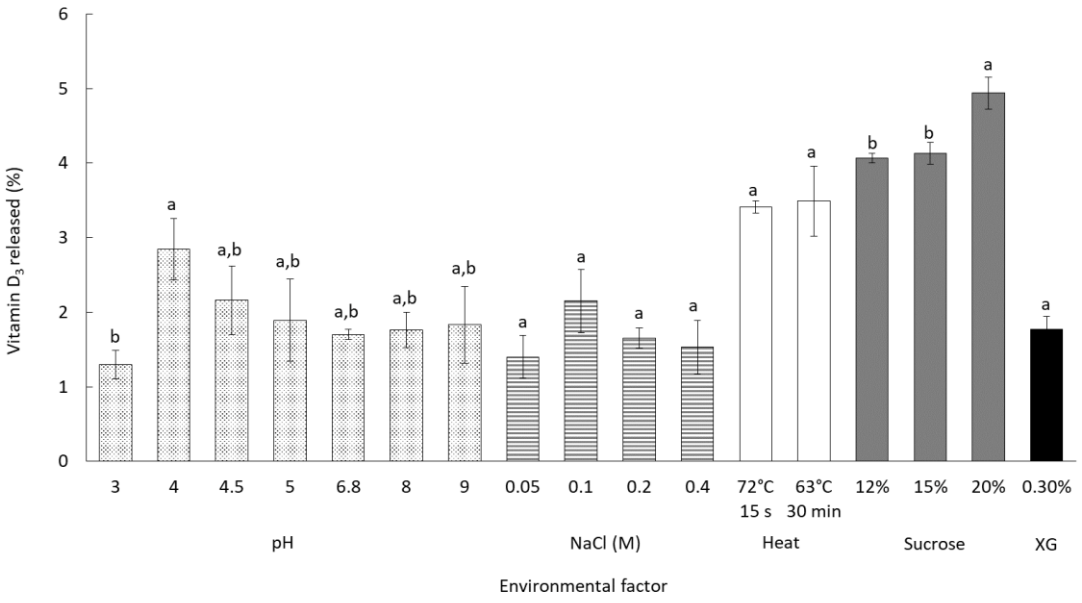

Fig. 7.12 Vitamin D_3 (%) stability after exposure to various environmental conditions followed by foaming. pH (polka dot), NaCl (stripes), heat (solid white), sucrose (solid grey) and xanthan gum (black). Data (n=3) are presented as the mean ± SD. Data with different letters within a condition indicate significant differences.

On addition of 0.05 – 0.4 M NaCl, there was a loss of 1.41 – 2.04 % vitamin D_3 across the four salt concentrations and the addition of XG led to 1.77 % VD_3 loss at the end of the fourth week. Foaming of the microgels in the presence of sucrose was found to be the most detrimental to VD_3 stability regardless of concentration, losing

approximately 4 % VD_3 at the end of the fourth week. However, this percentage loss is still considered a small loss.

Pasteurisation is important in food production, but the process is destructive to sensitive compounds such as vitamin D_3 (David and Livney, 2016). In chapter 6 of this thesis, the unwhipped WPI microgels were found to protect VD_3, as 97 % remained after heat exposure. After whipping the heated WPI/VD_3 microgels small losses occurred. When heated at 72 °C for 15 s or 63 °C for 30 min there was a loss of 3.41 or 3.50 % VD_3 respectively.

For native proteins mechanical whipping partially denatures protein solutions causing the protein molecules to undergo conformational changes at the air-water interface (Damodaran *et al.*, 2007). Due to this whipping effect, it is possible that the protein microgels were partially disrupted which led to some vitamin D_3 release. However, the amount of vitamin D_3 release was low, and it is hypothesised that the cross-linked microgel network was stable enough to withstand mechanical whipping and continued to protect the majority of vitamin D_3.

7.3 Conclusion

Encapsulation of vitamin D_3 did not negatively affect the foaming properties of WPI microgels. Results indicated that the rheological, foaming and foam textural properties of the microgels can be tailored by altering environmental conditions, however, in most cases there was no significant change from the control. The WPI/VD_3 microgels were also capable of protecting vitamin D_3 after mechanical whipping as very little losses of vitamin D_3 occurred.

This study demonstrates the potential of WPI microgels to act as delivery vehicles for vitamin D_3, while also producing stable foams, giving background for incorporating WPI/VD_3 microgels into real food systems for vitamin D_3 delivery.

Chapter 8
Incorporation of WPI/VD_3 microgels into ice cream

8.1 Introduction

A study by the World Health Organisation stated that the population growth of older persons is occurring on a global scale. By 2050, the population of people over the age of 60 is estimated to double to 2.1 billion, while the number of persons aged 80 or over is expected to triple by 2050 reaching 426 million (World Health Organization, 2021). As people age, physiological changes occur which can cause osteoarthritis, diabetes, increased blood pressure, dysphagia, osteoporosis etc. that can lead to reduced appetite and inadequate food intake.

Today, there is still a lack of choice of food products available that target the nutritional requirements needed by the elderly (Keršienė *et al*., 2020). This is limited by micronutrient degradation due to food processing or storage conditions because of the sensitive nature of micronutrients that are susceptible to light, temperature, or oxygen. These problems can be overcome by encapsulation within a carrier material before being incorporated into a food product.

In Chapter 6, WPI microgels proved to be a suitable vehicle for encapsulating and protecting vitamin D_3 on exposure to pasteurisation, UV-light and long-term storage. In Chapter 7, the vitamin D_3 loaded microgels displayed their ability to be mechanically whipped and still provide protection for vitamin D_3 while maintaining a stable foam.

This chapter therefore investigates the incorporation of WPI/VD_3 microgels into a real food matrix, ice cream. Ice cream is a popular dessert across the globe and could be explored as a vehicle for providing nutrition to elderly people (Spence *et al*., 2019). Studies suggest that soft and moist foods are most suitable for the elderly due to their ease of consumption, the incorporated air makes foams soft, easy to chew and digest (Aguilera and Park, 2016). Ice cream's creamy cold mouthfeel may stimulate the ageing palate, making it an effective vehicle for the delivery of calories and nutrients (Spence *et al*., 2019).

As the WPI microgels have already proved to protect vitamin D_3, the WPI microgels ability to withstand mixing, shearing and freezing during ice cream manufacture was analysed. The addition of WPI/VD_3 microgels on the rheological properties of the ice cream mixture and on the overrun, hardness and melting properties of ice cream was assessed to determine if microgel incorporation significantly affected the ice cream. Vitamin D_3 retention within the ice cream was also analysed to determine the protective effect of WPI microgels. The outcome of this study will therefore determine if WPI/VD_3 microgels have use in real life food systems.

8.2 Results & discussion

8.2.1 Ice cream rheological properties

The vitamin D_3 loaded microgels were added to the ice cream mixture (ICM) at different concentrations ranging from 3 – 17 % to determine the quantity of microgels that could be added before causing a significant change to the ice cream. The effect of WPI/VD_3 microgel concentration on the ICM rheological properties was firstly examined. When the microgels were added to the ICM, there was an increase in viscosity with increasing microgel concentration (Table 8.1). The viscosity of the ICM containing 17 % of microgels was almost five times greater than the control. Similar results have been found by Roy *et al*. (2022), Akalın *et al*. (2008) and Dervisoglu *et al*. (2005), whereby addition of protein to ice cream increased the mix viscosity due to the formation of protein networks and also due to the high molecular weight of whey protein.

Table 8.1 Viscosity of ice cream mixture and overrun of ice cream incorporating 0 – 17 % WPI/VD_3 microgels. Data (n=3) are presented as the mean ± SD. Data with different superscript letters within a column indicate significant differences.

WPI/VD_3 microgels	Viscosity (mPa)	Overrun (%)
0 %	42.52 ± 3.42^{c}	14.87 ± 0.02^{a}
3 %	51.22 ± 6.19^{c}	14.66 ± 0.35^{a}
7 %	$56.66 \pm 1.26^{b,c}$	12.17 ± 0.19^{b}
10 %	$67.56 \pm 1.51^{b,c}$	10.41 ± 1.05^{b}
13 %	$91.86 \pm 15.13^{b,c}$	10.00 ± 0.99^{b}
17 %	207.09 ± 32.08^{a}	7.41 ± 0.45^{c}

Fig. 8.1 and 8.2 display a strain, frequency, and time sweep of the samples. Each graph only shows the storage modulus for clarity. A strain sweep was firstly carried out to determine the linear viscoelastic region of each sample. All samples displayed a similar trend, with the network structures beginning to break down at approx. 0.8 % strain (Fig. 8.1 A). Further increasing strain led to a crossover point i.e. G' = G", indicating a structural breakdown from an elastic to a more viscous regime. The crossover point occurred at increasing strain with increasing microgel concentration. For example, a strain of ~ 2 %

caused G" > G' on addition of 0 and 3 % microgels, whereas G" > G' at ~ 31 % strain on addition of 17 % microgels (Fig. 8.1 B), indicating how the microgels strengthened the structure within the ICM. A strain of 0.2 % was chosen for further tests as this is well within the linear viscoelastic region.

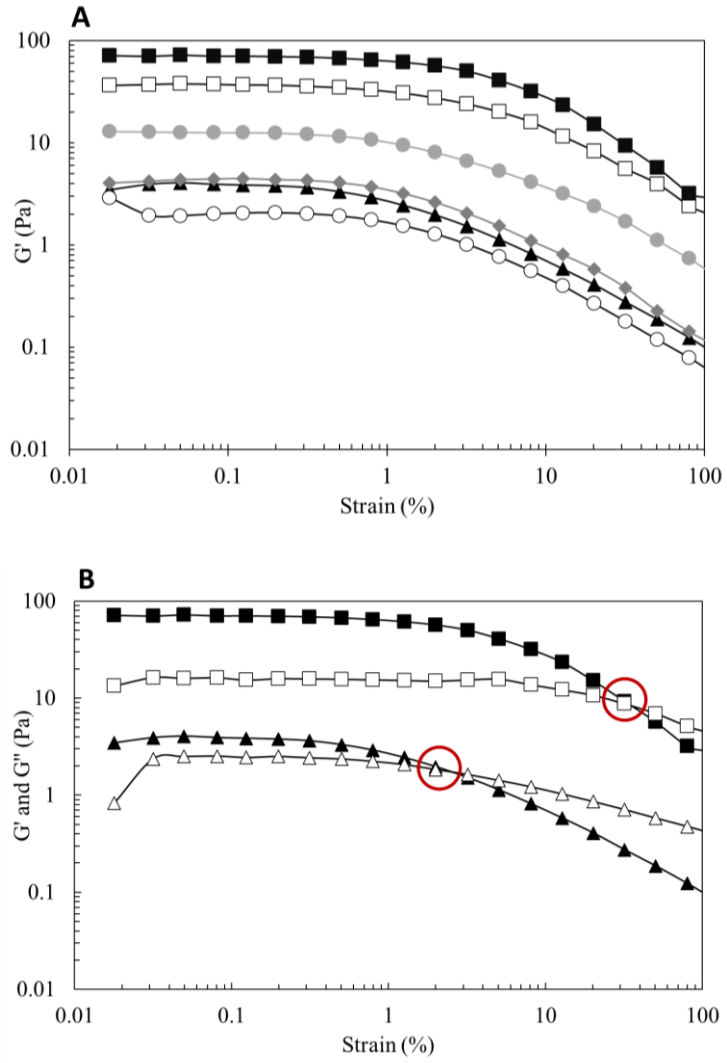

Fig. 8.1 (A) Strain sweep, G' of ice cream mixture containing 0 % (▲), 3 % (○), 7 % (♦), 10 % (●), 13 % (□) and 17 % (■) WPI/VD_3 microgels respectively. (B) Strain sweep, G' (closed symbols) and G" (open symbols) of ice cream mixture containing 0 % (▲) and 17 % (■) WPI/VD_3 microgels respectively. Red circle indicates crossover of moduli. Data (n=3).

All samples including the control were found to be marginally frequency dependent as G' and G" increased slightly as the frequency increased from 0.01 – 10 Hz and they were found to be more elastic than viscous (Fig. 8.2 A). The storage and loss

modulus were not significantly different comparing the control ICM and the ICM containing 3 – 7 % microgels. However, increasing to 10 – 17 % WPI/VD_3 microgels, G' and G" significantly increased.

The storage and loss moduli were monitored over a period of 120 min. Over that duration all ICM samples with or without microgels remained stable and displayed a predominantly elastic behaviour (Fig. 8.2 B). The incorporation of WPI/VD_3 microgels improved the viscoelastic strength of the ice cream, which increased with increasing microgel concentration.

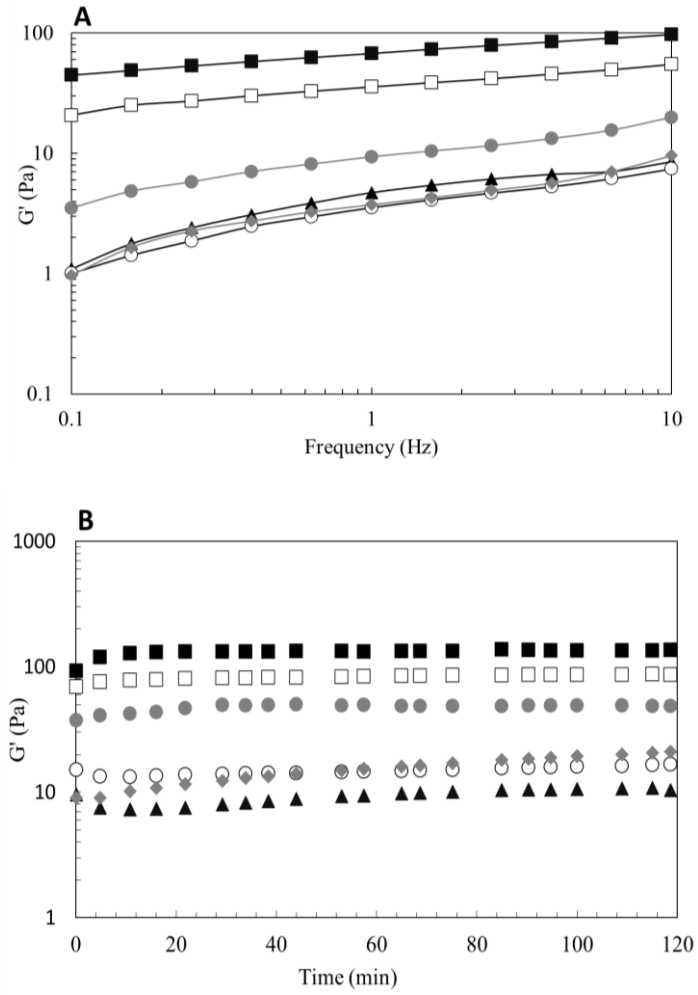

Fig. 8.2 Storage modulus (G') of ice cream mixture containing 0 % (▲), 3 % (○), 7 % (♦), 10 % (●), 13 % (□) and 17 % (■) WPI/VD_3 microgels respectively. (A) Frequency sweep and (B) Time sweep. Data (n=3).

These results suggest that incorporation of low levels of WPI/VD_3 microgels did not have much of an effect on the ICM, but, with increasing amounts of microgels the

viscoelasticity of the mixture increased. Similar results were found by Sun *et al*. (2015), whereby soy protein isolate/ cellulose nanofiber gels improved the viscoelasticity of ice cream. Similarly, Saraiva *et al*. (2020) found that on increasing the protein content of ice cream, G' and G" increased, with G' > G", due to the strong network formation of protein in the mixture.

It is possible that the WPI/VD_3 microgels might have bound to fat globules present in the ice cream mixture, further increasing the storage and loss moduli (Provost *et al*., 2016). Proteins are known to adsorb to fat globules due to their amphiphilic nature (Goff *et al*., 1989). This process was observed in Chapter 4, as the microgels stabilised air bubbles in foams. Yu *et al.* (2021) also found that the addition of nano fibrillated cellulose from grapefruit peel increased the viscoelastic strength of the ice cream mixture as G' and G" increased. The authors suggested that the nano-fibrillated cellulose could have bound to water or other components in the ice cream such as protein or fat through hydrogen bonds causing a positive effect on the ice cream structure.

8.2.2 Ice cream microstructure

The scanning electron microscopy images represent the control ice cream (without microgels) (Fig. 8.3 A) and 3 % WPI/VD_3 loaded ice cream (Fig. 8.3 B) respectively. Distinct differences were evident between both ice cream samples. The control ice cream sample appeared as a large mass with fat globules covering most of the surface creating a bumpy, uneven surface with some pores present. The addition of WPI/VD_3 microgels led to an ice cream with a smoother appearance. As indicated by the red circles, fat globules were still present on the surface, however, they were not as pronounced as the control (Fig. 8.3 B). It is proposed that the network formed by WPI/VD_3 microgels might be due to the microgels bridging multiple fat droplets causing coalescence into larger clusters forming a smoother surface. This fat bridging effect of the microgels could help to explain the increased storage and loss moduli values of the microgel loaded ice cream in Section 8.2.1. Similar results have been found by Deloid *et al*. (2018) and Yu *et al.* (2021). The smooth continuous three-dimensional network of the microgel loaded ice cream could also be due to the improved water holding capacity of the microgels as proposed by Hu *et al.* (2019). This suggests that the microgel loaded ice cream could provide a smoother mouthfeel when consumed.

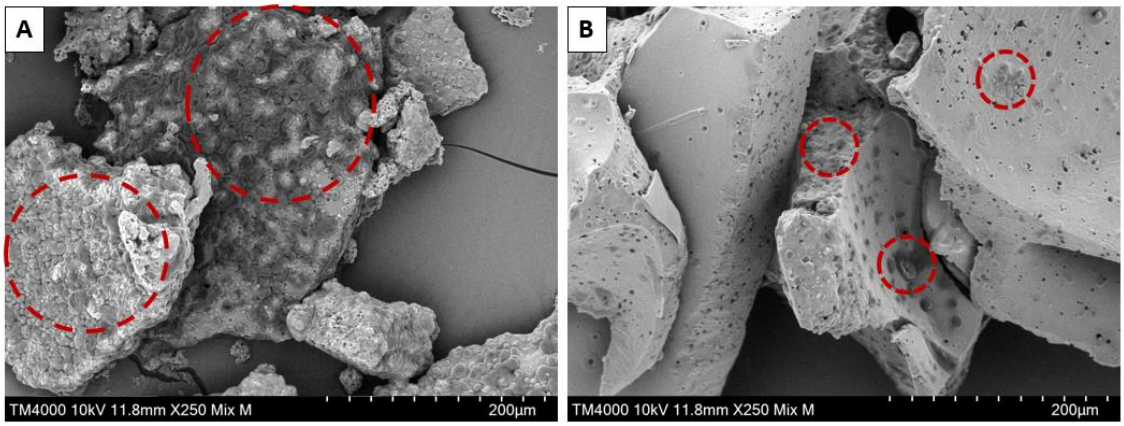

Fig. 8.3 Scanning electron microscopy micrographs of (A) control ice cream and (B) WPI/VD_3 microgel ice cream. Red dashed circles indicate fat globules.

8.2.3 Ice cream overrun (%)

The overrun which represents the air content in ice cream affects ice cream properties such as foam stability, melting behaviour and texture (Yan *et al*., 2021 & Soukoulis *et al*., 2008). In this study, the overrun of all the ice cream samples was relatively low (~ 7 – 15 %) and decreased with increasing WPI/VD_3 microgel concentration (Table 8.1). The addition of 3 % WPI/VD_3 microgels did not significantly alter the overrun compared to the control, however, further addition to 7 % or more significantly decreased the ice cream overrun. In fact, the overrun reduced by half on addition of 17 % WPI/VD_3 microgels compared to the control. The decreasing overrun with increasing microgel concentration could be attributed to the increasing ice cream mix viscosity. Increased viscosity decreases the amount of air that can be incorporated into a sample. Chansathirapanich *et al*. (2016) also found that more viscous ice cream mixtures incorporated less air resulting in lower overrun. More viscous ice cream systems require higher agitation and air incorporation due to the strong matrix that increases the resistance of the mixture to move (Roy *et al*., 2022).

Other studies have manufactured ice cream with overrun values of 28 – 55 % (Tipchuwong *et al*., 2017; Chansathirapanich *et al*., 2016; Yan *et al*., 2021 & Biasutti *et al*., 2013). The difference in overrun values could occur due to the ice cream mixture ingredients (Biasutti *et al*., 2013); in the other studies, authors added emulsifiers, stabilisers, milk powder or different sugars such as glucose syrup, which all could have influenced the overrun.

Nevertheless, the overall low overrun of all samples was probably due to the low power of the small benchtop ice cream machine which would be weaker than a commercial ice cream machine, being less capable of incorporating air. Overrun is found to be affected by dasher speed (Biasutti *et al*., 2013); the low power machine used in this study would work at a much lower speed and power churning the ice cream mixture at a slower rate affecting overrun.

8.2.4 Ice cream hardness

Ice cream hardness is the resistance of ice cream to deform upon an external force and is known to be affected by overrun, ice crystals, fat destabilization and viscosity (Muse and Hartel, 2004). After ice cream manufacture, the soft ice cream with or without WPI/VD_3 microgels was stored at -20 °C and the hardness was measured after 24 h and once a week for four weeks.

The hardness of ice cream with 3 % WPI/VD_3 microgels did not significantly differ from the control at any time point (Fig. 8.4), however, the hardness significantly increased with increasing microgel concentration across the four weeks. Ice cream with added 17 % microgels had the highest hardness (49 N), which was more than twice as much as the lowest hardness (23 N) at the end of the four weeks.

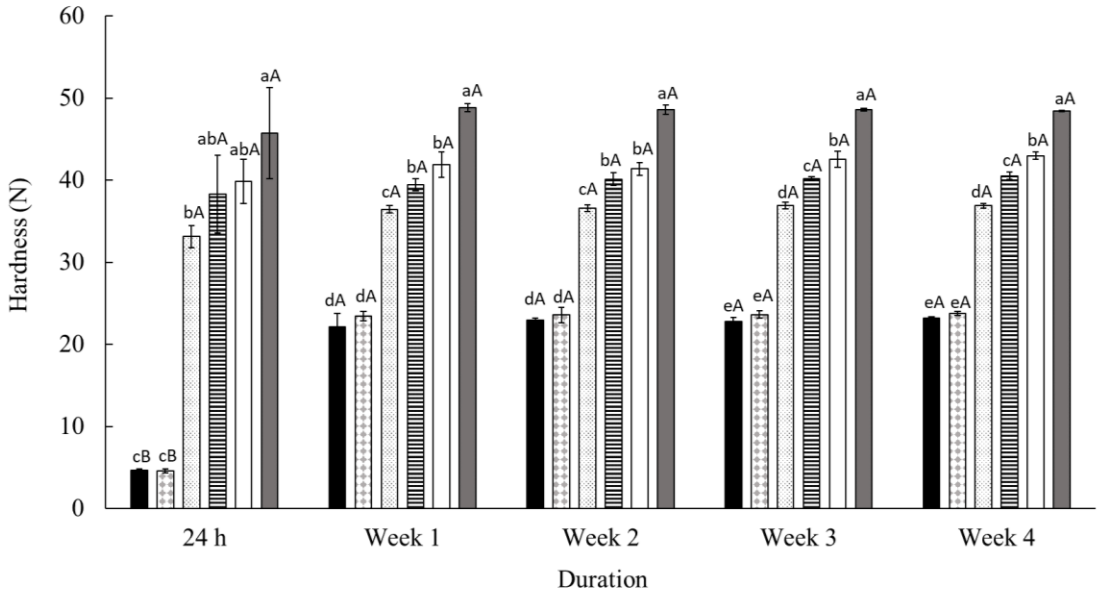

Fig. 8.4 Hardness of ice cream with 3 – 17 % WPI/VD_3 microgels. Concentration of WPI/VD_3 microgels; 0 % (black), 3 % (checked), 7 % (spotted), 10 % (striped), 13 % (white), 17 % (grey). Data (n=3) are presented as the mean ± SD. Data with different lowercase letters within a time frame and different uppercase letters between microgel concentration indicate significant differences.

The hardness of the control and the ice cream containing 3 % WPI/VD_3 microgels increased more than fourfold after one week of storage from ~ 5 N to 23 N, which then remained the same for the four weeks. The hardness of the ice creams containing 7 – 17 % microgels did not significantly change over the four weeks.

Previous studies have found that overrun, viscosity and fat content affect ice cream hardness (Chansathirapanich *et al.*, 2016; Yu *et al*., 2021; Yan *et al*., 2021; Biasutti *et al.*, 2013). Hardness is inversely proportional to overrun (Liu *et al.*, 2018). As found in the previous sections, the viscosity increase and overrun decrease on addition of > 3 % microgels could explain the textural difference and increased hardness with increasing microgel concentration. Ice cream with greater overrun is softer due to the incorporated air. Decreased air incorporation leading to lower overrun means there is an increase in the total solids content which leads to increased hardness. More viscous systems increase the resistance of penetration by the probe (Muse and Hartel, 2004). Akalın *et al*. (2008) and Roy *et al*. (2022) found that addition of WPI increased the hardness of their ice cream due to the formation of protein networks, which when combined with relatively lower overrun and increased storage modulus, increased the ice cream hardness.

8.2.5 Ice cream meltdown

When the ice crystals in ice cream begin to melt, gravity causes water to flow downward through the air bubbles and fat globules, causing the ice cream to melt (Muse and Hartel, 2004). The melting rate of ice creams with/ without WPI/VD_3 microgels (3 – 17 %) was analysed after 24 h and again after four week storage at -20 °C. The meltdown of ice creams with 0 - 17 % microgels stored for 24 h are displayed in Fig. 8.5. After 100 min, the control ice cream completely melted, whereas approx. 2 – 4 g ice cream remained for each sample containing WPI/VD_3 microgels. There was no significant difference in melting rate between similar samples stored for 24 h or four weeks (Table 8.2). The control ice cream was found to melt at a much faster rate than the WPI/VD_3 ice cream regardless of microgel concentration. In fact, the presence of WPI/VD_3 microgels resulted in an ice cream that melted at almost half the rate compared to the control ice cream. The melting rate did not change when the WPI/VD_3 microgel concentration was altered from 3 % up to 17 %.

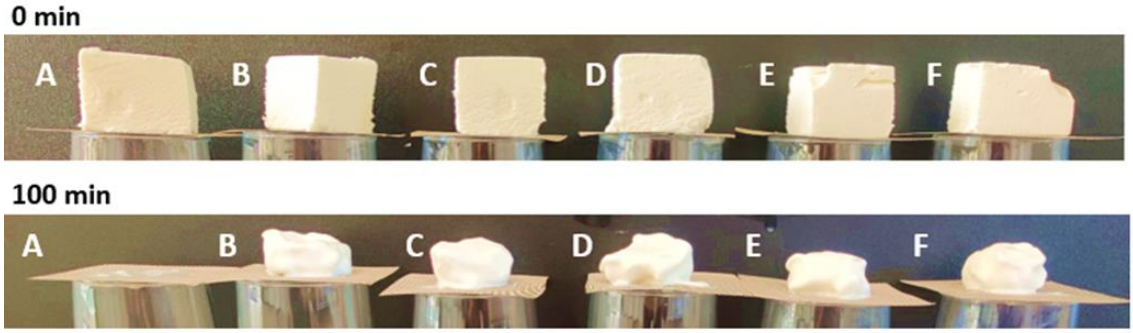

Fig. 8.5 Meltdown of ice cream stored for 24 h with (A) 0 %, (B) 3 % (C) 7 %, (D) 10 %, (E) 13 % and (F) 17 % microgels at 0 (top) and 100 min (bottom).

Table 8.2 Melting rate of ice cream samples with 0 – 17 % WPI/VD_3 microgels. Samples were measured after 24 h and four week storage at - 20 °C. Data (n=3) are presented as the mean ± SD. Data with different lowercase superscript letters within a column and uppercase superscript letters within a row indicate significant differences.

	Ice cream meltdown (g/min)	
WPI/VD_3 microgels	**24 h**	**Week 4**
0 %	0.679 ± 0.06^{aA}	0.678 ± 0.06^{aA}
3 %	0.387 ± 0.02^{bA}	0.384 ± 0.09^{bA}
7 %	0.390 ± 0.03^{bA}	0.391 ± 0.02^{bA}
10 %	0.389 ± 0.04^{bA}	0.386 ± 0.08^{bA}
13 %	0.385 ± 0.05^{bA}	0.387 ± 0.06^{bA}
17 %	0.389 ± 0.07^{bA}	0.388 ± 0.04^{bA}

The presence of WPI/VD_3 microgels significantly improved the melting resistance of the ice cream. In Chapter 5 and 7, the WPI/VD_3 microgels were capable at forming extremely stable foams by surrounding the air phase preventing gas diffusion as seen by image analysis. When incorporated within ice cream, it is possible that the microgels formed a stronger polymer network in the aqueous phase, which remained stable when the ice melted. This is similar to cryogelation, whereby gelation occurs under semi-frozen conditions, which forms a network cross-linked around ice crystals. When the ice crystals melt, the polymeric material is left forming a stable network (Rogers and Bencherif, 2019). It was proposed by Daw and Hartel (2015) that after the ice crystals begin to melt, the protein particles can coalesce fat globules which support the ice cream structure, reducing melting rates. Fat helps to structure ice cream and has a lower thermal conductivity than water (Liu *et al.*, 2018). The role of fat coupled with the microgels more than likely improved the melting rate of the ice cream.

Other studies have found that addition of nano-fibrillated cellulose or soy protein isolate/ cellulose nanofibers to ice cream reduced the melting rate compared to a control ice cream sample (Yu *et al*., 2021; Velasquez-Cock *et al.*, 2019; Sun *et al.*, 2015; Dervisoglu *et al*., 2005). Yu *et al*. (2021) found that the presence of nanomaterials significantly reinforced the mechanical properties and partially improved the thermal stability of ice cream. In this study, the rheological properties indicated that the addition of WPI/VD_3 microgels improved the viscoelastic strength of the ice cream, which could

have led to reduced melting properties. The interactions between the ice cream ingredients such as fat, air, protein and polymer network influenced ice cream melting rate. Akalın *et al.* (2008) also found that ice creams containing WPI had a lower melting rate than ice creams without, due to the formation of large protein networks.

In contrast, Roy *et al*. (2022) found that ice creams containing higher protein content had a higher melting rate due to decreased overrun and the inconsistencies in the fat globules formed which negatively affected fat destabilisation. Fat destabilisation causes the fat globules to coat and support air cells trapped within the ice cream mixture which contributes to slower melting rates (Muse and Hartel, 2004; Roy *et al*., 2022). Roy *et al*. (2022) further stated that the lower overrun resulted in a higher melting rate as air acts as an insulator for heat as it has low thermal conductivity.

8.2.6 Vitamin D stability in ice cream

Processing conditions have a negative impact on vitamin D stability leading to significant losses. In Chapter 6, the WPI microgels proved to be capable of protecting vitamin D_3 from pasteurisation temperatures, UV-light and long-term storage, while Chapter 6 showed their ability to withstand mechanical whipping. As a result, the stability of vitamin D_3 in ice cream following exposure to processing conditions was investigated over a four-week period.

As shown in Fig. 8.6, vitamin D_3 stability within the ice cream did not significantly change throughout the storage time regardless of microgel concentration. The control (0%) contained half the amount of VD_3 compared to the loaded microgel ice cream, as the dairy ingredients used to make ice cream contain vitamin D. The amount of VD_3 in the ice cream did not change throughout the four-week period. The low storage temperature of -20 °C and storage in the dark likely played a role in vitamin D_3 stability in the control. However, the incorporation of the WPI/VD_3 microgels increased the amount of VD_3 available in the product.

Vitamin D_3 is known to be unstable when exposed to air, however, in this study the presence of the incorporated air within the ice cream did not adversely affect VD_3 stability. Vitamin D_3 is also susceptible to light and heat; all samples were protected from light as they were stored in the dark and the WPI/VD_3 microgels were added after heat treatment but before homogenisation. This demonstrates that the microgels could withstand homogenisation at 8,000 rpm for 1 minute without disrupting the protective

effect of the microgels. These findings indicated that the cross-linked structure of the microgels could protect vitamin D_3 during processing and storage conditions.

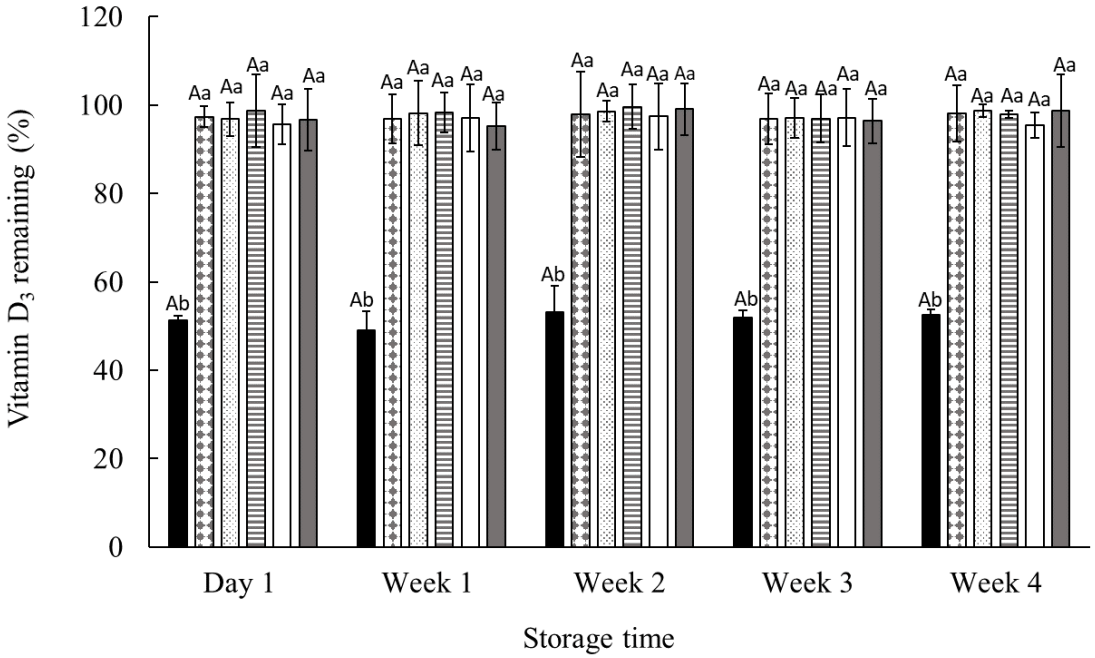

Fig. 8.6 Vitamin D_3 remaining in ice cream over a four-week period. WPI/VD_3 microgel concentration: 0 % (black), 3 % (checked), 7 % (spotted), 10 % (striped), 13 % (white), 17 % (grey). Data (n=3) are presented as the mean ± SD. Data with different lowercase letters within a timeframe indicate significant differences.

8.2.7 *In vitro* digestion

To study the *in vitro* digestion, samples containing 3 % WPI/VD_3 microgels were analysed, as at this concentration the microgels did not significantly alter the ice cream's properties, in comparison to the higher microgel concentrations. The WPI/VD_3 ice cream in dialysis bags were passed through a static *in vitro* digestion model, similar to Chapter 6. A sample containing ice cream without microgels was used as a control.

The cumulative release rate of VD_3 from the microgels and the loaded ice cream are shown in Fig. 8.7. The *in vitro* digestion data for the WPI/VD_3 microgels are also included in Fig. 8.7 for comparison purposes. During the first 120 min which represents the oral and gastric phase, 12 % and 2 % VD_3 was released from the microgels and ice

cream, respectively. As discussed in Chapter 6, the microgel complex formed due to cold-set gelation resulted in hydrophobic amino acids being protected within the protein network, forming a protective outer layer which would otherwise be destroyed by pepsin. This shows how the microgels continued to protect vitamin D_3 through gastric transit. Vitamin D_3 was released from the ice cream sample at a slower rate, and it is proposed that the complex food matrix acted as an additional barrier, as the gastric fluids would have taken longer to penetrate the ice cream formulation which contained several other ingredients.

On exposure to the intestinal fluids, the WPI microgels offered less protection to VD_3 for both samples. Again, vitamin D_3 was released from the microgels at a faster rate than the ice cream sample. After the first 30 min in the intestinal phase 33 and 23 % of VD_3 was released, which reached 64 and 48 % after one hour for the microgels and ice cream respectively. Although the release of vitamin D_3 was slower in the ice cream, at the end of digestion, the release of VD_3 from the microgels within the ice cream was not statistically different from that of the WPI/VD_3 microgels, reaching full release.

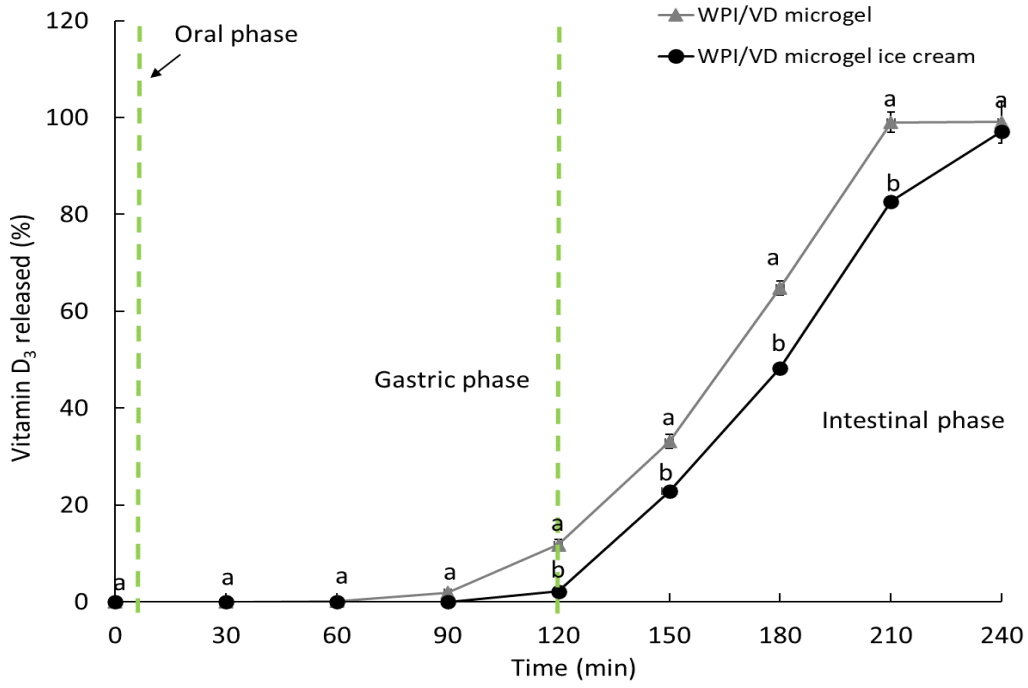

Fig. 8.7 Vitamin D_3 release (%) from WPI/VD_3 microgels (▲) and from WPI/VD_3 ice cream (●) after exposure to in vitro digestion. Data (n=3) are presented as the mean ± SD. Data with different letters indicate significant differences.

To further investigate the release mechanism of vitamin D_3 from the VD_3 loaded ice cream using a simulated *in vitro* digestion model, the cumulative release rate from WPI microgels were investigated by five kinetic models; zero order, first order, Korsmeyer-Peppas, Hixson Crowell and Higuchi and the related results are shown in Table 8.3.

Similar to Chapter 6, the release of VD_3 from the VD_3 loaded ice cream was not linear and the values from the regression coefficient (R^2) have shown best fit to Hixson-Crowell release model (R^2 = 0.885). The incorporation of WPI/VD_3 microgels in ice cream did not change the kinetic release of vitamin D_3, indicating that although VD_3 release was slower from the ice cream, it did not significantly change the release rate.

Table 8.3 Kinetic model fitting results of WPI/VD_3 loaded ice cream.

Model	WPI/VD_3 microgels	Ice cream
	R^2	R^2
Zero order	0.844	0.874
First order	0.693	0.771
Korsmeyer-Peppas	0.484	0.203
Hixson-Crowell	0.965	0.885
Higuchi	-0.730	-0.818

8.3 Conclusion

WPI/VD_3 microgels were successfully incorporated into a real food system, ice cream. The incorporation of the microgels into the ice cream mixture influenced the liquid rheological properties depending on microgel concentration. Increasing the concentration of microgels increased the viscoelastic strength of the ice cream mixture. Increasing concentration of microgels reduced the ice cream overrun which led to increased ice cream hardness. The addition of WPI/VD_3 microgels reduced the melting rate leading to the ice cream melting at half the rate of the control. This slower melting ice cream could be desirable to manufacturers for transportation and storage purposes. It could also be beneficial to slow eating elderly consumers. Vitamin D_3 was found to be stable over the four week period as the WPI microgels provided a protective barrier against processing and storage conditions.

Results indicated that low amounts of microgels such as 3 % did not significantly alter the ice cream characteristics, however further increase led to significant changes. The ice cream characteristics can be altered by changing the microgel concentration to suit the desired end product formulation. This reveals that WPI microgels may be used as a stabiliser for ice cream reducing meltdown while also being a suitable delivery system for VD_3 for fortification in ice cream.

Chapter 9
Conclusions and future work

9.1 Conclusions

This chapter will summarise the key research findings in relation to the research aims and discuss their significance in the area. This study aimed to gain an understanding of whey protein functionality upon exposure to various environmental conditions and the effect on WPI foamability and stability. This understanding is used to form the basis of creating whey protein isolate microgels for the stabilisation of foamed matrices. The WPI microgels are also used as a delivery vehicle to encapsulate and protect vitamin D_3. Both processes consisting of encapsulation and formation of stable foams are combined to form vitamin D_3 loaded microgel foams. Once the production of stable VD_3 loaded microgel foams is achieved, real food systems are looked at for the incorporation of microgel particles, followed by determining the *in vitro* digestibility of the food product.

Foams are made up of air bubbles surrounded by a continuous liquid phase, however, due to the pressure differences between the two phases they are susceptible to collapse. Foams, therefore, require surfactants to adsorb at the air/water interface to reduce the pressure disparity. Whey proteins are amphiphilic molecules containing both hydrophilic and hydrophobic regions, making them suitable for foam formation. The first research question was to determine the foaming ability of native WPI when subjected to different environmental conditions such as pH, ionic strength, heat treatment, sucrose concentration and xanthan gum addition. Altering the environmental conditions led to differences in the foaming properties of WPI, which indicated that the foaming properties could be manipulated to produce foams with high or low overrun or stability, which can be chosen to suit the product requirements. However, the WPI foams regardless of environmental factor only remained stable for several min or hours, which is not very useful from a food perspective.

After determining the requisite conditions for optimal foaming of WPI, microgels were fabricated and their foamability was examined. Pickering stabilised foams have gained interest in recent years as they can lead to dispersions being far more stable than those formed by surfactants. The cold-set gelation methods used formed novel microgel particle sols that could be manipulated depending on $CaCl_2$ concentration or cross-linking time to alter particle size, rheological and foaming properties. The microgel foams formed remained stable for a period of > 2 years, while also maintaining most of their foam shape. Light microscopy images revealed that the microgels were responsible for the stabilisation as cloudy gel-like white regions were present amongst the air bubbles. SEM images also revealed that the interconnected structure formed by the microgels trapped

and stabilised air bubbles. This is believed to be the first time that WPI microgel stabilised foams have shown stability over such a long period of time. Most studies in the literature do not state how long their particle stabilised foams remained stable, the authors simply just state that they improved the stability when compared to surfactants.

There have been several delivery systems for VD_3 such as nanoparticles, casein micelles, lipid nanocapsules etc., however, few studies have focused on using solely WPI microgels. In addition to having exceptional foaming properties, the whey protein microgels successfully encapsulated vitamin D_3. Hydrophobic interaction was the driving force for encapsulation between the unfolded protein molecules and VD_3. Vitamin D deficiency is prevalent worldwide and its fortification within food products is difficult due to its low water solubility and sensitivity to oxidation and UV-light. The WPI/VD_3 microgels when exposed to common environmental factors effectively protected VD_3 as $\geq$ 97 % VD_3 remained, indicating their potential use as a delivery system in foodstuffs, helping to solve the challenge of food fortification. If the microgels are to be incorporated into a food product, it must also deliver VD_3 to the correct site of action, so the microgels were assessed for their release properties *in vitro*. It was believed that the WPI microgels would breakdown in gastric transit due to the susceptibility of hydrophobic amino acids in β-lactoglobulin to pepsin present in the stomach. However, in this study, the complex structure formed by the microgels buried the hydrophobic amino acids within the core forming a protective outer layer resistant to pepsin. However, in the simulated intestinal phase the pancreatic proteases destroyed the protein structure and the microgels released VD_3. This suggests that the WPI microgels can be used as targeted delivery systems as they continue to protect VD_3 in harsh simulated gastric conditions but allows the release at the correct site of action, the small intestine.

Having established that the WPI microgels could successfully form ultra-stable foams and encapsulate, protect, and release vitamin D_3, the next step was to join both processes. To the authors knowledge, there has been no research in the literature that has formed vitamin D_3 loaded microgels for stabilisation of foams, so this is considered to be the first-time encapsulation and foaming have been combined to form VD_3 loaded microgel foams. The WPI/VD_3 microgel foaming properties were not found to be significantly different from the blank WPI microgel foams, indicating that the encapsulation of VD_3 did not have a negative effect. If the microgels are to be used in food products, it is essential to determine the effect of several environmental factors commonly found in food manufacture. The foaming properties of the microgels could be manipulated depending on the condition used. This is beneficial from a food perspective

as conditions can be chosen depending on whether a product with high or low volume is required.

Once the production of vitamin D_3 loaded stable foams was achieved, the WPI/VD_3 microgels were incorporated into ice cream, a more complex foamed food system. The ability of the WPI/VD_3 microgels to withstand the ice cream manufacturing conditions and continue to protect vitamin D_3 were analysed to determine if the microgels could be used as a delivery vehicle. The incorporation of low concentrations of WPI/VD_3 microgels did not significantly alter ice cream overrun, however, with increasing microgel concentration overrun decreased. Meltdown properties of the ice cream were greatly improved regardless of microgel concentration, with ice cream melting at half the rate of the control ice cream (without microgels). As the microgels have previously been found to form extremely stable foams in chapter 4, it is likely that the microgels formed a polymer network in the continuous phase reducing bubble coalescence. The microgels also continued to protect vitamin D_3 following ice cream manufacture as there was a high retention of the vitamin within the ice cream at the end of four-week storage at – 20 °C. Upon exposure to *in vitro* digestion, similar to the microgels, VD_3 was released in the small intestine, the optimum destination. This reveals that the WPI microgels can be used by manufacturers as a delivery vehicle for VD_3 fortification in ice cream.

The work from this thesis displays the effective use of WPI microgels for the uptake and release of vitamin D_3 while also forming ultra-stable foams and serving as a delivery vehicle in ice cream.

9.2 Future work

This work highlighted to effective use of WPI microgels to form ultra-stable foams while also having the capability of encapsulating and protecting VD_3. The ability of the WPI/VD_3 microgels to be incorporated into a food system was also shown. However, the following are particular areas that are suggested for further investigation.

The foamed systems in this work were formed by mechanical whipping and display good foaming properties. Continuing from this work it would be interesting to use a different foaming method for comparison, such as sparging to determine if better foaming properties were obtained. Additionally, light microscopy revealed that the microgels resided amongst the air bubbles leading to stabilisation. However, if equipment was available viewing these foams using confocal microscopy could give more visual information on the location of the microgels amongst the air bubbles. For example, Lazidis *et al*. (2016) found that WPI microgels surrounded air bubbles, which were distinctly visible using a fluorescent dye e.g., rhodamine B.

The WPI microgels displayed good encapsulation efficiency of vitamin D_3 (> 98 %). Scope for further investigation with the WPI microgels could be encapsulation of other hydrophobic compounds or to mask unpleasant flavours. This would help to make the microgels more desirable to manufacturers to create innovative value-added food products. Another area for future analysis is spray drying the WPI/VD_3 microgels. This would be more beneficial for manufacturers to increase the shelf life of the microgels by reducing the water activity. It would also allow for easier packaging and transport of the microgels to manufacturing plants. The effect of spray drying and rehydration on the microgel characteristics would also need to be assessed to determine the viability of the process.

It would be interesting to determine the microgels suitability as a food ingredient by performing a sensory analysis on the ice cream samples with and without WPI/VD_3 microgels. Additionally, inclusion of the microgels into other foamed food products would be beneficial to determine the versatility of the microgels regarding incorporation with various food ingredients.

The cellular uptake of vitamin D_3 could be carried out using Caco-2 cells. This is undoubtedly very important for food products intended for consumption. If the microgels are to be used as targeted delivery vehicles, vitamin D_3 needs to be adsorbed by the cells.

References

Abaee, A., Madadlou, A., Saboury, A.A., 2017. The formation of non-heat-treated whey protein cold-set hydrogels via non-toxic chemical cross-linking. Food Hydrocoll. 63, 43–49. https://doi.org/10.1016/j.foodhyd.2016.08.024

Abbasi, A., Emam-Djomeh, Z., Mousavi, M.A.E., Davoodi, D., 2014. Stability of vitamin D3 encapsulated in nanoparticles of whey protein isolate. Food Chem. 143, 379–383. https://doi.org/10.1016/j.foodchem.2013.08.018

Aguilera, J.M., Park, D.J., 2016. Texture-modified foods for the elderly: Status, technology and opportunities. Trends Food Sci. Technol. 57, 156–164. https://doi.org/10.1016/j.tifs.2016.10.001

Akalın, A.S., Karagözlü, C., Ünal, G., 2008. Rheological properties of reduced-fat and low-fat ice cream containing whey protein isolate and inulin. Eur. Food Res. Technol. 227, 889–895. https://doi.org/10.1007/s00217-007-0800-z

Alavi, F., Emam-Djomeh, Z., Mohammadian, M., Salami, M., Moosavi-Movahedi, A.A., 2020. Physico-chemical and foaming properties of nanofibrillated egg white protein and its functionality in meringue batter. Food Hydrocoll. 101, 105554. https://doi.org/10.1016/j.foodhyd.2019.105554

Alavi, F., Emam-Djomeh, Z., Yarmand, M.S., Salami, M., Momen, S., Moosavi-Movahedi, A.A., 2018a. Cold gelation of curcumin loaded whey protein aggregates mixed with k-carrageenan: Impact of gel microstructure on the gastrointestinal fate of curcumin. Food Hydrocoll. 85, 267–280. https://doi.org/10.1016/j.foodhyd.2018.07.012

Alavi, F., Momen, S., Emam-Djomeh, Z., Salami, M., Moosavi-Movahedi, A.A., 2018b. Radical cross-linked whey protein aggregates as building blocks of non-heated cold-set gels. Food Hydrocoll. 81, 429–441. https://doi.org/10.1016/j.foodhyd.2018.03.016

Alting, A.C., Hamer, R.J., De Kruif, C.G., Visschers, R.W., 2000. Formation of disulfide bonds in acid-induced gels of preheated whey protein isolate. J. Agric. Food Chem. 48, 5001–5007. https://doi.org/10.1021/jf000474h

Antipova, A.S., Semenova, M.G., Belyakova, L.E., 1999. Effect of sucrose on the

thermodynamic properties of ovalbumin and sodium caseinate in bulk solution and at air-water interface. Colloids Surfaces B Biointerfaces 12, 261–270. https://doi.org/10.1016/S0927-7765(98)00081-2

Arakawa, T., Timasheff, S.N., 1984. Mechanism of Protein Salting In and Salting Out by Divalent Cation Salts: Balance between Hydration and Salt Binding. Biochemistry 23, 5912–5923. https://doi.org/10.1021/bi00320a004

Arroyo-Maya, I.J., McClements, D.J., 2015. Biopolymer nanoparticles as potential delivery systems for anthocyanins: Fabrication and properties. Food Res. Int. 69, 1–8. https://doi.org/10.1016/j.foodres.2014.12.005

Asghari, A.K., Norton, I., Mills, T., Sadd, P., Spyropoulos, F., 2016. Interfacial and foaming characterisation of mixed protein-starch particle systems for food-foam applications. Food Hydrocoll. 53, 311–319. https://doi.org/10.1016/j.foodhyd.2015.09.007

Augustin, M.A., Hemar, Y., 2009. Nano- and micro-structured assemblies for encapsulation of food ingredients. Chem. Soc. Rev. 38, 902–912. https://doi.org/10.1039/b801739p

Bagheri, L., Yarmand, M., Madadlou, A., Mousavi, M.E., 2014. Transglutaminase-induced or citric acid-mediated cross-linking of whey proteins to tune the characteristics of subsequently desolvated sub-micron and nano-scaled particles. J. Microencapsul. 31, 636–643. https://doi.org/10.3109/02652048.2014.911377

Bajaj, S.R., Singhal, R.S., 2021. Fortification of wheat flour and oil with vitamins B12 and D3: Effect of processing and storage. J. Food Compos. Anal. 96, 103703. https://doi.org/10.1016/j.jfca.2020.103703

Bals, A., Kulozik, U., 2003a. Effect of pre-heating on the foaming properties of whey protein isolate using a membrane foaming apparatus. Int. Dairy J. 13, 903–908. https://doi.org/10.1016/S0958-6946(03)00111-0

Bals, A., Kulozik, U., 2003b. The influence of the pore size, the foaming temperature and the viscosity of the continuous phase on the properties of foams produced by membrane foaming. J. Memb. Sci. 220, 5–11. https://doi.org/10.1016/S0376-7388(03)00168-6

Bao, C., Jiang, P., Chai, J., Jiang, Y., Li, D., Bao, W., Liu, B., Liu, B., Norde, W., Li, Y., 2019. The delivery of sensitive food bioactive ingredients: Absorption mechanisms, influencing factors, encapsulation techniques and evaluation models. Food Res. Int. 120, 130–140. https://doi.org/10.1016/j.foodres.2019.02.024

Bayram, T., Pekmez, M., Arda, N., Yalçin, A.S., 2008. Antioxidant activity of whey protein fractions isolated by gel exclusion chromatography and protease treatment. Talanta 75, 705–709. https://doi.org/10.1016/j.talanta.2007.12.007

Beaulieu, L., Savoie, L., Paquin, P., Subirade, M., 2002. Elaboration and characterization of whey protein beads by an emulsification/cold gelation process: Application for the protection of retinol. Biomacromolecules 3, 239–248. https://doi.org/10.1021/bm010082z

Benichou, A., Aserin, A., Lutz, R., Garti, N., 2007. Formation and characterization of amphiphilic conjugates of whey protein isolate (WPI)/xanthan to improve surface activity. Food Hydrocoll. 21, 379–391. https://doi.org/10.1016/j.foodhyd.2006.04.013

Berino, R.P., Báez, G.D., Ballerini, G.A., Llopart, E.E., Busti, P.A., Moro, A., Delorenzi, N.J., 2019. Interaction of vitamin D3 with beta-lactoglobulin at high vitamin/protein ratios: Characterization of size and surface charge of nanoparticles. Food Hydrocoll. 90, 182–188. https://doi.org/10.1016/j.foodhyd.2018.11.027

Bertrand, M.E., Turgeon, S.L., 2007. Improved gelling properties of whey protein isolate by addition of xanthan gum. Food Hydrocoll. 21, 159–166. https://doi.org/10.1016/j.foodhyd.2006.03.005

Betz, M., Steiner, B., Schantz, M., Oidtmann, J., Mäder, K., Richling, E., Kulozik, U., 2012. Antioxidant capacity of bilberry extract microencapsulated in whey protein hydrogels. Food Res. Int. 47, 51–57. https://doi.org/10.1016/j.foodres.2012.01.010

Biasutti, M., Venir, E., Marino, M., Maifreni, M., Innocente, N., 2013. Effects of high pressure homogenisation of ice cream mix on the physical and structural properties of ice cream. Int. Dairy J. 32, 40–45. https://doi.org/10.1016/j.idairyj.2013.03.007

Bos, M.A., Dunnewind, B., Van Vliet, T., 2003. Foams and surface rheological properties of β-casein, gliadin and glycinin. Colloids Surfaces B Biointerfaces 31, 95–105. https://doi.org/10.1016/S0927-7765(03)00046-8

Bos, M.A., Van Vliet, T., 2001. Interfacial rheological properties of adsorbed protein layers and surfactants: A review. Adv. Colloid Interface Sci. 91, 441.

Britten, M., Lavoie, L., 1992. Foaming properties of protein as Affected by concentration 57, 1219–1241.

Brodkorb, A., Egger, L., Alminger, M., Alvito, P., Assunção, R., Ballance, S., Bohn, T., Bourlieu-Lacanal, C., Boutrou, R., Carrière, F., Clemente, A., Corredig, M., Dupont, D., Dufour, C., Edwards, C., Golding, M., Karakaya, S., Kirkhus, B., Le Feunteun, S., Lesmes, U., Macierzanka, A., Mackie, A.R., Martins, C., Marze, S., McClements, D.J., Ménard, O., Minekus, M., Portmann, R., Santos, C.N., Souchon, I., Singh, R.P., Vegarud, G.E., Wickham, M.S.J., Weitschies, W., Recio, I., 2019. INFOGEST static in vitro simulation of gastrointestinal food digestion. Nat. Protoc. 14, 991–1014. https://doi.org/10.1038/s41596-018-0119-1

Bruschi, M., 2015. Strategies to Modify the Drug Release from Pharmaceutical Systems, in: Strategies to Modify the Drug Release from Pharmaceutical Systems. Woodhead Publishing Ltd., pp. 63–86. https://doi.org/10.1016/b978-0-08-100092-2.00005-9

Bryant, C.., McClements. D.J, 2000. Influence of xanthan gum on physical characteristics of heat-denatured whey protein solutions and gels. Food Hydrocoll. 14, 383–390. https://doi.org/10.1016/s0268-005x(00)00018-7

Bryant, C.., McClements, D.J., 2000. Influence of xanthan gum on physical characteristics of heat-denatured whey protein solutions and gels. Food Hydrocoll. 14, 383–390. https://doi.org/10.1016/S0268-005X(00)00018-7

Bryant, C. M., McClements, D.J., 2000. Influence of sucrose on NaCl-induced gelation of heat denatured whey protein solutions. Food Res. Int. 33, 649–653. https://doi.org/10.1016/S0963-9969(00)00109-5

Bryant, C.M., McClements, D.J., 2000. Influence of sucrose on NaCl-induced gelation of heat denatured whey protein solutions. Food Res. Int. 33, 649–653. https://doi.org/10.1016/S0963-9969(00)00109-5

Campbell, G.M., Mougeot, E., 1999. Creation and characterization of aerated food products. Trends Food Sci. Technol. 10, 283–296.

Chansathirapanich, W., Ngamchuachit, P., Tansawat, R., 2016. Effect of fat content on characteristics of ice cream fortified with calcium and vitamin D3. Thai J. Pharm. Sci. 40, 132–138.

Chavoshpour-Natanzi, Z., Sahihi, M., 2019. Encapsulation of quercetin-loaded β-lactoglobulin for drug delivery using modified anti-solvent method. Food Hydrocoll. 96, 493–502. https://doi.org/10.1016/j.foodhyd.2019.05.051

Chen, J., Dickinson, E., 1998. Viscoelastic Properties of Protein-Stabilized Emulsions: Effect of Protein-Surfactant Interactions. J. Agric. Food Chem. 46, 91–97. https://doi.org/10.1021/jf970536c

Chen, L., Remondetto, G.E., Subirade, M., 2006. Food protein-based materials as nutraceutical delivery systems. Trends Food Sci. Technol. 17, 272–283. https://doi.org/10.1016/j.tifs.2005.12.011

Chen, L., Subirade, M., 2006. Alginate-whey protein granular microspheres as oral delivery vehicles for bioactive compounds. Biomaterials 27, 4646–4654. https://doi.org/10.1016/j.biomaterials.2006.04.037

Chen, M., Bleeker, R., Sala, G., Meinders, M.B.J., van Valenberg, H.J.F., van Hooijdonk, A.C.M., van der Linden, E., 2016. Particle size determines foam stability of casein micelle dispersions. Int. Dairy J. 56, 151–158. https://doi.org/10.1016/j.idairyj.2016.01.020

Chen, M., Feijen, S., Sala, G., Meinders, M.B.J., van Valenberg, H.J.F., van Hooijdonk, A.C.M., van der Linden, E., 2018. Foam stabilized by large casein micelle aggregates: The effect of aggregate number in foam lamella. Food Hydrocoll. 74, 342–348. https://doi.org/10.1016/j.foodhyd.2017.08.026

Chen, S., Li, Q., McClements, D.J., Han, Y., Dai, L., Mao, L., Gao, Y., 2020. Co-delivery of curcumin and piperine in zein-carrageenan core-shell nanoparticles: Formation, structure, stability and in vitro gastrointestinal digestion. Food Hydrocoll. 99, 105334. https://doi.org/10.1016/j.foodhyd.2019.105334

Cohen, Y., Levi, M., Lesmes, U., Margier, M., Reboul, E., Livney, Y.D., 2017. Re-assembled casein micelles improve in vitro bioavailability of Vitamin D in a Caco-2 cell model. Food Funct. 8, 2133–2141. https://doi.org/10.1039/c7fo00323d

Cook, M.T., Tzortzis, G., Charalampopoulos, D., Khutoryanskiy, V. V., 2012. Microencapsulation of probiotics for gastrointestinal delivery. J. Control. Release 162, 56–67. https://doi.org/10.1016/j.jconrel.2012.06.003

Cox, A.R., Aldred, D.L., Russell, A.B., 2009. Exceptional stability of food foams using class II hydrophobin HFBII. Food Hydrocoll. 23, 366–376. https://doi.org/10.1016/j.foodhyd.2008.03.001

Dabestani, M., Yeganehzad, S., 2019. Effect of Persian gum and Xanthan gum on foaming properties and stability of pasteurized fresh egg white foam. Food Hydrocoll. 87, 550–560. https://doi.org/10.1016/j.foodhyd.2018.08.030

Damodaran, S., 2005. R : Concise Reviews / Hypotheses in Food Science Protein Stabilization of Emulsions and Foams. J. food Sci. 70, 54–66.

Damodaran, S., Perkin, K.L., Fennema, O.R., 2007. Fennema's Food Chemistry (4th ed). CRC Press, Madison, Wisconsin.

David, S., Livney, Y.D., 2016. Potato protein based nanovehicles for health promoting hydrophobic bioactives in clear beverages. Food Hydrocoll. 57, 229–235. https://doi.org/10.1016/j.foodhyd.2016.01.027

Davidov-Pardo, G., Joye, I.J., McClements, D.J., 2015. Encapsulation of resveratrol in biopolymer particles produced using liquid antisolvent precipitation. Part 1: Preparation and characterization. Food Hydrocoll. 45, 309–316. https://doi.org/10.1016/j.foodhyd.2014.11.023

Davis, J.P., Foegeding, E.A., 2007. Comparisons of the foaming and interfacial properties of whey protein isolate and egg white proteins. Colloids Surfaces B Biointerfaces 54, 200–210. https://doi.org/10.1016/j.colsurfb.2006.10.017

Davis, J.P., Foegeding, E.A., 2004. Foaming and Interfacial Properties of Polymerized Whey Protein Isolate. J. Food Sci. 69, C404–C410. https://doi.org/10.1111/j.1365-2621.2004.tb10706.x

Daw, E., Hartel, R.W., 2015. Fat destabilization and melt-down of ice creams with increased protein content. Int. Dairy J. 43, 33–41. https://doi.org/10.1016/j.idairyj.2014.12.001

De Kruif, C.G., Weinbreck, F., De Vries, R., 2004. Complex coacervation of proteins

and anionic polysaccharides. Curr. Opin. Colloid Interface Sci. 9, 340–349. https://doi.org/10.1016/j.cocis.2004.09.006

Deloid, G.M., Sohal, I.S., Lorente, L.R., Molina, R.M., Pyrgiotakis, G., Stevanovic, A., Zhang, R., Mcclements, D.J., Geitner, N.K., Douglas, W., Ng, K.W., Chye, S., Loo, J., Bell, D.C., Brain, J., Demokritou, P., 2018. Reducing Intestinal Digestion and Absorption of Fat Using a Nature-Derived Biopolymer : Interference of Triglyceride Hydrolysis by Nanocellulose . Reducing Intestinal Digestion and Absorption of Fat Using a Nature-Derived Biopolymer : Interference of Trig. https://doi.org/10.1021/acsnano.8b03074

Dervisoglu, M., Yazici, F., Aydemir, O., 2005. The effect of soy protein concentrate addition on the physical, chemical, and sensory properties of strawberry flavored ice cream. Eur. Food Res. Technol. 221, 466–470. https://doi.org/10.1007/s00217-005-1207-3

Deshmukh, O.S., Van Den Ende, D., Stuart, M.C., Mugele, F., Duits, M.H.G., 2015. Hard and soft colloids at fluid interfaces: Adsorption, interactions, assembly & rheology. Adv. Colloid Interface Sci. 222, 215–227. https://doi.org/10.1016/j.cis.2014.09.003

Destribats, M., Wolfs, M., Pinaud, F., Lapeyre, V., Sellier, E., Schmitt, V., Ravaine, V., 2013. Pickering emulsions stabilized by soft microgels: Influence of the emulsification process on particle interfacial organization and emulsion properties. Langmuir 29, 12367–12374. https://doi.org/10.1021/la402921b

Dhakal, S.P., He, J., 2020. Microencapsulation of Vitamins in Food Applications to Prevent Losses in Processing and Storage : A Review. Food Res. Int. 109326. https://doi.org/10.1016/j.foodres.2020.109326

Dhayal, S.K., Delahaije, R.J.B.M., de Vries, R.J., Gruppen, H., Wierenga, P.A., 2015. Enzymatic cross-linking of α-lactalbumin to produce nanoparticles with increased foam stability. Soft Matter 11, 7888–7898. https://doi.org/10.1039/c5sm01112d

Diarrassouba, F., Garrait, G., Remondetto, G., Alvarez, P., Beyssac, E., Subirade, M., 2015. Food protein-based microspheres for increased uptake of Vitamin D3. Food Chem. 173, 1066–1072. https://doi.org/10.1016/j.foodchem.2014.10.112

Dickinson, E., 2017. Biopolymer-based particles as stabilizing agents for emulsions and

foams. Food Hydrocoll. 68, 219–231. https://doi.org/10.1016/j.foodhyd.2016.06.024

Dickinson, E., 2015. Microgels - An alternative colloidal ingredient for stabilization of food emulsions. Trends Food Sci. Technol. 43, 178–188. https://doi.org/10.1016/j.tifs.2015.02.006

Dickinson, E., 1999. Adsorbed protein layers at fluid interfaces: interactions, structure and surface rheology. Colloids Surfaces B Biointerfaces 15, 161–176.

Dima, C., Assadpour, E., Dima, S., Jafari, S.M., 2020. Bioactive-loaded nanocarriers for functional foods: from designing to bioavailability. Curr. Opin. Food Sci. 33, 21–29. https://doi.org/10.1016/j.cofs.2019.11.006

Djoullah, A., Saurel, R., 2021. Controlled release of riboflavin encapsulated in pea protein microparticles prepared by emulsion-enzymatic gelation process. J. Food Eng. 292. https://doi.org/10.1016/j.jfoodeng.2020.110276

Dollet, B., Raufaste, C., 2014. Rheology of aqueous foams. Comptes Rendus Phys. 15, 731–747. https://doi.org/10.1016/j.crhy.2014.09.008

Dombrowski, J., Johler, F., Warncke, M., Kulozik, U., 2016. Correlation between bulk characteristics of aggregated β-lactoglobulin and its surface and foaming properties. Food Hydrocoll. 61, 318–328.

Doublier, Garnier, Renard, Sanchez, 2000. Protein-polysaccharide interactions. Curr. Opin. Colloid Interface Sci. 5, 202–214.

Egan, T., Jacquier, J.C., Rosenberg, Y., Rosenberg, M., 2014. Cold-set whey protein microgels containing immobilised lipid phases to modulate matrix digestion and release of a water-soluble bioactive. J. Microencapsul. 31, 184–192. https://doi.org/10.3109/02652048.2013.824513

Egan, T., Jacquier, J.C., Rosenberg, Y., Rosenberg, M., 2013. Cold-set whey protein microgels for the stable immobilization of lipids. Food Hydrocoll. 31, 317–324. https://doi.org/10.1016/j.foodhyd.2012.11.008

Ellis, A.L., Mills, T.B., Norton, I.T., Norton-Welch, A.B., 2019. The hydrophobic modification of kappa carrageenan microgel particles for the stabilisation of foams. J. Colloid Interface Sci. 538, 165–173. https://doi.org/10.1016/j.jcis.2018.11.091

Engelhardt, K., Lexis, M., Gochev, G., Konnerth, C., Miller, R., Willenbacher, N., Peukert, W., Braunschweig, B., 2013. PH effects on the molecular structure of β-lactoglobulin modified air-water interfaces and its impact on foam rheology. Langmuir 29, 11646–11655. https://doi.org/10.1021/la402729g

ErÇelebi, E.A., IbanoĞlu, E., 2009. Effects of ionic strength on the foaming properties of whey protein isolate and egg white in the presence of polysaccharides. J. Food Process. Preserv. 33, 513–526. https://doi.org/10.1111/j.1745-4549.2008.00302.x

Ettelaie, R., Murray, B., 2014. Effect of particle adsorption rates on the disproportionation process in pickering stabilised bubbles. J. Chem. Phys. 140. https://doi.org/10.1063/1.4878501

Fameau, A.-L.L., Salonen, A., 2014. Effect of particles and aggregated structures on the foam stability and aging. Comptes Rendus Phys. 15, 748–760. https://doi.org/10.1016/j.crhy.2014.09.009

Farjami, T., Madadlou, A., 2017. Fabrication methods of biopolymeric microgels and microgel-based hydrogels. Food Hydrocoll. 62, 262–272. https://doi.org/10.1016/j.foodhyd.2016.08.017

Foegeding, E.A., Luck, P.J., Davis, J.P., 2006. Factors determining the physical properties of protein foams. Food Hydrocoll. 20, 284–292. https://doi.org/10.1016/j.foodhyd.2005.03.014

Food Safety Authority of Ireland, 2020. Vitamin D Scientific Recommendations for Food-based Dietary Guidelines for Older Adults in Ireland, FSAI.

Garrec, D.A., Norton, I.T., 2012. Understanding fluid gel formation and properties. J. Food Eng. 112, 175–182. https://doi.org/10.1016/j.jfoodeng.2012.04.001

Germain, J.C., Aguilera, J.M., 2014. Multi-scale properties of protein-stabilized foams. Food Struct. 1, 55–70. https://doi.org/10.1016/j.foostr.2014.01.001

Gharbi, N., Labbafi, M., 2019. Influence of treatment-induced modification of egg white proteins on foaming properties. Food Hydrocoll. 90, 72–81. https://doi.org/10.1016/j.foodhyd.2018.11.060

Ghosh, S., Rousseau, D., 2011. Fat crystals and water-in-oil emulsion stability. Curr. Opin. Colloid Interface Sci. 16, 421–431.

https://doi.org/10.1016/j.cocis.2011.06.006

Gill, H.S., Cross, M.L., 2000. Anticancer properties of bovine milk. Br. J. Nutr. 84, 161–166. https://doi.org/10.1017/s0007114500002397

Giroux, H.J., Houde, J., Britten, M., 2010. Preparation of nanoparticles from denatured whey protein by pH-cycling treatment. Food Hydrocoll. 24, 341–346. https://doi.org/10.1016/j.foodhyd.2009.10.013

Goff, H.D., 1997. Colloidal aspects of ice cream - A review. Int. Dairy J. 7, 363–373. https://doi.org/10.1016/S0958-6946(97)00040-X

Goff, H.D., Kinsella, J.E., Jordan, W.K., 1989. Influence of Various Milk Protein Isolates on Ice Cream Emulsion Stability. J. Dairy Sci. 72, 385–397. https://doi.org/10.3168/jds.S0022-0302(89)79120-7

Goldfein, K.R., Slavin, J.L., 2015. Why Sugar Is Added to Food: Food Science 101. Compr. Rev. Food Sci. Food Saf. 14, 644–656. https://doi.org/10.1111/1541-4337.12151

Gouin, S., 2004. Microencapsulation: Industrial appraisal of existing technologies and trends. Trends Food Sci. Technol. 15, 330–347. https://doi.org/10.1016/j.tifs.2003.10.005

Grossmann, L., Beicht, M., Reichert, C., Weiss, J., 2019. Foaming properties of heat-aggregated microparticles from whey proteins. Colloids Surfaces A Physicochem. Eng. Asp. 579, 123572. https://doi.org/10.1016/j.colsurfa.2019.06.037

Gunasekaran, S., Ko, S., Xiao, L., 2007. Use of whey proteins for encapsulation and controlled delivery applications. J. Food Eng. 83, 31–40. https://doi.org/10.1016/j.jfoodeng.2006.11.001

Guttoff, M., Saberi, A.H., Mcclements, D.J., 2015. Formation of vitamin D nanoemulsion-based delivery systems by spontaneous emulsification: Factors affecting particle size and stability. Food Chem. 171, 117–122. https://doi.org/10.1016/j.foodchem.2014.08.087

Ha, H.K., Rankin, S.A., Lee, M.R., Lee, W.J., 2019. Development and characterization of whey protein-based nano-delivery systems: A review. Molecules 24, 1–17. https://doi.org/10.3390/molecules24183254

Haham, M., Ish-Shalom, S., Nodelman, M., Duek, I., Segal, E., Kustanovich, M., Livney, Y.D., 2012. Stability and bioavailability of vitamin D nanoencapsulated in casein micelles. Food Funct. 3, 737–744. https://doi.org/10.1039/c2fo10249h

Hill, C., Eastoe, J., 2017. Foams: From nature to industry. Adv. Colloid Interface Sci. 247, 496–513. https://doi.org/10.1016/j.cis.2017.05.013

Hongsprabhas, P., Barbut, S., 1997. Structure-forming processes in Ca2+-induced whey protein isolate cold gelation. Int. Dairy J. 7, 827–834. https://doi.org/10.1016/S0958-6946(98)00011-9

Hu, Y., Li, C., Regenstein, J.M., Wang, L., 2019. Preparation and properties of potato amylose-based fat replacer using super- heated quenching. Carbohydr. Polym. 223, 115020. https://doi.org/10.1016/j.carbpol.2019.115020

Huang, W., Wang, L., Wei, Y., Cao, M., Xie, H., Wu, D., 2020. Fabrication of lysozyme κ-carrageenan complex nanoparticles as a novel. Internatioanl J. Biol. Macromol. 444–452.

Hunter, T.N., Pugh, R.J., Franks, G. V., Jameson, G.J., 2008. The role of particles in stabilising foams and emulsions. Adv. Colloid Interface Sci. 137, 57–81. https://doi.org/10.1016/j.cis.2007.07.007

Jakobsen, J., Knuthsen, P., 2014. Stability of vitamin D in foodstuffs during cooking. Food Chem. 148, 170–175. https://doi.org/10.1016/j.foodchem.2013.10.043

Je Lee, S., Rosenberg, M., 2000. Whey Protein-based Microcapsules Prepared by Double Emulsification and Heat Gelation. LWT - Food Sci. Technol. 33, 80–88. https://doi.org/10.1006/fstl.1999.0619

Jia, D., You, J., Hu, Y., Liu, R., Xiong, S., 2015. Effect of CaCl2 on denaturation and aggregation of silver carp myosin during setting. Food Chem. 185, 212–218. https://doi.org/10.1016/j.foodchem.2015.03.130

Jones, O.G., McClements, D.J., 2010. Functional biopolymer particles: Design, fabrication, and applications. Compr. Rev. Food Sci. Food Saf. 9, 374–397. https://doi.org/10.1111/j.1541-4337.2010.00118.x

Joye, I.J., Davidov-Pardo, G., McClements, D.J., 2015. Encapsulation of resveratrol in biopolymer particles produced using liquid antisolvent precipitation. Part 2:

Stability and functionality. Food Hydrocoll. 49, 127–134. https://doi.org/10.1016/j.foodhyd.2015.02.038

Joye, I.J., McClements, D.J., 2014. Biopolymer-based nanoparticles and microparticles: Fabrication, characterization, and application. Curr. Opin. Colloid Interface Sci. 19, 417–427. https://doi.org/10.1016/j.cocis.2014.07.002

Kakran, M., Sahoo, N.G., Li, L., Judeh, Z., 2012. Fabrication of quercetin nanoparticles by anti-solvent precipitation method for enhanced dissolution. Powder Technol. 223, 59–64. https://doi.org/10.1016/j.powtec.2011.08.021

Kampf, N., Martinez, C.G., Corradini, M.G., Peleg, M., 2003. Effect of two gums on the development, rheological properties and stability of egg albumen foams. Rheol. Acta 42, 259–268. https://doi.org/10.1007/s00397-002-0281-8

Katouzian, I., Jafari, S.M., 2016. Nano-encapsulation as a promising approach for targeted delivery and controlled release of vitamins. Trends Food Sci. Technol. 53, 34–48. https://doi.org/10.1016/j.tifs.2016.05.002

Kazmi, S.A., Vieth, R., Rousseau, D., 2007. Vitamin D3 fortification and quantification in processed dairy products. Int. Dairy J. 17, 753–759. https://doi.org/10.1016/j.idairyj.2006.09.009

Keršienė, M., Jasutienė, I., Eisinaitė, V., Pukalskienė, M., Venskutonis, P.R., Damulevičienė, G., Knašienė, J., Lesauskaitė, V., Leskauskaitė, D., 2020. Development of a high-protein yoghurt-type product enriched with bioactive compounds for the elderly. Lwt 131, 1–8. https://doi.org/10.1016/j.lwt.2020.109820

Khan, S. a, Royer, J.R., Raghavan, S.R., 1997. Rheology: Tools and Methods. Aviat. Fuels with Improv. Fire Saf. A Proc.

Khan, W.A., Butt, M.S., Pasha, I., Jamil, A., 2020. Microencapsulation of vitamin D in protein matrices: in vitro release and storage stability. J. Food Meas. Charact. 14, 1172–1182. https://doi.org/10.1007/s11694-019-00366-3

Kharlamova, A., Nicolai, T., Chassenieux, C., 2018. Calcium-induced gelation of whey protein aggregates: Kinetics, structure and rheological properties. Food Hydrocoll. 79, 145–157. https://doi.org/10.1016/j.foodhyd.2017.11.049

Khemakhem, M., Attia, H., Ayadi, M.A., 2019. The effect of pH, sucrose, salt and hydrocolloid gums on the gelling properties and water holding capacity of egg white gel. Food Hydrocoll. 87, 11–19. https://doi.org/10.1016/j.foodhyd.2018.07.041

Kiani, A., Fathi, M., Ghasemi, S.M., 2017. Production of novel vitamin D3 loaded lipid nanocapsules for milk fortification. Int. J. Food Prop. 20, 2466–2476. https://doi.org/10.1080/10942912.2016.1240690

Kinsella, J.E., 1981. Functional properties of proteins: Possible relationships between structure and function in foams. Food Chem. 7, 273–288. https://doi.org/10.1016/0308-8146(81)90033-9

Ko, S., Gunasekaran, S., 2006. Preparation of sub-100-nm β-lactoglobulin (BLG) nanoparticles. J. Microencapsul. 23, 887–898. https://doi.org/10.1080/02652040601035143

Krägel, J., Wüstneck, R., Husband, F., Wilde, P.J., Makievski, A. V., Grigoriev, D.O., Li, J.B., 1999. Properties of mixed protein/surfactant adsorption layers. Colloids Surfaces B Biointerfaces 12, 399–407. https://doi.org/10.1016/S0927-7765(98)00094-0

Kuhn, K.R., Cavallieri, Â.L.F., da Cunha, R.L., 2010. Cold-set whey protein gels induced by calcium or sodium salt addition. Int. J. Food Sci. Technol. 45, 348–357. https://doi.org/10.1111/j.1365-2621.2009.02145.x

Kuropatwa, M., Tolkach, A., Kulozik, U., 2009. Impact of pH on the interactions between whey and egg white proteins as assessed by the foamability of their mixtures. Food Hydrocoll. 23, 2174–2181. https://doi.org/10.1016/j.foodhyd.2009.05.001

Lajnaf, R., Picart-Palmade, L., Cases, E., Attia, H., Marchesseau, S., Ayadi, M.A., 2018. The foaming properties of camel and bovine whey: The impact of pH and heat treatment. Food Chem. 240, 295–303. https://doi.org/10.1016/j.foodchem.2017.07.064

Lam, S., Velikov, K.P., Velev, O.D., 2014. Pickering stabilization of foams and emulsions with particles of biological origin. Curr. Opin. Colloid Interface Sci. 19, 490–500. https://doi.org/10.1016/j.cocis.2014.07.003

Laneuville, S.I., Paquin, P., Turgeon, S.L., 2000. Effect of preparation conditions on the characteristics of whey protein - Xanthan gum complexes. Food Hydrocoll. 14, 305–314. https://doi.org/10.1016/S0268-005X(00)00003-5

Langevin, D., 2017. Aqueous foams and foam films stabilised by surfactants. Gravity-free studies. Comptes Rendus - Mec. 345, 47–55. https://doi.org/10.1016/j.crme.2016.10.009

Lau, C.K., Dickinson, E., 2005. Instability and structural change in an aerated system containing egg albumen and invert sugar. Food Hydrocoll. 19, 111–121. https://doi.org/10.1016/j.foodhyd.2004.04.020

Lau, K., Dickinson, E., 2006. Structural and Rheological Properties of Aerated High Sugar Systems Containing Egg Albumen. J. Food Sci. 69, E232–E239. https://doi.org/10.1111/j.1365-2621.2004.tb10714.x

Lau, K., Dickinson, E., 2004. Structural and Rheological Properties of Aerated High Sugar Systems Containing Egg Albumen. J. Food Sci. 69, E232–E239. https://doi.org/10.1111/j.1365-2621.2004.tb10714.x

Lazidis, A., de Almeida Parizotto, L., Spyropoulos, F., Norton, I.T., 2017. Microstructural design of aerated food systems by soft-solid materials. Food Hydrocoll. 73, 110–119. https://doi.org/10.1016/j.foodhyd.2017.06.032

Lazidis, A., Hancocks, R.D., Spyropoulos, F., Kreuß, M., Berrocal, R., Norton, I.T., 2016. Whey protein fluid gels for the stabilisation of foams. Food Hydrocoll. 53, 209–217. https://doi.org/10.1016/j.foodhyd.2015.02.022

Le, X.T., Rioux, L.E., Turgeon, S.L., 2017. Formation and functional properties of protein–polysaccharide electrostatic hydrogels in comparison to protein or polysaccharide hydrogels. Adv. Colloid Interface Sci. 239, 127–135. https://doi.org/10.1016/j.cis.2016.04.006

Lech, F.J., Delahaije, R.J.B.M., Meinders, M.B.J., Gruppen, H., Wierenga, P.A., 2016. Identification of critical concentrations determining foam ability and stability of β-lactoglobulin. Food Hydrocoll. 57, 46–54. https://doi.org/10.1016/j.foodhyd.2016.01.005

Lee, J., Duggan, E., 2022. Improved stability of vitamin D3 encapsulated in whey

protein isolate microgels. Int. Dairy J. 105351. https://doi.org/10.1016/j.idairyj.2022.105351

Levinson, Y., Israeli-Lev, G., Livney, Y.D., 2014. Soybean β-Conglycinin Nanoparticles for delivery of hydrophobic nutraceuticals. Food Biophys. 9, 332–340.

Li, H., Errington, A.D., Foegeding, E.A., 1999. Isostrength comparison of large-strain (fracture) rheological properties of egg white and whey protein gels. J. Food Sci. 64, 893–898. https://doi.org/10.1111/j.1365-2621.1999.tb15935.x

Li, J., Fu, J., Ma, Y., He, Y., Fu, R., Qayum, A., Jiang, Z., Wang, L., 2022. Low temperature extrusion promotes transglutaminase cross-linking of whey protein isolate and enhances its emulsifying properties and water holding capacity. Food Hydrocoll. 125, 107410. https://doi.org/10.1016/j.foodhyd.2021.107410

Li, J., Wang, C., Li, X., Su, Y., Yang, Y., Yu, X., 2018. Effects of pH and NaCl on the physicochemical and interfacial properties of egg white/yolk. Food Biosci. 23, 115–120. https://doi.org/10.1016/j.fbio.2017.12.004

Li, J.M., Nie, S.P., 2016. The functional and nutritional aspects of hydrocolloids in foods. Food Hydrocoll. 53, 46–61. https://doi.org/10.1016/j.foodhyd.2015.01.035

Li, R., Lund, P., Nielsen, S.B., Lund, M.N., 2022. Formation of whey protein aggregates by partial hydrolysis and reduced thermal treatment. Food Hydrocoll. 124. https://doi.org/10.1016/j.foodhyd.2021.107206

Li, X., Murray, B.S., Yang, Y., Sarkar, A., 2020a. Egg white protein microgels as aqueous Pickering foam stabilizers : Bubble stability and interfacial properties. Food Hydrocoll. 98, 105292. https://doi.org/10.1016/j.foodhyd.2019.105292

Li, X., Yang, Y., Murray, B.S., Sarkar, A., 2020b. Combination of egg white protein and microgels to stabilize foams: Impact of processing treatments. J. Food Eng. 275, 109860. https://doi.org/10.1016/j.jfoodeng.2019.109860

Liang, J., Yan, H., Wang, X., Zhou, Y., Gao, X., Puligundla, P., Wan, X., 2017. Encapsulation of epigallocatechin gallate in zein/chitosan nanoparticles for controlled applications in food systems. Food Chem. 231, 19–24. https://doi.org/10.1016/j.foodchem.2017.02.106

Liang, Y., Kristinsson, H.G., 2006. Influence of pH-Induced Unfolding and Refolding of Egg Albumen on Its Foaming Properties. J. Food Sci. 70, C222–C230. https://doi.org/10.1111/j.1365-2621.2005.tb07129.x

Lin, Y., Wang, Y.H., Yang, X.Q., Guo, J., Wang, J.M., 2016. Corn protein hydrolysate as a novel nano-vehicle: Enhanced physicochemical stability and in vitro bioaccessibility of vitamin D3. LWT - Food Sci. Technol. 72, 510–517. https://doi.org/10.1016/j.lwt.2016.05.020

Liszka-Skoczylas, M., Ptaszek, A., Zmudziński, D., 2014. The effect of hydrocolloids on producing stable foams based on the whey protein concentrate (WPC). J. Food Eng. 129, 1–11. https://doi.org/10.1016/j.jfoodeng.2014.01.002

Liu, K., Kong, X., Li, Q., Zhang, H., Zha, X., Luo, J., 2020a. Stability and bioavailability of vitamin D3 encapsulated in composite gels of whey protein isolate and lotus root amylopectin. Carbohydr. Polym. 227, 115337. https://doi.org/10.1016/j.carbpol.2019.115337

Liu, K., Li, Q.M., Zha, X.Q., Pan, L.H., Bao, L.J., Zhang, H.L., Luo, J.P., 2019. Effects of calcium or sodium ions on the properties of whey protein isolate-lotus root amylopectin composite gel, Food Hydrocolloids. Elsevier Ltd. https://doi.org/10.1016/j.foodhyd.2018.08.050

Liu, K., Zha, X.Q., Shen, W. Di, Li, Q.M., Pan, L.H., Luo, J.P., 2020b. The hydrogel of whey protein isolate coated by lotus root amylopectin enhance the stability and bioavailability of quercetin. Carbohydr. Polym. 236, 116009. https://doi.org/10.1016/j.carbpol.2020.116009

Liu, R., Wang, L., Liu, Y., Wu, T., Zhang, M., 2018. Fabricating soy protein hydrolysate/xanthan gum as fat replacer in ice cream by combined enzymatic and heat-shearing treatment. Food Hydrocoll. 81, 39–47. https://doi.org/10.1016/j.foodhyd.2018.01.031

Liu, W., Wang, J., McClements, D.J., Zou, L., 2018. Encapsulation of β-carotene-loaded oil droplets in caseinate/alginate microparticles: Enhancement of carotenoid stability and bioaccessibility. J. Funct. Foods 40, 527–535. https://doi.org/10.1016/j.jff.2017.11.046

Liu, Z., Liu, C., Sun, X., Zhang, S., Yuan, Y., Wang, D., Xu, Y., 2020. Fabrication and

characterization of cold-gelation whey protein-chitosan complex hydrogels for the controlled release of curcumin. Food Hydrocoll. 103, 105619. https://doi.org/10.1016/j.foodhyd.2019.105619

Loewen, A., Chan, B., Li-Chan, E.C.Y., 2018. Optimization of vitamins A and D3 loading in re-assembled casein micelles and effect of loading on stability of vitamin D3 during storage. Food Chem. 240, 472–481. https://doi.org/10.1016/j.foodchem.2017.07.126

Lomolino, G., Vincenzi, S., Gazzola, D., Crapisi, A., Curioni, A., 2015. Foaming properties of potato (Solanum tuberosum) proteins: A study by the gas sparging method. Colloids Surfaces A Physicochem. Eng. Asp. 475, 75–83. https://doi.org/10.1016/j.colsurfa.2015.01.093

Ložnjak, P., Jakobsen, J., 2018. Stability of vitamin D3 and vitamin D2 in oil, fish and mushrooms after household cooking. Food Chem. 254, 144–149. https://doi.org/10.1016/j.foodchem.2018.01.182

Luck, P.J., Bray, N., Foegeding, E.A., 2002. Factors determining yield stress and overrun of whey protein foams. J. Food Sci. 67, 1677–1681. https://doi.org/10.1111/j.1365-2621.2002.tb08704.x

Luo, Y., Teng, Z., Wang, Q., 2012. Development of Zein Nanoparticles Coated with Carboxymethyl Chitosn for Encapsulation and controlled release of vitamin D3. J. Agric. Food Chem. 60. https://doi.org/10.1021/jf204194z

Luo, Y., Zhang, B., Whent, M., Yu, L.L., Wang, Q., 2011. Preparation and characterization of zein/chitosan complex for encapsulation of α-tocopherol, and its in vitro controlled release study. Colloids Surfaces B Biointerfaces 85, 145–152. https://doi.org/10.1016/j.colsurfb.2011.02.020

Mackie, A.R., Gunning, A.P., Wilde, P.J., Morris, V.J., 2000. Competitive displacement of β-lactoglobulin from the air/water interface by sodium dodecyl sulfate. Langmuir 16, 8176–8181. https://doi.org/10.1021/la0003950

Madadlou, A., Famelart, M.H., Pezennec, S., Rousseau, F., Floury, J., Dupont, D., 2020. Interfacial and (emulsion) gel rheology of hydrophobised whey proteins. Int. Dairy J. 100. https://doi.org/10.1016/j.idairyj.2019.104556

Madalena, D.A., Ramos, Ó.L., Pereira, R.N., Bourbon, A.I., Pinheiro, A.C., Malcata, F.X., Teixeira, J.A., Vicente, A.A., 2016. In vitro digestion and stability assessment of β-lactoglobulin/riboflavin nanostructures. Food Hydrocoll. 58, 89–97. https://doi.org/10.1016/j.foodhyd.2016.02.015

Marinova, K.G., Basheva, E.S., Nenova, B., Temelska, M., Mirarefi, A.Y., Campbell, B., Ivanov, I.B., 2009. Physico-chemical factors controlling the foamability and foam stability of milk proteins: Sodium caseinate and whey protein concentrates. Food Hydrocoll. 23, 1864–1876. https://doi.org/10.1016/j.foodhyd.2009.03.003

Martin, A.H., Grolle, K., Bos, M.A., Cohen Stuart, M.A., Van Vliet, T., 2002. Network forming properties of various proteins adsorbed at the air/water interface in relation to foam stability. J. Colloid Interface Sci. 254, 175–183. https://doi.org/10.1006/jcis.2002.8592

Martínez-Padilla, L.P., García-Rivera, J.L., Romero-Arreola, V., Casas-Alencáster, N.B., 2015. Effects of xanthan gum rheology on the foaming properties of whey protein concentrate. J. Food Eng. 156, 22–30. https://doi.org/10.1016/j.jfoodeng.2015.01.018

Matalanis, A., Jones, O.G., McClements, D.J., 2011. Structured biopolymer-based delivery systems for encapsulation, protection, and release of lipophilic compounds. Food Hydrocoll. 25, 1865–1880. https://doi.org/10.1016/j.foodhyd.2011.04.014

Matalanis, A., Lesmes, U., Decker, E.A., McClements, D.J., 2010. Fabrication and characterization of filled hydrogel particles based on sequential segregative and aggregative biopolymer phase separation. Food Hydrocoll. 24, 689–701. https://doi.org/10.1016/j.foodhyd.2010.04.009

McClements, D.J., 2017a. Designing biopolymer microgels to encapsulate, protect and deliver bioactive components: Physicochemical aspects. Adv. Colloid Interface Sci. 240, 31–59. https://doi.org/10.1016/j.cis.2016.12.005

McClements, D.J., 2017b. Recent progress in hydrogel delivery systems for improving nutraceutical bioavailability. Food Hydrocoll. 68, 238–245. https://doi.org/10.1016/j.foodhyd.2016.05.037

McClements, D.J., Xiao, H., 2012. Potential biological fate of ingested nanoemulsions:

Influence of particle characteristics. Food Funct. 3, 202–220. https://doi.org/10.1039/c1fo10193e

Mendyk, A., Jachowicz, R., Fijorek, K., Dorozyński, P., Kulinowski, P., Polak, S., 2012. KinetDS: An open source software for dissolution test data analysis. Dissolution Technol. 19, 6–11. https://doi.org/10.14227/DT190112P6

Meunier-Goddik, L., Sandra, S., 2002. Liquid milk products. Encycl. dairy Sci. 1627–1632.

Minekus, M., Alminger, M., Alvito, P., Ballance, S., Bohn, T., Bourlieu, C., Carrière, F., Boutrou, R., Corredig, M., Dupont, D., Dufour, C., Egger, L., Golding, M., Karakaya, S., Kirkhus, B., Le Feunteun, S., Lesmes, U., MacIerzanka, A., MacKie, A., Marze, S., McClements, D.J., Ménard, O., Recio, I., Santos, C.N., Singh, R.P., Vegarud, G.E., Wickham, M.S.J., Weitschies, W., Brodkorb, A., 2014. A standardised static in vitro digestion method suitable for food-an international consensus. Food Funct. 5, 1113–1124. https://doi.org/10.1039/c3fo60702j

Mitbumrung, W., Suphantharika, M., McClements, D.J., Winuprasith, T., 2019. Encapsulation of Vitamin D3 in Pickering Emulsion Stabilized by Nanofibrillated Mangosteen Cellulose: Effect of Environmental Stresses. J. Food Sci. 84, 3213–3221. https://doi.org/10.1111/1750-3841.14835

Mleko, S., Kristinsson, H.G., Liang, Y., Gustaw, W., 2007. Rheological properties of foams generated from egg albumin after pH treatment. LWT - Food Sci. Technol. 40, 908–914. https://doi.org/10.1016/j.lwt.2006.04.007

Moakes, R.J.A., Sullo, A., Norton, I.T., 2015. Preparation and characterisation of whey protein fluid gels: The effects of shear and thermal history. Food Hydrocoll. 45, 227–235. https://doi.org/10.1016/j.foodhyd.2014.11.024

Moro, A., Báez, G.D., Busti, P.A., Ballerini, G.A., Delorenzi, N.J., 2011. Effects of heat-treated β-lactoglobulin and its aggregates on foaming properties. Food Hydrocoll. 25, 1009–1015. https://doi.org/10.1016/j.foodhyd.2010.09.021

Moschakis, T., Murray, B.S., Dickinson, E., 2005. Microstructural evolution of viscoelastic emulsions stabilised by sodium caseinate and xanthan gum. J. Colloid Interface Sci. 284, 714–728. https://doi.org/10.1016/j.jcis.2004.10.036

Mosekilde, L., 2005. Vitamin D and the elderly. Clin. Endocrinol. (Oxf). 62, 265–281. https://doi.org/10.1111/j.1365-2265.2005.02226.x

Murphy, R.W., Farkas, B.E., Jones, O.G., 2016. Dynamic and viscoelastic interfacial behavior of β-lactoglobulin microgels of varying sizes at fluid interfaces. J. Colloid Interface Sci. 466, 12–19. https://doi.org/10.1016/j.jcis.2015.12.012

Murray, B.S., 2019. Microgels at fluid-fluid interfaces for food and drinks. Adv. Colloid Interface Sci. 271, 101990. https://doi.org/10.1016/j.cis.2019.101990

Murray, B.S., Durga, K., Yusoff, A., Stoyanov, S.D., 2011. Stabilization of foams and emulsions by mixtures of surface active food-grade particles and proteins. Food Hydrocoll. 25, 627–638. https://doi.org/10.1016/j.foodhyd.2010.07.025

Murray, B.S., Ettelaie, R., 2004. Foam stability: Proteins and nanoparticles. Curr. Opin. Colloid Interface Sci. 9, 314–320. https://doi.org/10.1016/j.cocis.2004.09.004

Muse, M.R., Hartel, R.W., 2004. Ice cream structural elements that affect melting rate and hardness. J. Dairy Sci. 87, 1–10. https://doi.org/10.3168/jds.S0022-0302(04)73135-5

Nascimento, L.G.L., Casanova, F., Silva, N.F.N., Teixeira, Á.V.N. de C., Júnior, P.P. de S.P., Vidigal, M.C.T.R., Stringheta, P.C., Carvalho, A.F. de, 2020. Use of a crosslinked casein micelle hydrogel as a carrier for jaboticaba (Myrciaria cauliflora) extract. Food Hydrocoll. 106. https://doi.org/10.1016/j.foodhyd.2020.105872

Nastaj, M., 2021. Effect of Sucrose on Physicochemical Properties of High-Protein Meringues Obtained from Whey Protein Isolate. Appl. Sci.

Nedovic, V., Kalusevic, A., Manojlovic, V., Levic, S., Bugarski, B., 2011. An overview of encapsulation technologies for food applications. Procedia Food Sci. 1, 1806–1815. https://doi.org/10.1016/j.profoo.2011.09.265

Nicorescu, I., Loisel, C., Riaublanc, A., Vial, C., Djelveh, G., Cuvelier, G., Legrand, J., 2009. Effect of dynamic heat treatment on the physical properties of whey protein foams. Food Hydrocoll. 23, 1209–1219. https://doi.org/10.1016/j.foodhyd.2008.09.005

Nicorescu, I., Loisel, C., Vial, C., Riaublanc, A., Djelveh, G., Cuvelier, G., Legrand, J.,

2008. Combined effect of dynamic heat treatment and ionic strength on the properties of whey protein foams – Part II. Food Res. Int. 41, 980–988. https://doi.org/10.1016/j.foodres.2008.08.003

Nicorescu, I., Vial, C., Loisel, C., Riaublanc, A., Djelveh, G., Cuvelier, G., Legrand, J., 2010. Influence of protein heat treatment on the continuous production of food foams. Food Res. Int. 43, 1585–1593. https://doi.org/10.1016/j.foodres.2010.03.015

Nicorescu, I., Vial, C., Talansier, E., Lechevalier, V., Loisel, C., Della Valle, D., Riaublanc, A., Djelveh, G., Legrand, J., 2011. Comparative effect of thermal treatment on the physicochemical properties of whey and egg white protein foams. Food Hydrocoll. 25, 797–808. https://doi.org/10.1016/j.foodhyd.2010.09.020

Nooshkam, M., Varidi, M., Alkobeisi, F., 2022. Bioactive food foams stabilized by licorice extract/whey protein isolate/sodium alginate ternary complexes. Food Hydrocoll. 126, 107488. https://doi.org/10.1016/j.foodhyd.2022.107488

Norton, J.E., Gonzalez Espinosa, Y., Watson, R.L., Spyropoulos, F., Norton, I.T., 2015. Functional food microstructures for macronutrient release and delivery. Food Funct. 6, 663–678. https://doi.org/10.1039/c4fo00965g

O'Neill, G.J., Egan, T., Jacquier, J.C., O'Sullivan, M., Dolores O'Riordan, E., 2014. Whey microbeads as a matrix for the encapsulation and immobilisation of riboflavin and peptides. Food Chem. 160, 46–52. https://doi.org/10.1016/j.foodchem.2014.03.002

O'Neill, G.J., Jacquier, J.C., Mukhopadhya, A., Egan, T., O'Sullivan, M., Sweeney, T., O'Riordan, E.D., 2015. In vitro and in vivo evaluation of whey protein hydrogels for oral delivery of riboflavin. J. Funct. Foods 19, 512–521. https://doi.org/10.1016/j.jff.2015.09.043

Oboroceanu, D., Wang, L., Magner, E., Auty, M.A.E., 2014. Fibrillization of whey proteins improves foaming capacity and foam stability at low protein concentrations. J. Food Eng. 121, 102–111. https://doi.org/10.1016/j.jfoodeng.2013.08.023

Ochi, A., Katsuta, K., Maruyama, E., Kubo, M., Ueda, T., 2000. Effects of sugars on stability of egg foam and their rheological properties. Hydrocolloids 275–280.

Ozel, B., Zhang, Z., He, L., McClements, D.J., 2020. Digestion of animal- and plant-based proteins encapsulated in κ-carrageenan/protein beads under simulated gastrointestinal conditions. Food Res. Int. 137, 109662. https://doi.org/10.1016/j.foodres.2020.109662

Ozturk, B., Argin, S., Ozilgen, M., McClements, D.J., 2015. Nanoemulsion delivery systems for oil-soluble vitamins: Influence of carrier oil type on lipid digestion and vitamin D bioaccessibility. Food Chem. 187, 499–506. https://doi.org/10.1016/j.foodchem.2015.04.065

Panizzon, G.P., Bueno, F.G., Ueda-Nakamura, T., Nakamura, C.V., Filho, B.P.D., 2014. Preparation of spray-dried soy isoflavone-loaded gelatin microspheres for enhancement of dissolution: Formulation, characterization and in vitro evaluation. Pharmaceutics 6, 599–615. https://doi.org/10.3390/pharmaceutics6040599

Park, S.J., Garcia, C. V., Shin, G.H., Kim, J.T., 2017. Development of nanostructured lipid carriers for the encapsulation and controlled release of vitamin D3. Food Chem. 225, 213–219. https://doi.org/10.1016/j.foodchem.2017.01.015

Parker, M.L., Grant, A., Rigby, N.M., Belton, P.S., Taylor, J.R.N., 1999. Effects of popping on the endosperm cell walls of sorghum and maize. J. Cereal Sci. 30, 209–216. https://doi.org/10.1006/jcrs.1999.0281

Pelegrine, D.H.G., Gasparetto, C.A., 2005. Whey proteins solubility as function of temperature and pH. LWT - Food Sci. Technol. 38, 77–80. https://doi.org/10.1016/j.lwt.2004.03.013

Peng, D., Yang, J., Li, J., Tang, C., Li, B., 2017. Foams Stabilized by β-Lactoglobulin Amyloid Fibrils: Effect of pH. J. Agric. Food Chem. https://doi.org/10.1021/acs.jafc.7b03669

Peng, H., Chen, S., Luo, M., Ning, F., Zhu, X., Xiong, H., 2016. Preparation and self-assembly mechanism of bovine serum albumin-citrus peel pectin conjugated hydrogel: A potential delivery system for Vitamin C. J. Agric. Food Chem. 64, 7377–7384. https://doi.org/10.1021/acs.jafc.6b02966

Perez, A.A., Sánchez, C.C., Patino, J.M.R., Rubiolo, A.C., Santiago, L.G., 2010. Milk whey proteins and xanthan gum interactions in solution and at the air-water interface: A rheokinetic study. Colloids Surfaces B Biointerfaces 81, 50–57.

https://doi.org/10.1016/j.colsurfb.2010.06.021

Phillips, L.G., Schulman, W., Kinsella, J.E., 1990. pH and Heat Treatment Effects on Foaming of Whey Protein isolate. J. Food Sci. 55, 1116–1119. https://doi.org/10.1111/j.1365-2621.1990.tb01612.x

Phillips, L.G., Yang, S.T., Schulman, W., Kinsella, J.E., 1989. Effects of Lysozyme, Clupeine, and Sucrose on the Foaming Properties of Whey Protein Isolate and β-Lactoglobulin. J. Food Sci. 54, 743–747. https://doi.org/10.1111/j.1365-2621.1989.tb04694.x

Pinheiro, A.C., Gonçalves, R.F., Madalena, D.A., Vicente, A.A., 2017. Towards the understanding of the behavior of bio-based nanostructures during in vitro digestion. Curr. Opin. Food Sci. 15, 79–86. https://doi.org/10.1016/j.cofs.2017.06.005

Pithia, K.D., Edwards, S.F., 1994. Rheology of liquid foams. Phys. A Stat. Mech. its Appl. 205, 565–576. https://doi.org/10.1016/0378-4371(94)90221-6

Plamper, F.A., Richtering, W., 2017. Functional Microgels and Microgel Systems. Acc. Chem. Res. 50, 131–140. https://doi.org/10.1021/acs.accounts.6b00544

Provost, J., Colabroy, K., Kelly, B., Wallert, M., 2016. The Science of Cooking. John Wiley & Sons, Incorporated.

Raikos, V., Campbell, L., Euston, S.R., 2007. Effects of sucrose and sodium chloride on foaming properties of egg white proteins. Food Res. Int. 40, 347–355. https://doi.org/10.1016/j.foodres.2006.10.008

Ray, S., Raychaudhuri, U., Chakraborty, R., 2016. An overview of encapsulation of active compounds used in food products by drying technology. Food Biosci. 13, 76–83. https://doi.org/10.1016/j.fbio.2015.12.009

Rayner, M., 2015. Current status on novel ways for stabilizing food dispersions by oleosins, particles and microgels. Curr. Opin. Food Sci. 3, 94–109. https://doi.org/10.1016/j.cofs.2015.05.006

Remondetto, G.E., Beyssac, E., Subirade, M., 2004. Iron availability from whey protein hydrogels: An in vitro study. J. Agric. Food Chem. 52, 8137–8143. https://doi.org/10.1021/jf040286h

Rio, E., Drenckhan, W., Salonen, A., Langevin, D., 2014. Unusually stable liquid foams. Adv. Colloid Interface Sci. 205, 74–86. https://doi.org/10.1016/j.cis.2013.10.023

Rodríguez Niño, M.R., Rodríguez Patino, J.M., 2002. Effect of the aqueous phase composition on the adsorption of bovine serum albumin to the air-water interface. Ind. Eng. Chem. Res. 41, 1489–1495. https://doi.org/10.1021/ie010770z

Rodriguez Patino, J.M., Dolores Naranjo Delgado, M., Linares Fernández, J., 1995. Stability and Mechanical Strength of Aqueous Foams Containing Food Proteins. Colloids Surfaces A Physicochem. Eng. Asp. 99, 65–78.

Rodriguez Patino, J.M., Pilosof, A.M.R., 2011. Protein-polysaccharide interactions at fluid interfaces. Food Hydrocoll. 25, 1925–1937. https://doi.org/10.1016/j.foodhyd.2011.02.023

Rogers, Z.J., Bencherif, S.A., 2019. Cryogelation and cryogels. Gels 5, 6–7. https://doi.org/10.3390/gels5040046

Ron, N., Zimet, P., Bargarum, J., Livney, Y.D., 2010. Beta-lactoglobulin-polysaccharide complexes as nanovehicles for hydrophobic nutraceuticals in non-fat foods and clear beverages. Int. Dairy J. 20, 686–693. https://doi.org/10.1016/j.idairyj.2010.04.001

Rouimi, S., Schorsch, C., Valentini, C., Vaslin, S., 2005. Foam stability and interfacial properties of milk protein-surfactant systems. Food Hydrocoll. 19, 467–478. https://doi.org/10.1016/j.foodhyd.2004.10.032

Roy, S., Abdul, S., Prasad, W.G., Khetra, Y., 2022. Quality attributes of high protein ice cream prepared by incorporation of whey protein isolate. Appl. Food Res. 2, 100029. https://doi.org/10.1016/j.afres.2021.100029

Rullier, B., Axelos, M.A.V., Langevin, D., Novales, B., 2010. β-Lactoglobulin aggregates in foam films: Effect of the concentration and size of the protein aggregates. J. Colloid Interface Sci. 343, 330–337. https://doi.org/10.1016/j.jcis.2009.11.015

Rullier, B., Novales, B., Axelos, M.A.V., 2008. Effect of protein aggregates on foaming properties of β-lactoglobulin. Colloids Surfaces A Physicochem. Eng. Asp. 330,

96–102. https://doi.org/10.1016/j.colsurfa.2008.07.040

Sağlam, D., Venema, P., de Vries, R., van der Linden, E., 2014. Exceptional heat stability of high protein content dispersions containing whey protein particles. Food Hydrocoll. 34, 68–77. https://doi.org/10.1016/j.foodhyd.2012.12.016

Saraiva, B.R., da Silva, L.H.M., Anjo, F.A., Vital, A.C.P., Da Silva, J.B., Bruschi, M.L., Matumoto Pintro, P.T., 2020. Technological and sensorial properties of liquid nitrogen ice cream enriched with protein from brewing waste (trub). Int. J. Food Sci. Technol. 55, 1962–1970. https://doi.org/10.1111/ijfs.14484

Schmitt, C., Bovay, C., Rouvet, M., 2014. Bulk self-aggregation drives foam stabilization properties of whey protein microgels. Food Hydrocoll. 42, 139–148. https://doi.org/10.1016/j.foodhyd.2014.03.010

Schmitt, C., Bovay, C., Rouvet, M., Shojaei-Rami, S., Kolodziejczyk, E., 2007. Whey protein soluble aggregates from heating with NaCl: Physicochemical, interfacial, and foaming properties. Langmuir. https://doi.org/10.1021/la0632575

Schmitt, C., Moitzi, C., Bovay, C., Rouvet, M., Bovetto, L., Donato, L., Leser, M.E., Schurtenberger, P., Stradner, A., 2010. Internal structure and colloidal behaviour of covalent whey protein microgels obtained by heat treatment. Soft Matter 6, 4876–4884. https://doi.org/10.1039/c0sm00220h

Schmitt, V., Destribats, M., Backov, R., 2014. Colloidal particles as liquid dispersion stabilizer: Pickering emulsions and materials thereof. Comptes Rendus Phys. 15, 761–774. https://doi.org/10.1016/j.crhy.2014.09.010

Semo, E., Kesselman, E., Danino, D., Livney, Y.D., 2007. Casein micelle as a natural nano-capsular vehicle for nutraceuticals. Food Hydrocoll. 21, 936–942. https://doi.org/10.1016/j.foodhyd.2006.09.006

Shewan, H.M., Stokes, J.R., 2013. Review of techniques to manufacture micro-hydrogel particles for the food industry and their applications. J. Food Eng. 119, 781–792. https://doi.org/10.1016/j.jfoodeng.2013.06.046

Simoes, L.S., Martins, J., Pinheiro, A., Vicente, A., Ramos, O., 2020. β-lactoglobulin micro- and nanostructures as bioactive compounds vehicle.pdf.

Smithers, G.W., 2008. Whey and whey proteins-From “gutter-to-gold.” Int. Dairy J. 18,

695–704. https://doi.org/10.1016/j.idairyj.2008.03.008

Sobhaninia, M., Nasirpour, A., Shahedi, M., Golkar, A., Desobry, S., 2018. Fabrication of whey proteins aggregates by controlled heat treatment and pH: Factors affecting aggregate size. Int. J. Biol. Macromol. 112, 74–82. https://doi.org/10.1016/j.ijbiomac.2018.01.109

Soukoulis, C., Chandrinos, I., Tzia, C., 2008. Study of the functionality of selected hydrocolloids and their blends with κ-carrageenan on storage quality of vanilla ice cream. LWT - Food Sci. Technol. 41, 1816–1827. https://doi.org/10.1016/j.lwt.2007.12.009

Sousa, R., Portmann, R., Dubois, S., Recio, I., Egger, L., 2020. Protein digestion of different protein sources using the INFOGEST static digestion model. Food Res. Int. 130, 108996. https://doi.org/10.1016/j.foodres.2020.108996

Souza, C.J.F., Garcia-Rojas, E.E., 2017. Interpolymeric complexing between egg white proteins and xanthan gum: Effect of salt and protein/polysaccharide ratio. Food Hydrocoll. 66, 268–275. https://doi.org/10.1016/j.foodhyd.2016.11.032

Spence, C., Navarra, J., Youssef, J., 2019. Using ice-cream as an effective vehicle for energy/nutrient delivery in the elderly. Int. J. Gastron. Food Sci. 16, 100140. https://doi.org/10.1016/j.ijgfs.2019.100140

Stokes, J.R., 2011. Rheology of Industrially Relevant Microgels. Microgel Suspens. Fundam. Appl. 327–353. https://doi.org/10.1002/9783527632992.ch13

Su, Y., Gu, L., Zhang, Z., Chang, C., Li, J., McClements, D.J., Yang, Y., 2019. Encapsulation and release of egg white protein in alginate microgels: Impact of pH and thermal treatment. Food Res. Int. 120, 305–311. https://doi.org/10.1016/j.foodres.2019.02.048

Sun, L., Chen, W., Liu, Y., Li, J., Yu, H., 2015. Soy protein isolate/cellulose nanofiber complex gels as fat substitutes: rheological and textural properties and extent of cream imitation. Cellulose 22, 2619–2627. https://doi.org/10.1007/s10570-015-0681-4

Sung, M.R., Xiao, H., Decker, E.A., McClements, D.J., 2015. Fabrication, characterization and properties of filled hydrogel particles formed by the emulsion-

template method. J. Food Eng. 155, 16–21. https://doi.org/10.1016/j.jfoodeng.2015.01.007

Tabibian, M., Torbati, M., Mogaddam, M.R.A., Mirlohi, M., Sadeghi, M., Mohtadinia, J., 2017. Evaluation of vitamin D3 and D2 stability in fortified flat bread samples during dough fermentation, baking and storage. Adv. Pharm. Bull. 7, 323–328. https://doi.org/10.15171/apb.2017.038

TAInstruments, 2020. Basic Rheology, Module 3 - Oscillation : Amplitude and Frequency [WWW Document]. PowerPoint Slides. URL https://drive.google.com/file/d/1SEDMCigRftgFuF4swf07mtDS2Vuom0T_/view (accessed 6.2.20).

Talansier, E., Loisel, C., Dellavalle, D., Desrumaux, A., Lechevalier, V., Legrand, J., 2009. Optimization of dry heat treatment of egg white in relation to foam and interfacial properties. LWT - Food Sci. Technol. 42, 496–503. https://doi.org/10.1016/j.lwt.2008.09.013

Tan, Y., Liu, J., Zhou, H., Muriel Mundo, J., McClements, D.J., 2019. Impact of an indigestible oil phase (mineral oil) on the bioaccessibility of vitamin D 3 encapsulated in whey protein-stabilized nanoemulsions. Food Res. Int. 120, 264–274. https://doi.org/10.1016/j.foodres.2019.02.031

Tan, Y., McClements, D., 2021. Improving the bioavailability of oil-soluble vitamins by optimizing food matrix effects : A review. Food Chem. 348, 129148. https://doi.org/10.1016/j.foodchem.2021.129148

Teng, Z., Luo, Y., Wang, Q., 2013. Carboxymethyl chitosan-soy protein complex nanoparticles for the encapsulation and controlled release of vitamin D 3. Food Chem. 141, 524–532. https://doi.org/10.1016/j.foodchem.2013.03.043

ThermoScientific, 2020. Ellman’s Reagent.

Tipchuwong, N., Chatraporn, C., Ngamchuachit, P., Tansawat, R., 2017. Increasing retention of vitamin D3 in vitamin D3 fortified ice cream with milk protein emulsifier. Int. Dairy J. 74, 74–79. https://doi.org/10.1016/j.idairyj.2017.01.003

Tomczyńska-Mleko, M., 2013. Structure and stability of ion induced whey protein aerated gels. Czech J. Food Sci. 31, 211–216. https://doi.org/10.17221/247/2012-

cjfs

Torres, O., Murray, B., Sarkar, A., 2016. Emulsion microgel particles: Novel encapsulation strategy for lipophilic molecules. Trends Food Sci. Technol. 55, 98–108. https://doi.org/10.1016/j.tifs.2016.07.006

Totosaus, A., Montejano, J., Salazar, J., Guerrero, I., 2002. A review of physical and chemical protein-gel induction. Int. J. Food Sci. Technol. 37, 132–142. https://doi.org/10.1145/800219.806660

Ustunol, Z., 2014. Applied Food Protein Chemistry, 1st ed. John Wiley & Sons, Incorporated, Chicester.

Van der Plancken, I., Van Loey, A., Hendrickx, M.E., 2007. Foaming properties of egg white proteins affected by heat or high pressure treatment. J. Food Eng. 78, 1410–1426. https://doi.org/10.1016/j.jfoodeng.2006.01.013

Van Der Plancken, I., Van Loey, A., Hendrickx, M.E.G., 2005. Changes in sulfhydryl content of egg white proteins due to heat and pressure treatment. J. Agric. Food Chem. 53, 5726–5733. https://doi.org/10.1021/jf050289+

Vega, C., Sanghvi, A., 2012. Cooking Literacy: Meringues as Culinary Scaffoldings. Food Biophys. 7, 103–113. https://doi.org/10.1007/s11483-011-9247-7

Velasquez-Cock, J., Serpa, A., Vélez, L., Gañán, P., Hoyos, C.G., Castro, C., Duizer, L., Go, H.D., Zuluaga, R., 2019. Influence of cellulose nanofibrils on the structural elements of ice cream 87, 204–213. https://doi.org/10.1016/j.foodhyd.2018.07.035

Walia, N., Dasgupta, N., Ranjan, S., Chen, L., Ramalingam, C., 2017. Fish oil based vitamin D nanoencapsulation by ultrasonication and bioaccessibility analysis in simulated gastro-intestinal tract. Ultrason. Sonochem. 39, 623–635. https://doi.org/10.1016/j.ultsonch.2017.05.021

Wang, J., Nguyen, A. V., Farrokhpay, S., 2016. A critical review of the growth, drainage and collapse of foams. Adv. Colloid Interface Sci. 228, 55–70. https://doi.org/10.1016/j.cis.2015.11.009

Wang, K., Wang, G., Lu, C., Wang, Y., 2017. Preparation of amphiphilic Janus particles and their application in stabilising foams. Micro Nano Lett. 13, 397–402. https://doi.org/10.1049/mnl.2017.0597

Wang, X., Zeng, M., Qin, F., Adhikari, B., He, Z., Chen, J., 2018. Enhanced CaSO4-induced gelation properties of soy protein isolate emulsion by pre-aggregation. Food Chem. 242, 459–465. https://doi.org/10.1016/j.foodchem.2017.09.044

Weigle, D.S., Breen, P.A., Matthys, C.C., Callahan, H.S., Meeuws, K.E., Burden, V.R., Purnell, J.Q., 2005. A high-protein diet induces sustained reductions in appetite, ad libitum caloric intake, and body weight despite compensatory changes in diurnal plasma leptin and ghrelin concentrations. Am. J. Clin. Nutr. 82, 41–48. https://doi.org/10.1093/ajcn.82.1.41

Wierenga, P.A., Gruppen, H., 2010. New views on foams from protein solutions. Curr. Opin. Colloid Interface Sci. 15, 365–373. https://doi.org/10.1016/j.cocis.2010.05.017

Wilde, P.J., 2000. Interfaces: Their role in foam and emulsion behaviour. Curr. Opin. Colloid Interface Sci. 5, 176–181. https://doi.org/10.1016/S1359-0294(00)00056-X

Wimalawansa, S.J., 2018. Non-musculoskeletal benefits of vitamin D. J. Steroid Biochem. Mol. Biol. 175, 60–81. https://doi.org/10.1016/j.jsbmb.2016.09.016

Winuprasith, T., Khomein, P., Mitbumrung, W., Suphantharika, M., Nitithamyong, A., McClements, D.J., 2018. Encapsulation of vitamin D 3 in pickering emulsions stabilized by nano fi brillated mangosteen cellulose : Impact on in vitro digestion and bioaccessibility. Food Hydrocoll. 83, 153–164. https://doi.org/10.1016/j.foodhyd.2018.04.047

World Health Organization, 2021. Ageing and Health [WWW Document]. Ageing Heal. URL https://www.who.int/news-room/fact-sheets/detail/ageing-and-health (accessed 1.5.22).

World Health Organization, 2002. Keep fit for life. Meeting the nutritional needs of older persons. WHO Libr. Cat. Data 119. https://doi.org/10.1177/146642400312300228

Xiang, C., Gao, J., Ye, H., Ren, G., Ma, X., Xie, H., Fang, S., Lei, Q., Fang, W., 2020. Development of ovalbumin-pectin nanocomplexes for vitamin D3 encapsulation: Enhanced storage stability and sustained release in simulated gastrointestinal digestion. Food Hydrocoll. 106, 105926. https://doi.org/10.1016/j.foodhyd.2020.105926

Yan, L., Yu, D., Liu, R., Jia, Y., Zhang, M., Wu, T., Sui, W., 2021. Microstructure and meltdown properties of low-fat ice cream: Effects of microparticulated soy protein hydrolysate/xanthan gum (MSPH/XG) ratio and freezing time. J. Food Eng. 291, 110291. https://doi.org/10.1016/j.jfoodeng.2020.110291

Yang, J., Thielen, I., Berton-Carabin, C., Van der linden, E., Sagis, L., 2019. Nonlinear interfacial rheology and atomic force microscopy of air-water interfaces stabilized by whey protein beads and their constituents. Food Hydrocoll. 105466. https://doi.org/10.1016/j.foodhyd.2019.105466

Yang, X., Berry, T.K., Foegeding, E.A., 2009. Foams prepared from whey protein isolate and egg white protein: 1. physical, microstructural, and interfacialproperties. J. Food Sci. 74, 259–268. https://doi.org/10.1111/j.1750-3841.2009.01179.x

Yang, X., Foegeding, E.A., 2010. Effects of sucrose on egg white protein and whey protein isolate foams: Factors determining properties of wet and dry foams (cakes). Food Hydrocoll. 24, 227–238. https://doi.org/10.1016/j.foodhyd.2009.09.011

Yangchao Luo, Zhang, B., Whent, M., Yu, L. (Lucy), Wang, Q., 2011. Preparation and characterization of zeinchitosan complex for encapsulation of α-tocopherol.pdf. Colloids Surfaces B Biointerfaces.

Yin, X., Fu, X., Cheng, H., Wusigale, Liang, L., 2020. α-Tocopherol and naringenin in whey protein isolate particles: Partition, antioxidant activity, stability and bioaccessibility. Food Hydrocoll. 106, 105895. https://doi.org/10.1016/j.foodhyd.2020.105895

Yu, B., Zeng, X., Wang, L., Regenstein, J.M., 2021. Preparation of nanofibrillated cellulose from grapefruit peel and its application as fat substitute in ice cream. Carbohydr. Polym. 254, 117415. https://doi.org/10.1016/j.carbpol.2020.117415

Zagury, Y., David, S., Edelman, R., Hazan Brill, R., Livney, Y.D., 2021. Sugar beet pectin as a natural carrier for curcumin, a water-insoluble bioactive for food and beverage enrichment: Formation and characterization. Innov. Food Sci. Emerg. Technol. 74, 102858. https://doi.org/10.1016/j.ifset.2021.102858

Zareie, M., Abbasi, A., Faghih, S., 2019. Thermal Stability and Kinetic Study on Thermal Degradation of Vitamin D3in Fortified Canola Oil. J. Food Sci. 84, 2475–

2481.

Zayas, 2001. Functionality of proteins in food. https://doi.org/10.1007/978-3-642-56680-6

Zhang, A., Chen, S., Wang, Y., Wang, X., Xu, N., Jiang, L., 2020. Stability and in vitro digestion simulation of soy protein isolate-vitamin D3 nanocomposites. Lwt 117, 108647. https://doi.org/10.1016/j.lwt.2019.108647

Zhang, Z., Dalgleish, D.G., Goff, H.D., 2004. Effect of pH and ionic strength on competitive protein adsorption to air/water interfaces in aqueous foams made with mixed milk proteins. Colloids Surfaces B Biointerfaces 34, 113–121. https://doi.org/10.1016/j.colsurfb.2003.11.009

Zhang, Z., Zhang, R., Chen, L., Tong, Q., McClements, D.J., 2015a. Designing hydrogel particles for controlled or targeted release of lipophilic bioactive agents in the gastrointestinal tract. Eur. Polym. J. 72, 698–716. https://doi.org/10.1016/j.eurpolymj.2015.01.013

Zhang, Z., Zhang, R., Tong, Q., Decker, E.A., McClements, D.J., 2015b. Food-grade filled hydrogels for oral delivery of lipophilic active ingredients: Temperature-triggered release microgels. Food Res. Int. 69, 274–280. https://doi.org/10.1016/j.foodres.2015.01.004

Zhang, Z., Zhang, R., Zou, L., McClements, D.J., 2016. Protein encapsulation in alginate hydrogel beads: Effect of pH on microgel stability, protein retention and protein release. Food Hydrocoll. 58, 308–315. https://doi.org/10.1016/j.foodhyd.2016.03.015

Zhu, H., Damodaran, S., 1994a. Effects of Calcium and Magnesium Ions on Aggregation of Whey Protein Isolate and Its Effect on Foaming Properties. J. Agric. Food Chem. 42, 856–862. https://doi.org/10.1021/jf00040a003

Zhu, H., Damodaran, S., 1994b. Heat-Induced Conformational Changes in Whey Protein Isolate and Its Relation to Foaming Properties. J. Agric. Food Chem. 42, 846–855. https://doi.org/10.1021/jf00040a002

Zmudziński, D., Ptaszek, P., Kruk, J., Kaczmarczyk, K., Roznowski, W., Berski, W., Ptaszek, A., Grzesik, M., 2014. The role of hydrocolloids in mechanical properties

of fresh foams based on egg white proteins. J. Food Eng. 121, 128–134. https://doi.org/10.1016/j.jfoodeng.2013.08.020

Zou, L., Zheng, B., Zhang, R., Zhang, Z., Liu, W., Liu, C., Xiao, H., McClements, D.J., 2016. Enhancing the bioaccessibility of hydrophobic bioactive agents using mixed colloidal dispersions: Curcumin-loaded zein nanoparticles plus digestible lipid nanoparticles. Food Res. Int. https://doi.org/10.1016/j.foodres.2015.12.035

Appendix I

Research Outputs

11.1 List of outputs

Peer Reviewed Publications:

- Lee, J., Duggan, E., 2022. Improved stability of vitamin D_3 encapsulated in whey protein isolate microgels. International Dairy Journal. https://doi.org/10.1016/j.idairyj.2022.105351
- Lee, J., Duggan, E., 2022. Whey protein microgels for stabilisation of foams. International Dairy Journal. https://doi.org/10.1016/j.idairyj.2022.105399

Published abstracts:

- J. Lee, E. Duggan. 'Whey protein microgels for stabilisation of foams'. 48th Annual Food Science & Technology conference, Limerick, December 2019. Poster presentation. Awarded Best Poster.
- J. Lee, E. Duggan. 'Encapsulation of vitamin D in whey protein microgels: stability and foaming properties'. 49th Annual Food Science & Technology virtual conference, TUDublin December 2020. Oral presentation. Awarded Best Oral Presentation.
- J. Lee, E. Duggan. 'Encapsulation of vitamin D in whey protein microgels: stability and foaming properties'. Waterford Institute of Technology Virtual Postgraduate Conference 2021. Oral presentation.
- J. Lee, E. Duggan. 'The effect of vitamin D on the foaming properties of whey protein isolate microgels'. 4th Food Structure and Functionality Symposium, Structuring Foods for a Sustainable World virtual conference, Cork, October 2021. Poster presentation.
- J. Lee, E. Duggan. 'Stability and bioavailability of vitamin D encapsulated in whey protein isolate microgels'. 35th EFFoST International conference 2021, Healthy Individuals, Resilient Communities, and Global Food Security. Lausanne, Switzerland, November 2021. Oral presentation.

Other Dissemination:

- J. Lee. 'Foams for elderly nutrition' Waterford PubhD symposium in March 2019. An overview of the Task 1 was presented to the public. Oral presentation.
- An overview was presented to undergraduates and industry at the annual WIT Science Careers Day.